Allosteric interactions at the M_3 muscarinic acetylcholine receptor

Laura Iarriccio Silva

A Thesis submitted for the Degree of
Doctor of Philosophy

May, 2008

This work has been carried out at the Department of Chemical Engineering of the Polytechnic University and the Division of Physical Biochemistry, National Institute of Medical Research under the direction of Dr. Pere Garriga and Dr. Nigel Birdsall.

Dr. Pere Garriga Solé
Grupo de Biotecnología Molecular i Industrial, Departament d'Engenyeria Química, Secció de Terrassa, Universitat Politècnica de Catalunya

Dr. Nigel John Michael Birdsall
Division of Physical Biochemistry, MRC, National Institute of Medical Research, Mill Hill, London, UK

Barcelona, Londres 2 de mayo del 2008

A mi madre

Lo que no supimos decir nos dolerá eternamente
y sólo el valor de un corazón abierto
podrá liberarnos de esta congoja.
Nuestros encuentros en la vida son un momento fugaz
que debemos aprovechar con la verdad de la palabra
y la sutileza de los sentimientos.

Susanna Tamaro

ACTA DE QUALIFICACIÓ DE LA TESI DOCTORAL

Reunit el tribunal integrat pels sota signants per jutjar la tesi doctoral:

Títol de la tesi: .....

Autor de la tesi: .....

Acorda atorgar la qualificació de:

- ☐ No apte
- ☐ Aprovat
- ☐ Notable
- ☐ Excel·lent
- ☐ Excel·lent Cum Laude

Barcelona, …… de/d'…..……. de .....….

El President

.....
(nom i cognoms)

El Secretari

.....
(nom i cognoms)

El vocal

.....
(nom i cognoms)

El vocal

.....
(nom i cognoms)

El vocal

.....
(nom i cognoms)

Abstract

The extracellular loops of muscarinic acetylcholine receptors are predicted to play a role in the binding and regulation of allosteric modulators. Furthermore, the sequence of the five subtypes of muscarinic receptors shows a large degree of diversity in this region. M_3 receptor mutants, K523E, D518K and N132G, in which the substituted residues were those corresponding to the M_1 subtype, were studied. As the amino acids in positions 518 and 523 are charged, the uncharged mutants, K523Q and D518N, were also created in order to observe any possible effect of charge. One question examined is whether these mutations changed the binding of orthosteric and allosteric ligands, generating a M_1 receptor phenotype.

Radioligand binding experiments revealed that one mutant, K523E, had a profound potentiating effect on the binding of prototypical modulators like gallamine, strychnine, brucine and N-chloromethylbrucine, but had minimal effects on the binding of a number of orthosteric ligands, including [^{3}H]N-methylscopolamine ([^{3}H]NMS) and acetylcholine (ACh). The increase in affinity was found at both the unoccupied and [^{3}H]NMS-occupied receptors, with up to 70 fold increases in affinity being observed. Switches from negative to positive cooperativity for some strychnine-related compounds were found.

At K523E, the affinities of the strychnine-related ligands were also increased up to 160 fold at the receptor-ACh complex, with up to 35 fold positive cooperativity being observed. Positive cooperativity of this magnitude is the highest that has been reported for M_3 receptors.

The dramatic changes in cooperativities and affinities of allosteric ligands at K523E did not result in generation of the M_1 phenotype. The K523Q data suggest that the large changes in K523E result from the introduction of the negatively charged glutamate residue and not the loss of the positively charged lysine. The effect of K523E seems to be solely on the binding of allosteric ligands and the transmission of the effects of their binding to the orthosteric site.

For the ligands acting at the gallamine site, all the effects of the allosteric modulators on ACh binding have been reproduced in functional studies, indicating that the allosteric modulation, seen in binding, is transmitted to the cellular response. A novel and unexpected finding is that WIN62,577 is an allosteric agonist at M_3 muscarinic receptors and at K523E and N132G. The study also revealed that nanomolar concentrations of ACh may be present in assays of muscarinic receptor function and may give misleading interpretations of data. These artefacts were removed by preincubation with acetylcholinesterase, a control not previously used in functional studies of muscarinic receptors.

The sensitivity of the binding of both orthosteric and allosteric ligands to the composition of the binding assay buffer has also been investigated in detail. In a phosphate buffer of low ionic strength (PB) the affinity constants of all the compounds studied, both orthosteric and allosteric, were increased, relative to a Hepes buffer of higher ionic strength, except for WIN 62,577, an allosteric ligand which binds to a

different allosteric site from the prototypical modulators, and SVT-40776 a new M_3 selective antagonist, indicating their different modes of binding. Cooperativities have also been switched from negative to positive by changing buffer.

The two factors affecting the allosteric binding parameters of M_3 receptors, PB and the mutation K523E, mutually potentiate each others effects. We have been able to obtain up to 10,000 fold changes in the affinity at the unoccupied receptor and 6400 fold increases in affinity at the ACh occupied receptor.

The possible location of K523, relative to other residues on the external loops of muscarinic receptors shown to be important for the binding of allosteric ligands, has been explored using different models based on the X-ray structures of rhodopsin and the β_2 adrenergic receptor.

List of Abbreviations

α	Cooperativity between an allosteric modulator and NMS
β	Cooperativity between an allosteric modulator and ACh
δ	Sensitivity factor of the effects of the K523E mutation or PB buffer
Δ	Overall change in affinity from M_3 WT in Hepes to K523E in PB
[^{3}H]-NMS	(-)-[^{3}H]-N-methylscopolamine
[^{3}H]-QNB	(-)-[^{3}H]-3-Quinuclidinylbenzilate
AC	Adenylyl cyclase
AC-42	4-*n*-butyl-1-[4-(2-methylphenyl)-4-oxo-1-butyl]-piperidine
ACh	Acetylcholine
AChE	Acetylcholinesterase
ADP	Adenosine 5'-diphosphate
ASM	Airway smooth muscle
ATP	Adenosine 5'-triphosphate
ATCM	Allosteric ternary complex model
ATSM	Allosteric two-state model
B_{max}	Number of receptors expressed in the membranes
CAM	Constitutively active mutant
cAMP	2',3'-Cyclic adenosine monophosphate
CHO	Chinese hamster ovary cells
CMB	N-chloromethylbrucine
CNS	Central nervous system
COPD	Chronic obstructive pulmonary disease
DAG	Diacylglycerol
Darifenacin	(S)-2-[l-[2-(2,3-dihydrobenzofuran-5-yl)ethyl]-3-pyrrolidiny]-2,2-diphenylacetamide
DMEM	Dulbecco's modified Eagle's medium
DMSO	Dimethylsulfoxide
DNA	Deoxyribonucleic acid
Dpm	Disintegrations per minute
EC50	Drug concentration that produces 50% of the maximal effect
E1 Loop	First extracellular loop of the receptor
E2 Loop	Second extracellular loop of the receptor
E3 Loop	Third extracellular loop of the receptor
E_{max}	Maximum receptor induced signal
EDTA	Ethylenediamine-tetraacetic acid
EGTA	Ethyleneglycol-tetraacetic acid
ER	Endoplasmic reticulum
ERK	Extracellular regulated kinase
FBS	Foetal bovine serum
G-protein	Guanine nucleotide binding protein
GABA	γ-Amino-n-butyric acid
GDP	Guanosine 5'-diphosphate
GPCR	G-Protein Coupled Receptor
GSIS	Glucose-stimulated insulin secretion
GTP	Guanosine 5'-Triphosphate
GTPγS	Guanosine 5'-O-(3-thio)triphosphate
HEPES	N-[2-hydroxyethyl]piperazine-N'-[2-ethanesulphonic acid]

HEPES buffer	30ºC: 100 mM NaCl, 10 mM $MgCl_2$, 20 mM Hepes, pH 7.4
IC_{50}	Drug concentration that inhibits the maximum response by 50%
I Loop	Intracellular loop of the receptor
IP_3	Inositol 1,4,5-trisphosphate
K_A	Affinity constant of a competitive ligand
K_{app}	Measured apparent affinity constant
K_D	Dissociation constant
K_L	Affinity constant of the radioligand
Kocc	Affinity of an allosteric modulator when the receptor is occupied by an orthosteric ligand
Kx	Affinity constant of an allosteric modulator
LB broth	Luria Bertani broth
mAChR	Muscarinic acetylcholine receptor
McN-A-343	[4-[[N-(3-Chlorophenyl)carbamoyl]oxy]-2-butynyl]-trimethylammonium
mRNA	Messenger ribonucleic acid
ND	Not determined
NSB	Non-specific binding
n_H	Hill coefficient or slope factor
NK Receptor	Neurokinin receptor
NMS	N-Methylscopolamine
OAB	Overactive bladder
Oxo	Oxotremorine
PB buffer	Room temperature (20-24ºC): 5 mM, pH 7.4. Hypotonic buffer, pH 7.4
PBS	Phosphate buffered saline
PCR	Polymerase chain reaction
PI	Phosphoinositide
PIP_2	Phosphatidylinositol-4,5-bisphosphate
PKC	Protein kinase C
PLC	Phospholipase C
PNS	Peripheral nervous system
rpm	Revolutions per minute
R.T.	Room temperature
SAR	Structure-activity relationship
SEM	Standard error of the mean
Solifenacin	Solifenacin succinate [YM905; (3*R*)-1-azabicyclo[2.2.2]oct-3-yl(1*S*)-1-phenyl-3,4-dihydroisoquinoline-2(1*H*)-carboxylate monosuccinate)
SVT-40776	Quinuclidine carbamate derivative of an aralkylamine (WO 02/00652 and EP 1300407)
TE	Tris-acetate/EDTA Buffer
TM	Transmembrane
Tolterodine	[(*R*)-*N*,*N*-Diisopropyl-3-(2-hydroxy-5-methylphenyl)-3-phenylpropanamine]
TRIS buffer	37ºC: 50 mM Tris, 3 mM $MgCl_2$ and 0.2 mM EGTA, pH 7.4
WT	Wild Type

In this thesis the amino acids have been named following either the three letter or one letter code. When a mutation is referred to, the first original amino acid is named followed by the position that it has in the protein and in the last position is the amino acid that has been introduced.

Table of contents

List of figures

Chapter 1

Chapter 2

Chapter 3

Chapter 4

Chapter 5

Chapter 6

Chapter 7

Chapter 8

List of tables

Chapter 1

Chapter 2

Chapter 3

Chapter 4

Chapter 5

Chapter 6

Chapter 7

Chapter 1. Introduction

Cells receive information from their environment through a class of proteins known as receptors. In biochemistry, a receptor may be defined as a protein on the cell membrane, within the cytoplasm, or in the cell nucleus that binds to a specific molecule (a ligand), such as a neurotransmitter, hormone, cytokine, growth factor or other substances, and initiates the cellular response. The ligand-induced changes in the behaviour of receptor proteins result in physiological changes that constitute the biological actions of the ligands. The majority of hormone and neurotransmitter receptors are embedded in the phospholipid bilayer of cell membranes. There are different types of membrane spanning receptors:

1. ***Metabotropic receptors***: They, when activated, trigger a series of intracellular events which involve a range of second messengers and result in ion channel regulation or other cellular effects. The two main classes are:

1.1 G protein-coupled receptors: They have seven transmembrane (TM) domains and comprise a large family. Depending on the specific receptor, they may function as monomer, homodimers or heterodimers. These receptors are described in more detail in next section.

1.2 Receptor tyrosine kinases: They have a single TM segment and function as dimers. They have high affinity for many growth factors, cytokines and hormones (such as insulin) and can regulate their intrinsic tyrosine kinase activity.

2. ***Ionotropic receptors***: They contain a central pore which functions as ligand-gated ion channel.

2.1 Cys-loop receptors: These members are homo- or heteropentamers. Each subunit has four TM segments. They contain a characteristic loop formed by a disulfide bond between two cysteine residues. Some important examples are nicotinic acetylcholine and $GABA_A$ receptors.

2.2 Ionotropic glutamate receptors: These members are tetramers (dimers of dimers). Each subunit has three TM segments. They have glutamate as the neurotransmitter, for example NMDA (N-methyl *D*-aspartate) or kainate receptors.

2.3 ATP-gated channels: They are thought to be homo- or heterotrimers. Each subunit has two TM segments. They have ATP, ADP or adenosine as their main ligands and are called P2X receptors.

1.1 G-Protein Coupled Receptors (GPCRs)

G-Protein Coupled Receptors (GPCRs) (Pierce et al., 2002;Kristiansen, 2004) are integral membrane proteins that constitute the largest family of signal transduction molecules participating in the majority of normal physiological processes (Fredriksson and Schioth, 2005;Gether et al., 2002;Schoneberg et al., 2002). This family of receptors is being widely studied because of their potential use as pharmacological targets for drug development (Wise et al., 2002;Bosch et al., 2005). About 50% of drugs under current investigation are targets for these receptors (Drews, 2000) (Fig 1.1).

Fig.1.1: Current drug targets

Based on 483 drugs in Goodman and Gilman's "The Pharmacological basis of therapeutics". Ninth Ed. McGraw-Hill, New York

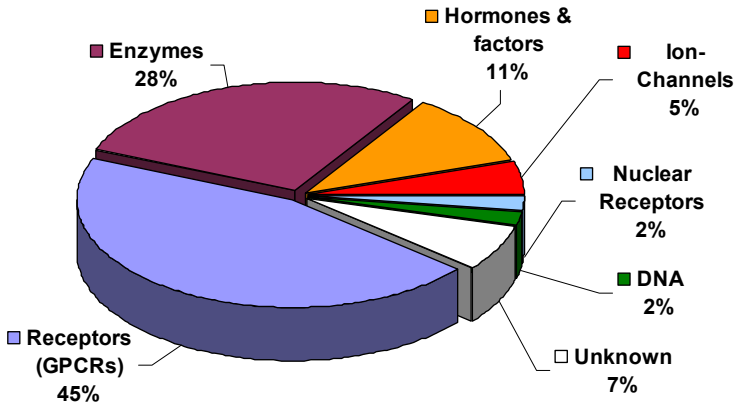

Members of the GPCR superfamily are responsible for the control of enzyme activity, ion channels and vesicle transport, and they respond to a wide variety of stimuli, such as sensory signals, hormones and neurotransmitters. Specific ligand binding triggers a conformational change in the receptor that leads to its active state, allowing binding and activation of a heterotrimeric G-protein (Wess, 1997;Gether et al., 2002). The activation of the G-protein results in inhibition or stimulation of the production of second

messengers that eventually elicit the linked cellular response (Fig. 1.2). Mutations in these receptors are responsible for a number of pathological processes, ranging from retinal degeneration in the case of the visual photoreceptor rhodopsin (Garriga and Manyosa, 2002;Rattner et al., 1999) to precocious puberty or hereditary obesity in the case of the lutropin receptor and the β_3-adrenergic receptor respectively (Themmen and Verhoef-Post, 2002;Strosberg, 1997).

Fig.1.2: GPCR signalling mechanisms

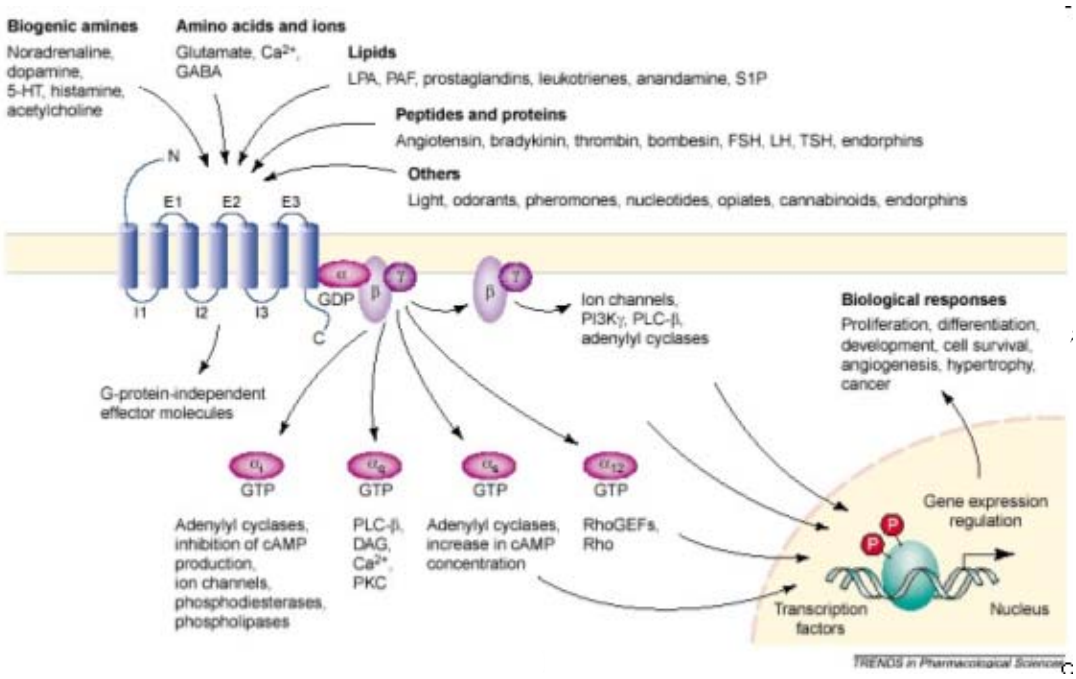

(Figure from http://nlp.postech.ac.kr/Research/POSBIOTM/content/intro.html)

1.1.1 Classification

There are ca 865 seven-transmembrane helix encoded GPCR-like sequences that have been identified in the human genome (Strosberg and Nahmias, 2007;Fredriksson and Schioth, 2005). The GPCRs maybe grouped into three main families based on their sequences and ligand binding properties (Figure 1.3. Family 1 (or A), the largest, includes the first GPCRs to be discovered; these GPCRs are closest in structure to rhodopsin since they have relatively short N- and C-termini. They are receptors for ligands as different as biogenic amines, chemokines, neuropeptides and prostanoids. Receptors in family 2 (or B) (which include those for adrenomedullin, calcitonin,

calcitonin gene-related peptide, glucagon, secretin and parathyroid hormone) have long N-termini containing several disulfide bonds, and those in family 3 (or C) (e.g. calcium-sensing and metabotropic glutamate receptors) have long N- and C-termini with the ligand-binding site in the N terminal domain. The rhodopsin like class 1 receptor family is by far the largest. Excluding odorant receptors (460) there are over 300 types. At least 210 receptors from families 1-3 have had their endogenous ligand identified. The other receptors are termed 'orphan' receptors.

Fig.1.3: Schematic diagram showing the structure of each of the three families into which GPCRs have been classified based on their sequences

(Figure 2 from (Strosberg and Nahmias, 2007))

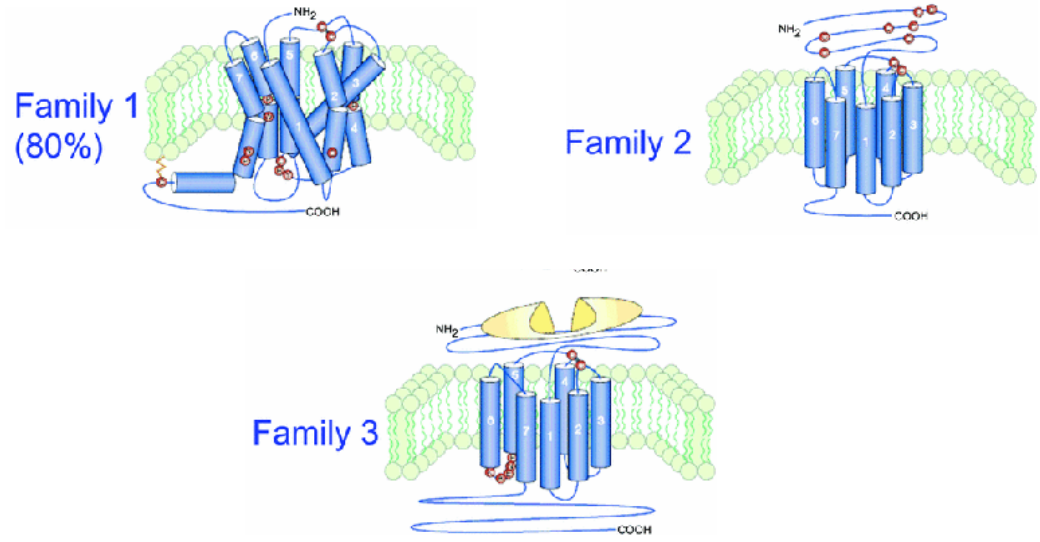

1.1.2 Receptor structure

As mentioned previously, GPCRs possess seven membrane-spanning domains. The extracellular parts of the receptor can be glycosylated. These extracellular loops in Family 1 receptors often contain two highly-conserved cysteine residues that form a disulfide bond to stabilize the receptor structure.

Early structural models for GPCRs were based on their weak homology to bacteriorhodopsin for which a structure had been determined by both electron diffraction (PDB 2BRD, 1AT9) (Grigorieff et al., 1996;Kimura et al., 1997) and X ray-based crystallography (1AP9) (Pebay-Peyroula et al., 1997). In 2000, the first crystal

structure of a mammalian GPCR, that of bovine rhodopsin (1F88) was solved ((Palczewski et al., 2000). While the main feature, the seven transmembrane helices, is conserved, the relative orientation of the helices differs significantly from that of bacteriorhodopsin. In 2007, the first structure of a human GPCR, the β_2-adrenergic receptor was solved (2R4R, 2R4S) (Rasmussen et al., 2007). This was followed immediately by a higher resolution structure of the same receptor (2RH1) (Cherezov et al., 2007) and(Rosenbaum et al., 2007). This structure proved to be highly similar to the bovine rhodopsin in terms of the relative orientations of the seven transmembrane helices. However the conformation of the second extracellular loop is entirely different between the two structures. Since this loop constitutes the "lid" that covers the top of the ligand binding site, this conformational difference highlights the difficulties in constructing homology models of other GPCRs based only on the rhodopsin structure.

1.1.3 Physiological roles

GPCRs are involved in a wide variety of physiological processes. Some examples of their physiological roles include:

1. the visual sense: the opsins use a photoisomerization reaction to translate electromagnetic radiation into cellular signals. Rhodopsin, for example, uses the conversion of *11-cis*-retinal to *all-trans*-retinal for this purpose
2. the sense of smell: receptors of the olfactory epithelium bind odorants (olfactory receptors) and pheromones (vomeronasal receptors)
3. behavioral and mood regulation: receptors in the mammalian brain bind several different neurotransmitters, including serotonin, dopamine, GABA and glutamate.
4. regulation of immune system activity and inflammation: Chemokine receptors bind ligands that mediate intercellular communication between cells of the immune system; receptors such as histamine receptors bind inflammatory mediators and engage target cell types in the inflammatory response.
5. autonomic nervous system transmission: both the sympathetic and parasympathetic nervous systems are regulated by GPCR pathways, responsible for control of many automatic functions of the body such as blood pressure, heart rate, and digestive processes.

1.2. Muscarinic receptors (mAChRs)

The first molecule identified positively as an endogenous neurotransmitter was acetylcholine (ACh) (Loewi and Navratil, 1926;Quastel et al., 1936;Feldberg and Krayer, 1933). The brilliant work done by these authors established the chemical basis of neurotransmission. Furthermore ACh is the neurotransmitter used by the motor nervous system, the presynaptic nerves of the autonomic nervous system and postsynaptic nerves of the parasympathetic nervous system, as well as being widely distributed in the central nervous system. Therefore ACh has achieved a very important position in the history of understanding neurotransmission. ACh acts at neuron-neuron and neuron-muscular cell synapses and binds to the cholinergic receptors, nicotinic and muscarinic receptors (Fig 1.4). The first definition of these two classes of receptor types was given by (Dale, 1914).

Acetylcholine (ACh) is synthesised from acetyl-CoA and choline in the cytoplasm of autonomic nerve terminals (Fig 1.4). The final step in the synthesis is catalysed by the enzyme choline acetyltransferase (CAT). Once formed, ACh is transported, packaged into synaptic vesicles and released at the nerve terminal where binds to muscarinic or nicotinic receptors, triggering the cell response. Cholinergic nerve transmission is terminated by the enzyme acetylcholinesterase (AChE). ACh binds to AChE and is hydrolysed to acetate and choline.

Fig.1.4: Synthesis and actions of ACh at synapses

Figure from presentation made by M.B. Gatch (University of North Texas at Fort Worth)

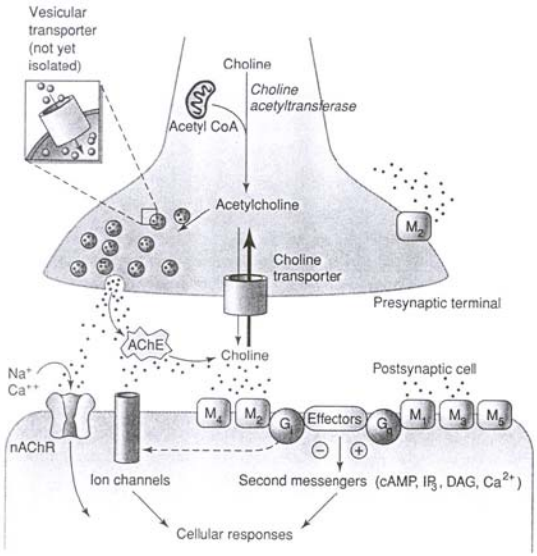

1.2.1 mAChR subtypes and localization

To date five subtypes of human muscarinic receptors (mAChRs) have been identified. The exact number of subtypes has only been known for 15 years. Cloning identified the five molecular subtypes, termed M_1-M_5 (Brown et al., 1980);(Hammer et al., 1980);(Hammer and Giachetti, 1982;Hulme et al., 1990). The M_1, M_2 and M_3 receptor subtypes had been postulated previously using pharmacological techniques (ROSZKOWSKI, 1961;Barlow et al., 1976;Hammer et al., 1980) and M_4 and M_5 subtypes were discovered using the molecular biology approach (Bonner et al., 1987;Bonner et al., 1987;Peralta et al., 1987;Bonner et al., 1988). The chromosomal locations of the five sub-types are based on further work by Bonner et al. are reported to be: **M_1**-11q12-13, **M_2**-7q35-36, **M_3**-1q43-44, **M_4**-11p12-11.2 and **M_5**-15q26 (Caulfield and Birdsall, 1998).

The distribution and tissue localization of the receptor subtypes has been studied extensively using pharmacological and molecular biological approaches for the past two decades. Pharmacologically, the receptor subtypes are classified based on their affinity for agonists and antagonists, although progress was hindered by the lack of selective ligands. There are indications in the early studies of the selective actions of gallamine on the heart (RIKER, Jr. and WESCOE, 1951) and of the agonist, McN-A-343 (4-*N*-[3-chlorophenyl]carbamoyloxy)-2-butynyltrimethylammonium chloride), on sympathetic ganglia (ROSZKOWSKI, 1961). The discovery of a ligand, pirenzepine, that has very high affinity for one subtype (M_1) relative to the others (Hammer et al., 1980) and the advent of radioligand binding and functional assays where accurate measurements of antagonist affinity constants were quantified (Hulme et al., 1978;Lazareno et al., 1990;Barlow et al., 1976) helped to overcome these difficulties.

Numerous studies have also explored the roles of specific mAChR subtypes (M_1-M_5) in mediating the diverse physiological actions of ACh. The experimental approaches, include immunohistochemical and mRNA hybridization studies, have shown mAChRs to be present in virtually all organs, tissues, or cell types (Caulfield, 1993;Levey, 1993;Vilaro et al., 1993;Wolfe and Yasuda, 1995). Such knowledge is considered essential for the development of novel therapeutic approaches aimed at inhibiting or enhancing signaling through specific mAChR subtypes. However, the task of assigning specific physiological functions to distinct mAChR subtypes has proven very

challenging, primarily owing to the lack of muscarinic agonists and antagonists that show a high degree of subtype selectivity for the individual mAChR subtypes (Eglen et al., 1999;Felder et al., 2000;Caulfield and Birdsall, 1998;Wess, 1996). Another complicating factor is that most organs, tissues, or cell types express multiple mAChR subtypes (Levey, 1993;Vilaro et al., 1993;Wolfe and Yasuda, 1995). Several laboratories have recently applied gene targeting techniques to generate mutant mouse lines deficient in one or more of the five mAChR genes (Hamilton et al., 1997;Gomeza et al., 1999a;Gomeza et al., 1999b;Matsui et al., 2000;Yamada et al., 2001;Takeuchi et al., 2002) in order to understand the physiological and pathophysiological roles of specific mAChR subtypes, particularly as far as the central muscarinic actions of ACh are concerned (Gautam et al., 2006;Kitazawa et al., 2007;LaCroix et al., 2008;Wess et al., 2007).

M_1 mAChRs are found predominantly in all the major regions of the forebrain, particularly the cerebral cortex, hippocampus and the striatum (Levey, 1993) and are the most abundantly expressed subtype in those regions. At these locations, the M_1 mAChRs are involved in higher cognitive processes such as learning and memory. M_1 receptors mediate most of the ACh-stimulated PIP_2 breakdown and MAP kinase activation in the hippocampus and cerebral cortex (Hamilton and Nathanson, 2001;Rosenblum et al., 2000) and activate ion channels underlying prolonged oscillations in the hippocampus (Fisahn et al., 2002). Pharmacological data supporting a role for the M_1 receptor in cognitive processes such as learning and memory are supported by studies with transgenic mice lacking the M_1 receptor, in which memory consolidation processes are impaired (Anagnostaras et al., 2003;Wess, 2003).

M_2 receptors are expressed throughout the central nervous system and in the periphery, especially in smooth muscle and tissues of the heart. In the heart, M_2 receptors are involved in the regulation of the force and rate of heart beating. Stimulation of the parasympathetic nervous system releases ACh from vagal nerve endings, which binds to (predominantly) M_2 mAChRs in the sinoatrial node, reducing heart beat frequency. M_2 mAChRs appear to be solely responsible for these regulatory effects despite the presence of the other mAChR subtypes in heart cardiac muscle (Caulfield and Birdsall, 1998). Stimulation of autoreceptors at cholinergic nerve endings allows acetylcholine to control its own release. For example, (Zhang et al., 2002a) showed that M_2 receptors

were responsible for the auto-inhibition of ACh release in the mouse hippocampus and cerebral.

M_4 receptors are preferentially expressed in the CNS forebrain (Levey, 1993) and are believed to regulate striatal dopamine release through action on the cell bodies of striatal GABAergic projection neurons (Zhang et al., 2002b). M_4-deficient mice show significant increases in basal locomotor activity and suggest a regulatory role of M_4 receptors on dopamine D_1 receptor locomotor activity. This highlights the fact that functional interactions between the cholinergic and dopaminergic pathways are important for striatal function and its control is relevant to the treatment of Parkinson's disease (Wess, 2003).

M_5 receptors, the last mAChR subtype to be cloned, are found in both neuronal and non-neuronal cells and are expressed at low levels. Until recently little was known about their physiological functions. The discovery of M_5 receptors in peripheral and cerebral blood vessel endothelium, has implicated M_5 receptors as being able to mediate ACh –induced dilation of arteries and arterioles. M_5 knockout mice have been shown to change drug seeking behaviours where effects of morphine and opioids were significantly reduced (Basile et al., 2002). The expression of M_5 receptors in the substantia nigra and the nucleus accumbens is consistent with their role as modulators of dopamine release in the mid-brain and their involvement in the rewarding effects of drug abuse. However the complex neuronal pathways that are involved these modulatory effects remain to be discovered.

M_3 receptors are also widely distributed in the CNS, located in various regions of the brain (Levey et al., 1994), although at lower levels than other receptor subtypes (Caulfield, 1993). A striking feature of M_3-deficient mice, observed by (Yamada et al., 2001) was their significant loss of body mass accompanied by reductions in serum leptin and insulin levels as a result of reduced food intake. Expressed at relatively high levels in the hypothalamus, M_3 receptors may be responsible, in part, for the regulation of appetite. At present little is known about the central physiological roles of the M_3 receptors. In the periphery is located in organs and tissues that are innervated by the parasympathetic nervous system (Caulfield, 1993;Eglen et al., 1994). They play a key role in actions associated with glandular function and regulation of smooth muscle contraction (Caulfield, 1993;Caulfield and Birdsall, 1998;Eglen et al., 1994;Wess,

2004). They have been found in salivary glands mediating primarily the stimulation of salivation and in the airway smooth muscle producing its contraction (Sarria et al., 2002;Fryer and Jacoby, 1998). The M_3 subtype is also involved in the parasympathetic control of pupillary sphincter muscle contractility. In vitro pharmacological studies using different isolated smooth muscle preparations (urinary bladder, ileum, stomach fundus, trachea and gall bladder) have shown the predominant role of M_3 receptor subtype in acetylcholine-mediated regulation of the contraction of these smooth muscle tissues. This M_3 smooth muscle mediation is especially important in the bladder, where enhanced urinary retention is present in M_3 receptor-deficient mice, suggesting this subtype is critical to urinary bladder voiding (Matsui et al., 2000;Stengel and Cohen, 2002;Stengel et al., 2002). Its physiological function and pathological implications in the bladder will be described in more detail later in this thesis.

Clearly the M_3 subtype performs multiple physiological actions and it is implicated in numerous pathological conditions. In this thesis, this is the main subtype that has been investigated.

The main distribution and function of the five muscarinic subtypes is summarised in Table 1.1. Fig. 1.5 illustrates the distribution of muscarinic receptors in the lung as an example of their location and functions. Acetylcholine (ACh) released acts via M_1 muscarinic receptors on postganglionic efferent nerves that innervate the submucosal glands and airway smooth muscle (ASM). Presynaptic M_2 muscarinic receptors are inhibitory autoreceptors on the postganglionic nerves. ACh released onto ASM causes bronchoconstriction via the M_3 muscarinic receptors and mucus secretion via the M_1 and M_3 muscarinic receptors.

Fig.1.5: Muscarinic receptors in the lung.

Figure from(Lee et al., 2001)

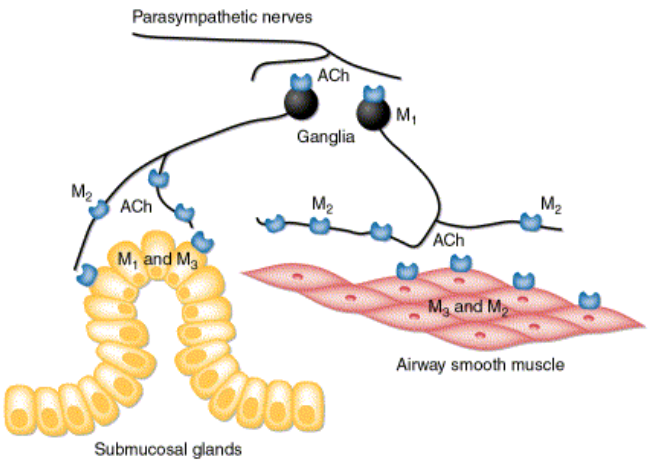

Table 1.1: Summary of the distribution, coupling and function of muscarinic receptor subtypes

(Adapted from (Caulfield and Birdsall, 1998), Table 4)

Subtype	*Distribution*	*G protein*	*Second messengers*[a]	*Functional responses*[b]
M_1	Brain (cortex, hippocampus) Glands Sympathetic ganglia	q/11	PLC IP_3/DAG Ca^{2+}/PKC	**M-current** inhibition
M_2	Heart Hindbrain Smooth muscle	i/o	AC (-)	K^+ channels Inhibit **Ca^{2+}** channels Decrease **heart** rate and force Decrease **neurotransmitter release** (presynaptic)
M_3	Smooth muscle Glands Brain	q/11	PLC IP_3/DAG Ca^{2+}/PKC	**Smooth muscle** contraction **Gland** secretion
M_4	Brain (forebrain, striatum)	i/o	AC (-)	Inhibit **Ca^{2+}**channels Decrease **neurotransmitter release** (presynaptic)
M_5	Brain (substantia nigra) Eye	q/11	PLC IP_3/DAG Ca^{2+}/PKC	

[a]: DAG, diacylglycerol; IP3, inositol 1,4,5-trisphosphate; PKC, protein kinase C; PLC, phospholipase C; AC, adenylyl cyclase.

[b]: Main responses; several other responses have been suggested to be elicited by defined subtypes.

1.2.2 Structure of muscarinic receptors

1.2.2.1 General structure

Muscarinic receptors have, in common with most members of the subgroup of G-protein-coupled receptor family whose ligand-recognition site binds small molecules, the major features of receptor structure which are (Caulfield & Birdsall 1998):

- The ligand recognition site is within the outer half of the membrane-embedded part of the protein. The transmembrane segments are probably α-helices, three oriented approximately perpendicular to the membrane, four at a more acute angle (Baldwin et al., 1997).
- There are two conserved cysteine residues that form a disulfide bond between the first and third extracellular loops (Kurtenbach et al., 1990;Savarese et al., 1992).
- At the cytoplasmic interface of TM III with the second intracellular loop there is a conserved triplet of amino acids (Asp Arg Tyr), which is important for both the expression and function of the receptor (Zhu et al., 1994;Jones et al., 1995;Lu et al., 1997).
- The carboxy-terminus is on the intracellular side of the membrane because antibodies to the C-terminus sequences recognize cell-surface receptors only when cells are permeabilized (e.g., (Lu et al., 1997). In this carboxyterminus, palmitoylation of a cysteine residue, C457 at M_2 receptors occurs in cells, but it is not an absolute requirement for the interaction with G-proteins even though function is enhanced (Hayashi and Haga, 1997).
- The N-terminus of the receptor is located in the extracellular part. On this N-terminus there are one or more glycosylation sites, but glycosylation apparently is not crucial for receptor expression and function, at least for the M_2 receptor (van Koppen and Nathanson, 1990).

1.2.2.2 Ligand binding site: Orthosteric site

Acetylcholine (ACh) is a ubiquitous neurotransmitter molecule and the natural agonist for muscarinic receptors, secreted from nerve terminals in the CNS and parasympathetic post-ganglionic neurons. Binding studies, alanine scanning mutagenesis and site-directed mutagenesis studies at M_1 and M_3 subtypes (Lu et al., 1997;Lu et al., 2001;Hulme et al., 2003b;Wess, 1996) have revealed the binding site for the classic muscarinic antagonist N-methylscopolamine (NMS) and ACh. The binding pocket is located approximately one third of the way down the transmembrane helical domains. The polar head group of the NMS molecule is believed to fit into a charge-stabilised aromatic cage. Mutagenesis studies suggest that the positively charged head group of ACh binds in a similar manner to that of NMS but that the side chain of ACh does not extend as deeply into the TM region (Wess et al., 1991;Hulme et al., 2003a). Fig 1.6 illustrates a model of the human M_1 muscarinic receptor with the molecules NMS and ACh docked at the predicted binding site. Residues homologous to those involved in ACh and NMS binding are found in other cationic amine receptor family members (Shi and Javitch, 2002) supporting the view that particular sequence positions are critical for ligand binding and consequent receptor activation. The most important residues for both ligands have been shown to be Asp(3.32), Tyr(3.33), Tyr(6.51), Tyr(7.39) and Tyr(7.43) of TM's III, VI & VII respectively; the numbering corresponds to the amino acid position according to the Ballesteros-Weinstein numbering system (Ballesteros and Weinstein, 1995). There are two threonine residues, conserved among the five subtypes of muscarinic receptors, Thr(5.42) and Thr(5.39), which are important for the binding of muscarinic agonists but not for antagonists (Wess et al., 1991;Wess et al., 1992;Wess et al., 1993). Asn(6.52) is been shown to be important for muscarinic antagonists like NMS, but not for agonists (Bluml et al., 1994a). This is also true for residues such as Asn(3.37), Val(3.40) and Phe(6.44).

Fig.1.6: M_1 muscarinic receptor model showing predicted ligand binding sites for acetylcholine & N-Methylscopolamine

Figure from (Lu et al., 2002)

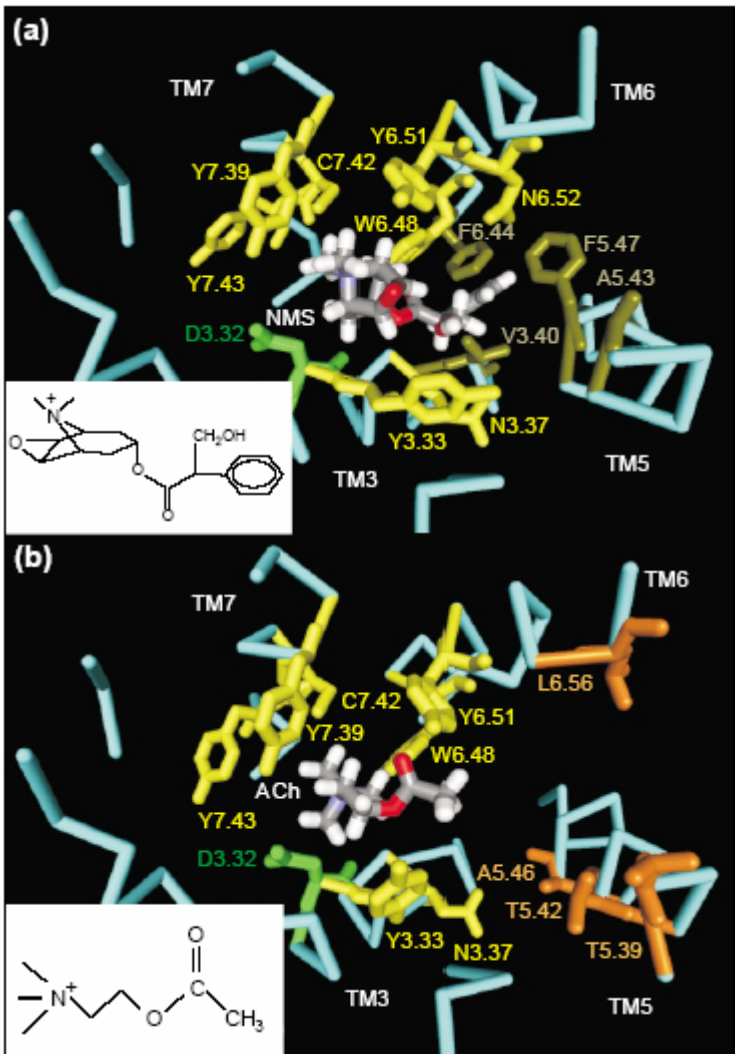

Alanine scanning mutagenesis (ASM) studies have suggested many of the residues involved in the binding of N-Methylscopolamine (a) and acetylcholine (b). Residues involved in the binding of the two molecules show some overlap. The positively charged head groups of both ACh and NMS are stabilised in an aromatic cage within the binding pocket and by interaction with Asp 3.32. ACh has a shorter side chain which appears not to extend as deeply into the binding pocket as does the bulkier side chain of NMS. The residues shown in the figure are known to play key roles in ACh and NMS binding to the five subtypes of muscarinic receptors (Lu et al., 2002).

There are other aspects of ligand binding that must also be considered. Some residues may form part of an entrance channel into the binding pocket. Residues of the 2nd extracellular loop of mAChRs may also be involved in ligand contact, by analogy with residues of the rhodopsin E2 loop (Shi and Javitch, 2002;Shi and Javitch, 2004), although the recent solution of the β_2 adrenergic receptor crystal structure revealed a different position of the E2 loop contributing to a different interpretation of the role of this loop and the mode of the entrance of the endogenous ligand (Rosenbaum et al., 2007;Cherezov et al., 2007). Moreover, recently random mutagenesis of the M_3 muscarinic receptor identified multiple residues in the E2 loop critical for activation (Scarselli et al., 2007). Radioligand binding and cell-based functional assays showed a 'gatekeeper' role of the E2 loop in the binding of both allosteric and orthosteric GPCRs ligands (Avlani et al., 2007).

The extracellular regions of GPCRs can also be targeted by allosteric modulators (May et al., 2007b;Christopoulos and Kenakin, 2002) which co-bind with orthosteric ligands and regulate their function. Muscarinic receptors are the best studied in this regard and prototypical modulators have been shown to play an important role not only in determining the actions of orthosteric ligands, but those of allosteric ligands as well. In the current study we have taken advantage of the opportunities given by the known modulators to investigate the involvement of the extracellular regions of the M_3 muscarinic receptors in the interaction between orthosteric ligands and allosteric ligands.

1.2.3 Functional response to receptor activation

1.2.3.1 Cascade of second messengers in signal transduction

Muscarinic receptors respond by activating different subtypes of G proteins upon activation by agonists. M_1, M_3 and M_5 mAChR subtypes activate primarily the G_q/G_{11} class of G-proteins stimulating phospholipase C_β isoforms to break down inositol 4,5 bisphosphate (PIP_2). Upon agonist binding to receptor, it undergoes a conformational change exposing a high affinity binding site for the G-protein heterotrimer which has GDP bound in an inactive state. Once the G protein binds to the receptor the GDP is released leaving an empty space for the nucleotide GTP, which exists at a higher

intracellular concentration than GDP, to bind. This exchange of GDP for GTP induces a conformational change causing dissociation of Gα from Gβγ dimer. The Gβ and Gγ subunits remain tightly associated and anchored into the lipid bilayer. Gα with the GTP bound activates phospholipase C (PLC) which promotes the hydrolysis of phosphatidylinositol 4,5-biphosphate (PIP_2) into the intracellular messengers 1,2-diacylglycerol (DAG) and inositol 1,4,5-triphosphate (IP_3). DAG remains bound to the membrane and activates protein kinase C (PKC) leading to effects including modulating slow potassium and calcium conductances. PKC also phosphorylates several mitogen-activated protein kinases (MAPKs), like ERK-1 and ERK-2, and activating various gene transcription factors involved in promoting smooth muscle growth. This activation appears to be dependent on PKC, although PKC independent pathway has been proposed by Tobin involving phosphorylation on sites in the third intracellular loop of the M_3 receptor by casein kinase 1α (CK1α) (Tobin, Totty, Sterlin 1997 and Budd, Tobin 2001).

The other product of PIP_2 hydrolysis, IP_3, translocates and binds to IP_3 receptors located in the sarcoplasmic calcium stores. When the IP_3 receptors are activated they release Ca^{2+} into the cytosol by opening Ca^{2+} channels. Intracellular calcium stores are the major source of Ca^{2+} for muscle contraction although influx from calcium channel receptors in the membrane can also contribute. Some of the effector proteins and the inositol phosphate signalling cascade are illustrated in Figure 1.7.

M_2 and M_4 mAChRs couple primarily to G-proteins of the G_i and G_o class, distinguishing the even numbered mAChRs from the odd numbered subtypes. The activation of αG_i inhibits adenylyl cyclase (AC) (Nasman et al., 2002) which primarily decreases the cellular cAMP level. The βγ subunits activate fast inward rectifier potassium channels and inhibit voltage sensitive calcium channels.

Fig.1.7: Gq-coupled receptor signaling in airway smooth muscle

(Figure from (Billington and Penn, 2003)

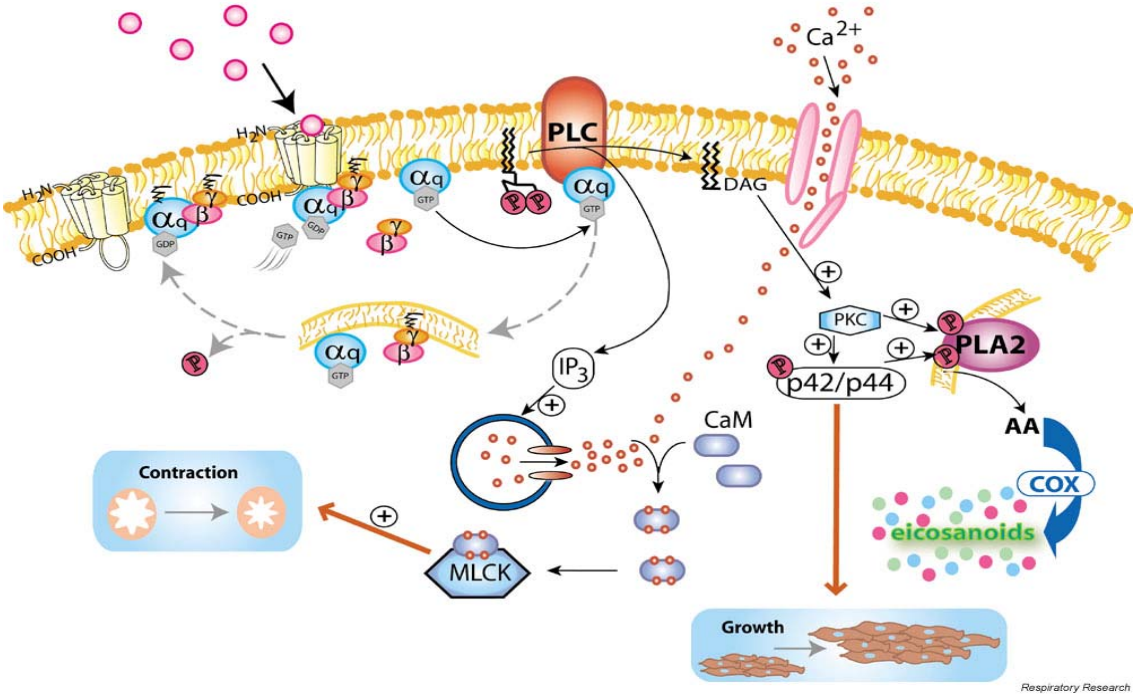

Key: CAM: calmodulin; MLCK: myosin light chain kinase: COX: cyclooxygenase: PLA2: phospholipase A_2: AA: arachidonic acid

1.2.3.2 Molecular mechanism of activation

The binding of agonists at the exofacial side activates the receptor leading to a series of pronounced structural changes on the cytoplasmic surface of the receptor (Hubbell et al., 2003;Gether and Kobilka, 1998;Bissantz, 2003;Kobilka, 2007) ultimately triggering G protein coupling to the receptor. These conformational changes are thought to be essential for productive receptor/G protein coupling. At present, little is known about the molecular mechanisms by which ligand binding to the extracellular receptor surface triggers the functionally critical conformational changes on the cytoplasmic side of the receptor. Thus, several *in situ* disulfide cross-linking studies at M_3 receptors have addressed this question (Ward et al., 2002;Han et al., 2005a;Li et al., 2007).

Accumulating evidence suggests that GPCR activation may involve a change in the relative disposition of TM III and VI (Bourne, 1997;Gether and Kobilka, 1998;Lin and Sakmar, 1996;Ramon et al., 2007;Farrens et al., 1996;Sheikh et al., 1996;Sheikh et al.,

1999;Kobilka, 2007). Site-directed spin labeling studies (Farrens et al., 1996) carried out with the photoreceptor, rhodopsin, indicated that rhodopsin activation may involve a rigid body movement of the cytoplasmic end of TM VI, away from the C terminus of TM III. In agreement with this concept, cross-linking of the cytoplasmic ends of TM III and TM VI, either via disulfide bonds in rhodopsin (Farrens et al., 1996) or via metal ion bridges in rhodopsin and other GPCRs (Sheikh et al., 1996;Sheikh et al., 1999), prevented receptor activation. A fluorescence spectroscopy study by Jensen et al on the β_2 adrenergic receptor (Jensen et al., 2001) added further evidence that an outward movement of the cytoplasmic region of TM VI follows agonist induced activation. The critical residue involved in this event for receptor signalling is Arg (3.50), again a highly conserved residue in the 'DRY' sequence in the I2 loop of the rhodopsin family of receptors (Lu et al., 1997), which forms a charge-stabilised hydrogen bond with Glu (6.30) at M_1 receptors (conserved in monoamine receptors and rhodopsin). Mutation of the Glu (6.30) residue produces constitutively active receptors, highlighting the constraining nature of this interaction in the native receptor (Hogger et al., 1995).

Numerous studies of disulfide cross-links, together with receptor modeling studies, strongly suggest that M_3 receptor activation increases the proximity of the cytoplasmic ends of TMs I and VII and TMs V and VI, associated with major rotational movements of the cytoplasmic portions of TMs VI (Ward et al., 2002) and VII (Han et al., 2005a). A likely scenario therefore is that the agonist induced conformational changes in TM VII are propagated to helix 8 via the short linker sequence connecting these two receptor regions. It is probable that the highly conserved NSXXNPXXY motif in TM VII is centrally involved in the conformational change that allows for a rearrangement of contacts to stabilise the activated state. The A91C/T549C and F92C/F550C receptors at M_3 receptors (located at TM I/TM VII) retained the ability to bind muscarinic ligands with high affinity and to couple to G proteins with high efficiency. However, when these two sites were linked via a disulfide bond, the receptor was unable to activate G proteins, suggesting that M_3 muscarinic activation requires a separation between these two residues (Li et al., 2007). An analogous rhodopsin mutant shows similar results (Fritze et al., 2003).

Based on sequence comparisons, the third intracellular loop of muscarinic receptors is suggested to determine the G protein coupling. The M_1, M_3 and M_5 receptor subtypes

which couple to same G protein show more similarities within this loop compared to M_2 and M_4 subtypes which couple to Gi type of G protein (Caulfield and Birdsall, 1998). Mutational analysis of the rat M_3 muscarinic receptor indicated that a limited number of amino acids located within the second (I2) and third intracellular (I3) loops and the adjacent cytoplasmic ends of TM III, V, and VI largely determine the Gq coupling preference of this receptor subtype (Bluml et al., 1994a;Bluml et al., 1994b). These findings are in agreement with a large number of studies using other classes of GPCRs (Strader et al., 1994;Wess, 1998).

Collectively, these structural changes are thought to enable heterotrimeric G proteins to contact previously inaccessible muscarinic receptor surfaces or residues, thus leading to productive receptor/G protein coupling. However, despite these findings, our knowledge of the molecular nature of the structural changes involved in GPCR activation is still very incomplete.

1.2.4 Targeting mAChRs for drug therapy

Muscarinic acetylcholine receptors (mAChRs), M_1–M_5, regulate the activity of numerous fundamental central and peripheral functions. Changes in level and activity of these receptors have been implicated in numerous major diseases of the CNS, and of the PNS. Unfortunately, it remains unclear in many cases which subtype is involved in mediating the different actions of ACh (Felder et al., 2000;Wess et al., 2007).

However, several muscarinic agonists or antagonists are currently approved for use in several clinical conditions. These include chronic obstructive pulmonary disease (COPD) and certain forms of bronchial asthma (where muscarinic antagonists such as ipratropium and tiotropium are effective drugs), peptic ulcer disease, Sjögren's syndrome, certain forms of cardiac arrhythmias, motion sickness and Parkinson's disease (Eglen, 2005;Felder et al., 2000) and in glaucoma, gastrointestinal and urinary bladder smooth-muscle disorders (OAB) (Taylor and Brown, 2006). The role of muscarinic M_3 receptors in OAB and the current drugs commercially available will be described more extensively in ***Chapter 3.3.***

Recently, phenotypic analysis of mutant mouse has identified specific mAChR regulated pathways as potentially novel targets for the treatment of several diseases. An

extensive description of these pathways and the collection of most important recent studies carried out with different *mAChR*-mutant mouse has been reviewed (Wess et al., 2007). Two examples of specific mAChR-regulated pathways as potentially novel targets are described. One is for the treatment of Alzheimer's disease (as a major relevant disease) and type 2 diabetes, as the M_3 subtype is directly implicated.

Alzheimer's disease

The overproduction of amyloid β peptide and its subsequent deposition as insoluble amyloid plaques is a key pathophysiological lesion leading to Alzheimer's disease. Consequently, reducing the production of this protein may slow the progression of the disease (Fisher et al., 2003). In isolated tissues, muscarinic M_1 agonism augments the release of the amino terminal form of amyloid precursor protein (Gu et al., 2003). Although the biochemical pathway underlying this effect is unclear, increases in Aβ protein promotes activation of protein kinase C and calcium/ calmodulin dependent kinase II: a process counteracted by M_1 receptors. This finding has been subsequently confirmed in Alzheimer's disease patients using the muscarinic M_1 receptor agonist, cevimeline, where Aβ levels declined after chronic treatment (Fisher et al., 2002). Similar observations in Alzheimer's disease patients are seen with the muscarinic M_1 agonists, alvameline, milameline, sabcomeline, RS 86, talsaclidine and xanomeline, suggesting that M_1 agonists, in general, lower Aβ (particularly Aβ42) levels (Hock et al., 2003). Long-term Phase III clinical trials have not, however, been conducted to assess the potential of these agents to retard progression of the disease. Indeed, current trials using muscarinic agonists in Alzheimer's disease are usually applied only to mild cognitive impairment and it thus is difficult to distinguish between symptomatic and disease-slowing effects of these compounds in most current trial designs (Longo and Massa, 2004).

Type 2 diabetes:

This occurs when β-cells fail to release sufficient amount of insulin, despite the elevated blood glucose levels (Kahn, 2001). Glucose-stimulated insulin secretion (GSIS) is regulated by numerous hormones and neurotransmitter, most of which bind to GPCRs expressed in pancreatic β-cells (Ahren, 2000). Many studies have demonstrated that GSIS could be stimulated by ACh release from intra-pancreatic parasympathetic nerves which acts on mAChRs of β-cells. This cholinergic amplification of GSIS is mediated

by the M_3 subtype (Duttaroy et al., 2004;Zawalich et al., 2004). In vivo studies of mutant mice that selectively lacked M_3 receptors in pancreatic β-cells showed reduced GSIS and significant impairments in glucose tolerance, probably due to reduced insulin release (Gautam et al., 2006). These authors also created transgenic mice that selectively overexpressed M_3 receptors in pancreatic β-cells in order to test the effects of enhanced signalling through β-cell M_3 receptors. Interestingly they found that glucose intolerance was dramatically improved and these mice showed pronounced reductions in blood glucose levels with increased serum insulin levels.

All these data, taken together, indicate that β-cell M_3 mAChRs play a crucial role in maintaining blood glucose homeostasis and that enhanced signalling through β-cell M_3 mAChRs leads to enhanced insulin release and greatly improved glucose tolerance. The mechanism of β-cell M_3 mAChRs is shown in Figure 1.8.

Fig.1.8: Scheme illustrating the central metabolic role of β-cell M_3 mAChRs.
(Figure 6 from (Wess et al., 2007))

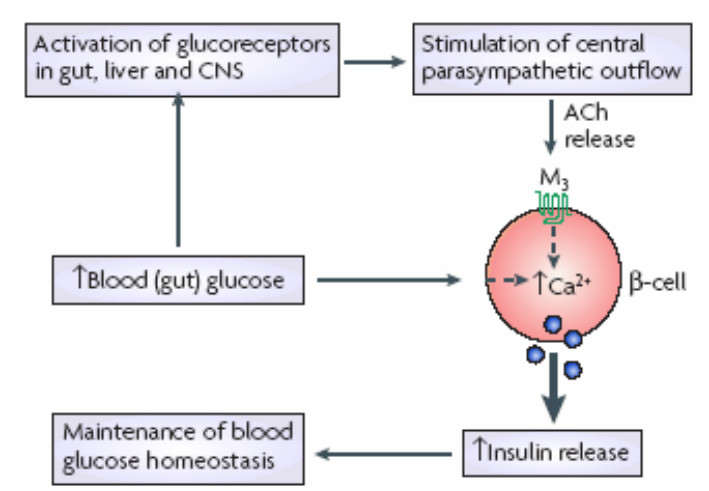

Figure 1.8: Mechanism of β-cell M_3 muscarinic receptors, where food intake triggers the stimulation of glucoreceptors in the gut, liver and brain producing an increase in central parasympathetic outflow (Gilon and Henquin, 2001;Niijima, 1989). The resulting stimulation of β-cell M_3 muscarinic receptors potentiates glucose-induced insulin release by increasing the intracellular calcium levels (Ahren, 2000;Gilon and Henquin, 2001). Mice lacking β-cell M_3 muscarinic receptors produce a disruption of this pathway causing a reduction in the insulin release and impaired glucose tolerance (Gautam et al., 2006). Contrarily, an overexpression of β-cell M_3 muscarinic receptors leads into an enhanced glucose-induced insulin release and a greatly improved glucose tolerance (Gautam et al., 2006).

The different potential therapeutic uses of subtype selective muscarinic agents based on gene targeting and/or pharmacological data are shown in Table 1.2. Blue coloured areas represent the disorders where the M_3 subtype, which is the main subtype studied in this thesis, is directly implicated and could be used as target in drug therapy. The areas coloured in yellow show the diseases where the other muscarinic subtypes could be potential targets. This table is adapted from Table 3 in (Wess et al., 2007).

Table 1.2: Potential therapeutic uses of mAChR subtype-selective compounds

Clinical condition	Drug
Alzheimer's disease	M_1, M_5 or mixed M_1/M_5 agonist; M_2 antagonist
Parkinson's disease	M_1, M_4 or mixed M_1/M_4 antagonist
Sjögren's syndrome	M_1, M_3 or mixed M_1/M_3 agonist
Schizophrenia	M_1, M_4 or mixed M_1/M_4 agonist
Type 2 diabetes	M_3 agonist (peripherally acting)
COPD (chronic obstructive pulmonary disease)	M_3 antagonist
OAB (overactive bladder)	M_3 antagonist
Obesity	M_3 antagonist (centrally acting)
Peptic ulcer disease	M_1 or mixed M_1/M_5 antagonist
Irritable bowel syndrome Gastrointestinal spasms	M_3 or mixed M_2/M_3 antagonist
Antinociception	M_4 agonist
Wound healing	M_4 agonist, M_3 antagonist
Cerebrovascular insufficiency	M_5 agonist
Drug addiction and withdrawal	M_5 antagonist

Table is adapted from Table 3 in (Wess et al., 2007)

1.3. Allosterism

1.3.1 Definition, concepts and historical perspective

The term "allosteric" (from the Greek meaning "other site") was defined by (MONOD et al., 1963) in a paper describing the ability of enzymes to have their biological activity modified, in either a positive or negative direction, by the binding of ligands to sites that were topographically distinct from the substrate-binding site. These distinct sites were defined as allosteric sites, in contrast to the substrate-binding (active) site.

There are two broad concepts which underline the majority of studies of allosterism. One of them, developed initially in the field of enzymology, is that many proteins possess more than one binding site and they can bind successively more than one ligand to these allosteric sites. This phenomenon is reflected in the earliest experimental model of allosterism, that of Bohr on oxygen binding to haemoglobin (Bohr C et al., 1904). The second important concept associated with allosterism is the ability of proteins to undergo conformational changes that yield an alteration in the affinity of the remaining (free) binding sites for ligands, highlighting the fact that the sites are conformationally linked (Wyman and Allen, 1951). When dealing with GPCRs, they are naturally allosteric in that they possess more than one type of binding site, with the G protein itself being the best-known allosteric modulator of agonist binding to GPCRs (Ehlert, 1985;Christopoulos and Kenakin, 2002).

Thus, the essential features of an allosteric interaction are:
- The binding sites are not overlapping.
- The binding of one ligand to its site affects the binding of the second ligand at the other site and vice versa. Allosteric interactions are, thus, reciprocal in nature.
- The effect of an allosteric modulator can be either negative of positive with respect to the binding and/or function of an orthosteric ligand.

1.3.2 Detection, quantification and validation of allosteric interactions

Affinity is defined by the ratio of the association and dissociation rate constants. When an allosteric ligand is bound to a receptor its conformational structure is changed and

therefore the rates with which an orthosteric ligand associates or dissociates from the new receptor conformation may be different from the rates for the unoccupied receptor. This may result in an alteration of the affinity of the orthosteric ligand for its binding site which is another manifestation of an allosteric interaction. Therefore an increase in ligand association rate and/or a decrease in ligand dissociation rate show an allosteric enhancement, whereas the opposite changes result in an allosteric inhibition. Both association and dissociation rates can also change in the same direction with enhancement or inhibition depending on the relative effects of one parameter compared with the other. A special case is when an allosteric interaction occurs but the affinity of the orthosteric ligand is not changed, i.e. the cooperativity is neutral. Kinetic measurements are a sensitive manifestation of allosterism.

1.3.2.1 Allosteric ternary complex model (ATCM)

To analyse both the equilibrium and kinetic manifestations of allosterism the simplest scheme is the allosteric ternary complex model, shown in Fig. (1.9). It is useful for both analysing the data and checking the validity of the results in the context of the scheme.

Fig.1.9: Representation of the ATCM

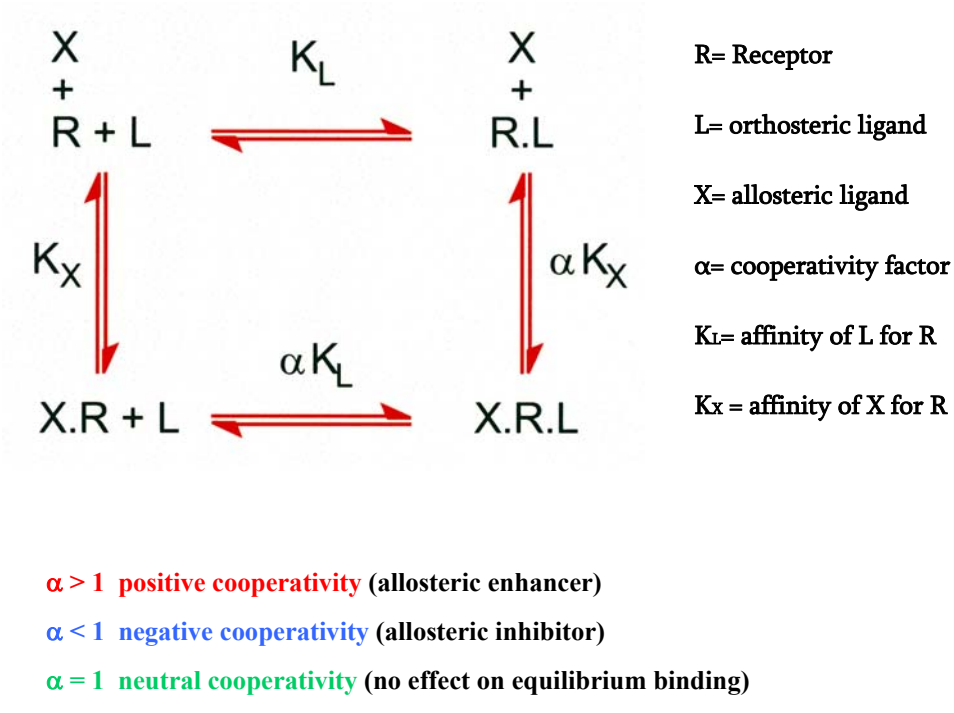

α > 1 positive cooperativity (allosteric enhancer)

α < 1 negative cooperativity (allosteric inhibitor)

α = 1 neutral cooperativity (no effect on equilibrium binding)

This is just a mathematical representation where the receptor can bind an orthosteric ligand [L] to one site on the 'right hand side' of the receptor. An allosteric ligand [X] binds to the separate site on 'the left hand side'. The allosterism is associated with the binding of the allosteric ligand (XR+ L) changing how L binds. Here the change is described by the factor alpha. This is the essence of the allosterism, where the receptor has two ligands bound simultaneously, with each having the ability to affect each others affinity equally.

In this model, orthosteric and allosteric ligands bind reversibly and saturably to their respective binding sites on the free receptor. The interaction is driven by the concentration of each ligand, their affinity constants (i.e., K_L, K_X) and an additional parameter, α, commonly referred to as the cooperativity factor (Ehlert 1988). This latter parameter describes the magnitude of the allosteric change in ligand affinity that occurs between two conformationally linked sites when they are both bound and represents the ratio of the affinity constants of the occupied receptor to that of the free receptor. Because of conformational linkage, the allosteric interaction between the two sites is reciprocal: what ligand L does to ligand X is the same as what ligand X does to ligand L. An α value >1 describes positive cooperativity (allosteric enhancement of binding), while an α value < 1 (but >0) describes negative cooperativity (allosteric inhibition of binding): α = 1 describes neutral cooperativity, i.e., no net effect on binding affinity at equilibrium, and α=0 describes a competitive interaction.

K_L, Kx, and α (and hence α.Kx) can be measured in **equilibrium** and **functional** studies. Independently, we can measure αKx in **kinetic** studies by measuring how the dissociation of L from the receptor changes in the presence of X. As X is progressively added, the observed dissociation rate constant changes that observed from RL to that found from XRL, and that change is governed by this binding constant, α.Kx. In all the cases the kinetic value and the equilibrium estimates of αKx have to agree with each other, if this model is to be valid.

1.3.2.2 Allosteric effects on binding (affinity)

For the detection of allosteric effects on the affinity of an orthosteric ligand, radioligand binding assays can be performed. The most common assays used are kinetic and equilibrium radioligand binding assays. They allow affinity binding constants of the allosteric ligand for the occupied and non-occupied receptor to be obtained. The

cooperativity value between the allosteric and the orthosteric ligand is also determined. The simplest way of describing allosteric interactions, which also forms the basis of many quantitative studies of GPCR allosterism, is the allosteric ternary complex model (ATCM) shown in Figure 1.9. An illustration comparing the theoretically infinite degree of inhibition obtained with a competitive orthosteric antagonist with the effects of an allosteric enhancer (α = 10) and an allosteric inhibitor (α= 0.1) on the receptor occupancy of an orthosteric ligand is shown in Figure 1.10(*a)* and *1.10(b)* respectively. The maximal displacement to the right of the orthosteric ligand curve by an allosteric antagonist approaches a limit which is defined by alpha. For an allosteric enhancer, the orthosteric occupancy curve is shifted to the left (Figure 1.10(*b)*). Figure 1.10(*c)* shows the same modulator interactions but from the point of view of a single ($1/K_A$) concentration of orthosteric ligand tested against increasing concentrations of modulator.

1.3.2.3 Allosteric effects on function (efficacy or potency)

Functional assays allow the detection of allosteric effects on the efficacy as well as the potency of agonists. Agonist concentration-effect curves are shifted to the left by positively cooperative allosteric agents and to the right by negatively cooperative agents. Allosteric function can also be measured using the ATCM. However certain assumptions have to be made: 1) affinity seen in function is what is seen in binding; 2) no constitutive activity of the system; 3) no agonism by the allosteric ligand and 4) efficacy of L at RL and XRL are the same, otherwise α estimated from binding and function will be different and additional assumptions are required. In those cases more complex models have to be used to analyse the data (Figure 1.11).

For a negatively cooperative interaction the data may be visualised as Schild plots of log (dose-ratio –1) versus log [allosteric agent], where dose-ratio is the ratio of equieffective agonist concentrations in the presence and absence of a particular concentration of allosteric agent, and can be analysed according to (Ehlert, 1988). The Schild Plot displays a linear portion (slope = 1) at low concentrations of allosteric ligand but this becomes flatter at higher concentrations, eventually becoming independent of [allosteric ligand] at high concentrations. The intercept of the plot at log(DR-1) = 0 gives the value of $-\log K_x$ (pA_2) and the plateau value of log(DR-1) gives the value of $-\log\alpha$.

Fig.1.10: Behavior of the ATCM

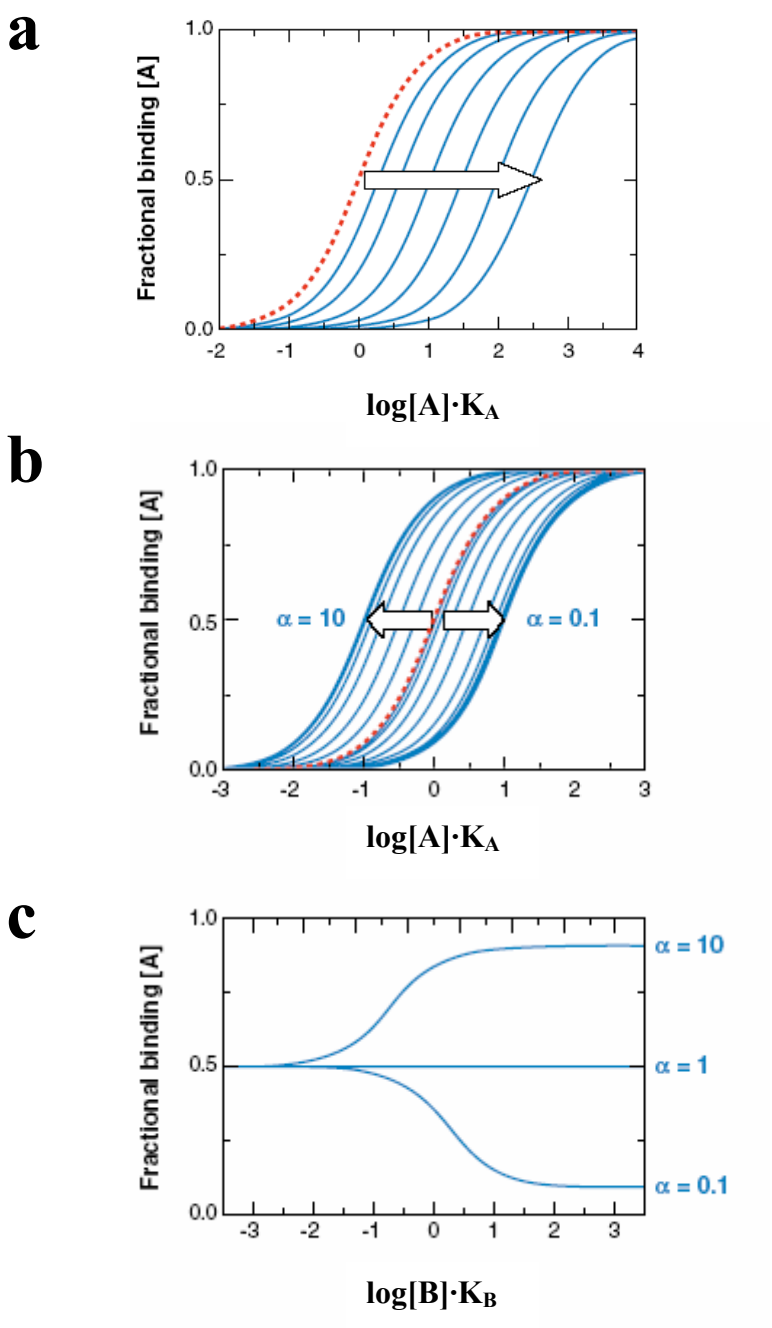

Fig 1.10: (*a*) A competitive interaction results in a theoretically limitless rightward shift of the concentration-occupancy curve for orthosteric ligand, A. (*b*) In contrast, an allosteric enhancer (α = 10) or allosteric inhibitor (α = 0.1) exhibits progressive inability to maximally shift the orthosteric ligand occupancy curve at maximal modulator concentrations. Arrows indicate increasing concentrations of ligand B. (*c*) The same interactions as shown in panel *b*, but using a fixed ($1/K_A$) concentration of orthosteric ligand and increasing concentrations of either a positive, negative, or neutral allosteric modulator. The Figure is from (May et al., 2007b).

1.3.2.4 Allosteric agonism

Ligands have been found which can activate the receptor from an allosteric site and not from the orthosteric site where the endogenous ligand binds, i.e. enrich the active state of GPCR conformations by themselves and thus showing agonism in the absence of a ligand bound orthosteric site (Bruns and Fergus, 1990;Langmead et al., 2006;Sachpatzidis et al., 2003). There are three potential advantages to allosteric agonists. The first is that allosteric agonism may be the best way to obtain selective agonists for certain receptors. This can be achieved on the basis of selective affinity for its nonconserved binding site or by selective signalling. The second advantage of allosteric agonists is that they may find clinical utility in combination therapies for certain disorders. Finally, allosteric agonists that act as enhancers of the endogenous agonist may prove clinically more efficacious compared with either agonists or allosteric enhancers alone.

1.3.2.5 More complex models

The quantification of the effects of allosteric modulators on orthosteric ligands efficacy requires an extension of the ATCM. A simple extension of the ATCM is the allosteric two-states model (ATSM) shown in Fig. 1.11 which describes allosteric modulator effects on affinity, efficacy, and the distribution of the receptor between active (R*) and inactive (R) states, determined by L, in terms of distinct conformations selected by ligands, an orthosteric ligand, A, and allosteric ligand, B, according to their cooperativity factors for the different states. In this model, there are three different molecular manifestations of the allosteric effect.

Thus, the cooperativity factors α and β determine the ability of the orthosteric and allosteric ligands, respectively, to promote an active receptor state; the cooperativity factor, γ, denotes the ability of each ligand to modulate the binding affinity of the other, whereas the factor, δ, denotes the ability of either ligand to modify the transition to the active state of the ternary complex.

Fig.1.11: Representation of the ATSM

Figure 1(b) from (May et al., 2007b). In this figure, dissociation constants are shown (1/affinity constant)

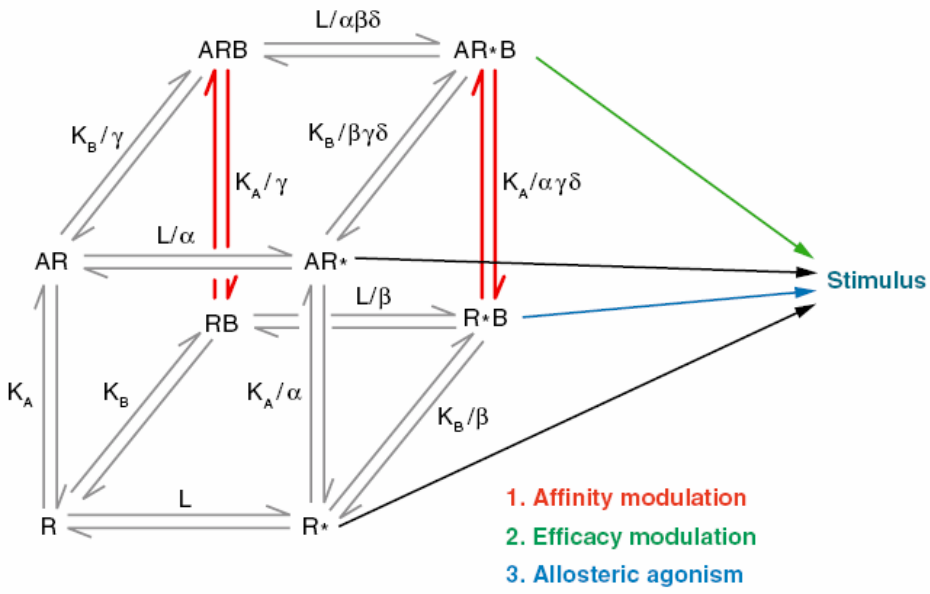

1.3.3 Therapeutic advantages of allosteric modulators

In terms of therapeutics, allosteric agents can be seen as stand-alone drugs which selectively enhance (or inhibit) the affinity of the endogenous ligand at the desired receptor subtype(s). They have the potential to provide a spatial and temporal selective action at a given receptor subtype that is not possible with orthosteric ligands. In addition, they have the capability to make an exogenous non subtype-selective orthosteric agonist or antagonist selective because of their different cooperativities at different subtypes. These therapeutic advantages that allosteric drugs offer are discussed in more detail in the following paragraphs. They can be applied to all GPCRs although muscarinic receptors are used as the main examples for being the receptor subfamily studied in this thesis:

1. Allosteric sites on muscarinic receptors have many attractions as therapeutic targets. They may be less well conserved across receptor subtypes than the orthosteric site, allowing a greater potential for ligands with a subtype selectivity based on affinity. It has been difficult to develop subtype-selective muscarinic agonists and antagonists,

perhaps because the structure of the binding region for ACh in the receptor (the orthosteric site) is strongly conserved across the muscarinic receptor subtypes (Hulme et al., 1990;Caulfield and Birdsall, 1998;Lu et al., 2002;Hulme et al., 2003b). It might be anticipated that an allosteric site on a receptor would be less strongly conserved across subtypes, provided the site is not the binding site for another endogenous ligand or is part of a domain of the receptor that performs another important function.

2. Allosteric ligands allow subtype selectivity based on cooperativity as well as affinity: they have the potential for 'absolute subtype selectivity', a new and powerful type of receptor subtype selectivity. An allosteric agent with positive or negative cooperativity with the endogenous ligand at one receptor subtype and neutral cooperativity at the other subtypes, regardless of the concentration or dose of the allosteric agent and regardless of its relative affinities for the receptor subtypes (Lazareno et al., 1998) would have absolute subtype selectivity. Clearly, allosteric agents have the potential to display many varied patterns of cooperativity with ACh or other orthosteric ligands across the muscarinic receptor subtypes.

The first example of 'absolute subtype selectivity' at M_1-M_4 receptors is thiochrome (2,7-dimethyl-5*H*-thiachromine-8-ethanol, Fig.1.12) an oxidation product and metabolite of thiamine. Thiochrome enhances ACh affinity at M_4 receptors and has neutral cooperativity at the other subtypes (Lazareno et al., 2004).

Fig.1.12: Chemical structure of thiochrome

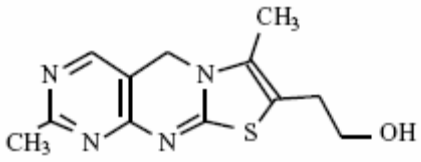

3. Allosteric ligands have the ability to 'tune' the effects of orthosteric agonists or antagonists as they may increase subtype-selectivity of orthosteric ligands, or modify their kinetics or efficacy therefore conferring a useful property to relatively non-selective exogenous orthosteric agonists or antagonists to generate a desired subtype selectivity.

4. Allosteric ligands may act as 'allosteric enhancers' to increase the affinity of the endogenous ligand, ACh, thus providing a use-dependent amplification of the endogenous signal, much as benzodiazepine tranquillisers such as diazepam act by allosterically enhancing the affinity for certain $GABA_A$ receptor subtypes for GABA (Whiting, 2003). A highly selective allosteric potentiator of the calcium-sensing receptor (family 3 GPCRs) termed cinacalcet (Sensipar, (Marino et al., 2003)) has now received US Food and Drug Administration approval for use in the treatment of hyperparathyroidism (Dong, 2005). Maraviroc (Celsentri, (Meanwell and Kadow, 2007)) is an allosteric CCR5 chemokine receptor antagonist that prevents HIV entry into the cells and it has also been approved by the FDA (*Pfizer, Inc. Pfizer Receives Approvable Letter from FDA for Maraviroc. Press Release. June 20, 2007).*

5. The actions of allosteric ligands have a 'ceiling'; i.e. their maximum effect is limited by their cooperativity. This is not just applicable to allosteric enhancers but also to allosteric inhibitors, which 'tune down' but do not abolish the signalling of a receptor molecule in the way that an orthosteric antagonist does.

6. Allosteric ligands, provided that they do not modulate constitutive activity, do not have an action on muscarinic receptor in the absence of ACh.

7. As most allosteric muscarinic ligands do not increase the maximum response to ACh, it is possible to envisage that an enhancer will have a selective action on tissues that are not being optimally stimulated because of a local ACh deficit.

Basically any muscarinic subtype or disease that is or has been a target for a selective muscarinic antagonist or agonist, e.g.(Felder et al., 2000;Eglen et al., 2001), but where the efficacy of the orthosteric ligands has been limited by its muscarinic side effects, is fair game for an allosteric approach. One example is that allosteric enhancers with selectivity for the M_1 receptor could be of use in the treatment of the cognitive decline in the earlier stages of Alzheimer's disease, where they would compensate for the effects of the localised ACh deficit.

1.3.4 Allosteric muscarinic ligands

The most extensive pharmacological studies of allosteric binding sites within the Family A (rhodopsin-like) of GPCRs have been on muscarinic receptors and as a result they

have become the prototypical GPCRs for the study of allosterism. This is in part due to the earliest evidence of allosteric modulation was found for this receptor family (Lullmann et al., 1969;Clark and Mitchelson, 1976) and to many allosteric ligands of different structures being described. They all appear to bind with different affinities to the five subtypes of muscarinic receptors. Furthermore many of the protocols used to study allosterism at GPCRs were originally developed using muscarinic receptors (Mohr et al., 2003;Birdsall and Lazareno, 2005;Waelbroeck, 2003).

1.3.4.1 Allosteric ligands that bind to the 'gallamine' binding site

The idea of the existence of a second ligand binding site on muscarinic receptors appeared when it was demonstrated that the effect caused by the neuromuscular blocker, gallamine (Fig 1.13), an inhibitor of the negative inotropic and chronotropic actions of muscarinic agonists in the heart, was not through a competitive mechanism (Clark and Mitchelson, 1976). Furthermore, it seemed to be a selective effect on the muscarinic receptors of the heart, as in similar studies in other types of tissues where muscarinic receptors are located, like salivary glands, ileum and bladder, showed that gallamine was less potent (RIKER, Jr. and WESCOE, 1951;Li and Mitchelson, 1980).

Subsequently, an extensive characterization of the gallamine binding properties of the binding of muscarinic receptors confirmed the existence of an allosteric site that, when it was occupied, modified the affinity of the ligand which was bound to the competitive site but it did not completely inhibit it (Stockton et al., 1983). These studies concluded with the fact that gallamine inhibited allosterically numerous agonists and antagonists, and that its potency in modulating these binding properties was different depending on the tissue, being most potent in the heart.

Allosteric modulators of muscarinic receptors can both diminish and increase the affinity of an antagonist or agonist. During last decade, the behaviour of different allosteric compounds on agonist and antagonist actions has been very extensively studied (Lazareno and Birdsall, 1995;Lazareno et al., 1998;Proska and Tucek, 1995;Jakubik et al., 1997;Tränkle and Mohr, 1997;Zahn et al., 2002).

Gallamine has become the prototypical muscarinic allosteric ligand. It is negatively cooperative with agonists and antagonists and, among the 5 subtypes of the muscarinic

receptors, has the highest affinity for M_2 subtype. It seems to act at the same site as other allosteric ligands such an obidoxime (Ellis and Seidenberg, 1992), and tubocurarine (Waelbroeck, 1994). Another neuromuscular blocking agent, alcuronium, was the first ligand where positive cooperativity with the muscarinic antagonist, [^{3}H]NMS, was demonstrated (Tucek et al., 1990). This enhancement of affinity at M_2 receptors also was observed, not only with the orthosteric antagonist [^{3}H]NMS but also with other muscarinic antagonists, such atropine (Hejnova et al., 1995). The fact that some allosteric agents were capable of producing an increase of the affinity of some muscarinic antagonists, lead to the thought that an equivalent enhancement could be produced with agonists, for instance, with the endogenous neurotransmitter acetylcholine.

Subsequently, strychnine, the precursor for the synthesis of alcuronium was discovered to have similar properties at muscarinic receptors as its functionalized dimer, alcuronium. A complete characterization of strychnine in binding assays has been done at all the muscarinic subtypes (Lazareno and Birdsall, 1995). The allosteric effects when NMS or ACh are bound to the receptor were also studied. The estimation of the affinities for the free and occupied receptor have been determined and hence the cooperativity that the modulator exerts on the ligands (antagonists and agonists) (Jakubik et al., 1997;Gharagozloo et al., 1999). Even though strychnine is smaller in size compared to alcuronium, it binds with comparable affinities to the free M_1, M_3 and M_4 receptors. However at M_2 receptors it has 10 fold lower affinity than alcuronium.

Strychnine enhances the affinity of the antagonist NMS at M_2 and M_4, being neutral at M_1 and inhibiting the NMS affinity at M_3 (Lazareno and Birdsall, 1995). However at all the subtypes it decreased the affinity of ACh, inhibiting its binding when the modulator was present (Lazareno and Birdsall, 1995;Jakubik et al., 1997).

Another alkaloid with a very similar structure to strychnine is brucine (10,11-dimethoxystrychnine). Although it binds with a lower affinity to muscarinic receptor than strychnine (2-10 fold lower), it was the first allosteric ligand shown to enhance both the affinity and functional potency of ACh at M_1 receptors (although only 2-fold), being negative or almost neutral with the other subtypes (Lazareno et al., 1998). In contrast (Jakubik et al., 1997) reported that, brucine was positively cooperative with ACh at M_3 as well as at M_1.

One quaternary analogue of brucine, N-chloromethylbrucine (CMB), has been found to increase ACh binding exclusively at M_3 receptors by up to 3-fold, with negative or neutral cooperativities at the other subtypes. The selectivity and the allosteric actions of brucine and N-chloromethylbrucine was confirmed in functional studies (Lazareno et al., 1998;Birdsall et al., 1999). This compound showed a different pattern of cooperative interactions with ACh and [^{3}H]NMS across the receptor subtypes. Some other N-substituted analogues, like brucine-N-oxide and N-benzyl-brucine, (Fig. 1.13) have been also studied and they exhibited a variety of affinities and cooperativities with different ligands and at different subtypes but no consistent picture of the SAR emerged (Lazareno et al., 1998;Gharagozloo et al., 1999).

Fig.1.13: Chemical structures of some different allosteric modulators for the 'gallamine' site that have been studied

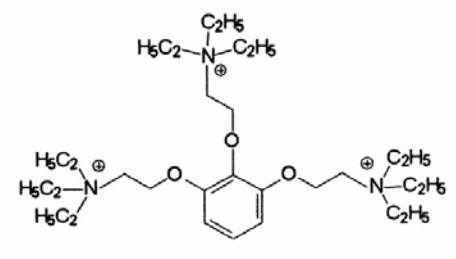

Gallamine

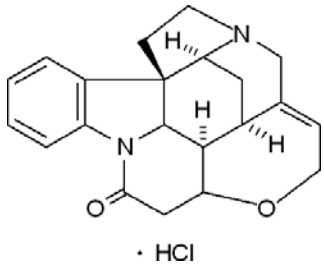

Strychnine

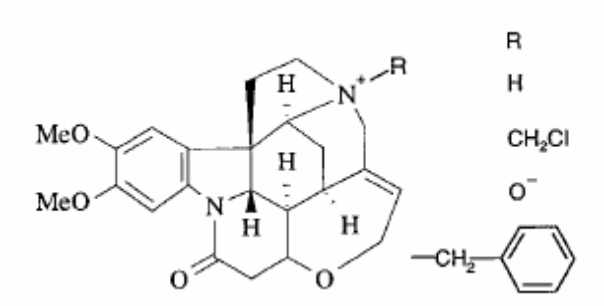

R	Name
H	Brucine
CH_2Cl	N-chloromethylbrucine(CMB)
O^-	Brucine-N-oxide
$-CH_2$	N-benzyl brucine

Brucine and its analogues

1.3.4.2 Allosteric ligands that bind to the 'WIN' binding site

A number of indolocarbazoles have been shown to be moderately potent allosteric muscarinic ligands at M_1-M_4 receptors, and exhibited a range of positive, neutral and negative cooperativities with NMS and ACh at the different subtypes (Lazareno et al., 2000). These are exemplified by staurosporine and KT5720 (Fig 1.14). KT5720 is an allosteric enhancer of ACh at M_1 receptors. Small changes in the structure of the indolocarbazoles produce significant changes in affinity and cooperativity.

These ligands differ in their allosteric behaviour from most other allosteric ligands in a number of ways. Firstly they have a tendency to be M_1 selective, in contrast to the M_2 selectivity exhibited by quaternary and bis-quaternary ligands. Secondly, some of these molecules do not have a positively charged nitrogen. Indeed the neutral KT5720 is more potent than the positively charged staurosporine. Thirdly, some of these allosteric ligands have very small or no (in the case of KT5720 at M_2 receptors) effect on [^{3}H]-NMS dissociation.

Another important difference between these molecules and the molecules which bind to the gallamine binding site is that they seem to bind in a different part of the receptor. Gallamine exhibited neutral cooperativity with KT5720 at M_1 receptors indicating that these molecules bound to spatially separated allosteric sites on the receptor (Lazareno et al., 2000). Similarly brucine exhibited neutral cooperativity with KT5720.

Two commercially available molecules, WIN 62,577 and its close analogue WIN 51,708, have been also reported to act as allosteric modulators at muscarinic receptors (Lazareno et al., 2002). They do not affect the dissociation rate of [^{3}H]NMS at M_3 receptors but their allosteric behaviour was demonstrated by another approaches which are explained in the next paragraph. WIN 62,577 is a weak allosteric enhancer of ACh at M_3 receptors and it seems to bind to the same site as staurosporine and KT5720.

A very particular and, at the same time, very useful finding is that an analogue of WIN 62,577 (PG987, 17-β-hydroxy-Δ4-androstano[3,2- *b*]pyrido[2,3-*b*]indole) uniquely speeds up the dissociation rate of [^{3}H]-NMS. It is therefore possible to easily monitor the kinetic interactions between PG987 and allosteric molecules that slow [^{3}H]-NMS

dissociation. It seems that PG987 binds to the same site as KT5720 and staurosporine on M_3 receptors but not to the site to which gallamine and strychnine bind. Using this approach it was possible to demonstrate that a ligand, WIN 51,708, that did not affect [^{3}H]-NMS dissociation at M_3 receptors nevertheless was binding to the same site as PG987. This approach was also utilised by (Ellis and Seidenberg, 2000) exploiting the finding that obidoxime acts allosterically with [^{3}H]QNB but has no effect on its dissociation rate at low ionic strength.

The allosteric site to which the indolocarbazoles and WIN 62,577 bind has been termed the 'WIN' site.

Fig.1.14: Chemical structure of staurosporine, KT5720, WIN 62,577 and PG 987

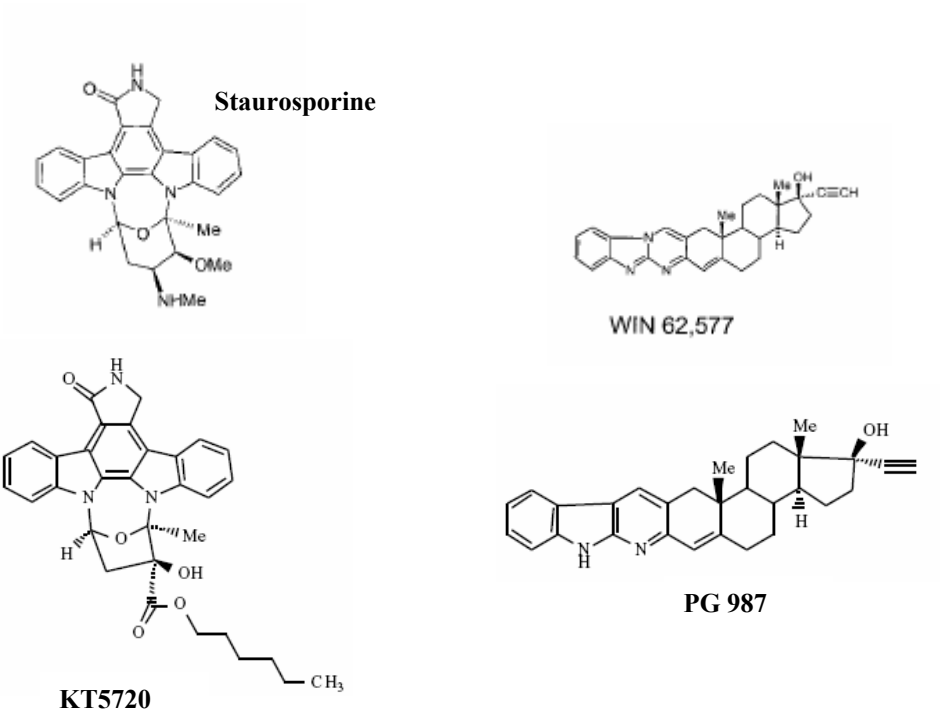

1.3.4.3 Allosteric ligands that bind in an atypical mode

McN-A-343 is a M_1/M_4 preferring agonist whose detailed mechanism of action is unknown. It is also of interest because it appears to interact allosterically with [^{3}H]NMS at M_2 receptors (Birdsall et al., 1983) causing incomplete inhibition of its binding when

present at a saturating concentration at rat M_2. A slowing effect of McN-A-343 on [^{3}H]NMS dissociation was also observed (Waelbroeck, 1994). Although it looks that this molecule binds in a more complicated mode, a theory was proposed that McN-A-343 binds to the orthosteric site on the unoccupied receptor; at somewhat higher concentrations it binds to the *d*-tubocurarine-occupied receptor and to its allosteric site when the orthosteric site is occupied by NMS. This fact would explain the fact that carbachol and McN-A-343 appear to interact competitively in functional studies at M_2 receptors (Christopoulos and Mitchelson, 1997) although their data could also be compatible with high negative cooperativity between the two agonists.

A selective agonist for M_1 subtype receptors has also been found recently which exerts a selectivity in functional responses (Spalding et al., 2002). The molecule is AC-42 (4-*n*-butyl-1-[4-(2-methylphenyl)-4-oxo-1-butyl]-piperidine) and it has the unusual property in that this subtype selectivity is not observed in binding where AC-42 appears to interact competitively with orthosteric muscarinic antagonists and with carbachol or with very high negative cooperativity. Nevertheless evidence for its binding allosteric behaviour at M_2 and M_1 has been reported recently (Langmead et al., 2006) and it has been classified as an allosteric agonist. Another special feature of this molecule is that it appears to utilise different binding epitopes on the receptor from orthosteric ligands such as ACh. Its binding site has been postulated to be an allosteric site or a different mode of binding to the orthosteric site. This 'ectopic' site seems to be located somewhere on the transmembrane domain 3 of the receptor, as the mutant W101A at M_1 receptors greatly enhanced the agonist actions of AC-42 (Spalding et al., 2002;Spalding et al., 2006).

However there are interesting similarities between McN-A-343 and AC-42. Not only is there an element of structural similarity between the two compounds but their agonist actions are both competitive (or highly negatively cooperative) with carbachol. It may be that McN-A-343 is binding to the same allosteric or 'ectopic' site as AC-42 (which is a different site from the allosteric site to which tubocurarine binds) and activates the receptor from that site.

The atypical antipsychotic clozapine (R = Me in Fig 1.15), an effective drug for the treatment of schizophrenia, and some other atypical neuroleptics are potent muscarinic agonists at M_4 receptors (Zorn et al., 1994;Zeng et al., 1997;Olianas et al., 1999). No

evidence has been found of the agonist clozapine acting allosterically (Michal et al., 1999). In addition, it has been reported recently that a major metabolite of clozapine, N-desmethylclozapine (R = H in Fig 1.15) is a potent muscarinic agonist with some M_1 selectivity (Sur et al., 2003). It has also been suggested to bind to M_1 receptors at a site distinct from the acetylcholine-binding site. The interaction of desmethylclozapine and clozapine with the Y381A mutant of the human M_1 receptor has been investigated (Sur et al., 2003). This tyrosine residue is considered to be very important for ACh binding and agonism, as the Y381A mutant exhibits strongly decreased ACh potency (up to 3,000 fold) (Sur et al., 2003;Lu et al., 2001;Ward et al., 1999). In contrast to the deleterious effects of this mutation on ACh actions, the efficacy of both N-desmethylclozapine and clozapine was *increased* considerably at the Y381A mutant, with their potencies being unchanged or increased. This result indicates a different mode of binding between both N-desmethylclozapine (and clozapine) and ACh. Because the potency and efficacy of AC-42 are also increased or unchanged in the Y381A mutant (Spalding et al., 2006), it is possible that N-desmethylclozapine and clozapine could be binding to the same site as AC-42 (and possibly McN-A-343) at an allosteric site, and are not just binding in a different mode to the orthosteric site. Structural and further mutagenesis studies should resolve the issue.

Another class of allosteric ligands are termed atypical because they bind with slope factors (Hill coefficient) greater than 1, even when the orthosteric site of the receptor is occupied. Some examples of this class of ligands are tacrine (Potter 1989), Duo3 (4,4'-bis-[(2,6- dichloro-benzyloxy-imino)-methyl]-1,1'-propane-1,3-diylbis-pyridinium dibromide) (Tränkle and Mohr, 1997) and some pentacyclic carbazoles (Gharagozloo et al., 2002). Furthermore obidoxime, a competitive ligand at the 'gallamine' allosteric site with a slope factor less than 1, (Ellis and Seidenberg, 1992) inhibits the actions of Duo3 only weakly and in a non competitive fashion (Tränkle and Mohr, 1997). In addition the affinity of Duo3 is much less sensitive to the buffer composition than the typical allosteric agents (Schröter et al., 2000) and the interactions between Duo and WDuo3 (1,3-bis[4-(phthalimidomethoxyimino-methyl)-pyridinium-1-yl]propane dibromide) with obidoxime are different. For these reasons, it has been suggested that Duo3 might be binding to a different allosteric site (Tränkle and Mohr, 1997). A similar behaviour to obidoxime has been shown by Mg^{2+} in its interaction with Duo3 and WDuo3 (Burgmer et al., 1998). The binding of tacrine and WDuo3, a typical allosteric agent

with slope factor equal to 1, have been shown to be affected by mutation of residues like Tyr177 and Thr423 at M_2 receptors (Ellis and Seidenberg, 2000). Duo3 seems to be binding to the same cavity than the other ligands but in an atypical mode (Tränkle et al., 2005).

Fig.1.15: Chemical structure of some atypical ligands

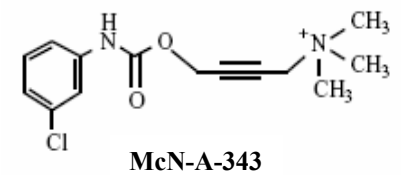

McN-A-343

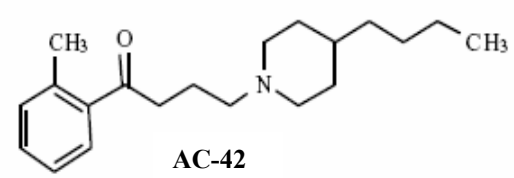

AC-42

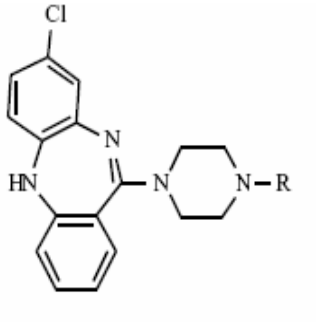

R= Me Clozapine

R= H Desmethyl clozapine

1.3.5 Where are the allosteric binding sites?

The precise location of the allosteric sites of the muscarinic receptor subfamily is largely unknown. This is a drawback that has limited efforts to better understand the mechanism of allosteric modulation.

To date, investigations within this field have been predominantly focused on the localization of extracellular allosteric domains that could be targeted by small molecules, and as such would represent attractive targets in terms of drug discovery and therapeutics. Furthermore, muscarinic receptors subtypes share a high degree of homology in transmembrane segments whereas the extracellular loops display greater diversity, making it potentially easier to reveal pharmacological differences between subtypes and define the structural basis of modulator selectivity. Taking into account these two facts, two basic approaches generally have been used in most mutagenesis studies of mACh receptor allosterism. The first has used site-directed mutagenesis of residues which are conserved among the five subtypes of receptors, with the aim of localizing common patterns across them. The second approach has involved the creation

of chimeras and single residue substitution of the non-conserved residues, mainly located at the external loops.

Following chimeric and single mutation studies candidate residues responsible for the M_2 selectivity of gallamine have been suggested. The acidic sequence EDGE of M_2 located at the second extracellular loop, immediately before the conserved Cys residue that forms the disulphide bond, has been mutated into the corresponding neutral sequence LAGQ of M_1, considerably lowering the affinity of gallamine, and vice versa (Leppik et al., 1994;Gnagey et al., 1999). Furthermore, acidic residues (D393 and E397) located at the third extracellular loop of M_1 (Gnagey et al., 1999) have also been implicated. The nature of residue 410 in M_5, equivalent to S388 in M_1 and to N514 in M_3, has also been shown to regulate gallamine binding (Spalding et al., 1997). Prototypical modulators, gallamine among others, were proposed to function as a cap by binding above the extracellular domain E2 lid stabilizing its closure and thereby slowing the rate of dissociation of the trapped ligand (Proska and Tucek, 1994), in a clear analogy to the role of this domain in rhodopsin (Shi and Javitch, 2002;Shi and Javitch, 2004). However, the simple model of a cap cannot explain cooperativity values different from neutral as a change of conformation is required, invalidating this simple interpretation in those cases. The group of Arthur Christopoulos has provided recently evidence of the importance of the E2 loop for the modulation of allosteric ligands constituting a major contact point for direct modulator-receptor interactions. They have shown that the mutants V171C and N419C have strong inhibitory effects on the access of orthosteric ligands suggesting that the E2 loop is flexible and that these residues represent the main points of it to adopt an open or closed conformation to regulate access (Avlani et al., 2007).

A three-dimensional model of the M_2 receptor in the NMS-occupied state was built on the basis of the crystal structure of bovine rhodopsin by (Jöhren and Höltje, 2002). Structurally different ligands such as gallamine, WDuo3, caracurine V salts or W84 (a hexamethonium-derivative) have been docked. (Ellis and Seidenberg, 2000;Buller et al., 2002;Voigtländer et al., 2003;Huang et al., 2005). By using molecular modelling and site- directed mutagenesis they have found that residues as Tyr177, N419 and Thr423 are also important for the allosteric modulation of these compounds, although they indicated that each modulator has a different selectivity pattern, i.e. the residue Thr423

has been found to be critical for the binding of WDuo3 and caracurine V related compounds, whereas for gallamine binding Asn419 plays a more important role but not for W84, which interacts with Tyr177 at M_2. The atypical molecules such a tacrine and Duo3 might be binding to this cavity too but in an atypical mode (Tränkle et al., 2005). At the M_3 receptor the triplet of residues (KFN) located in the third extracellular loop, has been determined as being responsible of determining the cooperativity of certain modulators (Krejci and Tucek, 2001;Jakubik et al., 2005). Acidic residues in this loop have also been postulated important for the binding and modulation of orthosteric ligands. Specifically, in the M_2 receptor changing N419 to E or D (found in M_1 and M_4 receptors), increased the affinity of gallamine for the NMS-occupied receptor. On the other hand the substitution of N419 by a K (M_3) reduced the affinity of gallamine for the NMS-occupied receptor (Gnagey et al., 1999).

Most mutagenesis studies of non conserved residues that are most likely located in the "gallamine" binding site have been done mainly on the M_2 subtype, the subtype with the highest affinity for gallamine. Some of these residues may be distanced from this site, but nevertheless induce changes in the structure of the binding site by indirect mechanisms. Out of the 24 conserved amino acids located extracellularly, two (W101 and W400) have been described as important residues for the binding of gallamine to the unbound and NMS-bound M_1 receptor (Matsui et al., 1995). A snake diagram illustrating the important residues for allosteric (black) and orthosteric (green) ligands binding is shown in Fig. 1.16. The conserved disulfide bond is also shown.

Fig.1.16: 'Snake' diagram of the M_2 mAChR

Figure from (Avlani et al., 2007)

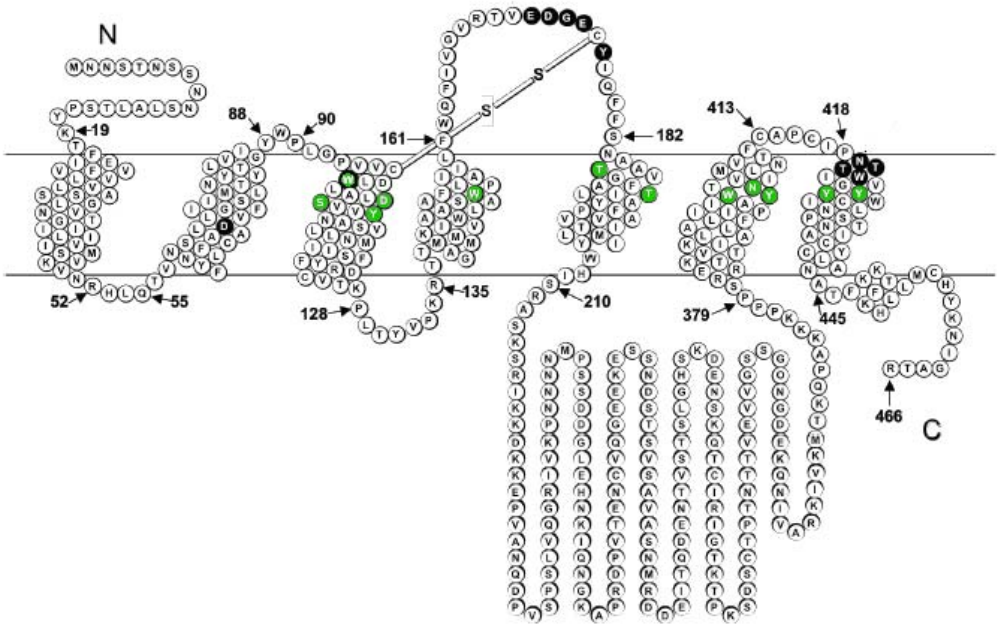

The location of the second allosteric site, the WIN site, is also largely unknown. There has been only reported one residue at M_1 subtype, Y82, a tyrosine located in the second transmembrane helix, that when mutated to alanine showed an increase in the cooperativity of WIN 51,708 and WIN 62,577 with ACh (Baig et al., 2005). This indicates that the tyrosine might be interfering in the binding of both WIN compounds.

The binding site of the atypical ligands like molecules as AC-42 or NDMC is not known. It seems that the binding site for these molecules share part of the orthosteric binding site utilising another 'ectopic' part of the receptor in which residues as W101 in the TM III of M_1 might be interfering, as the mutant W101A at the M_1 subtype substantially decreased the binding of ACh or carbachol whereas the agonist action of AC-42 was potentiated (Spalding et al., 2006). The binding of McN-A-343 is likely to use a different epitopes on the M_2 receptors than the prototypical modulators, as the mutant ^{172}EDGE^{175}-QNGQ _ Y^{177}A _ T^{423}A at M_2 receptors enhanced the maximal response without affecting the binding properties of McN-A-343 (May et al., 2007a). It remains to be determined whether its binding site overlaps at all with the 'gallamine' allosteric site or whether those effects were mediated indirectly through conformational changes transmitted between distinct binding sites.

To facilitate the development and design of new agents with high receptor subtype selectivity, an understanding of the receptor residues that govern the affinity of the allosteric ligands and the pattern of cooperative interactions between modulators and orthosteric ligands, such as ACh and [^{3}H]NMS, across the muscarinic subtypes is necessary.

1.4 Aims of the study

The overall aim of this thesis was to investigate the relative contribution that some non-conserved residues, located in the extracellular loops of the human M_3 muscarinic receptors, play in the modulation by allosteric modulators. This study will attempt to explore the molecular determinants of their subtype selectivity (for M_3 and M_1 receptors). The specific aims were as follows:

1. To design and construct human M_3 receptors, mutated at residues located in the extracellular loops.

2. To examine the effects of the mutations on binding under different ionic conditions where changes in binding properties may be amplified or attenuated.

3. To investigate the possible participation of individual amino acids residues in the binding of different prototypical allosteric modulators and some others postulated to bind to a second allosteric site.

4. To study the effects of the mutants on the modulation by allosteric modulators of ACh function.

5. To relate the effects of the mutations to their locations in possible receptor structures.

Chapter 2. Materials and methods

2.1 Materials

Chinese Hamster Ovary cells (CHO), stably transfected with the human M_3 mAChR (M_3 CHO-FlpIn cells) and the human M_1 mAChR (M_1 CHO-FlpIn cells) were kindly provided by Dr. A. Christopoulos (Department of Pharmacology, University of Melbourne, Australia). Chinese Hamster Ovary cells (CHO), stably transfected with the human M_1 mAChR (M_1 CHO-pCD cells) were kindly provided by Dr. Nigel Birdsall (Division of Physical Biochemistry, NIMR, Mill Hill, U.K.).

Oligonucleotides were manufactured and supplied by GeneWorks (Hindmarsh, Australia). Dulbecco's modified Eagle's medium (DMEM), penicillin-G, streptomycin, hygromycin-B and foetal bovine serum certified, origin USA (FBS) were purchased from Invitrogen. Easy Flasks 175F sterile for cell culture were obtained from Fisher Scientific UK (Nunc).

[^{3}H]-(-)-N-methylscopolamine 82-84 Ci.mmol^{-1} and [^{3}H]-myo-inositol 37 mBq/ml was from Amersham Biosciences. Liquid scintillation solution, Liquiscint, was supplied by National Diagnostics.

Darifenacin ((S)-2-[l-[2-(2,3-dihydrobenzofuran-5-yl)ethyl]-3-pyrrolidinyl]-2,2-diphenylacetamide), solifenacin succinate [YM905; (3*R*)-1-azabicyclo[2.2.2]oct-3-yl(1*S*)-1-phenyl-3,4-dihydroisoquinoline-2(1*H*)-carboxylate monosuccinate) and tolterodine [(*R*)-*N*,*N*-diisopropyl-3-(2-hydroxy-5-methylphenyl)-3-phenylpropanamine] were kindly provided by SALVAT (Esplugues de Llobregat, Barcelona). SVT-40776 (quinuclidine carbamate derivative of an aralkylamine (WO 02/00652 and EP 1300407), molecular weight: 558.48) was provided by SALVAT. This company has the full right to the patent of its structure (http://pharmalicensing.com/public/outlicensing/view/2661/salvat-svt-40776). The structure has not been disclosed to us. The structures of darifenacin and solifenacin were confirmed by mass spectra measured by Dr. Steve Howell at NIMR on a Bruker MicroTOF-Q ESI spectrometer.

N-chloromethyl brucine (CMB) was synthesized by Dr. P. Gharagozloo at MRC Technology, Mill Hill.

All other reagents were purchased from Sigma-Aldrich (London, UK).

2.2 Methods

2.2.1 Introduction of mutations into the M_3 gene

The coding sequence of the human M_3 mAChR was subcloned into a pEFS/FRT/V5-DEST Gateway destination vector (Invitrogen). This was achieved using the LR Clonase enzyme mix kit (Invitrogen). This subcloned coding sequence of the human M_3 WT was kindly provided by the lab of Dr. Arthur Christopoulos in Melbourne, Australia.

The following point mutations were introduced by QuickChange site-directed mutagenesis into the M_3 WT sequence: N132G, D518N, D518K, K523E and K523Q. Oligonucleotide primer pairs (one forward, one reverse) were designed to incorporate the desired mutations (Table 2.1).

The primer pairs were used in the **PCR-based QuickChange site-directed mutagenesis kit**. For each reaction, the following reagents were added: 5 µl of 10x reaction buffer (100 mM KCl, 100 mM $(NH_4)_2SO_4$, 200 mM Tris-HCl (pH 8.8), 20 mM $MgSO_4$, 1% Triton X-100 and 1 mg/ml nuclease free BSA), 50 ng DNA template, 125 ng of sense primer, 125 ng of antisense primer, 1µl dNTP mix, 1 µl pf *pfuTurbo* DNA polymerase and double-distilled water to a final volume of 50 µl.

PCR amplification was performed using 1 cycle of 95°C for 60 sec, 25 cycles of denaturation for 30 sec at 95°C, annealing for 60 sec at 55°C and extension for 255 sec at 68°C. The amplification reactions were then digested at 37°C with 1 µl of the *Dpn*I restriction enzyme to digest the parent DNA. The PCR products were chemically **transformed** into *E. coli* XL1-Blue supercompetent cells according to manufacturer's protocol. The transformed cells were plated on bacteriologic agar plates containing 50µg/ml ampicillin and incubated at 37°C overnight. Selected bacterial colonies were

chosen to inoculate in 5 ml of LB broth containing 150 µg/ml ampicillin for small scale plasmid isolation using Wizard *Plus* SV Minipreps DNA purification kit (Promega, Madison, WI, USA). The resultant DNA having the M_3 receptor gene with the desired mutations were verified by sequencing the product using primers provided in the kit (T7 forward and reverse sequencing primers) (See section 2.2.2 for sequencing protocol).

Positive bacterial mutations having the pEF5/FRT/V5-DEST vector from FlpIn system containing the M_3 muscarinic mutation genes were grown overnight in 50 ml LB broth containing 150µg/ml ampicillin. The overnight culture was spun down and the pellet was resuspended in 1 ml LB broth containing 20% glycerol and was frozen down at -70°C. Maxi preparations of the vectors were also prepared using a QIAGEN kit.

Table 2.1: Oligonucleotides used for M_3 receptor gene point mutagenesis and nucleotides changed in the M_3 receptor gene for the point mutations

Mutation	Sequence from 5´to 3´	Sequence change
K523E	5′ for GCTGCATACCCGAAACCTTTTGGAATCTGGG 5′ rev CCCAGATTCCAAAAGGTTTCGGGTATGCAGC	AAA →GAA
K523Q	5′ for GCTGCATACCCCAAACCTTTTGGAATCTGGG 5′ rev CCCAGATTCCAAAAGGTTTGGGGTATGCAGC	AAA →CAA
D518N	5′ for GGTGAACACCTTTTGTAACAGCTGCATACCC 5′ rev GGGTATGCAGCTGTTACAAAAGGTGTTCACC	GAC →AAC
D518K	5′ for GGTGAACACCTTTTGTAAGAGCTGCATACCC 5′ rev GGGTATGCAGCTCTTACAAAAGGTGTTCACC	GAC →AAG
N132G	5′ for CCTACATCATCATG GGT CGATGGGCCTTAGGG 5′ rev CCTAAGGCCCATCG ACC CATGATGATGTAGG	AAT →GGT

2.2.2 DNA Sequencing

The miniprep double stranded DNA template was used in cycle-sequencing reactions using the ABI Prism BigDye Terminator v3.1 Ready Reaction Cycle Sequencing Kit (Applied Biosystems; California, USA). The Terminator Ready Reaction Mix contains the dye terminators, deoxynucleoside triphosphates, AmpliTaq DNA polymerase (Taq-FS), magnesium chloride and Tris-HCl buffer (pH 9.0). For each reaction the following reagents were added: 8 µl of Terminator Ready Reaction Mix, 500 ng template DNA, 3.2 pmol sequencing primer (T7 forward primer) and deionized water to a final volume of 10 µl. The PCR amplification was carried out for 35 cycles, each comprising denaturation for 30 sec at 96°C, annealing for 15 sec at 50°C and extension for 4 min at 60°C.

Following PCR, the product was purified by ethanol/sodium acetate precipitation to completely remove unincorporated dye terminators that could obscure data at the beginning of the sequence before the samples can be analyzed by electrophoresis. For each 20 µl of reaction mixture, the following reagents were added: 3 µl of 3 M sodium acetate (pH 4.6), 62.5 µl of non-denatured 95% ethanol and 14.5 µl of deionized water. The samples were left at room temperature for 30 min to precipitate the PCR products and then spun for 20 min at 14,000 rpm to pellet down the PCR products. The supernatants were carefully discarded and the DNA pellets were washed once with 250 µl of 70% ethanol followed by a spin for 5 min at 14,000 rpm. The samples were air-dried for 1 hour.

The dried down DNA pellets were sent over to Australian Genome Research Facility (Parkville, Australia) for electrophoresis and data analysis by ABI Prism 373xI 96-capillary automated DNA sequencers to confirm the fidelity of the mutations.

The results of the confirmation of the introduction of the mutation are shown in Fig. 2.1 where a chronogram illustrates the position of the desired mutation with a red square.

Fig.2.1: Sequence confirmation of the mutations

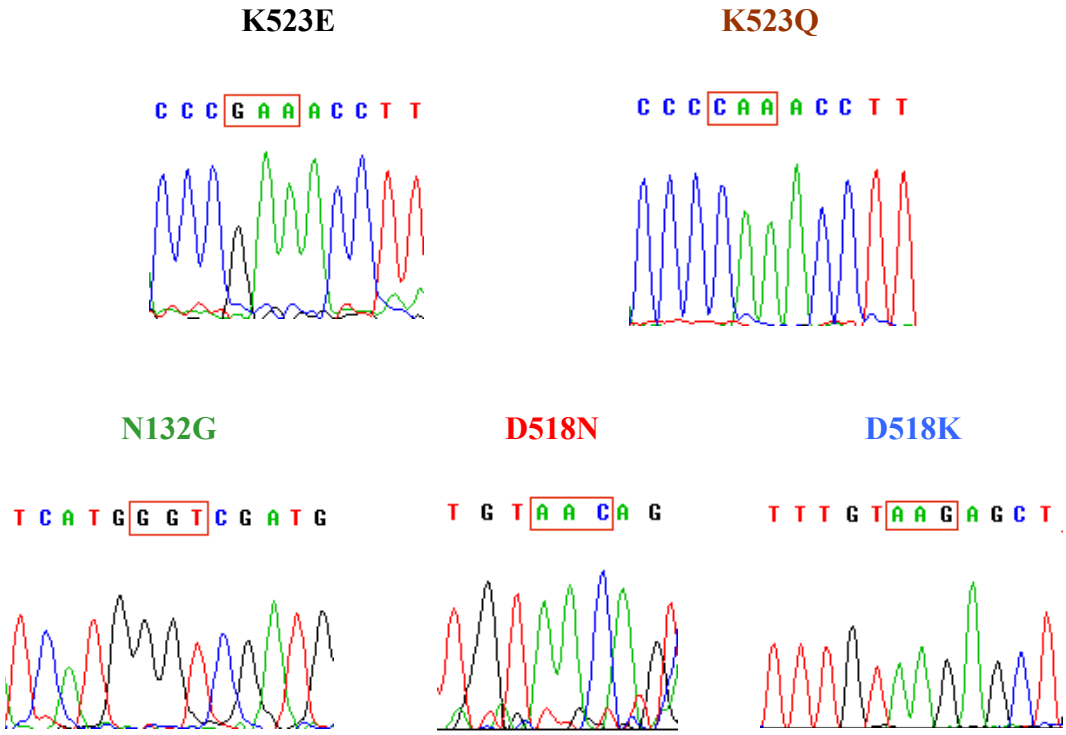

2.2.3 Maxi Preparation of DNA

Once the authenticity of gene was confirmed by sequencing, large scale plasmid DNA purifications were using the QIAGEN Kit (Qiagen Plasmid Purification Kits, La Jolla, CA) which is based on a modified alkaline lysis procedure, followed by binding of plasmid DNA to QIAGEN Anion-Exchange Resin under appropriate low-salt and pH conditions. The DNA yield was determined by both UV spectrophotometry by measuring the absorbance at 260 nm and 280 nm and quantitative analysis on a 0.8 % agarose gel. The plasmid DNAs were stored at -20°C in TE buffer (10 mM Tris-HCl, pH 7.5, 1mM EDTA) until use.

2.2.4 Sterile Cell Culture Techniques

2.2.4.1 Stable transfection of the receptors in CHO FlpIn cells

Chinese Hamster Ovary cells (CHO), stably transfected with the human M_3 mAChR (M_3 CHO cells) were kindly provided by Dr. A. Christopoulos (Department of Pharmacology, University of Melbourne, Australia).

To stably transfect the M_3 muscarinic mutants, 75 cm^2 flasks with CHO FlpIn cells at 70-75 % confluency were used for each transfection. The cells were transfected in serum and antibiotic-free DMEM (Dulbecco's modified Eagle's medium) using lipid based transfection protocol. The procedure is as follows: 1 μg of pEFS/FRT/V5-DEST vector containing the mutant M_3 mAChR gene, 9 μg POG44 vector (containing the FlpIn enzyme) were mixed with DMEM. Parallely 75 μl of lipofectamine was mixed with DMEM. These two tubes were mixed and incubated for 30 min at room temperature for lipid-DNA complex formation. This mixture was diluted with DMEM and overlaid onto the cells DMEM. The cells were incubated at 37 °C in a CO_2 incubator for 4 hr and then the media was replaced with complete DMEM containing 10 % FBS.

Once the cells were confluent, they were passaged with a confluency of 20 %, incubated at 37 °C in a CO_2 incubator for 4 hrs, and then the media was replaced with complete DMEM containing 10 % FBS and 400 μg/ml hygromycin-B (for selection of cells transfected with M_3 mAChR gene). The cells were kept at 37 °C in a CO_2 incubator, replacing with fresh DMEM media containing 10 % FBS and 400 μg/ml hygromycin-B every two days until colonies were obtained. These colonies, resistant to hygromycin-B, were collected and passaged 5 times to get cells stably transfected with the wt and mutant M_3 mAChR gene. The cells were characterized for the receptor expression by a radioligand binding assay.

2.2.4.2 Cell Culture Maintenance

Chinese Hamster Ovary (CHO) cells were routinely cultured in complete DMEM supplemented with 5% heat-inactivated FBS (56°C for 30 min to inactivate the complement protein preventing any immunological reaction), 100 units/ml penicillin-G, 100 µg/ml Streptomycin, and the selection antibiotic (50 µg /ml zeocin) for untransfected CHO FlpIn cells and 200 µg /ml hygromycin-B for CHO FlpIn cells stably transfected. The cells were incubated at 37°C in a 5% CO_2 humidified incubator.

Cells were passaged once they were 95% confluent. Adherent monolayer cells were washed with 1 x Versene (140 mM NaCl, 2 mM KCl, 8 mM Na_2HPO_4, 1 mM KH_2PO_4, 0.05 M EDTA, pH 7.4) to remove dead cells and any residual FBS that may inhibit the action of trypsin. The cells were then trypsinized by 1 x Versene/Trypsin treatment (0.05% trypsin in 1 x versene) for 3-5 min. 5 ml of complete DMEM was added to inactivate the trypsin and the cells were spun down by centrifuging at 300*g* for 5 min. The cells were then resuspended in complete DMEM and dispensed in flasks at the dilutions required and incubated in the 37°C – 5% CO_2 incubator until ready to use.

2.2.4.3 Freezing and Recovering Cells

Cell lines were frozen for long-term storage to preserve cells, avoid senescence and any effects of genetic drift. After trypsinisation, cells were spun down and the cell pellets were resuspended in 2 ml per 175cm^2 flask of the freeze mix (45% DMEM, 45% FBS, 5% DMSO and 5% Glycerol). From this mixture, 1ml aliquots were pipetted into labeled cryotubes and the cryotubes were placed into the fridge for 2 hours. Then they were transferred into the freezer until the cells were frozen. After that cryotubes were immediately frozen at -70°C overnight before transferring to liquid nitrogen for long term storage. To recover cells, the cryotubes were placed directly in 37°C water bath to thaw. Once thawed the outside of cryotube was wiped with 70% ethanol and the content was resuspended in 1ml complete DMEM containing 20% FBS and no selection antibiotic and transferred to 75cm^2 flask and maintained in the 37°C – 5% CO_2 incubator until confluent. The media was replaced with fresh media after 24 hrs and when required thereafter.

2.2.5 Cell membrane preparation:

For membrane-based radioligand binding assays, M_3 CHO cells, M_1 CHO cells and mutant CHO cells, were grown, harvested, and centrifuged as described above, with the final pellet resuspended in 5 ml of ice-cold homogenization buffer (20 mM HEPES, 10 mM EDTA) and then homogenized using a Polytron homogenizer for three 10-s intervals at maximum setting with 30-s cooling periods used between each burst. The homogenate was centrifuged (1000*g*, 10 min, 25°C), the pellet discarded and the supernatant was recentrifuged at 30,000*g* for 30 min at 4°C. The resulting pellet was resuspended in 5 ml of resuspension buffer (20 mM HEPES, 0,1mM EDTA), and the protein content was determined using the method of (Bradford, 1976). The homogenate was then aliquoted into 1-ml amounts and either used immediately or stored frozen at -80°C until required for radioligand binding assays.

2.2.6 Radioligand binding assays

2.2.6.1 Buffer composition

In this thesis different buffers have been used. The composition of each buffer was as follows:

1-Tris buffer (TRIS)**:** 37ºC: 50 mM Tris, 3 mM $MgCl_2$ and 0.2 mM EGTA, pH 7.4.
2-Hepes buffer (HEPES)**:** 30ºC: 100 mM NaCl, 10 mM $MgCl_2$, 20 mM Hepes, pH 7.4
3-Phosphate Buffer (PB)**:** room temperature (20-24ºC): 5 mM (4mM Na_2HPO_4 and 1mM KH_2PO_4). Hypotonic buffer, pH 7.4
4-Jakubik buffer**:** 25 ºC: 136 mM NaCl**,** 5 mM KCl**,** 1 mM MgSO4**,** 1 mM Na-phosphate buffer, pH 7.4, 10 mM Na-Hepes buffer, pH 7.4.

2.2.6.2 Saturation Binding Assays:

M_3, M_1 and mutant CHO cell membranes (5-10 μg/ml) were incubated in 1-ml total volume of TRIS buffer, HEPES buffer or PB buffer containing concentrations of [^{3}H]NMS ranging from 0.02 to 5 nM, for 90 min at 37°, 30° or room temperature, depending on the buffer used. Nonspecific binding was defined using 10 μM atropine. Incubation was terminated by rapid filtration through Whatman GF/B filters ((Brandel,

USA) using a Brandell cell harvester. Filters were washed three times with 3-ml aliquots of ice-cold milliQ water and dried before the addition of 4 ml of scintillation cocktail. Vials were then left to stand until the filters became uniformly translucent before radioactivity was determined using scintillation counting. The determination of nonspecific binding, the filtration and the counting procedure was used in all the binding assay protocols described subsequently.

2.2.6.3 Equilibrium Binding Assays:

M_3, M_1 and mutant CHO cell membranes (5-10 μg/ml) were incubated in 1-ml total volume of TRIS, HEPES or PB buffer containing either 0.2 or 0.1 nM [^{3}H]NMS (as indicated under *Results*), and a range of concentrations of the orthosteric or allosteric modulators at 37°C, 30°C or R.T., depending the buffer used, for 3 hours, as indicated under *Results*.

2.2.6.4 Dissociation Kinetic Assays:

2.2.6.4.1 Full time course

Initial experiments were performed to investigate the complete time course of [^{3}H]NMS dissociation, in the absence or presence of allosteric modulators, using a reverse time protocol. For these experiments, M_3, M_1 and mutant CHO cell membranes (5-10 μg/ml) were equilibrated with 0.2 nM [^{3}H]NMS in 1-ml total volume of TRIS buffer for 60 min at 37°C. Atropine (10 μM), either alone or together with 100 μM of the indicated allosteric modulator, was then added at various time points to prevent radioligand reassociation to mAChRs, *see Results*.

2.2.6.4.2 Two and one point kinetics

In subsequent experiments, designed to investigate the effects of a range of modulator concentrations on the [^{3}H]NMS dissociation rate, a "two-point kinetic" approach was used, where the effect on radioligand dissociation of each test ligand was determined at 0 min and two other time points (60 and 120 min). Another approach was also used, the "one-point kinetic assay" where only one time point, at, ca 2.5 dissociation half-lives of [^{3}H]NMS alone was used. This simplified approach for the determination of radioligand dissociation rate constants is valid when the dissociation characteristics of the radioligand are found to be monophasic in the absence and presence of any of the

modulators tested (Lazareno and Birdsall, 1995), as found for [^{3}H]NMS in the present study (see *Results*). A high concentration of membranes (50-75 μg/ml) was incubated with a high concentration of [^{3}H]NMS (1 nM) for about 30-60 min. Then 200 μl aliquots were distributed to tubes, which contained 100 μl of 10^{-5} M atropine alone or in the presence of a number of concentrations of allosteric agent (typically three concentrations) in 1-ml total volume of TRIS, HEPES or PB buffer. The time zero data point was obtained using only 200 μl of the mixture. Nonspecific binding was measured in separately prepared tubes pre-incubated with 100 μl of 10^{-5} M atropine alone in 1-ml total volume of TRIS, HEPES or PB buffer before addition of containing 200 μl of a mix of membranes + [^{3}H]NMS. Some time later, (about 2.5 dissociation half-lives) the samples were filtered, see *Results*.

2.2.6.5 Inhibition of [^{3}H]NMS binding by a fixed concentration of ACh and different concentrations of the modulator

M_3, M_1 and mutant CHO cell membranes (5 μg/ml) were incubated in 1-ml total volume of HEPES and PB buffer with a fixed concentration of [^{3}H]NMS, 0.2 and 0.1 nM respectively (as indicated under *Results*) at 30ºC or R.T. for 3 hours. The binding of [^{3}H]NMS was measured alone and in the presence of one concentration of ACh, 20 μM, and a range of concentrations of the allosteric modulators. All the experiments were performed in presence of 0.2 mM of GTP.

2.2.6.6 Inhibition of [^{3}H]NMS binding by different concentrations of ACh and a fixed concentration of the modulator.

M_3, M_1 and mutant CHO cell membranes (5 μg/ml) were incubated in 1-ml total volume of HEPES and PB buffer with a fixed concentration of [^{3}H]NMS, 0.2 and 0.1 nM respectively (as indicated under *Results*) at 30ºC or R.T. for 3 hours. The binding of [^{3}H]NMS was measured alone and in the presence of a single concentration of the allosteric modulator and a range of concentrations of the ACh (0.1μM-100μM). All the experiments were performed in presence of 0.2 mM of GTP.

2.2.6.7 Equilibrium binding assay with different concentrations of modulator and ACh

M_3, M_1 and mutant CHO cell membranes (5 μg/ml) were incubated in 1-ml total volume of HEPES and PB buffer with a fixed concentration of [^{3}H]NMS, 0.2 and 0.1 nM respectively (as indicated under *Results*) at 30ºC or R.T. for 3 hours. The binding of [^{3}H]NMS was measured alone and in the presence of three concentrations of the allosteric modulator and a range of concentrations of the ACh (0.1μM-100μM). All the experiments were performed in presence of 0.2 mM of GTP. Determination of nonspecific binding, termination of reaction, and determination of radioactivity were performed as described above.

2.2.7 Phosphoinositide Turnover Assays

Wild-type M_3 receptor (WT) and its N132G and K523E mutants were stably expressed using the Flp-In expression vector in CHO cell lines. The cells were grown in 12-well plates at 37^{o}C, 5% CO_2 and labelled with 2μCi/ml *myo*-[^{3}H]inositol for 18 hours, allowing incorporation of the *myo*-[^{3}H]inositol into phosphatidylinositol-4,5-bisphosphate (PIP_2) within the cell. The medium containing the *myo*-[^{3}H]inositol was removed and the cells were incubated for 30 min in warm Krebs-bicarbonate solution (120mM NaCl, 3.1mM KCl, 1.2mM $MgSO_4$, 2.6mM $CaCl_2$, 10mM glucose and 25mM $NaHCO_3$, pH 7.4) containing 10mM LiCl (to inhibit inositol phosphatases), that had been pre-incubated at 37^{o}C. Following addition of a series of increasing concentrations of acetylcholine in the presence or absence of other ligands made up in the Krebs-bicarbonate solution the cells were incubated a further 60 minutes at 37^{o}C in 5% CO_2 (*See Results*). The stimulation of PI hydrolysis was terminated by removal of the agonist containing medium, the addition of 5% ice-cold perchloric acid and incubation at 4^{o}C for 20 minutes. 0.4ml of the lysate was then added to 0.1ml of 10mM EDTA and 0.5 ml of a 1:1 ratio (v/v) of tri-n-octylamine and 1,1,2 trichlorotrifluoroethane (Freon) solution. The samples were then vortexed and centrifuged at 4,000 rpm for 10 minutes in a Heraeus Megafuge to separate aqueous phase containing the inositol phosphates from the non-aqueous phase. Then, 0.3 ml of the aqueous upper phase was added to columns containing Dowex AG 1 x 8 resin (formate form dry mesh size 100-200). The columns were washed with 10ml milliQ H_2O, then 25mM ammonium formate, and

finally the ^{3}H-inositol phosphates were eluted with 1M ammonium formate, 0.1M formic acid. 1ml of the eluted sample was collected and 10 ml Liquiscint scintillation fluid was added. Samples were counted on a Wallac 1409 counter.

2.2.8 Data analysis:

Data generated from binding assays were analysed using Prism 4.0 (GraphPad Software Inc., San Diego, CA). Data points were fitted to models using non-linear regression equations.

Saturation binding assays

Data sets of total and nonspecific binding obtained from each saturation binding assay were analyzed according to the following equation analysis:

$$B_{L^*} = R_T \times \frac{K_L \times L^*}{\left(1 + K_L \times L^*\right)} + NS \times L^* \qquad \textbf{(1)}$$

where $[R_T]$ is the total receptor concentration, K_L is the radioligand equilibrium association constant, L* is the free radioligand concentration, BL* is the bound radioligand concentration and NS is the fraction of nonspecific binding. The hyperbolic term in eq. 1 was not used when fitting the nonspecific binding data, whereas the parameter NS was shared between both total and nonspecific binding data sets.

Competition assays

The equation that describes the effect of an orthosteric ligand on the binding of a radioligand is:

$$RL^* = \frac{R_{Lo^*}}{1 + (Kapp_A \times A)^{n_H}} \qquad \textbf{(2)}$$

where K_{app} is the apparent affinity constant of the competing ligand and A is its free concentration. RLo* is the bound radioligand in absence of A and RL* is the measured bound radioligand. The Hill coefficient or slope factor is represented by n_H.

The data were actually fitted in GraphPad Prism using the following equation

$$Y = Bottom + \frac{(Top - Bottom)}{(1 + 10\hat{}((\log EC50 - X) \times HillSlope))} \quad \textbf{(3)}$$

where Y is the concentration of radioligand bound to the receptor, X is the logarithm of the concentration of the competing ligand and EC50 is the midpoint of the curve which is the inverse of the apparent affinity constant ($EC50=1/Kapp_A$). Y starts at the Top and goes to the Bottom with a sigmoid shape. HillSlope is the negative of the Hill coefficient or slope factor.

When the Hill coefficient is not constrained it is an indicator of the shape of the inhibition curve. If the value is equal to 1 the competition curve is consistent with the ligands binding to a homogenous set of binding sites. If the value is greater than 1, then there may be positive co-operativity in ligand binding. Conversely, if the value is significantly less than 1, then negative co-operativity may be occurring or the ligand could be binding to a heterogeneous population of receptors.

The apparent affinity constant obtained from competition binding assays using the Hill equation or one site model were corrected to take into account the receptor's affinity for the radioligand. This was achieved by using the Cheng Prusoff correction factor (Cheng and Prusoff 1973).

Thus:

$$K_A = Kapp_A\left(1 + K_{L^*}\left[L^*\right]\right) \quad \textbf{(4)}$$

where $Kapp_A$ is the apparent affinity constant of the competing ligand, L* is the free concentrations of the radioligand at equilibrium, K_{L^*} and K_A are the affinity constants for the radioligand and the competitor respectively.

Radioligand kinetics assays.

Radioligand dissociation rates were analysed by non-linear regression according the following equation for mono-exponential decay using Prism 4.0:

$$Y = Span \times \exp(-K \times X) + Plateau \qquad \textbf{(5)}$$

where Span is the specific binding of the radioligand, at time=0, before dissociation was initiated. Y is bound radioligand (specific binding) after dissociation for time X. The equation starts at (Span + Plateau) at time = 0 and decays to Plateau with a rate constant K. The half life is 0.69/K. K is the k_{offobs} and denotes the observed radioligand dissociation rate constant in absence or presence of the allosteric modulator. For mono-exponential and fully reversible binding it is predicted that the curve would decay to Plateau=0. These values were finally expressed as percentage inhibition of the true [^{3}H]NMS dissociation rate constant *(k_{-1}* in the absence of allosteric agent) and fitted to a hyperbolic function using nonlinear regression analysis (*eq. **2***). The curve corresponds to the occupancy curve for the allosteric agent at the [^{3}H]NMS occupied site.

Estimation of the affinity of an allosteric agent for the [^{3}H]NMS-occupied receptor.

An alternative method of obtaining estimates of the affinity of the allosteric agent for the [^{3}H]NMS occupied receptor in a single step has also been used. Equation **(5)** was modified by substituting K(= k_{offobs}) by:

$$\frac{k_{-1}}{(1 + Kocc[X])} \qquad \textbf{(6)}$$

The equation introduced in GraphPad Prism was:

$$\mathrm{Y} = \mathrm{Span} \times \exp\left(\frac{-\mathrm{t} \times \mathrm{k}_{-1}}{(1 + 10\text{^}(\log\mathrm{Kocc} + \mathrm{X}))}\right) \qquad \textbf{(7)}$$

The specific binding of the radioligand at t=0 is Bo (Span) and this decays during dissociation to a value at time t with a rate constant which is slowed to zero by increasing concentrations of allosteric ligand X. k_{-1} is the dissociation rate constant of the radioligand in the absence of X. logKocc is the log affinity constant of the allosteric

ligand for the occupied receptor. This equation can also be used to directly estimate logKocc even when Span is not known ASSUMING that X binds according to the law of mass action and totally inhibits radioligand dissociation when it is bound to the ternary complex.

Equilibrium radioligand binding assays in presence of an allosteric modulator:

The equation introduced in GraphPad Prism describing the binding of radioligand in the presence of allosteric agent was:

$$Y = \frac{BoundLo \times (1 + 10\text{^}(\log K_L + \log L)) \times (1 + 10\text{^}(\log Kocc + X))}{(1 + 10\text{^}(\log K_X + X) + 10\text{^}(\log K_L + \log L) \times (1 + 10\text{^}(\log Kocc + X)))} \quad \textbf{(8)}$$

where logL is log[radioligand] e.g -9 for 1 nM, could be a variable ; $\log K_L$ is the log affinity of the radioligand ;X is the log concentration of the allosteric ligand, X, log affinity $\log K_X$; BoundLo is the bound radioligand in absence of any radioligand in dpm ;logKocc is the affinity of X for the L-occupied receptor and, by the allosteric ternary complex model, should be the same as that obtained in the off-rate assay. The cooperativity between X and L is given by Kocc/Kx.

Estimation of the cooperativity between an agent and both [^{3}H]NMS and unlabeled ACh and the affinity of the agent for the receptor.

The equation introduced into the GraphPad Prism for the binding of radioligand in the presence of competitor and allosteric agent was:

$$Y = \frac{BoundLo \times (1 + 10\text{^}(\log K_L + \log L)) \times (1 + 10\text{^}(\log Kocc + A))}{(1 + 10\text{^}(\log K_A + A) + 10\text{^}(\log K_X + X) \times (1 + bet \times 10\text{^}(\log K_A + A)) + 10\text{^}(\log K_L + \log L) \times (1 + 10\text{^}(\log Kocc + A)))} \quad \textbf{(9)}$$

This equation could be used even when the allosteric ligand only has a small effect on both the radioligand and orthosteric ligand binding. In such situations the affinity of the allosteric ligand for the [^{3}H]NMS occupied receptor might have to be fixed at Kocc (from off rate - alph*K_A) in order to get estimates of alpha and beta. The log concentration of allosteric ligand was on the header of each column of data; logL is log[radioligand] e.g -9 for 1 nM; $\log K_L$ is the log affinity of the radioligand; A is the allosteric ligand, log concentration logA (column title), log affinity $\log K_A$ and logKocc

at the unliganded and radioligand occupied receptor respectively; logX is the log concentration of the competing orthosteric ligand, X , log affinity $\log K_X$; BoundLo is the bound radioligand in absence of any radioligand in dpm ;bet is the cooperativity between X and A

Functional assays

The equation used in GraphPad Prism describing the functional effect of an agonist alone is similar to the equation **(3)** but with the difference that Y is response, X is the logarithm of the agonist concentration and EC50 is the midpoint of the curve which is the inverse of the apparent potency. Y starts at the Bottom and goes to the Top with a sigmoid shape. HillSlope is now the slope factor which normally was constrained to 1 as the dose-response curves gave slope factors not significantly different from unity.

The equation used in GraphPad Prism describing the functional effect in presence of an allosteric ligand:

$$Y = Basal + \frac{\left(E\max - basal\right)}{\left(\frac{1+\left(10\text{^}\left(\log EC50 - X\right)\right)\times\left(1+10\text{^}\left(\log K_A + \log A\right)\right)}{\left(1+bet\times 10\text{^}\left(\log K_A + \log A\right)\right)^n}\right)} \qquad \textbf{(10)}$$

analyses functional data where X is the concentration of agonist and interacts allosterically with A with a cooperativity factor bet; this model assumes that A does not affect the Emax of A; logEC50 is the log potency of the agonist in the absence of A.

For statistical analysis of differences between parameters, in general, paired or unpaired t-tests, and one way ANOVA were used as appropriate. Data are expressed as mean±SEM(n). When n=2, the error is denoted by range/2.

2.2.9 Modelling programs

The three dimensional images of the human M_1 muscarinic, the rat M_3 muscarinic and the human β_2 adrenergic receptors structures were constructed using PyMol (DeLano Scientific LLC) by introducing the coordinates from protein data bank (PDB) kindly provided by Ed Hulme (NIMR) and Jürgen Wess (NIH) for the M_1 and M_3 receptors respectively. The β_2 adrenergic receptor coordinates were obtained from the PDB (2RH1).

Chapter 3. Choice of the M_3 mutants and the characterization of their interactions with orthosteric ligands

The majority of studies on Family A (rhodopsin-like) GPCRs have focused on ligand binding in the TM regions. Less is known about the role of the extracellular regions. The discovery of allosteric ligands that use the extracellular loops of the muscarinic receptors to mediate their effects has provided a good reason to further investigate the role of muscarinic receptors extracellular loops in drug actions. Moreover this region is less conserved among the five subtypes than the TM domains, giving an opportunity to find a role for it in drug selectivity.

3.1 Sequence alignment of muscarinic receptor subtypes and the choice of M_3 mutants

The sequences of the three extracellular loops of the five muscarinic receptors have been aligned in order to identify non conserved residues in this region which could have a potential subtype selectivity role. The alignment of the first and third extracellular loop is shown in Fig 3.1 and 3.2.

Fig.3.1: Alignment of the first extracellular loop sequences of the five muscarinic subtypes and some related GPCRs

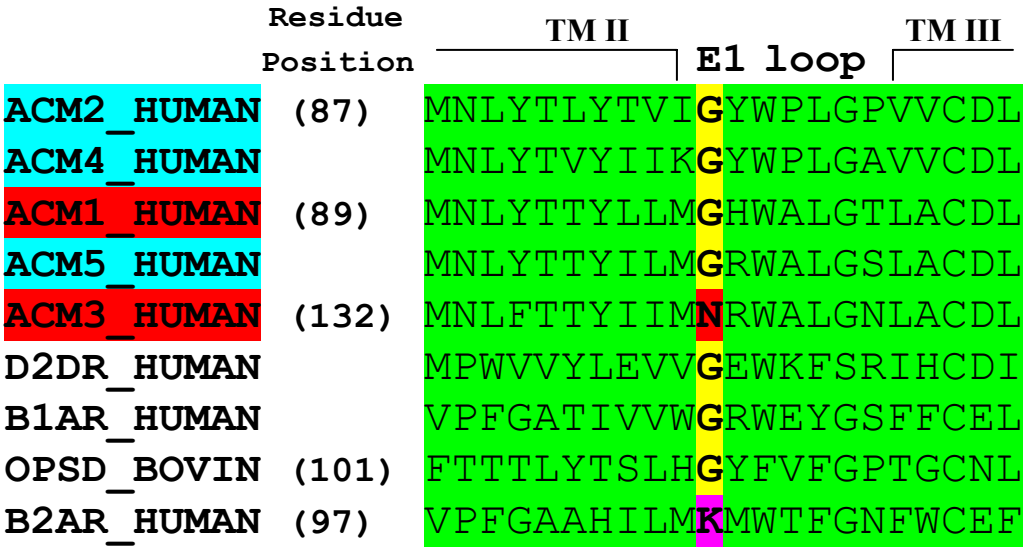

Some other prototypical members of the Family A of GPCRs, like human D_2 dopamine receptor (D2DR), human beta 1 adrenergic receptor (B1AR), bovine rhodopsin receptor (OPSD) and beta 2 adrenergic receptor (B2AR) are included in the alignment.

In Fig 3.1 we have highlighted the position of the first extracellular loop sequences, which corresponds to the position 132 in M_3 human receptor. It is worth noting that in all muscarinic subtypes, there is a glycine, except for the M_3 subtype, which contains an asparagine. Three of the other GPCRs shown in the figure also contain a glycine, including rhodopsin. Therefore we decided to mutate this asparagine to the glycine that the rest of muscarinic subtypes contain in order to test the possible effect of this residue in generating M_3 subtype selectivity.

Fig.3.2: Alignment of the third extracellular loop sequences of the five muscarinic subtypes and some related GPCRs

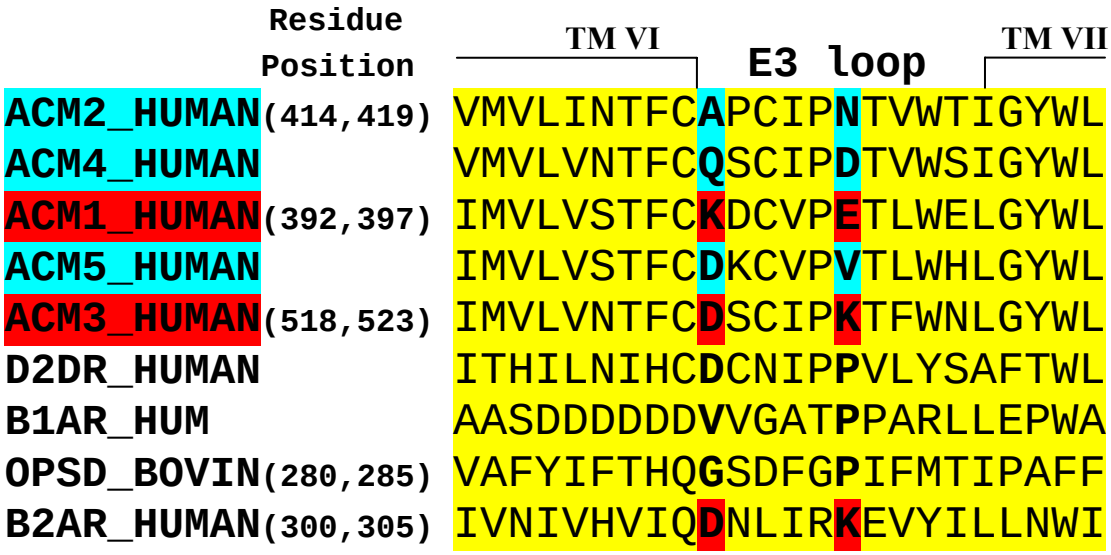

In the alignment of the sequences of the third extracellular loop there are two highlighted positions in Fig 3.2 (corresponding to residues 518 and 523 of the M_3 human subtype). In each position all the residues within the five subtypes are different from each other. Furthermore, the residues of M_3 are charged, one **negatively**, Asp^{518} (D) and the other **positively**, Lys^{523} (K). In the same position at the M_1 subtype, there are also charged residues but they are reversed. Therefore we decided to change the residues of the M_3 receptor to the reversed residues corresponding to the M_1 subtype. We also made the neutral mutant to study the effect of the charges. It is worth noting

that the corresponding residues in the recent crystal structure of the beta 2 adrenergic receptor are the same as those in M_3 subtype. This is important because if a selective role is found for those residues at the M_3 receptor, it can be similar in the beta 2 adrenergic receptor. However, allosteric ligands for this last receptor are not known. A summary of the mutants constructed is shown in Table 3.1

Table 3.1: Mutants constructed on the M_3 muscarinic receptor at the extracellular loops

	Mutants receptors	Subtype residue substitution	Charges on residues in E3 loop 518	523
	M_3 WT		-	+
	M_1 WT		+	-
E3 loop	K523E	$M_3 \rightarrow M_1$	-	-
	D518K	$M_3 \rightarrow M_1$	+	+
	K523Q		-	0
	D518N		0	+
E1 loop	N132G	M_3→all other subtypes		

The residues selected are specific for each muscarinic receptor subtype. Moreover they are large and **charged amino acids** being more likely to affect the allosteric ligand binding to the receptor by ionic interactions. Interestingly, the common allosteric binding site is believed to be situated over the cleft of the orthosteric site and it may represent an access route for agonists and antagonists. Some acidic amino acid of the E2 loop and E3 loop are involved in the allosteric interactions of modulators (Leppik et al., 1994;Gnagey et al., 1999;Krejci and Tucek, 2001;Voigtländer et al., 2003), making these positions potentially important candidates contributing to the allosteric binding site.

The effects of the mutations on the binding of orthosteric ligands such as ACh and NMS, relative to M_3 WT receptor is described in subsequent sections. It is necessary to perform these initial studies to be sure that mutations are not affecting the main structure of the receptor and the orthosteric site.

The choice of buffers for binding studies often depends on the receptor subtype and the specific purpose of the experiment. In general is difficult to stimulate genuinely physiological conditions using membrane preparations in vitro, for the simple reason that, because of their vectorial insertion in the cell-surface membrane, the extracellular and the intracellular surfaces of receptors are exposed to different ionic conditions. It may be possible to remedy this defect in reconstitution system in which receptors are inserted into phospholipid vesicles. Studies on whole cells are generally complicated by processes occurring inside of them as internalisation, phosphorylation, etc. However these problems are often circumvented by using low temperatures.

For the study of ligand binding, the use of simple buffers usually suffices. The choice is dictated by the desired pH. For studies around neutral pH, Hepes, phosphate, or Tris buffers are often used in the concentration range, 5-50 mM. The "Good" buffers (Hepes, Mes, Pipes,etc.) seem, generally, to be fairly innocuous for receptor binding studies. These buffers can be supplemented with the salts of monovalent cations (NaCl, KCl) to produce the desired ionic strength. Because receptor-specific ligands are almost invariable charged, ionic strength often exerts a strong effect on the effective affinity constant of the receptor-ligand interactions, through the screening of charge-charge interaction. High ionic strength will also promote hydrophobic interactions. Variations on the pH within the physiological range can produce large effects on receptor-ligand interactions. These can be due either effect on the ionization of groups within the receptor's ligand binding site or on a group which affects receptor-effector interactions, which may be on the receptor itself, or on the effector if these are separate entities, as in the case of G-protein coupled receptors. Alternatively, the protonation or ionization of groups on the ligand may change with pH and affect its interaction with the receptor. Such pH-dependent effects may influence both the equilibrium binding constant and the kinetic rate constants of binding. The interplay of these effects can be very complex.

The binding properties of the orthosteric ligands for the mutants, relative to M_3 WT, have been studied in different buffers. This was thought to be useful to expose or amplify differences found in the binding properties of the mutants from those of the WT receptors and allows us to compare the results found with those in the literature. The ligands used were NMS, atropine, ACh and a number of putative M_3 selective antagonists that are being used clinically or have been designed to treat the overactive bladder.

3.2 Effects of the mutations on the binding of the radioligand, [^{3}H]NMS

3.2.1 Initial studies of the effects of the mutations on the affinity of [^{3}H]NMS. [Tris buffer]

The initial characterization of the constructions of FlpInCHO_M_3 and mutants was carried out in saturation binding assays where different concentrations of a radiolabelled ligand were added to a fixed concentration of membranes. In this study, the radiolabelled ligand chosen was the muscarinic antagonist, [^{3}H]-N-methyl-scopolamine [^{3}H]NMS.

One of the reasons for choosing it was because in general its binding is simple. Antagonists generally bind with the same affinity to all states of the receptors, unlike agonists which have different affinity for the receptor when bound to G protein, thus making the analysis of the binding more complex. In addition, it has relatively fast kinetics and high affinity, and a good ratio between specific to non-specific binding. Furthermore, it has a comparable affinity for all the subtypes.

The experiments were carried out initially in a buffer composed of 50 mM Tris, 3 mM $MgCl_2$ and 0.2 mM EGTA, at a temperature of 37 ºC for 2 hours. This buffer, together with the conditions, will be named 'Tris buffer' from now on. The reason for the choice of this buffer was that the laboratory of Prof. Christopoulos in Australia (where the constructions were made) was using it as one of their incubation binding buffers. The non-specific (NSB) binding was measured using a high concentration (10μM) of the non-labelled specific muscarinic antagonist, atropine, to prevent the binding of the [^{3}H]NMS to the receptors.

In Figure 3.3.A a representative saturation curve of the M_3 WT with increasing concentrations of [^{3}H]NMS is shown. The total binding curve increases progressively as the concentration of radioligand increases. The non-specific binding is a straight line showing a linear increase with concentration of [^{3}H]NMS. The higher the non-specific binding, the higher is the background noise and this is one parameter which determines the choice of concentration of radioligand to be used in the assay. The specific binding

shows the real presence and number of receptors that exist in the membrane preparation tested, with the binding being saturable at high concentrations of [^{3}H]NMS. The K_{NMS} and Bmax parameters are obtained by fitting the data to the equation (described in *Material and Methods*) using non linear regression. The concentration of free [^{3}H]NMS is shown on the x-axis in Figure 3.3.A as that is the parameter used in the equation formulated to analyse the data. If only a small fraction of radioligand binds the receptor, the free concentration is essentially identical to the concentration added and the total concentration may be used in the analysis. If this does not occur, ligand depletion is occurring and an incorrect estimate of the affinity constant will be obtained if total [^{3}H]NMS total is used instead of free [^{3}H]NMS. This type of graph is a very common way of representing the data for saturation assays as it illustrates saturability. There is an alternative mode of representing the data which clearly depicts the whole nature of the binding process. This uses a logarithmic scale to represent the concentration of free [^{3}H]NMS (figure 3.3.B) and allows large range of concentrations, over 300 fold (10pM-3nM), to be represented.

The radiolabelled antagonist [^{3}H]NMS bound specifically and saturably to CHO cell membranes expressing either M_3 or M_1 muscarinic receptors. [^{3}H]NMS bound to M_3 WT and M_1 WT membranes with a log affinity constant (Log K_{NMS}) of 9.65±0.04 and 10.16±0.07 respectively. The maximum binding capacities (Bmax) of the M_3 and M_1 preparations were 2552±115 and 511±151 fmol/mg protein respectively (n=6, n=2). In Figure 3.4, [^{3}H]NMS saturation curves at M_1 WT and the mutated M_3 receptors are illustrated. The logarithm of the affinity constants of [^{3}H]NMS for the mutated receptors did not significantly differ between constructs or from M_3 WT receptors (Table 3.2).

Fig.3.3: Representative [^{3}H]NMS saturation curve at the M_3 WT

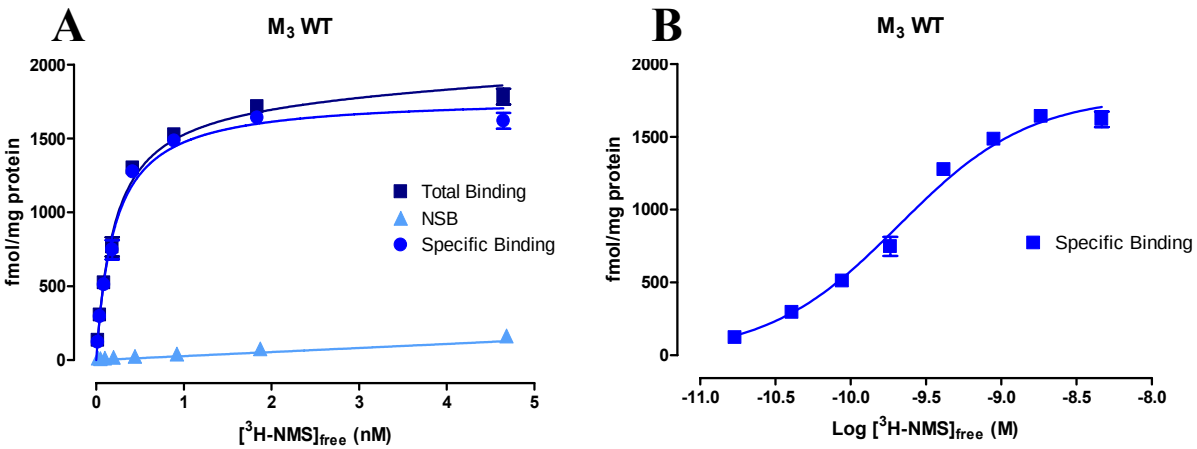

Figure 3.3: [^{3}H]NMS saturation binding assays were performed on a membrane preparation of M_3 receptors stably expressed in CHO cells, in Tris buffer at 37ºC for 2 hours. The protein concentration used was 10 µg/mL.

A: represents total, non-specific (NSB) and specific binding expressed in fmol/mg protein plotted against increasing free concentration of [^{3}H]NMS. The curves through the data points are the nonlinear least squares fit to the data.

B: The same data for specific binding as in Figure 3.1.A are plotted using Log free [^{3}H]NMS as abscissa. The curve through the data points is the nonlinear least squares fit to the data and shows an excellent fit between the predicted and observed values of the bound radioligand over the whole 300 fold range of [^{3}H]NMS concentrations used.

In this experiment the log K_{NMS} was 9.68±0.02 and Bmax 1781±38.

Fig.3.4: [^{3}H]NMS saturation curves at M_1 WT receptors and the mutated M_3 receptors

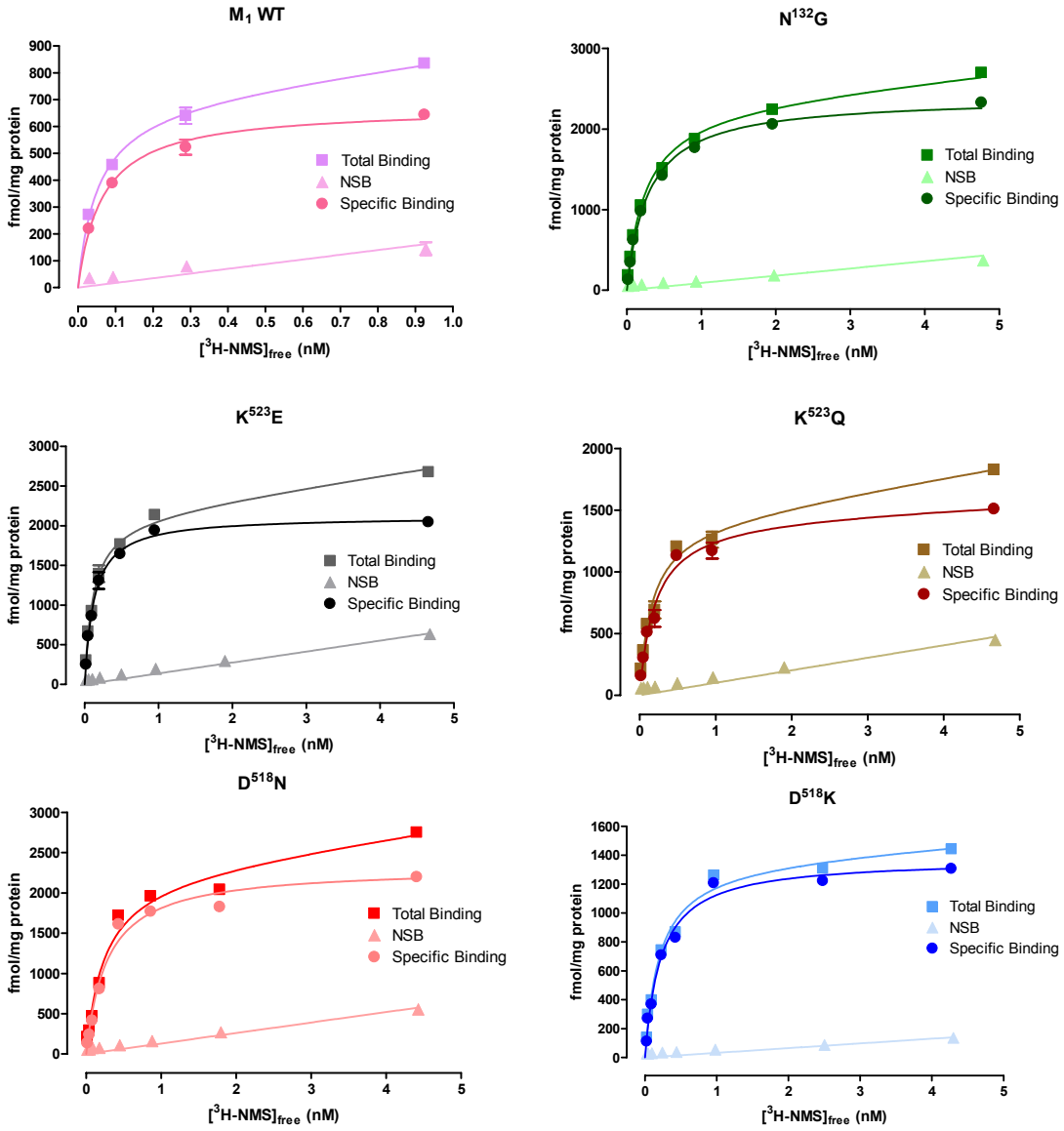

Figure 3.4: Representative [^{3}H]NMS saturation binding curves for M_1 WT and mutated M_3 receptors stably expressed in CHO cells. The membranes were incubated with increasing concentration of [^{3}H]NMS in Tris buffer at 37ºC for 2 hours. The protein concentration used was ca 10 µg/mL. The total, specific and non-specific binding (NSB) is expressed in fmol/mg protein. The curves represent the non-linear squares fits to the experimental data.

Table 3.2: The log affinity constants of [^{3}H]NMS at M_3, M_1, and the mutated M_3 receptors in Tris buffer

	[^{3}H]-N-Methyl Scopolamine		
Receptor	**Log K_{NMS}**	**B_{max} (fmol/mg protein)**	**n**
Wild Type M_3	9.65±0.04	2552±115	3
Wild Type M_1	10.16±0.07	511±151	2
$K^{523}E$ mutant	9.76±0.09	2404±284	4
$K^{523}Q$ mutant	9.77±0.07	1603±84	5
$N^{132}G$ mutant	9.72±0.07	2814±419	5
$D^{518}N$ mutant	9.67±0.07	2291±421	2
$D^{518}K$ mutant	9.60±0.06	1066±167	2

Table 3.2: [^{3}H]NMS binding properties of wild type M_3, M_1 and mutant M_3 muscarinic receptors stably expressed in CHO cells. The affinity constants are shown as the log values ± standard error

3.2.2 Initial studies of the effects of the mutations on the dissociation rate of [^{3}H]NMS. [Tris buffer]

Among the experiments to establish in the experimental characterization of a receptor-ligand interaction, there should be studies of the kinetics of its binding to the orthosteric or allosteric site on the receptor. These are exponential processes if the binding is simple. The actual rate constants that govern the ligand association (k_{+1}) and dissociation (k_{-1}) can be determined experimentally from kinetic experiments that measure radioligand binding as a function of time. They are very sensitive indicators of the interaction of the ligand with a particular conformation of the receptor.

An additional aim of these studies was to estimate the half-life of the radioligand binding in order to establish the incubation time needed in subsequent experiments to ensure binding is in equilibrium. A further objective of these assays was to compare the rate of the dissociation of the radioligand [^{3}H]NMS from the M_3 WT with those of the mutants, in order to investigate the possible involvement of the mutated amino acids in this process.

The dissociation of L* from the receptor-ligand complex can be studied by pre-incubation of the receptor with L* until some chosen level of binding has been achieved, followed by the prevention of its rebinding by adding, at different times, a concentration of unlabelled competitive ligand sufficient to saturate all the receptors. This effective reduction of association rate of L* to zero will cause only the dissociation of L* to be observed. As the only ligand measured is that of L* bound to the receptor, which decreases over time, this decrease provides the quantification of the rate of dissociation of L* from the receptor.

The reaction that describes the L*R complex dissociating to generate L* and R is determined by the concentration of the complex of L*R and the magnitude of the reverse rate constant (k_{-1}). This constant is expressed in units of time^{-1}. The half time of the dissociation ($0.69/k_{-1}$) is independent of the initial value of L*R. This is because the exponent which governs the rate of breakdown depends only on k_{-1}.

To investigate the time course of the [^{3}H]NMS dissociation, initial studies were designed using a reverse time protocol as described in Material and Methods. In order to prevent the reassociation of the radioligand, 10 μM atropine was added at different time points, over a one hour time period (0, 3, 5, 10, 20, 40 and 60 min).

Representative dissociation curves of [^{3}H]NMS from the WT receptor and the mutants, are shown in Figure 3.5. The results are summarized in Table 3.3. All the experiments were performed on membranes from CHO cells stably expressing the M_3 WT receptor or the mutants in Tris buffer at 37ºC. All data, without exception, were analysed and fitted well to a single exponential model of dissociation. The mean rate of dissociation of [^{3}H]NMS from M_3_wt was 0.032±0.002 min^{-1}, which equates to a mean half-life of dissociation of 22 minutes, i.e, the time that the radioligand needs to dissociate from 50 % of the receptors. This is a very useful parameter, as 5 times its value indicates the time that the receptor needs to be incubated with the radioligand to reach >97% of the true equilibrium value. For example, at M_3 WT, (5x22 mins= ca 2h) and therefore this is the optimal incubation time for equilibrium assays on this receptor under these conditions.

For the mutated receptors, small changes in dissociation compared to wild type, were detected (Table 3.3). The largest difference in the dissociation rate of the [^{3}H]NMS was seen for the mutant K523E, k_{-1}= 0.062±0.016 min^{-1}($t_{1/2}$= 11 min), which is 2 fold faster than the WT receptor. For the N132G mutant, k_{-1}= 0.021±0.001 min^{-1}($t_{1/2}$= 33 min) which is significantly slower than WT. However, in subsequent experiments, this difference was not observed. There is no explanation for this discrepancy except that these data are only from two experiments. The remainder of the mutants had similar off-rates to M_3 WT.

Fig.3.5: Full time course curves for the dissociation of [^{3}H]NMS from M_3 WT membranes and the mutated M_3 receptors [Tris buffer]

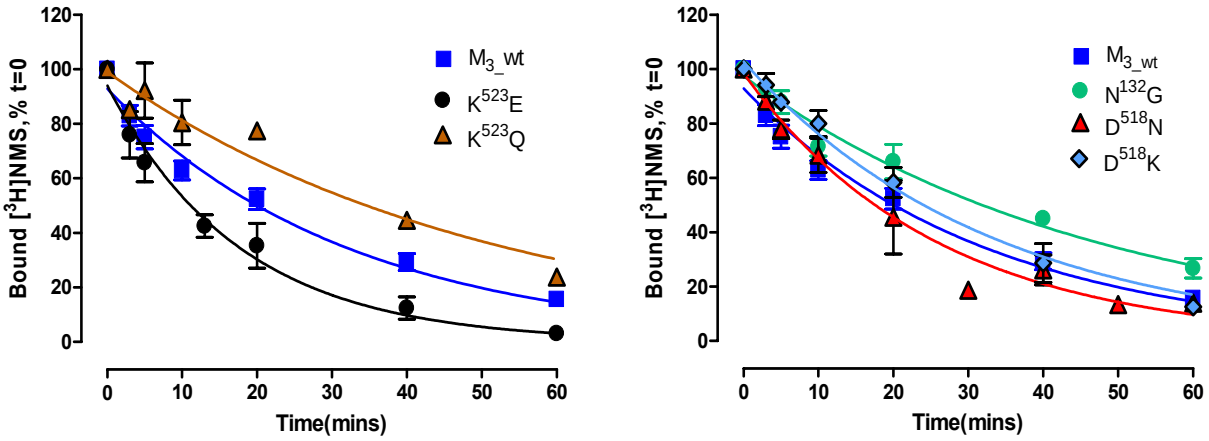

Fig.3.5: Representative full time course curves of the dissociation of [^{3}H]NMS from M_3_wt and the mutant receptors. All the dissociation experiments were performed at 37ºC in Tris Buffer.

Table 3.3: The dissociation rate constants of [^{3}H]NMS from M_3, M_1 WT and the mutated M_3 receptors [Tris buffer].

	[^{3}H]-N-Methyl Scopolamine		
Receptor	**k_{-1}**	**$T_{1/2}$ (min)**	**n**
Wild Type M_3	**0.032±0.002**	**22**	**9**
Wild Type M_1	**0.076±0.008**	**9**	**2**
$K^{523}E$ mutant	**0.062±0.016***	**11**	**4**
$K^{523}Q$ mutant	**0.033±0.009**	**21**	**4**
$N^{132}G$ mutant	**0.021±0.001***	**33**	**2**
$D^{518}N$ mutant	**0.038±0.004**	**18**	**3**
$D^{518}K$ mutant	**0.026±0.008**	**27**	**3**

Table 3.3.: Dissociation rate constants of [^{3}H]NMS obtained by full time course assays performed in Tris buffer. Values are shown as mean ± standard error.

* Significantly different from WT M_3 values ($p<0.05$, 2 tailed t-test)

3.2.3 Influence of different incubation conditions on [^{3}H]NMS affinity and kinetics at M_3 and M_1 receptors

The previous experiments were carried out in one buffer system, Tris buffer at 37ºC. However, it is known that the affinity constants of ligands are sensitive to the nature of the buffer (Birdsall et al., 1979). In addition, it was previously shown that, for some antagonists, the lowering of ionic strength (Barlow et al., 1979) and temperature (Waelbroeck et al., 1989) of the incubation increases their affinity for the muscarinic receptors in rat cerebral cortex.

Furthermore, there is a considerable variety of incubation conditions and little consensus between laboratories in their choice. In order to study in outline the influence of ionic composition and temperature on the affinity and kinetics of [^{3}H]NMS at M_3 and M_1 receptors, we decided to employ three different incubation conditions, chosen because they were quite different from each other and they have been used extensively by a number of major laboratories in the field. In subsequent discussion, these conditions will be referred to as 'Tris', 'Hepes' and 'PB':

1. Tris buffer, 37ºC (Tris): 50 mM Tris, 3 mM $MgCl_2$ and 0.2 mM EGTA, pH 7.4. This was used for the initial studies in the laboratory of Dr. Arthur Christopoulos in Australia.
2. Hepes buffer, 30ºC (Hepes): 100 mM NaCl, 10 mM $MgCl_2$, 20 mM Hepes, pH 7.4: A simplified, close to isotonic, buffer in which GTPγ^{35}S studies of GPCR activation, can also be measured. The antagonist affinity constants measured in this buffer are close to those measured in functional studies. The temperature was 30ºC as the receptors are more stable than at 37ºC. These conditions were developed and have been used for many years in the Dr. Nigel Birdsall laboratory, where I performed the main body of my experiments.
3. Phosphate Buffer (PB): 5 mM, pH 7.4. Hypotonic buffer, room temperature (20-24ºC): These conditions are used in the laboratories of the Dr. John Ellis (Penn State University College of Medicine, USA) and Prof. Klaus Mohr and Dr. Christian Tränkle (Univ. of Bonn) and have been used extensively in the determination of the affinities of allosteric ligands, especially gallamine, in dissociation kinetics experiments (Ellis et al., 1991; Waelbroeck, 1994; Tränkle et al., 1996).

The idea is that we could investigate the effects of the mutations under a variety of conditions that could both maximise differences in the observed affinities and rates and also allow comparison with literature values for different allosteric and orthosteric ligands. This study is novel as there has been, to our knowledge, no side by side investigation of the effects of buffer on the affinities and cooperativities of a range of allosteric ligands at mutated muscarinic receptors.

Here, we describe the binding properties of muscarinic receptors in three different conditions, basically when membrane-bound receptors are perturbed by changes in ionic strength and temperature. We can observe whether the structure-binding relationships for the receptors can be altered such that drug selectivity or dissociation rate constants are considerably enhanced or attenuated.

Table 3.4 shows the [^{3}H]NMS affinities for M_1 and M_3 receptors under the different conditions. The log affinity of NMS for the M_3 WT receptor in Tris Buffer is 9.65±0.04. This was unchanged in Hepes buffer but in PB buffer the affinity increased ca 5 fold to 10.31±0.20. A similar behaviour was found for M_1 WT receptors, where the log affinity of NMS for the receptor is not changed much between Tris and Hepes buffer (10.16±0.07 versus 9.98±0.02 respectively) but is significantly higher (3-5 fold) in PB buffer. Comparing the two wt receptors, it is worth noting that the affinity of NMS was always 2-3 fold higher at M_1 than at M_3, independent of the buffer used.

Regarding the number of receptors expressed in the membranes (the Bmax parameter), there is a large range of values caused by using different membrane preparations from the same receptor. The range of the data obtained is shown in the table 3.4. It seems possible that the Bmax is higher in PB buffer than in the rest of buffers, Tris being the one which has a lower Bmax but no explicit experiments were carried out to detect Bmax changes between assays in different buffers. This may be difficult to carry out as the filters may not retain the same % of membranes in the different buffers. There is no reason to expect differences in Bmax values under the different conditions.

Full time course experiments of radioligand dissociation where the half-life is obtained, have been described previously in section 3.2.2. For subsequent experiments the extent of dissociation at only one time point was measured and a one time-point estimate of k_{-1}

determined. This method and its analysis are described in Material and Methods. The initial criterion for deciding the time-point for the incubation was ca 2.5 times the estimated half-life. Under these conditions ca 20 % binding will remain and this is appropriate to give an accurate estimate of k_{-1}. For example for M_3 WT receptors in Tris Buffer at 37ºC where the half-life is 22 min, the incubation time chosen was ca 55 min. For much longer incubation times the specific [^{3}H]NMS binding will be lower and close to the NSB. Hence the larger errors in the estimate of the specific binding will tend to give larger errors in the estimate of k_{-1}.

To have an initial idea of the $t_{1/2}$ values in Hepes and PB buffer of [^{3}H]NMS at M_3 and M_1 receptors, we looked at the literature values. The half-life in Hepes of M_3 and M_1 are reported to be 10 and 9 min respectively (Lazareno and Birdsall, 1995) and in PB buffer, 35 and 22 min respectively (Gnagey et al., 1999). This enabled us to set the dissociation time point at ca 25 min in Hepes and 90 and 55 min in PB.

The dissociation rate constants for [^{3}H]NMS at M_1 and M_3 receptors for the different conditions are shown in Table 3.5. For M_3 receptors the fastest dissociation rate was observed in Hepes buffer (0.071±0.004 min^{-1}) and was significantly slower in PB buffer (0.028±0.002 min^{-1}). At M_1 receptors the fastest dissociation rate constant was observed in Tris buffer (0.076±0.008 min^{-1}), and the slowest again in PB buffer (0.032±0.001 min^{-1}).

Table 3.4: The affinity constants of [^{3}H]NMS at M_1 and M_3 receptors under different incubation conditions

	[^{3}H]-N-Methyl Scopolamine			
Buffer	**Log K_{NMS}**		**B_{max} (fmol/mg protein)**	
	Wild Type M_3	**Wild Type M_1**	**Wild Type M_3**	**Wild Type M_1**
Tris	**9.65±0.04 (5)**	**10.16±0.07 (2)**	**1490-1540(4)**	**360-660(2)**
Hepes	**9.70±0.06 (6)**	**9.98±0.02 (2)**	**1250-3370(4)**	**215-510(2)**
PB	**10.31±0.20 (4)**	**10.66±0.01 (2)**	**3620-4370(3)**	**1220-1270(2)**

Table 3.4: Log affinity constants of [^{3}H]NMS at wild type M_3, M_1 receptors stably expressed in CHO cells under three different incubation conditions. The ranges of the Bmax values (fmol/mg protein) are also shown. Values are shown as mean ± standard error (n)

Table 3.5: The dissociation rate constants of [^{3}H]NMS from M_1 and M_3 receptors under different incubation conditions

	[^{3}H]-N-Methyl Scopolamine			
Buffer	**k_{-1}**		**$t_{1/2}$ (min) Half Life**	
	Wild Type M_3	**Wild Type M_1**	**Wild Type M_3**	**WildType M_1**
Tris	**0.045±0.006 (7)**	**0.076±0.008 (2)**	**15**	**9**
Hepes	**0.071±0.004 (6)**	**0.061±0.006 (2)**	**10**	**11**
PB	**0.028±0.002 (7)**	**0.032±0.001 (2)**	**25**	**22**

Table 3.5: Dissociation rate constants of [^{3}H]NMS obtained from one time-point assays. The k_{-1} for M_3 in Hepes was significantly faster than that in Tris or PB ($p<0.01$, $p<0.001$ respectively). The value in Tris was also significantly different from that found in PB ($p<0.05$). At M_1, the k_{-1} in PB was significantly slower than in Tris or Hepes ($p<0.05$). Values are shown as mean ± standard error (n)

3.2.4 Effect of the mutations on [^{3}H]NMS affinity and its kinetics under different incubation conditions

Knowing the affinity and kinetic constants of [^{3}H]NMS at both M_3 and M_1 receptors under the different conditions, it was then possible to compare these values with those for the mutant receptors under three conditions in order to maximise the potential to observe differences in the parameters.

At this point in my studies, given the lack of time and the use of three different conditions that increase the number of experiments, we decided to select only three mutants out of the five for this investigation. K523E was selected as it was the mutant that had shown a large difference in the rate of dissociation of [^{3}H]NMS in Tris buffer. K523Q, was selected to allow us to compare the possible involvement of the charge in explaining this difference and to investigate whether any difference is amplified or attenuated in the different buffers. N132G is a potential selectivity mutation as the asparagine at that position is unique to the M_3 subtype of muscarinic receptor. Binding experiments equivalent to those previously described for the wild type receptors were performed on the mutants.

There were no significant changes in affinity constants between the mutants and M_3 WT regardless of the buffer used. In PB buffer [^{3}H]NMS had the highest affinity ($p<0.01$) in all the cases, compared to Tris and Hepes buffer, with the latter two buffers yielding very similar affinity constants (Table 3.6).

Regarding the number of receptors measured on the membranes (Bmax Table 3.7), there are large differences in these values resulting from very different dates on which the experiments were performed and different membrane preparations being used, so that only the range of Bmax values are shown. In contrast to the data for the WT receptors, there was no suggestion that the Bmax values were higher in PB buffer.

One point kinetic curves for the M_3 WT and the three mutants selected in Hepes and PB buffer are illustrated in Figure 3.6. The mutants show the same pattern as the WT receptor regarding the influence of the incubation conditions on the k_{-1}. So the

incubation buffer affects equally the k_{-1} values of the wild type receptors and the mutants. With respect the dissociation rate constants, the k_{-1} of K523E was 2.0-2.7 fold faster compared to the wild type receptors in all the buffers. This is illustrated in Figure 3.7 for a comparison of Hepes and PB buffers. This is the example of the most prominent differences found in this kind of assay. M_3 WT and K523E mutant in Hepes and PB buffer were chosen as they showed the greatest difference of dissociation rate constants. The M_3 WT in PB buffer was the slowest, with a half-life of 25 min. On the other hand, the half-life for K523E in the same buffer condition was only 9 min. In Hepes buffer, [^{3}H]NMS dissociation was even faster from K523E with a half-life of 4 min compared to 10 min for the M_3 WT receptor. It is noteworthy that the mutant K523Q also showed an increase in the dissociation rate constant relative to the M_3 WT (1.5-1.9 times faster, depending on the buffer used) (Table 3.8).

A summary of the ratio of dissociation rate constants between mutants and M_3 and M_1 WT phenotypes under different conditions is given in table 3.9. Looking solely at the ratios in Tris buffer, one can conclude that the k_{-1} values of M_1 and M_3 are different and that the mutated M_3 receptors, K523E and K523Q, have reached the k_{-1} of the M_1 phenotype in that buffer. However, in both Hepes and PB buffer, the k_{-1} values at M_3 and M_1 are similar to each other, whereas the mutations K523E and K523Q are different from M_3 or M_1. Because we have looked at three buffers, we can conclude that K523E or K523Q do not have the M_1 phenotype with the concordance of the k_{-1} values in Tris being serendipitous.

Table 3.6: Log affinity constants of [^{3}H]NMS at M_3 and M_1 WT receptors and mutated M_3 receptors under different incubation conditions

Receptor	[^{3}H]-N-Methyl Scopolamine		
	Log K_{NMS}		
	Tris Buffer	Hepes Buffer	PB Buffer
Wild Type M_3	9.65±0.04 (4)	9.70±0.06 (6)	10.31±0.20 (4)
$K^{523}E$ mutant	9.76±0.09 (4)	9.62±0.07 (4)	10.29±0.21 (3)
$K^{523}Q$ mutant	9.77±0.07 (5)	9.71±0.07 (4)	10.34±0.07 (3)
$N^{132}G$ mutant	9.72±0.07 (5)	9.71±0.04 (4)	10.38±0.18 (2)
Wild Type M_1	10.16±0.07 (2)	9.98±0.02 (2)	10.65±0.01 (2)

Table 3.6: Log affinity constants of [^{3}H]NMS for wild type M_3, M_1 receptors and mutated M_3 receptors stably expressed in CHO cells under three different incubation conditions. The K_{NMS} values were significantly higher for all the constructs in PB buffer ($p<0.01$) than those in either Tris or Hepes. The [^{3}H]NMS affinity constants of the mutant receptors were not significantly different from M_3 WT. Values are shown as mean ± standard error (n)

Table 3.7: Bmax values of [^{3}H]NMS at M_3 and M_1 WT receptors and mutated M_3 receptors under different incubation conditions

Receptor	[^{3}H]-N-Methyl Scopolamine		
	B_{max}(fmol/mg protein)		
	Tris Buffer	Hepes Buffer	PB Buffer
Wild Type M_3	1040-3050(6)	1250-3370(4)	3620-4370(4)
$K^{523}E$ mutant	1450-2690(4)	1070-2370(4)	1260-2070(3)
$K^{523}Q$ mutant	1470-4060(5)	1080-2590(4)	1370-1980(3)
$N^{132}G$ mutant	2130-5110(5)	2325-3110(4)	1790-2330(2)
Wild Type M_1	360-660(2)	215-510(2)	1220-1270(2)

Table 3.7: Range of Bmax values for [^{3}H]NMS at M_3 and M_1 WT receptors and the mutated M_3 receptors stably expressed in CHO cells under three different conditions. The data represent values from 2-6 independent experiments.

Fig.3.6: Representative one point kinetic assay curves of the dissociation of [^{3}H]NMS from M_3 WT receptors and mutated M_3 receptors in two different conditions: Hepes and PB buffer

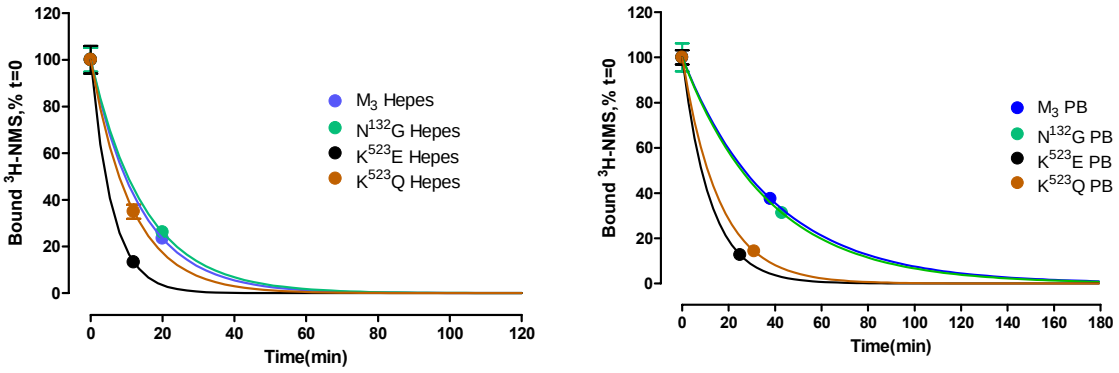

Figure 3.6: Dissociation rate curves of [^{3}H]NMS using only one time point (ca 2.5 dissociation half-lives for each construct). Each data point is the mean of duplicate estimates and representative of 2-7 experiments. The data were fitted using the one point kinetic equation described in *Material and Methods*. Note the difference in the scale of the x-axes

Fig.3.7: One point kinetic assay curves comparing the dissociation of [^{3}H]NMS from M_3 WT membranes and the mutant K^{523}E in Hepes and PB buffer

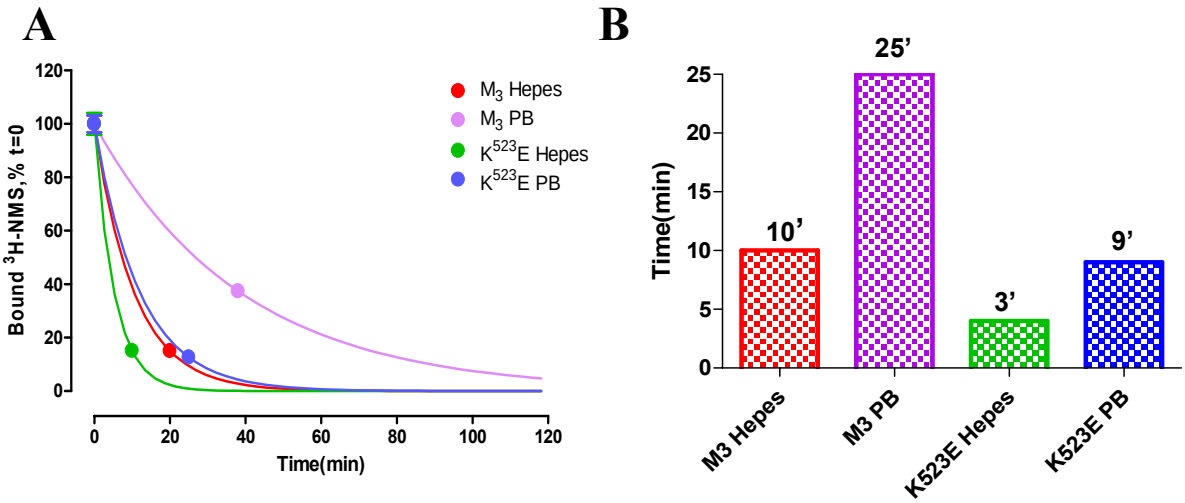

Figure 3.7: Dissociation rate curves of [^{3}H]NMS using only one time point (approximately 2.5 dissociation half-lives). Each data point is the mean of duplicate estimates and representative of 2-7 experiments. The data were fitted using the one point kinetic equation described in *Material and Methods*. In graph B the calculated half-lives (min) are illustrated

Table 3.8: The dissociation rate constants of [^{3}H]NMS from M_3 and M_1 WT receptors and mutated M_3 receptors under different incubation conditions

Receptor	[^{3}H]-N-Methyl Scopolamine		
	k_{-1} (min^{-1})		
	Tris Buffer	Hepes Buffer	PB Buffer
Wild Type M_3	0.045±0.006 (6)	0.071±0.004 (6)	0.028±0.002 (7)
$K^{523}E$ mutant	0.088±0.017 (4)	0.186±0.011 (7)	0.076±0.008 (6)
$K^{523}Q$ mutant	0.065±0.008 (7)	0.137±0.013 (7)	0.051±0.010 (5)
$N^{132}G$ mutant	0.042±0.009 (4)	0.072±0.004 (5)	0.030±0.002 (4)
Wild Type M_1	0.076±0.008 (2)	0.061±0.006 (2)	0.032±0.001 (2)

Table 3.8: Dissociation rate constants of [^{3}H]NMS obtained from one time-point assays performed in the three different incubation buffers. The k_{-1} for K523E compared to M_3 WT in Tris was significantly faster ($p<0.01$). This difference was even greater in Hepes and PB buffer ($p<0.001$). On the other hand, the k_{-1} of K523Q was faster than the k_{-1} of M_3 WT in Tris ($p<0.05$). This value was also significantly higher in Hepes and PB ($p<0.05$, $p<0.001$ respectively). The k_{-1} values of N132G were not significantly different from the value of M_3 WT. Values are shown as mean ± standard error (n)

Table 3.9: Ratios of dissociation rate constants between WT phenotypes and mutated M_3 receptors under different incubation conditions

Ratio	[^{3}H]-N-Methyl Scopolamine		
	Tris Buffer	Hepes Buffer	PB Buffer
$K^{523}E$/ M_3	2.0	2.6	2.7
$K^{523}Q$/ M_3	1.5	1.9	1.8
M_1/ M_3	1.7	0.9	1.2
$K^{523}E$/ M_1	1.2	2.9	2.5
$K^{523}Q$/ M_1	0.9	2.3	1.6

Table 3.9: Ratios were calculated using the data in Table 3.8 (above)

Given the fact that $K_{NMS} = k_{+1}/k_{-1,}$ estimates of the association rate constants (k_{+1}) for the wild type and mutants can be calculated using the data gained from dissociation and saturation assays. It is assumed that the binding and release of ligand are monophasic processes and that receptor isomerisation on binding ligand is not an issue. Table 3.10 shows the calculated k_{+1} values. The increase of the $k_{+1,}$ observed in PB buffer for all the constructs compared to the k_{+1} in Tris and Hepes, is compatible with the increase in [^{3}H]NMS affinity in PB buffer. Under this incubation condition, the antagonist [^{3}H]NMS is slower to dissociate from the receptor and faster to associate to the receptor than is observed either in Tris or Hepes. It is also worth noting that the k_{+1} at M_1 receptors is faster than that at M_3 receptors, the ratio being greatest (5 fold) in Tris.

Table 3.10: Calculated association rate constants of [^{3}H]NMS at the M_3 and M_1 WT receptors and the mutated M_3 receptors under different incubation conditions

Receptor	[^{3}H]-N-Methyl Scopolamine k_{+1} ($x10^8\ M^{-1}x\ min^{-1}$) [Calculated]		
	Tris Buffer	Hepes Buffer	PB Buffer
Wild Type M_3	2	4	6
$K^{523}E$ mutant	5	8	15
$K^{523}Q$ mutant	4	7	11
$N^{132}G$ mutant	2	4	7
Wild Type M_1	11	6	15

3.2.5 Discussion

This section (3.2) has described the characterization of the interactions of the well known antagonist and radioligand [^{3}H]NMS at M_3, M_1 receptors and the mutant receptors.

These initial studies and the results obtained are important in deciding the incubation conditions that need to be used in experiments described in subsequent chapters. The saturation experiments give us an indication of the appropriate concentration of radioligand [^{3}H]NMS to be used subsequent experiments. We will be using the concentration of [^{3}H]NMS which corresponds approximately to the K_D of the radioligand because there is a good ratio between specific and non-specific binding at that concentration, which would decrease if higher concentrations were used. The determination of the $t_{1/2}$ values is important in terms of deciding the incubation time for the kinetic experiments (ca 2.5 times the $t_{1/2}$) and the time necessary of the interaction of [^{3}H]NMS and the receptor to reach the equilibrium (5 times $t_{1/2}$).

During our initial studies at NIMR, we found a problem with the cells containing the FlpIn M_1 construct that was made in the lab in Australia. The properties looked unusual because the NMS affinity was much lower than expected in Hepes buffer, with log values in the range 9.3-9.6 (expected value ca 10.1) and the dissociation kinetics much faster, ca 0.25 min^{-1}, than those reported for M_1 receptors under the same conditions. We did side by side comparisons in the 3 buffer systems and found differences in the $logK_{NMS}$ (up to 4 fold), and in its dissociation kinetics (up to 6-fold) (data not shown). For these reasons we decided to change to the construct of M_1 receptor used in the NIMR lab, in the following experiments reported in this chapter and subsequently to be sure of having a valid comparison. At the time of writing this thesis, the FlpIn M_1 receptor construct has just been resequenced in the Christopoulos lab in Australia. The result has confirmed that the construct did have a mutation, at residue 193 (A193T). (A. Christopoulos, personal communication).

This body of data, reported in 3.2, allows comparison with existing published data to assure the quality of results (Table 3.11).

Table 3.11: Comparison between affinity and dissociation rate constants estimated in this study with published data

	$LogK_{NMS}$ published	*$LogK_{NMS}$ in this thesis*	*k_{-1} published*	*k_{-1} in this thesis*
Tris				
M_1	**9.66[1]**	**10.16**	**-**	**0.076**
M_3	**9.83[1]**	**9.65**	**-**	**0.045**
Hepes				
M_1	**9.92[2,3]**	**9.98**	**0.076[2], 0.074[3]**	**0.061**
M_3	**9.66[2]**	**9.70**	**0.069[2]**	**0.071**
PB				
M_1	**10.74[5]**	**10.65**	**0.032[4]**	**0.032**
M_3	**10.74[5],10.35[6]**	**10.31**	**0.020[4]**	**0.028**

[1] (Ohtake et al., 2007)
[2] (Lazareno and Birdsall, 1995)
[3] (Matsui et al., 1995)
[4] (Gnagey et al., 1999)
[5] (Ford et al., 2002)
[6] (Huang and Ellis, 2007)

We found an excellent agreement on the data obtained in Hepes and PB and the published data. Limited or no comparisons are possible in Tris buffer as there is no published data using these precise conditions. What data are published is from Ohtake et al., 2007 but these measurements were at room temperature, not 37°. The authors do not explicitly state the NMS affinity constants. We have calculated the affinity constants of [^{3}H]NMS for M_1 and M_3 receptors in this Tris buffer from the IC50 data in their published inhibition curves and the tabulated affinity constants in the papers, using the Cheng-Prusoff correction equation:

$$K_{NMS} = \frac{\left(IC_{50}\, from \cdot their \cdot graph \times K_A\, from \cdot their \cdot Table1\right) - 1}{[NMS]}$$

where K_{NMS} is the [^{3}H]NMS affinity constant.

The results obtained also indicate that the different incubation conditions produce substantial perturbations of the binding properties of [^{3}H]NMS. These perturbations could also be different for different orthosteric and allosteric ligands and so could give more information about the nature of the binding processes and the modes of binding.

PB buffer increases the affinity of K_{NMS} ca 5 fold at the two subtypes, M_1 and M_3, without exception (P>H=T) [P=PB, H=Hepes, T=Tris) and, in this buffer condition, k_{-1} was always slower for all the WT receptors and mutants, with the same fold change relative to Hepes and Tris (H=T>P). Therefore k_{-1} and K_{NMS} values were also equally affected by buffer conditions at the WT receptor indicating that the M_1/M_3 subtype selectivity of NMS is observed in all buffers and showing that the selectivity of NMS is an intrinsic property of the receptor and not the buffer in which the affinity is measured. The same pattern of buffer sensitivity of K_{NMS} and k_{-1} were found for the mutants. In PB buffer k_{+1} values were always faster in PB than in Tris or Hepes at the two subtypes. However, at M_3 and mutants, the increase k_{+1} followed the pattern P>H>T whereas at M_1 WT was P>T>H. This is an indication of a different effect of M_1 on k_{+1} of NMS relative to M_3, not due a buffer effect. In PB buffer, there is an increase of k_{+1} despite lower temperatures. This is opposite to the expected effect (k_{+1} increases as temperature increases). In this example buffer effects appear to dominate over temperature effects.

One of the explanations for the effect of PB buffer on the NMS binding properties is that the low ionic strength of the PB buffer might be facilitating the binding of the NMS, there being less interference from cations. This may explain why the k_{+1} was faster at RT in PB than 37° in Hepes.

Regarding the effect of mutants on [^{3}H]NMS binding properties we found that none of the mutations changed the K_{NMS}. Therefore the aminoacids mutated are not individually responsible for the M_1/M_3 selectivity of NMS or its binding to the orthosteric site. The k_{-1} of K523E is always 2.0-2.7 faster compared to WT regardless the incubation buffer. This mutant possesses a negative charge corresponding to that found in M_1 WT. The

mutant K523Q also had an increase in the k_{-1} of ca 1.5-1.9 fold, regardless of the buffer condition. So the positively charged residue at position 523 seems to be slowing the dissociation (and association) of the NMS at the receptor.

The k_{+1} values of K523E and K523Q were also increased by the same factor as the k_{-1} values because the NMS affinity did not change. The residue does participate in the conformation of the orthosteric site of the receptor but it might be on the pathway taken by the orthosteric ligand, NMS, to and from its binding site.

Regarding the change of k_{+1} in different buffer conditions, we mentioned before that it followed the pattern P>H>T for the M_3 receptors and the mutants. The mutant K523E did keep the same pattern as M_3 showing another indication that the change observed between the rank order of k_{+1} of M_1 and M_3 is not only due to the replacement of the amino acid K by E.

Looking at three different buffers prevented us from the misleading conclusion that the change of the residue for the equivalent present in M_1 in the mutant K523E, reached the k_{-1} of M_1. This was observed in Tris buffer. However, the changed dissociation rate constants in the other two buffers made the values for M_1 and M_3 the same but the dissociation rate constants were even faster in the mutants. Therefore the differences in observed [^{3}H]NMS dissociation kinetics of M_1 and M_3 are not solely due to replacement of K by E.

The replacement of the residue N132 by G, which corresponds to the residue present in M_1 subtype, did not result in any change in NMS binding parameters, indicating there is no evidence that N132 is important for NMS binding.

Finally, it is worth noting that the big difference (6 fold) in [^{3}H]NMS dissociation rate constants found between M_3 WT rate in PB and K523E in Hepes show that both factors together, buffer conditions and the mutation, can create a major effect on the value of this constant whereas almost no change in association rate constant is observed. This amplification effect will be exploited in subsequent chapters which look at the effects of buffer conditions and mutations on the binding of allosteric ligands.

3.3 Effect of different incubation conditions on the binding of orthosteric ligands

3.3.1 Introduction

Competition or displacement binding assays were performed to study the binding of the classical orthosteric ligands, atropine, ACh and various selective M_3 antagonists to M_3 WT and mutant muscarinic receptor. In these experiments increasing concentrations of unlabeled ligands compete for the receptor with a fixed concentration of radioligand, [^{3}H]NMS. The data were analysed using the 'Hill equation' providing apparent log affinity constants (pIC_{50}) and a slope factor (n_H) which describes the 'steepness' of the inhibition curve. A slope factor = 1 indicates that competition between the two ligands is for a single class of binding site. A slope factor less than 1 indicates the presence of two separate populations of binding sites or a more complex binding process.

3.3.2 Initial studies

3.3.2.1 Atropine

Atropine is the archetypical non-selective competitive antagonist for the muscarinic acetylcholine receptors. Competition assays were designed to analyse the binding of atropine to M_3 WT and M_3 mutant muscarinic receptors.

In Figure 3.8 a representative competition curve of the M_3 WT with increasing concentrations of atropine in Tris buffer is shown. Usually, the inhibition curves are normalized to show the percentage of inhibition of the initial amount of RL* complex formed in absence of the competitive ligand. The point at which the complex RL* is reduced by 50% is defined as IC50 (inhibitory concentration producing 50% of inhibition). The IC50 was converted to an affinity constant using the Cheng & Prussoff (1973) equation (*See Materials and Methods*). Analysis was performed using a one-site competition equation which describes the competition of an unlabelled ligand to a single binding site identified with a radiolabelled ligand. The atropine competition curve gave a Log K_A value of 8.77±0.04 at M_3 WT in Tris buffer. The affinity constants of atropine for the M_3 receptor and the mutants were not significantly different (Table 3.12).

3.3.2.2 Acetylcholine (ACh)

Competition binding experiments were also perfomed to calculate the affinity that ACh has for the M_3 WT and M_3 mutant receptors in three incubation conditions.

In Figure 3.8 a representative ACh inhibition curve of the M_3 WT in Tris buffer is shown. Analysis was performed using the 'Hill equation' without constraining the coefficient Hill factor to 1. This equation is described in more detail in Material and Methods.

The ACh competition curve gave a Log K_A value of 5.11±0.09 at M_3 WT in Tris buffer. The logarithm of the affinity constants of ACh for the mutations did not significantly differ between constructs (Table 3.12). The affinity value of ACh in Hepes at M_3 WT was not significantly different in Hepes relative to Tris but in PB buffer the affinity increased ca 2 fold to (5.20±0.03) relative to Hepes. This increase of affinity in PB buffer relative to Hepes was found equally in the M_3 mutants and the M_1 WT (log difference 0.35±0.02, n=5, Table 3.12). The Hill factor was ca 0.7 in all the cases indicating more than one population of binding sites for ACh.

Fig.3.8: [^{3}H]NMS inhibition curves of the antagonist atropine and the agonist ACh at the M_3 WT in Tris buffer

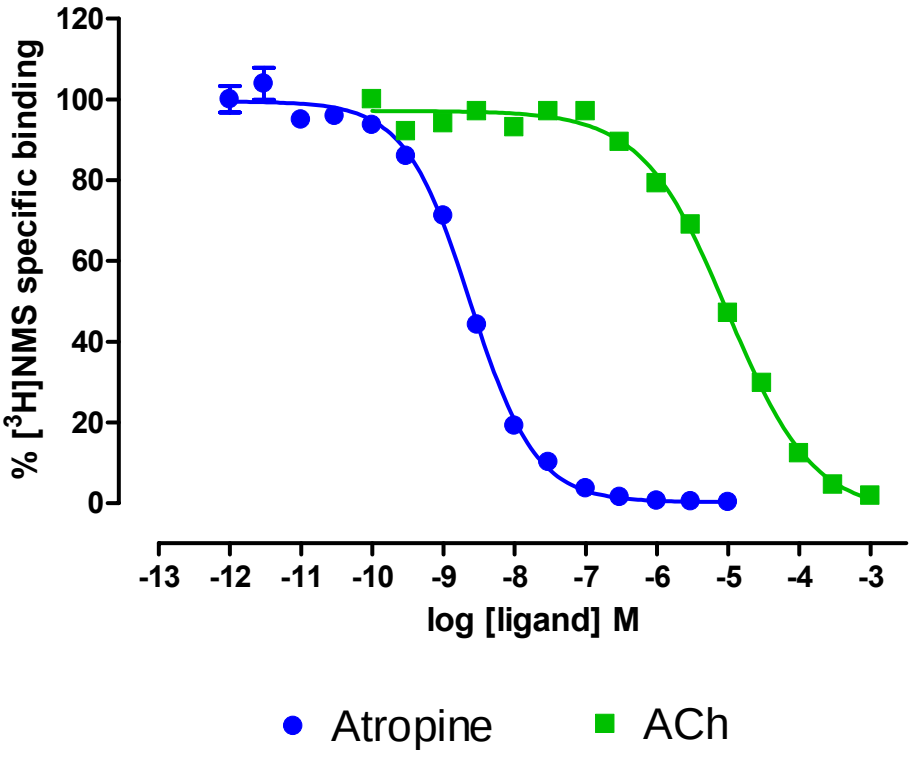

Table 3.12: Affinity constants for atropine and ACh at the M_3 WT, M_1 WT and the M_3 mutant muscarinic receptors under three different incubation conditions

Receptor	Atropine (log K_A)	ACh (log K_A)		
	Tris	Tris	Hepes	PB
M_3 WT	8.77±0.04	5.11±0.09	4.90±0.08	5.20±0.03
M_1 WT	N.D.	N.D.	4.60±0.11	5.09±0.06
K523E	8.79±0.04	5.09±0.04	4.72±0.11	5.01±0.09
K523Q	8.89±0.03	4.86±0.06	4.70±0.05	4.97±0.03
N132G	9.00±0.05	4.84±0.10	4.77±0.04	5.19±0.07
D518N	8.95±0.04	5.21±0.12	N.D.	N.D.
D518K	8.90±0.04	4.95±0.29	N.D.	N.D.

Table 3.12: Log affinity values for the muscarinic antagonist atropine and the endogenous agonist ACh at the M_3 WT and the M_3 mutant muscarinic receptors stably expressed in CHO cells in Tris, Hepes and PB buffer. The membranes were incubated with a fixed concentration of [^{3}H]NMS, 0.2 nM in Tris and Hepes and 0.1 nM in PB at 37ºC, 30ºC or R.T. depending on the buffer for 3 hours. Different concentrations of atropine (1fM-1μM) or ACh (1pM-1mM), were added. Each estimate is the mean ± SEM from 2-15 independent experiments. N.D. Not determined.

The next section reviews briefly the use of M_3 antagonists to treat overactive bladder and examines whether the binding of those antagonists may be sensitive to the mutations of the M_3 receptors and thus affect the subtype selectivity of these ligands.

3.3.3 M_3 selective antagonists of therapeutic importance

3.3.3.1 Introduction (OAB)

Under normal conditions, human urinary bladder smooth muscle contractility is predominantly under the control of the parasympathetic nervous system, where acetylcholine is the primary contractile neurotransmitter in the human detrusor acting on muscarinic receptors modulating urinary bladder contraction during voiding phase and control detrusor tone during the filling phase.

Overactive bladder (OAB) is a highly prevalent disorder characterized as a syndrome consisting of 'urgency with or without urgency incontinence, usually accompanied by frequency and nocturia' (see (Wang et al., 1995;Hegde and Eglen, 1999;Chess-Williams et al., 2001;Fetscher et al., 2002). These symptoms can result from detrusor overactivity with contraction of the bladder mediated primarily by activation of muscarinic M_3 receptors. This major role of the M_3 subtype is shown in radioligand (Matsui et al., 2000) and in vivo (Chapple and Nilvebrant, 2002) studies. Antimuscarinic agents are therefore the first line pharmacotherapy for treating OAB, but a lack of M_3 receptor subtype selectivity with these agents can generate a range of side effects that limits their effectiveness. Worldwide, there are six antimuscarinic drugs currently marketed for the treatment of OAB: oxybutynin, tolterodine, propiverine, trospium, darifenacin, and solifenacin. Each has demonstrated efficacy for the treatment of OAB symptoms, but their pharmacokinetic and adverse event profiles differ somewhat due to structural differences (tertiary vs quaternary amines), muscarinic receptor subtype selectivities, and organ selectivities. The most frequently reported adverse events in clinical studies of antimuscarinics are dry mouth, constipation, headache, and blurred vision; however few patients withdraw from clinical trials because of adverse events.

These molecules differ in their reported pharmacological profile at the five human recombinant muscarinic receptors. Tolterodine (including its 5-hydroxymethyl metabolite) and trospium essentially do not discriminate between the five subtypes. Their mechanism of action remains unclear as they exhibit selective actions *in vivo* (Fetscher et al., 2002). Oxybutynin (and its N-desethyl metabolite) and solifenacin have

been reported to possess marginal selectivity (~10-fold) for M_3 over the M_2/M_5 subtypes, but do not distinguish between M_3 and M_1/M_4 subtypes. In contrast, darifenacin, which behaves as an insurmountable antagonist (Gillberg et al., 1998;Nilvebrant et al., 1997), has been reported to have a high degree of selectivity for M_3 over the M_2/M_4 subtypes and modest selectivity for M_3 over the M_1/M_5 subtypes. In animal models, greater bladder-to salivary gland selectivity ratios have been reported for tolterodine (Gupta et al., 2002), darifenacin (Ikeda et al., 2002) and solifenacin (Chapple, 2000) compared to oxybutynin. Despite the subtype selectivity of darifenacin and solifenacin, they still present antimuscarinic side effects such as dry mouth. Contrarily, tolterodine shows a greater selectivity for bladder than for salivary gland. With the exception of trospium, which is dosed twice daily, the remaining four oral drugs (tolterdoine-ER, oxybutynin-ER, solifenacin and darifenacin) are dosed once daily.

SVT-40776 is a novel substituted quinuclidine derivative with high human M_3 receptor affinity and claimed elevated selectivity versus human M_2 muscarinic receptor. This compound is reported to have a unique profile, with reduced side effects, like dry mouth and cardiac effects. Its state of development is in Phase II as a potential drug of a new generation to treat OAB. The pharmaceutical company, SALVAT, has the full rights on this patent.

In this study we have investigated the binding of the clinically used drugs, darifenacin, solifenacin and SVT-40776 with M_3 and M_1 WT receptors and the M_3 mutants in order to study the possible role of the targeted amino acids in the binding of these competitive antagonists. Binding studies with tolterodine have also been carried out, but only in Tris buffer due to time restriction. The chemical structure, function and clinical status of antagonists are shown in Fig. 3.9 and Table 3.13.

Fig.3.9: Chemical structure of three selective M_3 muscarinic antagonists, solifenacin, darifenacin and tolterodine, which are currently clinically used for the treatment of overactive bladder (OAB)

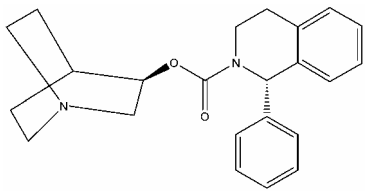

Solifenacin

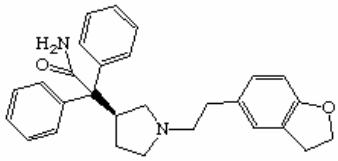

Darifenacin

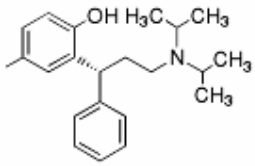

Tolterodine

Table 3.13: Function and status of the four selective M_3 muscarinic antagonists studied

Compound	*Receptor selectivity*	*Tissue selectivity*	*Status*
Darifenacin (Enablex,Novartis)	M_3-selective	Slightly bladder selective	Approved
Solifenacin (Vesicare,Astellas Pharma)	M_3-selective	Non selective	Approved
Tolterodine (Detrol, Pfizer)	Non-selective	Bladder selective over salivary glands	Approved
SVT-40776 (Salvat)	M_3-selective	Bladder selective	Phase II

3.3.3.2 Darifenacin, Solifenacin, SVT-40776 and Tolterodine

Competition binding assays were carried out to analyse the binding of the four selective M_3 antagonists, darifenacin, solifenacin, SVT-40776 and tolterodine at M_3 WT, M_1 WT and M_3 mutant muscarinic receptors in three buffer conditions (except for tolterodine which was analyzed only in Tris buffer because of time limitations).

Fig 3.10 shows a representative [^{3}H]NMS inhibition binding curve of darifenacin, solifenacin, tolterodine and SVT-40776 at M_3 WT and M_1 WT in Hepes. Non linear regression using the one site competition equation with slope factor equal to 1 was used to analyse the data. The pIC50 values obtained were mathematically corrected using the Cheng-Prusoff equation. Table 3.14 shows the affinities of darifenacin, solifenacin, tolterodine and SVT-40776 for M_1 and M_3 receptors under the different conditions.

The log affinity of darifenacin for the M_3 WT receptor in Tris buffer was 8.25±0.12. This was unchanged in Hepes buffer but in PB buffer the affinity increased ca 3 fold to 8.71±0.15. A different behaviour was found for M_1 WT receptors, where the log affinity of darifenacin for the receptor is not changed much between Tris and PB buffer (7.85±0.15 versus 8.10±0.17 respectively) but is significantly lower (3 fold) in Hepes buffer, relative to PB, but not showing significant difference relative to Tris. Comparing the two WT receptors, it is worth noting that the affinity of darifenacin was always 2-4 fold higher at M_3 than at M_1, independent of the buffer used.

The log affinity of solifenacin for the M_3 WT receptor in Tris Buffer was 8.48±0.16. This was unchanged in Hepes buffer but in PB buffer the affinity increased ca 2 fold to 8.81±0.15. A different behaviour was found for M_1 WT receptors, where the log affinity of solifenacin for the receptor is not changed much between Tris and PB buffer (9.50±0.13 versus 9.62±0.17 respectively) but is significantly lower (2 fold) in Hepes buffer relative to PB but not showing a significant difference relative to Tris. Comparing the two WT receptors it is worth noting that, contrary with that seen for affinity values of darifenacin, the affinity of solifenacin was always ca 10 fold higher at M_1 than at M_3, independent of the buffer used.

The log affinity of SVT-40776 for the M_3 WT receptor in Tris Buffer was 9.34±0.14. This was unchanged in Hepes and in PB buffer. At M_1 WT receptors the log affinity of SVT-40776 in Tris buffer was 9.84±0.12 with no significant change in Hepes or PB. This shows that this particular compound is not sensitive to buffer conditions at both M_3 and M_1 WT.

Regarding the effects of the mutants on affinity values of darifenacin, solifenacin, tolterodine and SVT-40776 the mean values of pIC50 were not significantly different at any of the mutants relative M_3 WT under any condition, indicating that none of the residues studied are implicated the binding selectivity of the M_3 antagonists tested (Table 3.15).

Fig.3.10: [^{3}H]NMS inhibition curves of darifenacin, solifenacin and SVT-40776 at the M_3 WT and M_1 WT in Hepes buffer

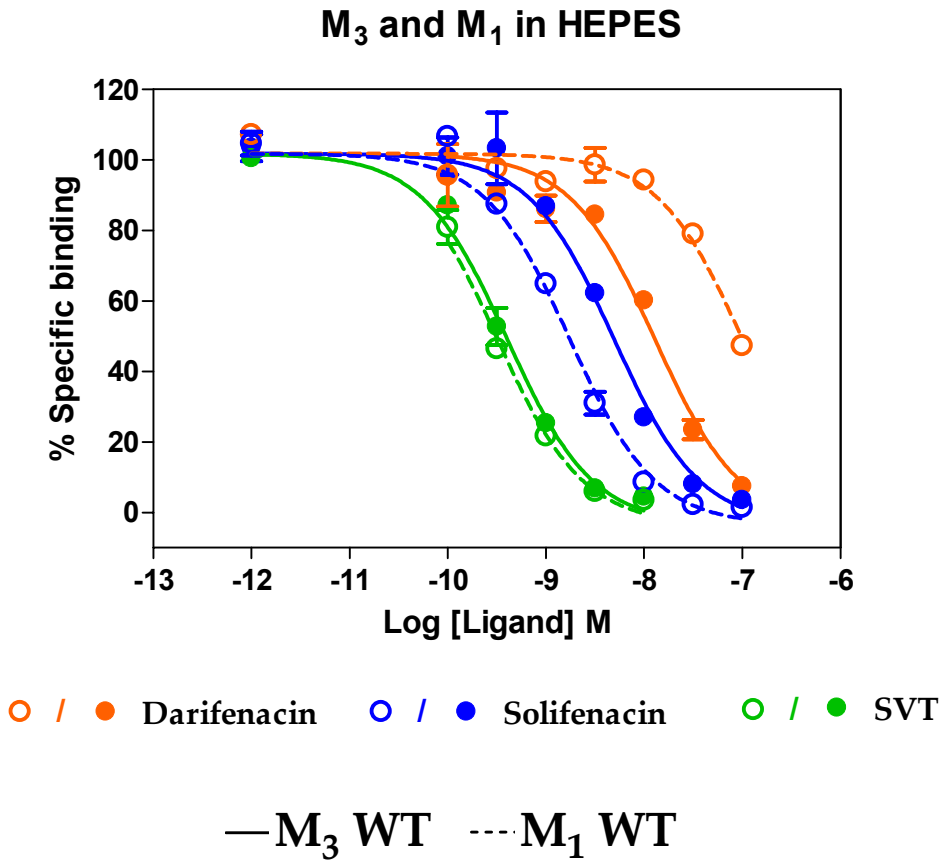

Table 3.14: Affinity constants for the antagonists darifenacin, solifenacin, tolterodine and SVT-40776 at the M_3, and M_1 WT muscarinic receptors under three different incubation conditions

	Tolterodine		Darifenacin		Solifenacin		SVT-40776	
Buffer	M_3	M_1	M_3	M_1	M_3	M_1	M_3	M_1
TRIS	8.49±0.25	N.D.	8.25±0.12	7.85±0.15	8.48±0.16	9.50±0.13	9.52±0.14	9.84±0.12
HEPES	N.D.	N.D.	8.11±0.05	7.07±0.16	8.47±0.09	9.28±0.15	9.40±0.14	9.72±0.12
PB	N.D.	N.D.	8.71±0.15	8.10±0.17	8.81±0.15	9.62±0.17	9.52±0.13	9.95±0.12

Each estimate is the mean value from 2-6 independent experiments

N.D. Not determined

Table 3.15: Affinity constants for the antagonists darifenacin, solifenacin, tolterodine (only in Tris) and SVT-40776 at the M_3 mutant receptors under three different incubation conditions

	Tolterodine	Darifenacin			Solifenacin			SVT-40776		
	TRIS	TRIS	HEPES	PB	TRIS	HEPES	PB	TRIS	HEPES	PB
K523E	8.57±0.40*	8.47±0.01	8.39±0.01	8.90±0.04	8.60±0.01	8.62±0.09	8.96±0.11	9.35±0.14	9.36±0.01	9.57±0.25
K523Q	8.48±0.05*	8.50±0.20	8.31±0.04	9.01±0.06	8.67±0.06	8.60±0.11	9.10±0.05	9.47±0.15	9.35±0.16	9.77±0.12
N132G	8.59±0.60*	8.45±0.12	8.33±0.07	9.00±0.03	8.55±0.06	8.58±0.14	8.99±0.08	9.44±0.10	9.42±0.16	9.66±0.18
D518N	8.45±0.40*	N.D.	N.D.	N.D.	N.D.	N.D.	N.D.	N.D.	N.D.	N.D.
D518K	8.36±0.70*	N.D.	N.D.	N.D.	N.D.	N.D.	N.D.	N.D.	N.D.	N.D.

Each estimate is the mean value from 2-6 independent experiments

N.D. Not determined

* Results obtained by SALVAT (Alicia Enrich, personal communication)

3.3.4 Discussion

This section describes the characterization of the interactions of different orthosteric ligands at M_3, M_1 receptors and the mutant receptors. Among these orthosteric ligands are the archetypical muscarinic antagonist, atropine and the endogenous agonist, ACh.

Radioligand binding inhibition curves have been performed in order to study these orthosteric interactions. These studies are important to check whether any of the M_3 mutations affected the conformation of the orthosteric site. The affinity of the atropine and ACh was not significantly changed by any of the M_3 muscarinic mutants studied, indicating that the residue located in the extracellular loops of the M_3 muscarinic receptors, N132G, D518 and K523 are not important for the binding of orthosteric ligands, at least for atropine and ACh.

The effect of three buffer incubation conditions on the ACh affinity at the M_3, M_1 and M_3 mutant receptors have been also tested. Incubating in PB buffer increased equally the affinity of ACh for M_3, M_1 and the M_3 mutants ca 2 fold, showing an effect of PB favouring ACh binding although the affinity changes were not as large as those found for [^{3}H]NMS.

One of the aims of this thesis is to study the effects of the selected non-conserved residues, located on the extracellular loops, of the human M_3 receptor, on the allosteric interactions, which will be described in next section. It is important that the orthosteric site is not affected by these mutations as, if we observe changes produced by the mutations in subsequent experiments studying the allosteric interactions, it will be due to an effect of the residue, on the allosteric site(s) and not on the overall receptor structure.

The interactions of another set of antimuscarinic drugs, darifenacin, solifenacin and SVT-40776 with M_3, M_1 and the M_3 mutants have been also studied. These selective M_3 compounds are currently used for the treatment of OAB. They are supposed to bind to the orthosteric site. We have checked the effect of the M_3 mutations on the binding of these ligands in three different buffers. None of the mutations significantly affected the affinity constants of these drugs indicating that the residues N132, D518 and K523 are not important for the selectivity of these compounds.

The effects of the three different buffers on the binding of darifenacin, solifenacin and SVT-40776 were also tested. We have found that the affinity constants of darifenacin and solifenacin, which are structurally related, were similarly sensitive to PB buffer at M_3 and M_1 WT whereas the affinity constants of SVT-40776, which has a different structure, was not affected by PB buffer at any subtype indicating an involvement of the structure of the ligand in the buffer sensitivity.

Table 3.16 illustrates the comparison between the log affinity constants obtained in this thesis for darifenacin, solifenacin and SVT-40776 in three different buffers and the affinity values reported in the literature.

We have shown that darifenacin was M_3 selective over M_1 whereas solifenacin and SVT-40776 were M_1 selective over M_3. However there are discrepancies within and between literature values and our data (Table 3.16). In the case of darifenacin all the data shown in the literature have reported that darifenacin is M_3 selective. Nevertheless, contrary to what we have seen, solifenacin has been shown to be M_3 selective by two groups and M_1 selective by one group. This discrepancy might be due to not using exactly the same conditions. We do not have published data to compare with our estimates of the affinity of SVT-40776 at M_1.

Furthermore we have also found some discrepancies in the range of the affinity values. The values of affinity for darifenacin were in some cases 1 log unit different between our results and those reported in the literature, although there are some values which agree. In the case of solifenacin we have found that it is over 1 log unit more potent at M_1 than the one published estimate. The conditions for the binding assays are similar, but not identical. These differences, however, are unlikely to account for the different affinity estimates.

All these discrepancies concerned us and we decided to analyse by mass spectrometry our samples of darifenacin and solifenacin to confirm their structures. The mass spectra of both compounds confirmed the correct structures (Fig 3.11). [Darifenacin (MH^+ major isotopic species: expected value 427.23, observed 427.24) and solifenacin (MH^+ major isotopic species: expected value 363.22, observed 363.2).

Table 3.16: Comparison between affinity constants estimated in this study with published data:

	Darifenacin		Solifenacin		SVT-40776	
	In this thesis	***Published***	***In this thesis***	***Published***	***In this thesis***	***Published***
TRIS						
M_3	8.25	8.70[3], 8.8[4], 9.31[7]	8.48	7.92 [3,4], 9.08[7]	9.52	10.00[7]
M_1	7.85	7.51[3], 7.8[4]	9.50	7.59 [3,4], 9.75[7]	9.84	
HEPES						
M_3	8.11	9.12 [2], 8.42 [5], 8.14[6]	8.47		9.40	
M_1	7.07	8.15 [2], 7.46 [5]	9.28		9.72	
PB						
M_3	8.71	8.92[1]	8.81		9.52	
M_1	8.10	7.46[1]	9.62		9.95	

[1] (Chapple, 2000)

[2] (Wallis and Napier, 1999)

[3] (Ohtake et al., 2007)

[4] (Ikeda et al., 2002)

[5] (Nelson et al., 2004)

[6] (Wallis, 1996)

[7] Results of experiments performed by Salvat (Alicia Enrich, personal communication)

Fig.3.11: Mass spectra of darifenacin and solifenacin

DARIFENACIN

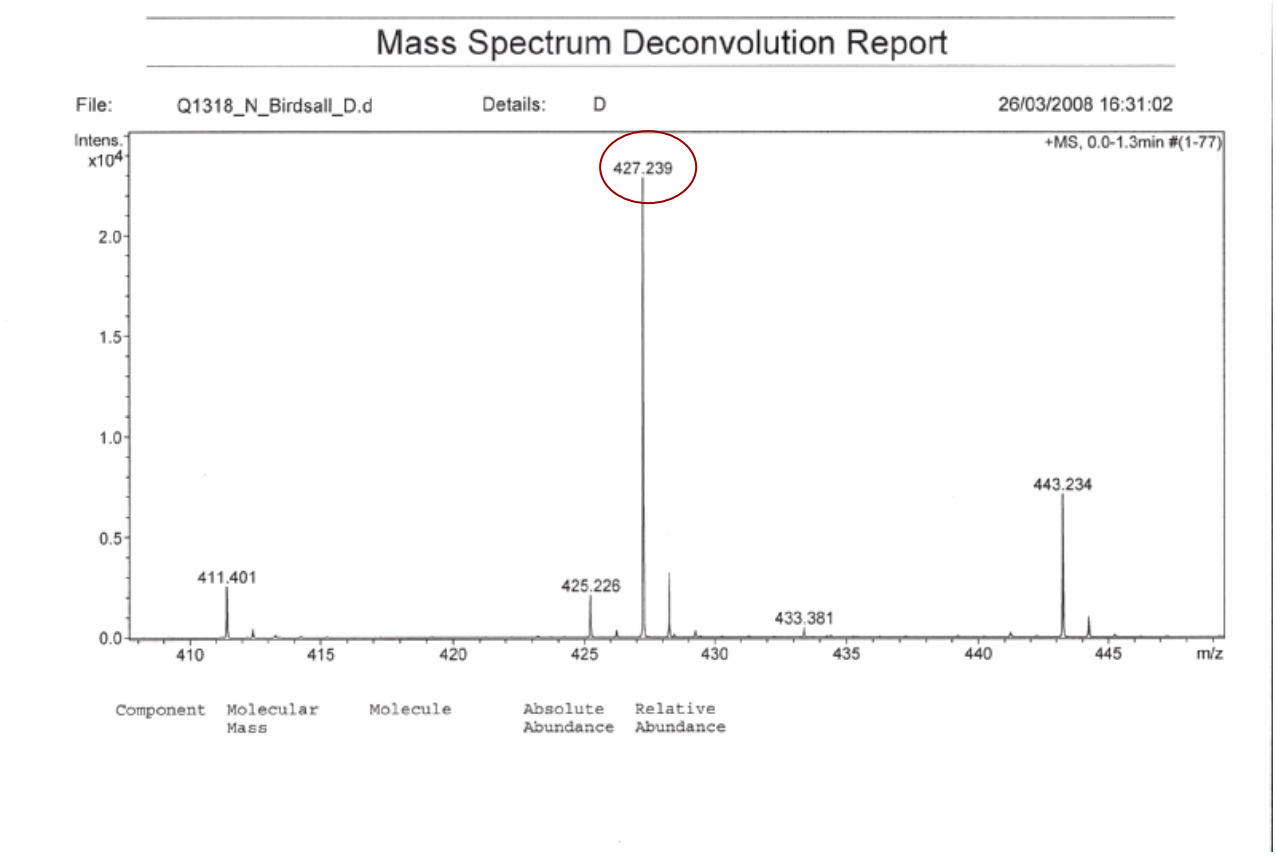

SOLIFENACIN

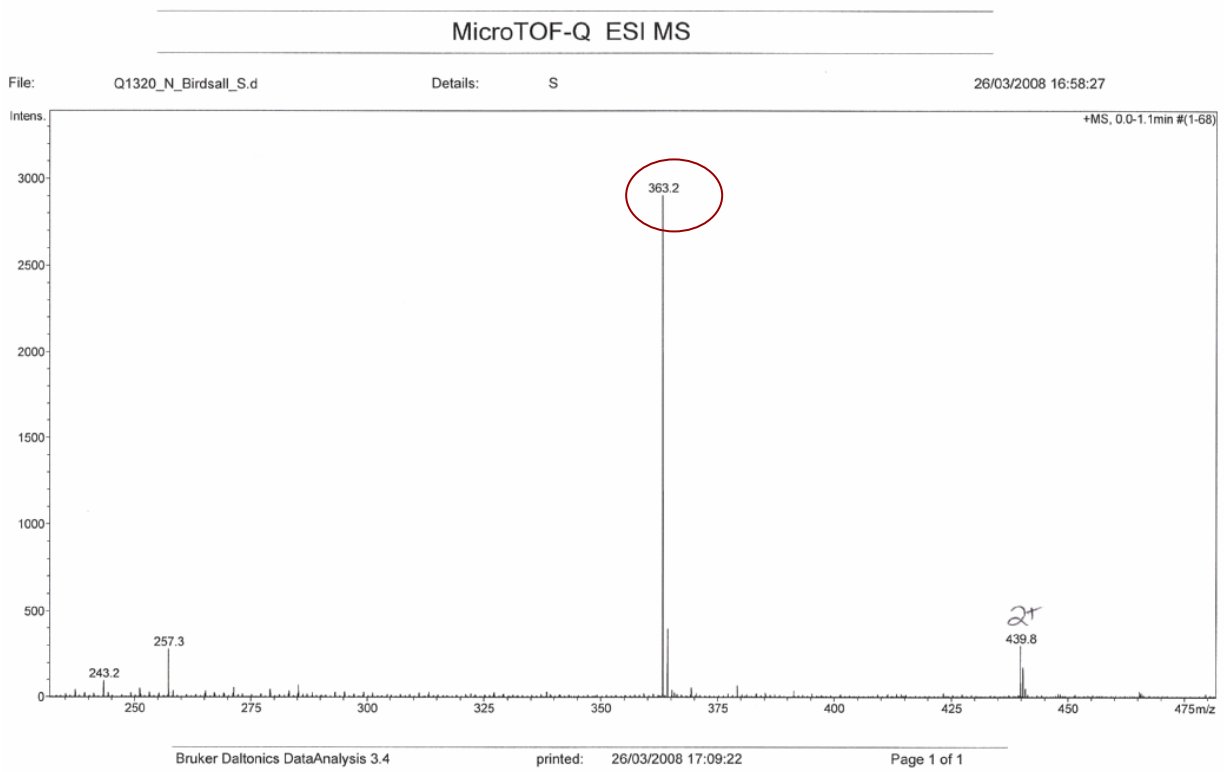

In conclusion, we have shown that K523, N132 and D518 in M_3 receptors are not important for the affinity and subtype selectivity of all the orthosteric ligands examined. However, K523 affects NMS kinetics and by virtue of its charge, appears to slow the access and egress of NMS to and from the orthosteric site.

The studies of different buffers reveal that the M_1/M_3 selectivity of NMS, darifenacin, solifenacin and SVT-40776 are retained. In contrast to some published data, solifenacin, a putative M_3 selective antagonist, has a higher affinity (10 fold) for M_1 receptors.

With the exception of SVT-40776, the affinities of the ligands are higher in PB, relative to Hepes. We do not see the high buffer sensitivity found for the binding of gallamine and AF-DX 116 to muscarinic receptors. However, gallamine (and probably AF-DX 116) are allosteric, not orthosteric ligands.

The effects of the mutations and buffer conditions on the binding of allosteric ligands will be described in the next chapter.

Chapter 4. Characterization of the interactions between [^{3}H]NMS and allosteric ligands that bind to the 'gallamine' binding site

4.1 Allosteric ligands that bind to the 'gallamine' binding site

4.1.1 Introduction

Most of the current drugs targeting muscarinic receptors bind to the orthosteric site of the receptor following the classical strategy of mimicking the action of the endogenous ligand, ACh. The development of small-molecule orthosteric ligands with high degree of selectivity remains a major challenge, as the orthosteric site is strongly conserved between the 5 subtypes of muscarinic receptors and it is difficult to discriminate between them. In addition using an agonist or antagonist which prevents ACh binding to its site, results in continuous receptor stimulation or inhibition of receptor function. This may not be physiologically or therapeutically beneficial.

However, there is an allosteric site in all muscarinic receptors, called the 'gallamine site' which is located on the extracellular loops. This part of the receptor is much less conserved than the orthosteric site, therefore becoming a potential target for subtype-selective compounds. Allosteric modulators, compared to orthosteric ligands, have the advantage, in addition to the potential of achieving selective affinity, of achieving selectivity through cooperativity (Lazareno and Birdsall, 1995). Molecules like gallamine, strychnine, brucine and CMB bind to this site. The chemical structure of these four allosteric ligands is shown in the *Introduction* section in Fig 1.13.

Equilibrium and kinetic studies of these four allosteric agents have been made at the five subtypes of muscarinic receptors (Lazareno and Birdsall, 1995;Lazareno et al., 1998;Ellis and Seidenberg, 1992). Gallamine, is a polycationic drug which has been shown to be negatively cooperative with the orthosteric ligand, [^{3}H]NMS, at all the subtypes of muscarinic receptors, having the highest affinity for the M_2 subtype (Ellis and Seidenberg, 1992;Stockton et al., 1983). The alkaloid strychnine, on the other hand, shows positive cooperativity with [^{3}H]NMS at the M_2 and M_4 subtypes, being

neutral at M_1 and negatively cooperative at M_3 (Lazareno and Birdsall, 1995). The very close analogue of strychnine, brucine, has the same pattern of cooperativities with [^{3}H]NMS as strychnine, positive at M_2, neutral at M_1 and negative at M_3 (Gharagozloo et al., 1999). The final compound in this group, CMB, has negative cooperativity with [^{3}H]NMS at M_1 and M_3, whereas at M_2 the cooperativity with [^{3}H]NMS is positive (Lazareno et al., 1998).

The action of allosteric ligands depends on the ionic composition of the incubation medium (Ellis et al., 1991). (Tränkle et al., 1996) investigated the potency of several allosteric modulators to retard [^{3}H]NMS dissociation from porcine heart muscarinic M_2 receptors under two different assay conditions: in a phosphate buffer of low ionic strength and in absence of divalent cations and in a Tris buffer in presence of divalent cations. Those two buffer compositions resemble our PB and Tris buffers. They found that generally the allosteric agents were more potent to retard the [^{3}H]NMS dissociation at M_2 in the low ionic strength buffer.

Acidic and other residues of the extracellular loops of muscarinic receptors have been shown to be important for the regulation of the binding of allosteric ligands (Leppik et al., 1994;Gnagey et al., 1999). In order to further understand better the mechanism underlying the changes of patterns of cooperativities between modulators and orthosteric ligands, we have studied five different mutations of non-conserved residues located in the extracellular loops of the M_3 receptor.

A possible strategy to develop novel modulators is to use the most selective allosteric modulators described to date as lead structures and to design new compounds by applying information about quantitative structure-activity relationships of these compounds. For this approach, it is a prerequisite to have potency data for the compounds that can be directly compared. However, such data are available to only a limited extent. First, the allosteric potency depends on the assay conditions, and these are not very uniform among the various groups of investigators. Second, either the logKx in equilibrium or the logKocc value, are reported. Rarely are the two values, which are necessary to fully describe an allosteric interaction, are described.

Qualitatively different cooperative effects have been reported by another group, with positive effects of strychnine with [^{3}H]NMS at both, M_1 and M_3 subtypes (Jakubik et al., 1997;Jakubik et al., 2005) and also some different behaviours have been reported by the same group with brucine, being positive with [^{3}H]NMS at M_1 and negative at M_2 (Jakubik et al., 1997). In view of the fact that there are some discrepancies between laboratories in the cooperativities shown by some allosteric agents with [^{3}H]NMS, we decided to look at the cooperativities of the above allosteric agents with [^{3}H]NMS under similar incubation conditions to those that this particular group uses.

Therefore, to fully describe the allosteric interaction, the aim of the present study was to directly compare the potency of a number of representative allosteric compounds and define the rank order of potency for the free and for the [^{3}H]NMS occupied receptor. Kinetic and equilibrium binding studies of gallamine, strychnine, brucine and CMB and [^{3}H]NMS at M_3 WT and the mutated M_3 receptors have been performed under the same three different buffer conditions used in the previous chapter.

4.1.2 Preliminary experiments to set up the assay conditions to examine the effects of allosteric modulators on [^{3}H]NMS dissociation from the M_3 receptor

One of the characteristics that differentiate an allosteric modulator from an orthosteric ligand is its capacity to modify the kinetic properties of the orthosteric ligand for the receptor, because it binds to a different site on the receptor and changes its conformation. This phenomenon provides a very useful tool to identify and quantify allosteric interactions.

There are several methods that can be used experimentally to quantify an allosteric interaction, based on the change of the kinetic properties of an orthosteric ligand bound to the receptor in the absence or presence of an allosteric modulator. The methods described below are based on monitoring the extent of radioligand dissociation over time in the absence or presence of different concentrations of modulator.

The effects of the different allosteric modulators on [^{3}H]NMS dissociation were studied at the M_3 receptor using three different assay protocols. These preliminary

experiments were necessary in order to set up the assay conditions for subsequent experiments.

Initially, full time course experiments of [^{3}H]NMS dissociation at M_3 WT membranes in Tris buffer at 37ºC were performed in absence and in presence of a single concentration of an allosteric modulator at different times. In these experiments the modulators gallamine and strychnine were used. The concentration chosen was 100 μM of the modulator, a relatively high concentration where it would be expected that substantial effects on [^{3}H]NMS dissociation would occur. These experiments allowed the change in k_{-1} of the radioligand from the receptor in presence of a high concentration of the modulator to be detected and quantitated. In addition they show whether dissociation in presence of a modulator is monoexponential. If this is observed it is possible to readily quantitate the allosteric interactions in terms of a simple model, the allosteric ternary complex model.

The data were analysed and fitted well to a single exponential model of dissociation with the fitted parameters indicated by **(a)** in Table 4.1 (See *equation **5*** in *Materials and Methods*). The mean rate of dissociation of [^{3}H]NMS from M_3 WT in Tris buffer at 37ºC was 0.032 min^{-1} and was slowed down, to 0.025 min^{-1} in presence of 100 μM gallamine and to 0.015 min^{-1} in 100 μM strychnine. This represented a significant slowing of 1.3 ($p<0.05$) and 2.1 ($p<0.01$) fold respectively. Representative time course curves are shown in Fig 4.1.

These assays established the monoexponential dissociation of [^{3}H]NMS in the presence of these allosteric ligands in this buffer but were long, generated an unnecessary number of data points, and only examined a single concentration of allosteric ligand. Therefore a different assay was used. This is a two point dissociation kinetic assay. In these experiments, an estimation of [^{3}H]NMS dissociation rate is made by measuring the [^{3}H]NMS bound at three time points (0, 60 and 120 min) in the presence of a range of drug concentrations, typically between 1-10^4 μM.

Fig.4.1: Full time course curves for the dissociation of [^{3}H]NMS from M_3 WT membranes in the absence and presence of a single concentration of gallamine or strychnine

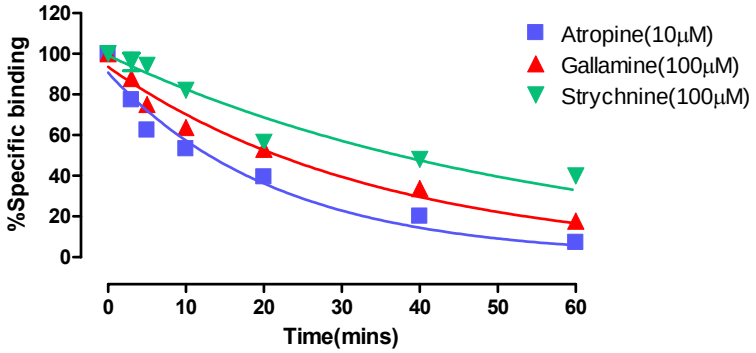

Fig. 4.1: Representative full time course curve of the dissociation of [^{3}H]NMS from M_3 WT receptors in the presence of 10 μM atropine and the absence or presence of 100 μM gallamine or strychnine. These experiements were all performed in Tris buffer. The curves represent the non-linear square fits to the experimental data using the one phase exponential decay equation to analyze the data. The data has been normalized to the percentage of specific [^{3}H]NMS bound to the M_3 receptor at time t=0.

This protocol allowed an additional parameter to be calculated, the concentration of modulator that inhibits the rate of the dissociation of [^{3}H]NMS by a factor of 2, i.e. to halve the k_{-1}. The reciprocal of this concentration corresponds to the affinity of the modulator for the receptor when is occupied by the orthosteric ligand (Log Kocc) (Lazareno and Birdsall, 1995).

The method of doing these experiments and the equations used to analyse the data are described in *Material and Methods* (*equations **5** and **2***). Two different analyses have been performed on these data. The first equation initially fits the data at each concentration of modulator to a single exponential model of dissociation (**a**) and subsequently the different values obtained for the dissociation rate of M_3 WT in absence and presence of the modulators gallamine and strychnine are plotted against the log concentration of the allosteric modulators and fitted using a sigmoidal dose response curve equation (named **b**). The resulting graph shows the excellent fit to the experimental data (Fig. 4.2). The calculated IC50 corresponds to the reciprocal of the

affinity of the modulator when the receptor is occupied by the orthosteric ligand, [^{3}H]NMS.

A representative graph of the different time course curves obtained in presence of different concentrations of gallamine, and the subsequent plot of the calculated k_{-1} values against the log concentration of gallamine is shown in Fig. 4.2 A and B respectively.

In the experiments using gallamine, the mean rate of dissociation of [^{3}H]NMS in Tris buffer at 37ºC using two point kinetic method from M_3 WT was significantly different ($p<0.05$) from the k_{-1} obtained in full time course experiments, being 0.020±0.003 min^{-1}. Nevertheless, the k_{-1} of [^{3}H]NMS was reduced 1.5 fold ($p<0.05$) in presence of 100 μM gallamine, which is comparable with the slowing factor found in full time course experiments. We have no explanation for this change value. The Log Kocc for gallamine was 3.85±0.10 (3). We also fitted the data in Fig. 4.2B without constraining the slope factor to 1 and a slope factor of 1.8 was obtained. Homotropic positive cooperativity for gallamine at human M_3 receptors, a slope factor of ca 1.2 has been reported (Huang and Ellis, 2007).

On the other hand, when similar experiments were performed in presence of 100 μM strychnine, the mean rate of dissociation of [^{3}H]NMS in Tris buffer at 37ºC from M_3 WT was not significantly different from that obtained in full time course experiments and, in presence of strychnine, was reduced 1.9 fold ($p<0.01$), also comparable with the one obtained in full time experiments. The Log Kocc for strychnine was 4.13±0.09 (4). These data are summarized in Table 4.1.

A second way of analysing the data in the 2 point kinetic method was used. It differs from the previous approach in that only one equation was used to fit the data. This equation directly gives the k_{-1} and an estimate of Log Kocc by analysing the amount of the radioligand [^{3}H]NMS remaining at certain times at different concentrations of the allosteric modulator. The equation used is named as **c** in the Table 4.1 and is described in Material and Methods (*equation 7*). The numbers obtained of the k_{-1} and the Log Kocc using the two different analyses in the 2 point kinetics are not significantly different, validating both approaches (Table 4.1).

Fig.4.2: Two point kinetics curves for the dissociation of [^{3}H]NMS from M_3 WT membranes in the absence and presence of nine different concentrations of gallamine

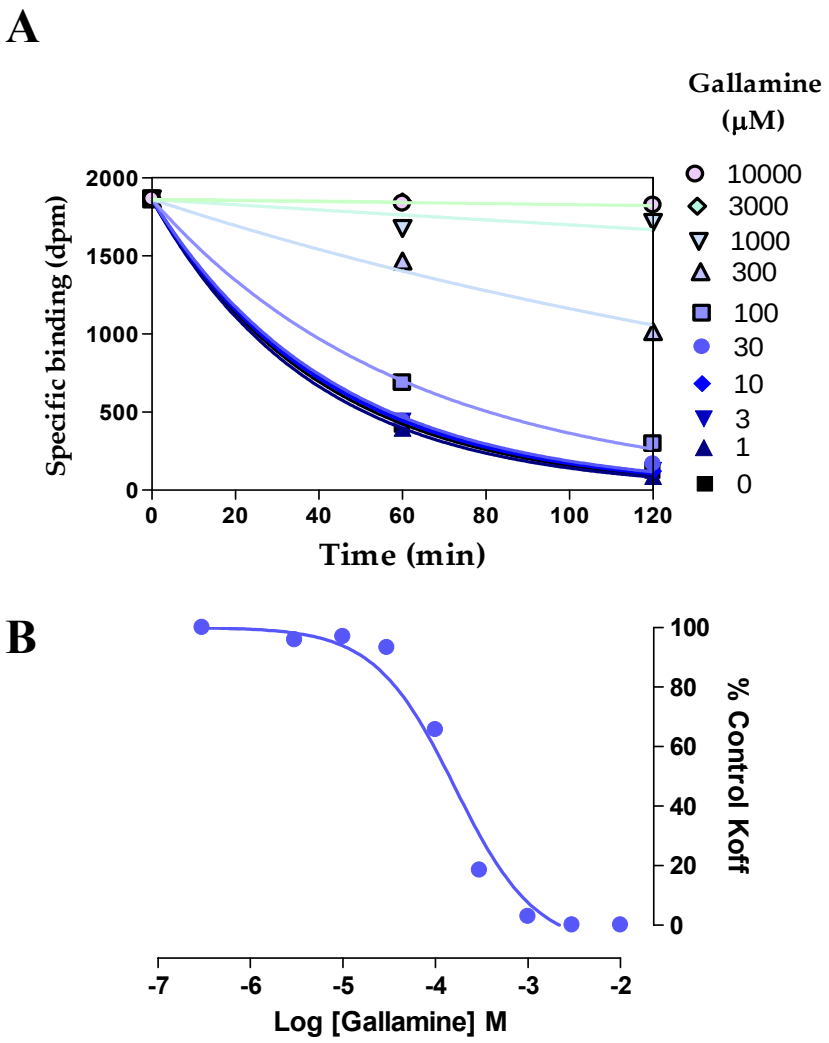

Fig. 4.2: Representative graphs of the two point kinetic assay at M_3 WT receptors. These experiments were performed in Tris Buffer. Graph A represents time course curves of the dissociation of [^{3}H]NMS from M_3 WT receptors in the presence of 10 μM atropine and the absence or presence of nine different concentration of gallamine (1-10^4 μM).

Graph B represents the percentages of the control k_{-1}, plotted against log concentration of gallamine. The log affinity of gallamine when the receptor is occupied by [^{3}H]NMS is the pIC50 of this curve. The curves represent the non-linear square fits to the experimental data using the one phase exponential decay equation in graph A and a dose-response curve equation in graph B.

Table 4.1: Three different experimental methods of measuring the dissociation rate constants of [^{3}H]NMS in the absence and presence of an allosteric modulator, gallamine and strychnine, at M_3 WT

	M_3_wt Receptor	Full Time Course	2 point kinetics		1 point kinetic		
		Tris	Tris		Tris	Hepes	PB
Gallamine	k_{obs}/k_{-1}	1.3* [a]	1.5* [a]	-	-	-	-
	Log Kocc	-	3.85 [b] (0.10;3)	3.98 [c] (0.09;3)	3.91 [c] (0.05;4)	3.65 [c] (0.04;4)	4.92 [c] (0.06;5)
Strychnine	k_{obs}/k_{-1}	2.1** [a]	1.9** [a]	-	-	-	-
	Log Kocc	-	4.13 [b] (0.09;4)	4.04 [c] (0.09;4)	4.27 [c] (0.02;2)	4.09 [c] (0.10;4)	5.25 [c] (0.01;2)

Equations used to analyse the data:

[a] One phase exponential decay

[b] Sigmoidal dose-curve

[c] Allosteric dissociation assay for estimate of allosteric potency

* Significantly different ($p<0.05$)

** Significantly different ($p<0.01$)

Table 4.1: Ratios between dissociation rate constants of [^{3}H]NMS from M_3 WT in presence (k_{obs}) and absence (k_{-1}) gallamine or strychnine, using different protocols and equations to analyze the data. The equations used to analyse each body of data indicated by **a**, **b** and **c**, are described in more detail in the *Materials and Methods* section. The LogKocc of gallamine and strychnine obtained in the different protocols are also shown. In the full time course and 2 point kinetics assays, only Tris Buffer was used. In 1 point kinetic assay, three different incubation conditions were studied. Data are shown as mean (sem; n).

Finally, the third method used was the one point kinetic assay under three different incubation conditions, where an estimation of [^{3}H]NMS dissociation was made by measuring the [^{3}H]NMS bound at only one time point (relative to that at time t=0) in the presence of a range of three concentrations of an allosteric ligand under three different conditions. The incubation time point was around 2.5 times the half-life of the [^{3}H]NMS from the M_3 WT receptor, also measured in these assays. Three concentrations of gallamine and strychnine were used, a range of 10-1000 μM in Tris and Hepes Buffer and 1-100 μM if the buffer was PB. The non-linear square fits to the experimental data is represented in Fig. 4.3 using equation **c** as previously described. The parameters obtained are summarized in Table 4.1.

Significant differences in the dissociation rate constants between the three conditions tested were found by using the unpaired two tailed t-test (Table 4.1). The fastest rate constant was observed in Hepes buffer, k_{-1}=0.071±0.004 min^{-1} and was significantly slower in PB buffer, k_{-1}=0.028±0.002 min^{-1} ($p<0.001$). The Log Kocc of gallamine was also significantly different, being 3.65 in Hepes buffer and 4.90 in PB buffer ($p<0.001$). A similar phenomenom occurs with Log Kocc of strychnine which changes from 4.09 to 5.25 ($p<0.001$) between Hepes and PB buffers.

To conclude, the single one point dissociation assay provides a valid method of estimating k_{-1} and log Kocc.

Fig.4.3: One time point kinetic analysis of the dissociation of [^{3}H]NMS from M_3 WT membranes in the absence and presence of three different concentrations of gallamine and strychnine under three different incubation conditions

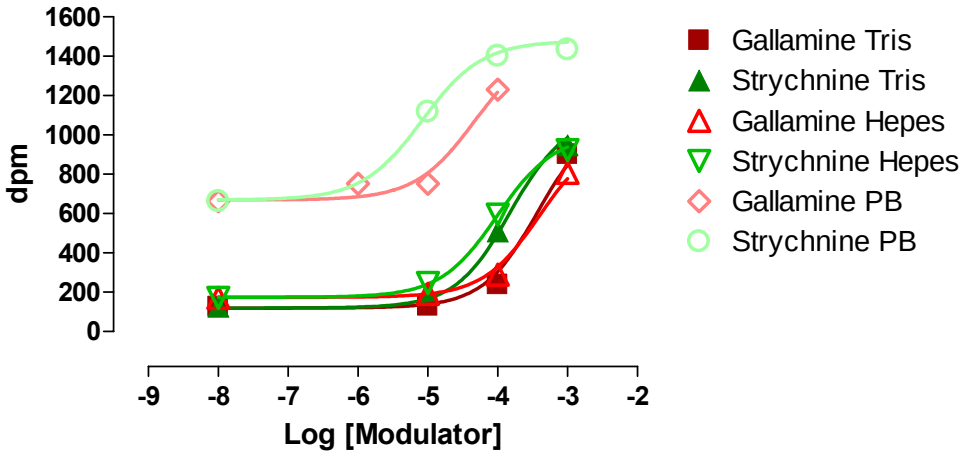

Fig. 4.3: Representative graphs of the one point kinetic assay for the determination of the affinity of two allosteric ligands at [^{3}H]NMS occupied M_3 WT receptor under three different incubation conditions. This graph shows the increase of the [^{3}H]NMS bound to the receptor as the concentration of the modulator increases. This is due to the reduction of the rate of the dissociation of [^{3}H]NMS in presence of increasing concentration of modulator.

The allosteric modulators studied were gallamine and strychnine and the incubation point time selected in each case was around 2.5 times the k_{-1} of the M_3 WT in Hepes in this experiment. The range of concentrations used of the two agents in Tris and Hepes buffer was 10-1000 μM and in PB buffer was 1-100 μM in addition of 10 μM of atropine.

The curves represent the non-linear square fits to the experimental data using the equation (named **c**) described in *Material and Methods* that provides estimates of allosteric potency when the receptor is occupied by an orthosteric ligand.

4.1.3 Effect of mutations on [^{3}H]NMS dissociation in absence and presence of different concentrations of allosteric ligands using three different incubation conditions

As described earlier, five mutants of the M_3 receptor were created where the residues substituted were those corresponding to the M_1 subtype: K523E, D518K and N132G. As the amino acids in positions 518 and 523 are charged, the uncharged mutants, K523Q and D518N, were also created in order to observe any possible effect of the charge.

These mutations were evaluated for their effects on the ability of four allosteric agents to allosterically regulate the receptor, relative to their effects on the wild-type M_3. The method used in this study was one point kinetic assay described in the previous section, and the incubation time point selected was based on the k_{-1} of the construct, ca. 2.5 times the half-life. The orthosteric ligand used was [^{3}H]NMS and four allosteric ligands were studied, gallamine, strychnine, brucine and CMB (all of which are considered to bind to the 'Gallamine binding site'). This study used the three different incubation conditions previously employed. The different values obtained for the affinity of the modulators at the [^{3}H]NMS occupied receptor (log Kocc) are summarised in Table 4.2 (page 134).

The mutation N132G (Table 4.2) did not change log Kocc relative to M_3 WT for all ligands under any conditions.

Preliminary experiments also showed that the D518K and D518N mutations did not change log Kocc (data not shown). Shortage of time prevented further studies of these mutants.

Gallamine affinity at the [^{3}H]NMS occupied receptor.

At M_3 WT, the log Kocc of gallamine was increased 4 fold and 15 fold in Tris and PB relative to Hepes. At K523E log Kocc increased 2.5 fold in Tris and Hepes and 25-30 fold in PB buffer relative to M_3 WT. If we compare Log Kocc gallamine of K523E in Hepes with the one in PB, there is a remarkable increase of 250 fold in affinity. At K523Q, log Kocc gallamine was unaffected in both Tris and Hepes conditions. However, it showed a 4 fold increase in PB. This is an example where the mutation produces a change in binding in one buffer but not the two other buffers.

Strychnine and brucine affinity at the [^{3}H]NMS occupied receptor.

The Log Kocc values of brucine and strychnine were comparable in Tris and Hepes and ca 10 fold higher in PB for M_3 WT and all mutants. This suggests a common mechanism of the PB buffer in affecting the affinity of these two ligands which does not involve the mutated residues. At K523E the affinities were increased ca 10 fold in all buffers, indicating that this mutation produced a change in the basic binding of brucine and strychnine, independent of buffer. At K523Q the log Kocc values were unaffected, relative to M_3 WT, in all buffers, except the log Kocc of strychnine (but not brucine) which was increased 2 fold in PB. This is a very different pattern of behaviour from the K523E mutant, both because of its buffer dependence and the differentiation between brucine and strychnine.

CMB affinity at the [^{3}H]NMS occupied receptor.

At M_3 WT, the log Kocc of CMB was increased in PB relative to the two other buffers but to a smaller extent than for the other ligands. At K523E, the log Kocc of CMB relative to WT was increased 3-5 fold in Tris and Hepes and ca 12 fold in PB. At K523Q, the log Kocc relative to WT was unaffected in Tris, but was increased 4 fold in Hepes and only ca 1.5 fold in PB. This is an example where a difference is observed between Tris and Hepes buffer but with only a small change in PB. This is a different behaviour from that observed for the other allosteric ligands.

Fig. 4.4 shows the difference of the Log Kocc obtained for these four allosteric modulators at the three mutated M_3 receptors relative to M_3 WT in two buffers, Hepes and PB.

Fig.4.4: Log difference in Kocc of four allosteric modulators at three mutated M_3 receptors relative to M_3 WT in Hepes and PB buffers

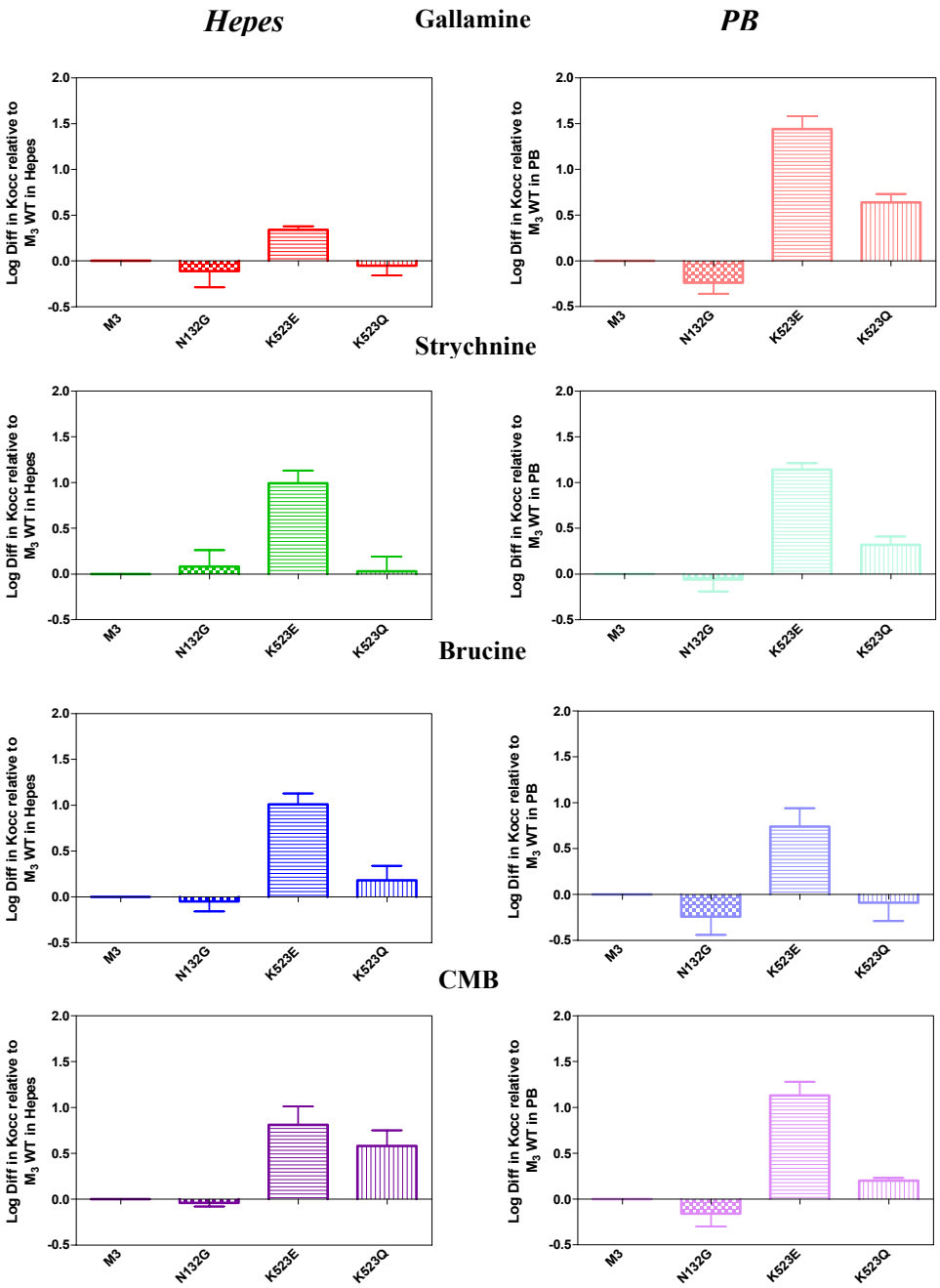

4.1.4 Effect of allosteric modulators on the equilibrium binding of [^{3}H]NMS to M_3 WT receptor

The previous section dealt with the investigation of the effects of incubation conditions on the ability of four allosteric ligands to inhibit the dissociation rate of [^{3}H]NMS from M_3 and mutated M_3 receptors. This section describes the effects of the three different incubation conditions on the binding of the four allosteric ligands to the unoccupied receptor, measured in equilibrium binding experiments.

Five different concentrations of the modulators were used. The range selected was based on the Kocc value. The maximal concentration used cannot be significantly more than the reciprocal of this value as a kinetic artefact is generated. If the concentration of modulator is higher than 0.5 log unit above log Kocc, there is such an increase in slowing of the kinetic association and dissociation rate constants, that it would take a very long time to reach equilibrium, and it would be extremely difficult to measure the binding of [^{3}H]NMS at equilibrium. The affinities (Log Kx) of the agents for M_3 WT receptors for the unoccupied receptor are summarised in Table 4.2.

If we compare the affinity of a modulator, obtained in equilibrium binding assays, with the affinity of the modulator when the receptor is occupied by the orthosteric ligand, we can obtain the cooperativity between both ligands when they are bound to the receptor at the same time. This is given by the ratio between Kocc and Kx, which gives us alpha. The cooperativity can also be obtained from equilibrium assays directly, and if the cooperativity from equilibrium and the cooperativity calculated from the ratio of Kocc and Kx agree, it can be established that the ternary complex model is valid to analyze the data. The cooperativities calculated from kinetic and equilibrium experiments for each allosteric ligand and [^{3}H]NMS, together with their affinities in equilibrium assays in three different buffer conditions, are discussed in the following paragraphs. In some cases where the cooperativity is very close to 1 or, contrarily, is very close to zero, being almost competitive, the cooperativity is difficult to determine in equilibrium experiments without constraining the log Kocc in the equation used to analyse the data in equilibrium assays (number **8** in *Material and Methdos*) to that measured in the kinetic studies. In Fig. 4.5 is shown an example of

the difference between constraining or not. In these cases, both methods of analysis give excellent fits and the effect of constraining log Kocc is minimal. This suggests that, for the quality of the experimental data, the allosteric ternary complex model is a viable method of analysing the data.

Fig.4.5: Comparison of the fits of the equilibrium binding curves of four different allosteric modulators at M_3 WT receptor in PB buffer, with log Kocc unconstrained or constrained to the values found in the [^{3}H]NMS dissociation experiments

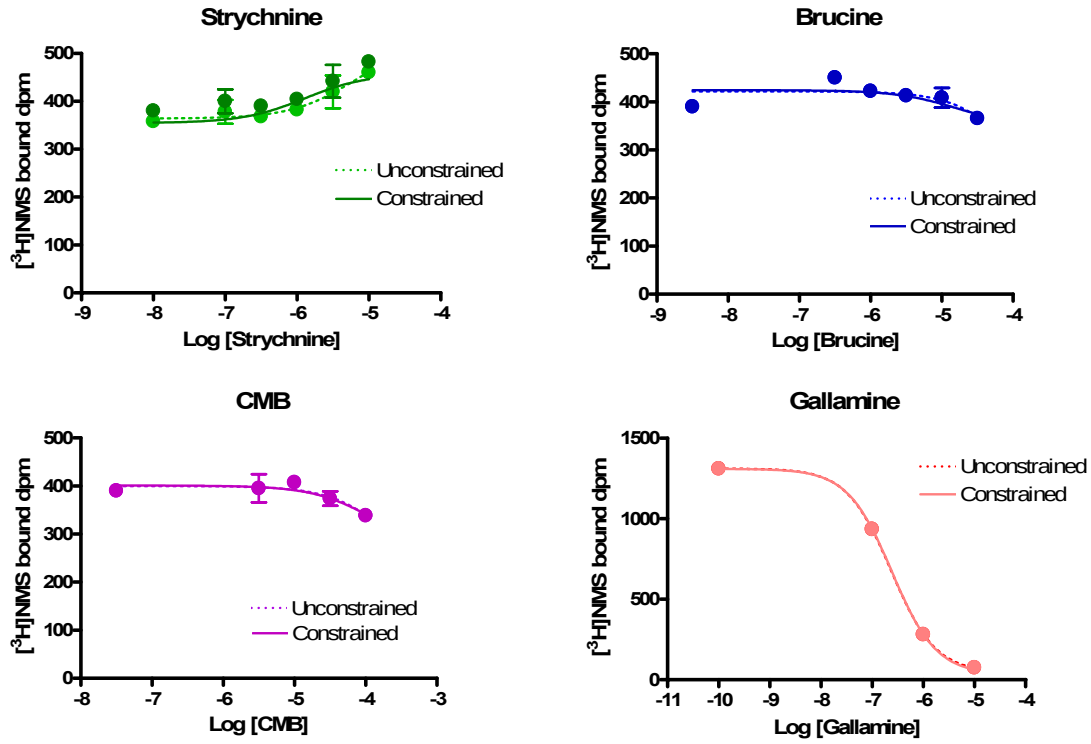

Gallamine affinity and cooperativity

The affinity of gallamine is somewhat higher (3 fold, $p<0.01$) in Tris compared to Hepes. In PB it is very much higher, 50-150 fold, compared to that found in either the other two buffers ($p<0.001$). The observed cooperativity in Tris and Hepes is strongly negative, α ca 0.03. In PB buffer this cooperativity is even more negative, $\alpha = 0.005$, reflecting the fact that gallamine binding to the unoccupied receptor is more sensitive to buffer than its binding to the NMS occupied receptor.

Strychnine affinity and cooperativity

The affinity of strychnine is similar in both Tris and Hepes buffer. In PB this affinity significantly increased 5 fold ($p<0.001$), but this is less than that observed at the NMS-occupied receptor (10-14 fold) indicating that strychnine binding to the unoccupied receptor (in contrast to gallamine) is less sensitive to buffer than its binding to the NMS occupied receptor. In Tris buffer the cooperativity observed between strychnine and [^{3}H]NMS was neutral whereas in Hepes buffer was negative (ca 0.6). On the other hand in PB, this cooperativity was switched to positive. This is the first time that this finding has been observed, where a change in the direction of cooperativity is created by a different incubation buffer.

Brucine affinity (Log Kx)

The affinity of brucine was, in contrast with the pattern observed for the previous two ligands, comparable in Tris and PB buffer, being still significantly different, $p<0.05$. In contrast, brucine affinity was ca 10 fold lower ($p<0.001$) in Hepes, indicating a brucine binding sensitivity to Tris buffer not previously observed. On the other hand, there was a different influence of buffer on the cooperativity, it being slightly negative and comparable in PB and Hepes (ca 0.5) and strongly negative in Tris (ca 0.04). This suggests a different mechanism of strychnine and brucine binding to the unoccupied receptor, in contrast with what it was observed in the binding to the NMS-occupied receptor.

CMB affinity and cooperativity

The affinity of CMB to the unoccupied receptor was comparable in Tris and Hepes buffer, but in PB this affinity was increased ca 5 fold ($p<0.001$). The cooperativities observed (ca 0.4) were not affected by the different buffers used, indicating a different mechanism of CMB binding to the unoccupied receptor from that observed with strychnine.

The affinity of the four allosteric ligands studied at the unoccupied M_3 WT receptor, were all different diminishing in the following order: gallamine > strychnine > brucine > CMB except in Tris buffer where brucine was higher than strychnine.

In Fig. 4.6 the effect of the allosteric modulators gallamine, strychnine, brucine and CMB in PB buffer on the binding of [^{3}H]NMS at M_3 WT receptors is illustrated. It showed the variability of extent and the direction of cooperativities between NMS and the four allosteric modulators. The interaction between gallamine and [^{3}H]NMS results in almost complete inhibition, which corresponds to negative cooperativity. On the other hand, there is practically no inhibition of CMB and brucine binding, the manifestation of very weak negative cooperativity with [^{3}H]NMS and strychnine shows positive cooperativity, indicated by an increase in the binding curve.

Fig.4.6: Effects of gallamine, strychnine, brucine and CMB on [^{3}H]NMS equilibrium binding curves in PB buffer, illustrating the different observed cooperativities for those ligands

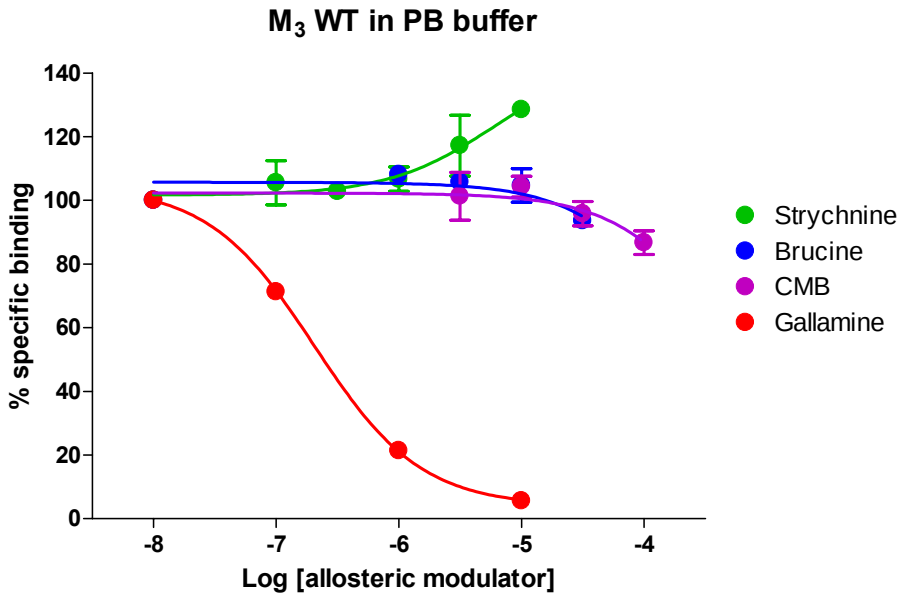

4.1.5 Effect of mutations on the affinity and cooperativity of four allosteric modulators estimated from [^{3}H]NMS equilibrium binding assays

Because of the importance of some single amino acid residues located on the extracellular loops on the binding characteristics of various allosteric modulators, the role of two individual aminoacids was studied in detail. In these experiments the effect of the four allosteric agents used previously on the equilibrium binding of [^{3}H]NMS to the K523E, K523Q and N132G mutants was examined.

In these assays, the selection of the range of the concentration of modulators used was chosen using the same criteria of using the Kocc values for the mutant and thereby avoiding kinetic artefact, as was done on the M_3 WT (Section 4.1.4). The effects of the three different incubation buffers were also tested.

Fig. 4.7 shows the difference of the Log Kx obtained for these four allosteric modulators at the three mutated M_3 receptors relative to M_3 WT in two buffers.

Gallamine affinity for the unoccupied receptor relative to M_3 WT.

The N132G mutation did not affect gallamine binding in any buffer. The two other mutants showed their biggest effect in PB buffer. K523E showed a 7 fold increase in affinity in Tris and Hepes relative to WT. This increase was 60 fold in PB, with the Kx now being 10^9 M^{-1}, which is an extremely high affinity for an allosteric ligand. The K523Q mutation also increased the gallamine affinity but the increase was attenuated relative to what was seen for K523E: only a 2-3 fold increase was observed in Tris and Hepes whereas ca 15 fold increase was seen in PB buffer. The positive charge at position 523 inhibits gallamine binding to M_3 receptors.

The cooperativity of gallamine with [^{3}H]NMS in Tris at K523E and K523Q became more negative relative to WT, with values lower than 0.01. This effect was not seen in Hepes buffer, indicating a Tris buffer sensitivity in gallamine binding at K523E and K523Q. In PB buffer the cooperativities observed were also strongly negative, with values lower than 0.01, indicating that this decrease in cooperativity is buffer dependent.

Fig.4.7: Equilibrium binding bar graphs for the log difference in affinity of gallamine, strychnine, brucine and CMB at the mutated M_3 receptors relative to M_3 WT receptors, in two different incubation conditions

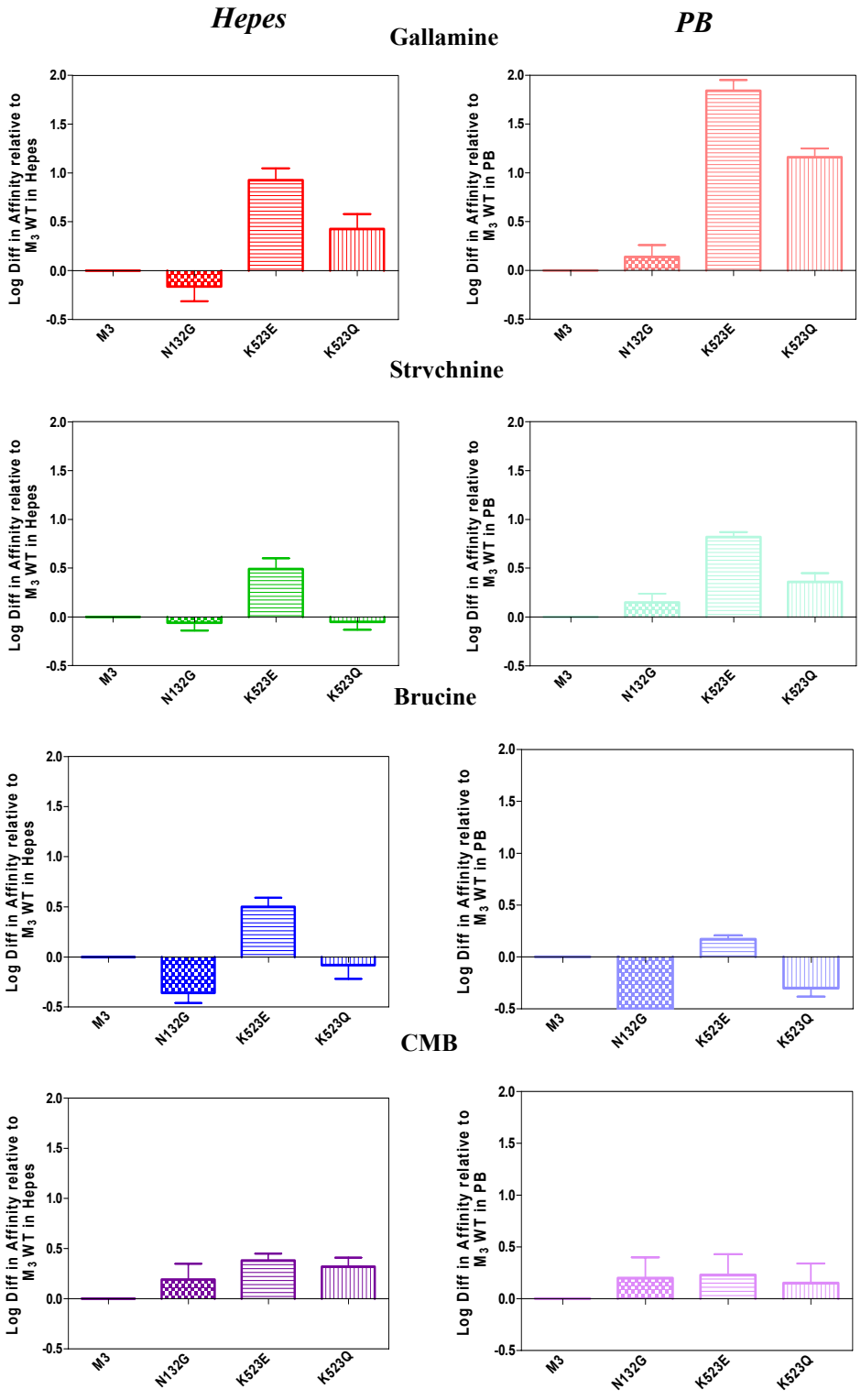

Strychnine affinity for the unoccupied receptor relative to M_3 WT.

The N132G and K523Q mutation increased the affinity of strychnine ca 2 fold in Tris and PB buffer, with no effects seen in Hepes. The increase of strychnine affinity was greater at K523E, ca 4-6 fold in all buffers. The K523E mutation also switched the negative cooperativity seen in M_3 WT to positive cooperativity in Tris and Hepes (0.6 to 2.1), suggesting that the incorporation of a negative charge in that position in M_3 receptors could be important for observing positive cooperativity between [^{3}H]NMS and strychnine. This switch was not observed in the K523Q mutation indicating that a positive cooperativity between these two ligands requires a negative charge in the 523 position and not just removal of the positive charge. In PB buffer the positive cooperativity seen in M_3 WT, increased ca 2.6 fold at K523E suggesting that PB buffer is also important for increasing the cooperativity of these two ligands.

Brucine affinity for the unoccupied receptor relative to M_3 WT.

The N132G and K523Q mutation decreased the affinity of brucine, ca 2 fold in Tris and PB buffers. The K523E mutation caused only a small increase of brucine affinity (if any) relative to strychnine in the buffers Tris and PB. In Hepes buffer the increase of brucine affinity, ca 3 fold, was higher than the increase observed in PB buffer, ca 1.5 fold. This is a different behaviour from that observed for other allosteric ligands. The K523E mutation changed the negative cooperativity seen at M_3 to neutral cooperativity in Hepes and to positive cooperativity (ca 2) in PB buffer.

CMB affinity for the unoccupied receptor relative to M_3 WT.

Only small effects, if any, were observed. There was a small but significant increase in affinity (ca 2.5 fold) at K523E and K523Q in Hepes that was not found in PB. This effect indicates a similarity with brucine binding to the unoccupied receptor. This is the only case where an effect in Hepes is observed and not in PB. Only at the K523E mutant in PB was the alpha changed to positive compared with the negative cooperativity seen at M_3 WT. This indicates a buffer dependence in this particular mutant for the interactions between [^{3}H]NMS and CMB.

Table 4.2: Binding parameters for the allosteric interactions of four allosteric modulators with NMS obtained from equilibrium (log Kx) and kinetic (log Kocc) experiments

	Gallamine		Strychnine		Brucine		CMB	
	logKx	logKocc	logKx	logKocc	logKx	logKocc	logKx	logKocc
Tris								
M3	5.56±0.05(3)	3.91±0.05(4)	4.33±0.03(2)	4.27±0.01(2)	4.81±0.01(2)	3.44±0.06(2)	3.37±0.06(2)	3.10±0.17(2)
N132G	5.41±0.11(4)	3.83±0.06(2)	4.59±0.01(2)	4.19±0.09(4)	4.50±0.04(2)	3.48±0.08(2)	3.24±0.16(2)	3.02±0.18(2)
K523E	6.47±0.06(4)	4.31±0.03(2)	4.78±0.10(2)	5.12±0.12(6)	4.86±0.02(2)	4.49±0.10(3)	3.76±0.06(2)	3.60±0.05(2)
K523Q	6.11±0.13(3)	3.80±0.16(3)	4.54±0.01(2)	4.22±0.12(6)	4.52±0.07(2)	3.50±0.10(3)	3.65±0.11(2)	3.24±0.15(2)
Hepes								
M3	5.01±0.08(4)	3.65±0.04(4)	4.30±0.07(5)	4.09±0.10(4)	3.89±0.05(5)	3.37±0.11(4)	3.46±0.05(7)	2.92±0.02(2)
N132G	4.85±0.13(3)	3.54±0.18(3)	4.25±0.05(4)	4.17±0.16(3)	3.61±0.05(3)	3.30±0.05(3)	3.65±0.16(7)	2.88±0.04(2)
K523E	5.94±0.09(4)	4.00±0.02(2)	4.80±0.09(5)	5.09±0.11(2)	4.39±0.08(6)	4.38±0.04(2)	3.84±0.05(8)	3.73±0.20(4)
K523Q	5.44±0.13(4)	3.76±0.10(3)	4.26±0.03(3)	4.12±0.12(3)	3.81±0.14(4)	3.55±0.11(3)	3.78±0.08(5)	3.51±0.17(4)
PB								
M3	7.20±0.08(2)	4.92±0.05(5)	5.03±0.08(3)	5.25±0.01(2)	4.89±0.02(6)	4.65±0.18(2)	4.18±0.13(5)	3.71±0.01(2)
N132G	7.34±0.09(3)	4.68±0.16(2)	5.18±0.03(3)	5.19±0.13(2)	4.38±0.06(3)	4.41±0.09(2)	4.32±0.16(2)	3.56±0.14(2)
K523E	9.04±0.08(2)	6.37±0.13(4)	5.81±0.01(4)	6.39±0.07(2)	5.06±0.04(6)	5.38±0.09(4)	4.41±0.15(5)	4.84±0.15(4)
K523Q	8.36±0.04(3)	5.56±0.06(3)	5.39±0.03(2)	5.57±0.09(3)	4.58±0.08(3)	4.55±0.08(2)	4.33±0.14(2)	3.91±0.03(2)

4.1.6 Examination of a discrepancy in the literature in the allosteric actions of strychnine and brucine at M_3 and M_1 receptors

The study of the effects of two structural related compounds, strychnine and brucine on their affinities with all the subtypes muscarinic receptors (M_1-M_4 subtypes) and their effect on [^{3}H]NMS binding, has also been reported by another group (Jakubik et al., 1997). We found a discrepancy between their results and ours in two of the parameters measured.

We looked at the differences in methodology and composition of the incubation buffer. Their buffer was similar to our Hepes buffer in terms of its having high ionic strength, so its use might be expected to give similar results to ours in Hepes buffer. Equilibrium and kinetic experiments were performed in M_1 and M_3 receptors with [^{3}H]NMS and brucine and strychnine respectively in Hepes and Jakubik buffer. The values of the affinities and the alpha values observed by them and by us are shown in Table 4.3, as well as previously published data from NIMR (Lazareno and Birdsall, 1995;Lazareno et al., 1998;Gharagozloo et al., 1999).

Although their data for the affinities of brucine at M_3 receptors and strychnine at M_1 receptors agree with our data and the published data, their affinities of brucine at M_1 receptors and strychnine at M_3 receptors do not agree with ours. They are at least one log unit higher than the ones that we obtained. The directions of alpha are also different. In the case of the effect of brucine on [^{3}H]NMS binding to M_1 receptors they obtained positive cooperativity, (α= 2), whereas we obtained neutral cooperativity, i.e. α= 1. In addition, they reported the cooperativity of strychnine with [^{3}H]NMS at M_3 receptors to be neutral, and we obtained negative cooperativity (α=0.7), shown in Table 4.3 and Fig. 4.8. In the graphs that they show, the positive allosteric effect of brucine with [^{3}H]NMS at M_1 receptors is manifest as an increase in binding. As it has been shown that the allosteric modulators prevent the degradation of the receptors (May et al., 2005), one possible interpretation of these graphs is that during the incubation for 21 hours in the Jakubik experiments the receptors have degraded and the amount of receptor bound to [^{3}H]NMS has decreased. This could have been prevented by increasing concentrations of modulator and resulted in an increase in binding, and therefore apparent positive

cooperativity. To test this theory we incubated for 3 hours, which was enough to reach equilibrium according to our k_{-1} and log Kocc values and therefore avoid the kinetic artefact at the higher concentrations of allosteric ligands that we use, and for 21 hours which is the time that Jakubik used.

Comparing the graphs incubating for 3 and 21 hours, there was a decrease in [^{3}H]NMS bound at 21 hours confirming possible receptor degradation. However, we did not find the positive effect of brucine with [^{3}H[NMS at M_1 that they reported (data not shown).

The affinities obtained at 3 and 21 hours agreed with the ones that we obtained under our Hepes buffer conditions. These, together with the cooperativity values obtained in both Hepes and Jakubik buffer, are shown in Table 4.3. We also performed one point kinetic experiments in order to obtain the k_{-1} of [^{3}H]NMS and the Kocc of strychnine and brucine at M_3 and M_1 subtypes under Hepes and Jakubik buffer (Table 4.3). [Jakubik et al., did not perform any kinetic experiments].

We did not see the strong positive cooperative effect of brucine in [^{3}H]NMS at M_1 receptors that they found. Fitting the experimental equilibrium data using the ternary complex model gave values of log $\alpha \cdot Kx$ that were compatible with the log Kocc that we have obtained. On the other hand the equilibrium data obtained is incompatible with $\alpha=2$ between brucine and NMS. The binding affinities of strychnine at M_3 receptors in Jakubik buffer obtained in our equilibrium assays was comparable with that obtained in Hepes buffer.

These results emphasize the caution that must be used in quantitatively analysing allosteric data in the absence of kinetic data.

Further discrepancies with the results of the Jakubik group were also observed when cooperativity with ACh was measured (described in the discussion of Chapter 5).

Table 4.3: Comparison of the binding properties of brucine and strychnine for M_1 and M_3 WT muscarinic receptors in Hepes (*section 4.1.4*), by Jakubik et al., and from our experimental data obtained using Jakubik conditions

	Brucine			Strychnine		
	M_1			M_3		
	logKx (α)	***Log Kocc***	***k_{-1} (min^{-1})***	***logKx (α)***	***Log Kocc***	***k_{-1} (min^{-1})***
HEPES	4.60 (1.0)	4.60[a]	0.06	4.30 (0.7)	4.10[a]	0.08
Jakubik data	5.70 (2.0)	6.00[b]	N.D.	5.70 (1.0)	5.70[b]	N.D.
Jakubik buffer[c]	4.70 (0.8)	4.60[a]	0.10	4.40 (0.7)	4.11[a]	0.10
HEPES[d]	4.73 (0.9)	4.50	0.07	4.16(0.7)	4.02	0.07
HEPES[e]	4.60 (0.8)	4.50	0.08	4.20(0.7)	4.00	0.06

[a]: Parameter obtained from kinetic experiments

[b]: Parameter calculated from Log Kx and the alpha obtained in equilibrium assays.

[c]: Experimental data obtained using Jakubik conditions.

[d]: Published data (Lazareno and Birdsall, 1995;Lazareno et al., 1998)

[e]: Published data (Gharagozloo et al., 1999)

Table 4.3: Discrepancies of brucine and strychnine binding parameters log Kx and log Kocc, obtained by equilibrium and kinetic experiments using Hepes and Jakubik buffer at the M_1 and the M_3 receptors respectively. Data are means of three experiments. The S.E.M. value of each parameter was always less than 0.10. The value of the cooperativity obtained is shown in brackets

N.D. Not determined

Fig.4.8: Discrepancy between two allosteric modulators behaviour found by Jakubik et al and the experimental data that we obtained using the same conditions

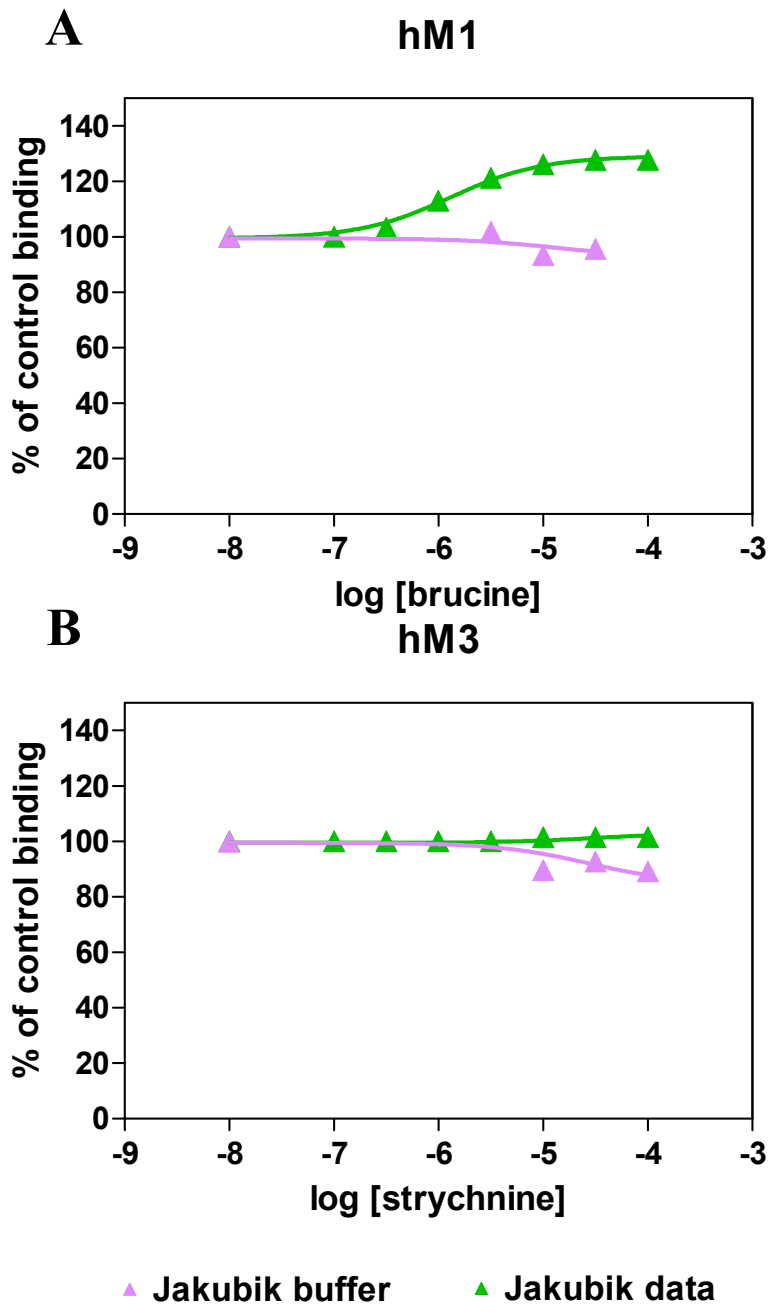

Fig. 4.8: Binding of [^{3}H]NMS in the presence of brucine at the human M_1 WT (hM_1) receptors on the curve on the top and in the presence of strychnine at the human M_3 WT (hM_3) on the curve below at the concentrations shown in the abscissas. The data obtained by Jakubik et al is illustrated in green triangles and the data that we obtained in Jakubik buffer is shown in pink triangles.

4.1.7 Discussion

The initial full time-course experiments showed that, in presence of gallamine and strychnine in Tris buffer at M_3 receptors, [^{3}H]NMS dissociation was monoexponential, verifying that the allosteric ternary complex can be used to analyse the effects of those allosteric modulators on [^{3}H]NMS dissociation and to quantify allosteric interactions. Both agents, gallamine and strychnine, were able to slow the rate of [^{3}H]NMS dissociation from M_3 WT verifying their allosteric behaviour, with strychnine being able to slow the dissociation more than gallamine at the same concentration. We have also performed two point kinetic experiments which give us an extra parameter, logKocc of the modulator, which is the concentration required to halve the rate of [^{3}H]NMS dissociation. This is equivalent to the affinity of the allosteric agent for the receptor when NMS is already bound to it. These experiments take a relatively long time to perform relative to the information content and we showed that one time point kinetic assays are more efficient and the data can be analysed with only one equation in order to obtain LogKocc values which agreed with the other assays. Therefore one point kinetic assays were made to study the effect of the mutations on the Log Kocc of gallamine (G), strychnine (S), brucine (B) and CMB under three buffer conditions. It is possible to analyse the results in several different ways.

Qualitative effects of the mutations on the rank order of log Kocc values

The rank order of log Kocc at M_3 WT and for N132G, D518N and D518K mutations in all buffer conditions was: S > G > B > CMB. This indicates that the different buffers used and those mutations do not change the basic structure-activity relationships (SAR), at the NMS-occupied receptor. Only the K523E mutation changed the SAR to: S > B > G > CMB in Hepes buffer. With this single mutation the structure of the receptor has been changed substantially and now this receptor structure (and the SAR also) becomes buffer sensitive. In PB buffer the SAR became, S = G > B > CMB. So the structure of this site is not the same in Hepes and in PB. The rank order of log Kocc at K523Q mutation in PB buffer was S = G > B > CMB, matching with the one observed in the K523E mutation in PB buffer. It could indicate that the positive charge of lysine is interfering with gallamine binding, and when it is replaced by E or Q (but only in PB buffer), gallamine affinity is increased.

Quantitative effects of the mutations on the log Kocc values

It is also possible to analyse quantitatively the magnitude of the changes that mutations have on the Log Kocc values of the four allosteric modulators under three different conditions relative to M_3 WT. This provides twelve different measures. The mutations N132G, D518K and D518N did not change any of those parameters (0/12). In contrast, the mutation K523E changed all 12 factors, (12/12 relative to M_3 WT). The quantitative changes of the log Kocc values of the K523E mutation, relative to M_3 WT, for the four allosteric modulators was buffer sensitive: in Tris buffer the order of the magnitude of the changes in log Kocc relative to M_3 WT was S = B > G = CMB, in Hepes S = B > CMB > G and in PB, G > S = CMB > B. This is illustrated in Fig. 4.9 (for Hepes and PB). In the three buffer conditions studied, the difference of log Kocc of strychnine and brucine for K523E relative to M_3 WT were ca 10 fold, indicating that this increase is dependent only on the mutation. It seems than brucine and strychnine share a common mechanism in the way they bind to the NMS occupied receptor and they are unlike gallamine or CMB, which undergo an increase in log Kocc only in PB buffer. We can conclude that the effect of K523E on gallamine and CMB binding to the NMS occupied receptor relative to M_3 is sensitive to ionic conditions.

The K523Q mutation changed quantitatively and selectively the Log Kocc of CMB relative to M_3 WT in Tris and Hepes buffer, (CMB > S = B = G). This large difference in the quantitative change of Log Kocc of CMB relative to M_3 is a unique property of this mutation. This indicates a possible disfavouring role of the charges, positive or negative, in the binding of CMB when NMS is bound to the receptor. However in PB buffer the quantitative changes of the log Kocc values of the K523Q mutation relative M_3 WT are: G > S > CMB > B, matching the SAR of K523E in that buffer.

Fig.4.9: Quantitative effect of the K523E mutation on the Log Kocc value of the four allosteric modulators relative to the M_3 WT in Hepes and PB

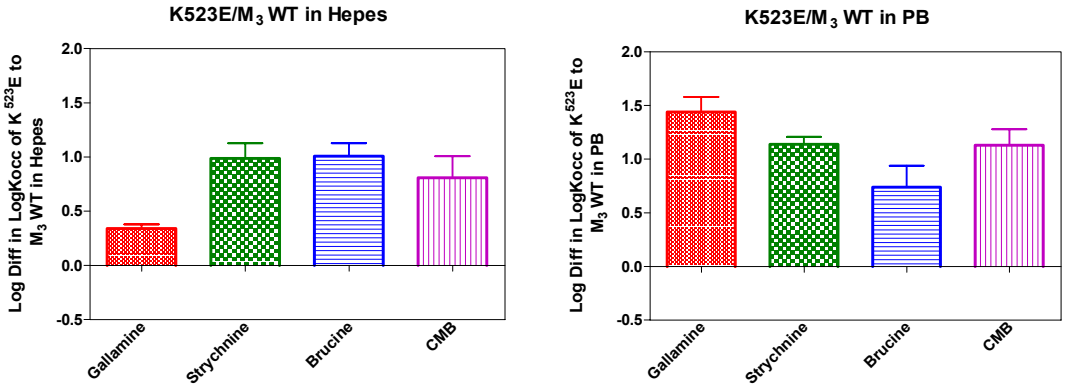

"Square diagrams"

This is a third method of looking at the changes in Kocc. The absolute numbers for the change in Kocc of the modulators at M_3 WT and K523E in Hepes and PB, obtained individually from four different experiments are shown in a different form in Fig. 4.10. For example, the four different Log Kocc values of gallamine obtained at M_3 WT and the K523E mutation in Hepes and PB are shown as circles in a square arrangement analogous to the ATCM. The circle at the top left hand side represents symbolically the log Kocc value of gallamine for M_3 WT in Hepes buffer. This is the starting point of the diagram and is the parameter which is going to be compared with that produced by the K523E mutation (change of colour from blue to red in circle) and the effect of the buffer (moving from top to bottom within the scheme). The fold change in Kocc is shown as a number accompanying the arrow representing the transition between two 'states' of the receptor. For example the Kocc of gallamine is increased 2 fold by the K523E mutation when binding is measured in Hepes buffer and the Kocc of gallamine at the WT M_3 receptor is increased 20 fold in PB relative to Hepes. This square is completed by measurements of the effect of the mutation K523E in PB buffer (28 fold) and the buffer effect on the binding of gallamine to K523E (235 fold). The overall fold increase in gallamine potency from M_3 WT in Hepes to K523E in PB from the data from the four experiments, either following one path or the other, has to be the same. This is a consequence of the law of microscopic reversibility which says that in the absence of an

external energy source there is the same energy change between two points in a cycle independent of the pathway taken between those two points. Within the errors of the individual estimates, this is true for all the squares in the following figures (B, C, D) representing strychnine, brucine and CMB effects.

There are two product components which show how much the log Kocc values of gallamine (or the other allosteric ligands) have increased by these two processes. One is given by the product of the two fold-increases that the gallamine Kocc has undergone either following one path or the other, which has been mentioned previously. In this case, the product for gallamine is 500 and this represents the overall change (Δ) in Kocc of gallamine between M_3 in Hepes and K523E in PB. The other parameter (δ) is the ratio of the two constants on the opposite sides of the square, which is a 'sensitivity factor'. It represents either how much the mutant has changed the buffer sensitivity (δ=12 for gallamine) or equally how much the buffer has changed the ability of the mutation to modify gallamine affinity.

Fig.4.10: Diagram illustrating that the two pathways of the different factors (K523E mutation and switching to PB buffer) that increase the Kocc values of allosteric modulators relative to that found at M_3 WT in Hepes lead to the same effect

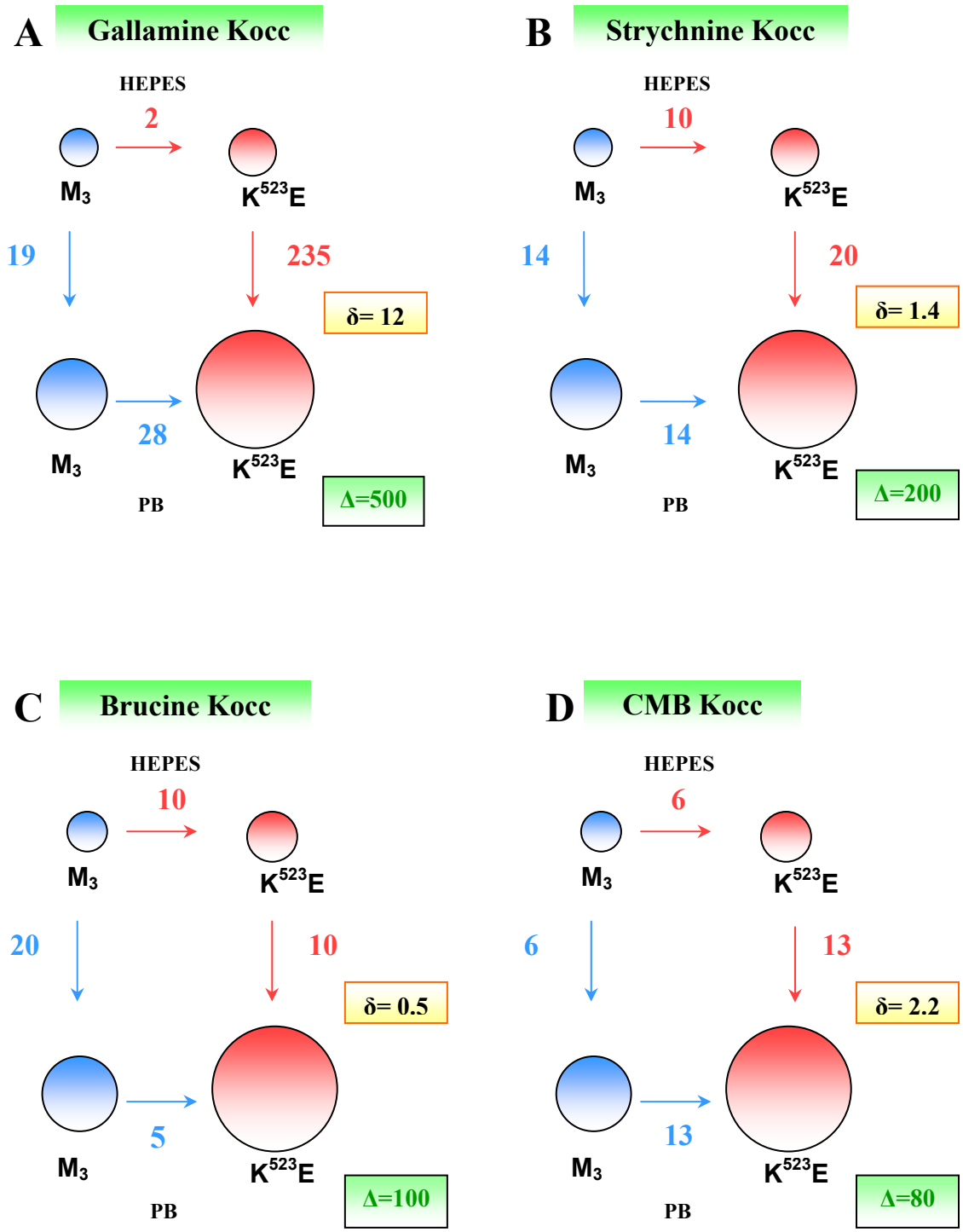

The same approaches have been applied to the affinities of the four allosteric ligands for the unoccupied receptor (log Kx).

Qualitative effects of the mutations on the rank order of log Kx values

These values were from equilibrium experiments on the M_3 WT and mutant receptors under three buffer conditions. The rank order of the log Kx obtained at M_3 WT and N132G, K523Q and K523E receptors was: G > S > B > CMB in Hepes and also in PB, but the difference between gallamine and the other three agents was even higher in this buffer. Therefore the relative SARs of these four ligands at the unoccupied receptor are independent of the buffer and the mutations. Although the relative SARs were not buffer sensitive, it is worth noting that the affinities of the four allosteric ligands studied were always increased in PB buffer relative to Hepes and Tris. This SAR pattern for Log Kx is different than the one found for Log Kocc, but this is logical as gallamine has a strong negative cooperativity with NMS, and thus Kx>>Kocc whereas Kx ≈ Kocc for the other allosteric ligands.

Quantitative effects of the mutations on the log Kx values

We also have quantified the effects that mutations have on the Log Kx of four allosteric modulators under three different conditions relative to M_3 WT, just as we did for the Log Kocc values. Again, there are twelve different ratios for each mutant. The log Kx values of the K523E mutation for the allosteric ligands increased in 11 out of 12 examples, clearly showing that the receptor structure produced by this mutation is more favourable for the binding of all the allosteric ligands tested.

The N132G mutation did not affect the log Kx values of gallamine, strychnine or CMB relative to M_3 WT in 8 of 9 conditions, (8/9). Interestingly a decrease in affinity for brucine was observed (3/3), unlike what was happening with the Log Kocc, where there was no change in affinity. Therefore the N132G mutation only affects brucine binding to the unoccupied receptor. The K523Q mutation increases affinity for gallamine, strychnine and CMB in 7/9 examples, showing a clear involvement of this residue in regulating Log Kx, unlike the Log Kocc where no change was observed (9/9). It seems that the positive charge of K may be perturbing in the binding of the allosteric ligands

when the receptor is unliganded, but not when is occupied by NMS. The K523Q mutation in contrast decreases the affinity for brucine (2/3). The K523Q mutation therefore affects the binding of all four ligands to the unoccupied receptor.

The quantitative changes of the log Kx values of the K523E mutation relative to M_3 WT in Hepes and PB buffer are shown in Fig. 4.11. As we found for the NMS occupied receptor, the K523E mutation produced larger effects on the log Kx for the four allosteric ligands than the other mutants. An increase in affinity was observed in all the conditions (12/12). The changes for gallamine were the highest of the allosteric ligands in Hepes and PB buffer unlike the changes in log Kocc values where strychnine was the largest in Hepes (but not in PB). Gallamine also was the ligand most sensitive to the mutation and this sensitivity was greater in PB than in Hepes. In contrast strychnine does not have as a big change in PB compared to Hepes, and the change in log Kx for brucine and possibly CMB was lower in PB than in Hepes. We can conclude that the effect of K523E on gallamine and brucine binding relative to M_3 when the receptor is not bound to NMS is affected by ionic conditions.

Fig.4.11: Quantitative effect of the K523E mutation on the Log Kx values of the four allosteric modulators, relative to the M_3 WT in Hepes and PB

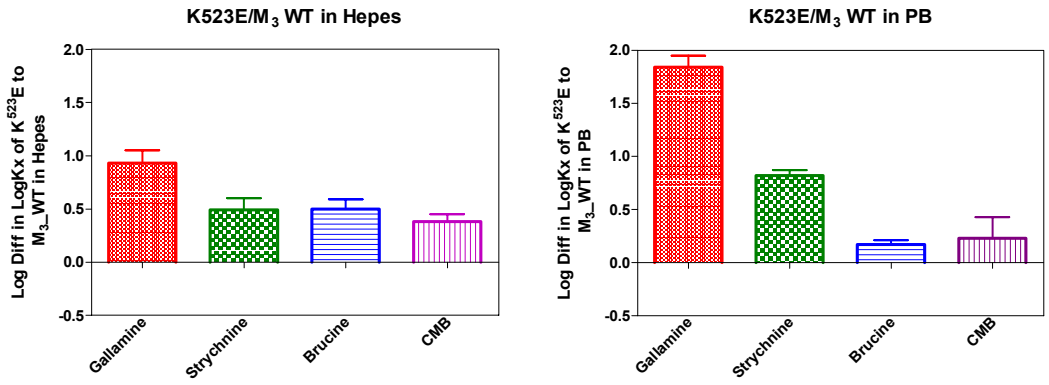

Square diagrams for Kx

An analogous diagram of squares to that shown in Fig. 4.10, illustrating the differences of Kx values obtained between M_3 WT and the K523E mutant in Hepes and in PB is shown in Fig. 4.12.

The overall changes in Kocc and Kx of gallamine, strychnine, brucine and CMB between M_3 and K523E in Hepes and PB buffer are also summarised in Table 4.4. We can observe, by looking at these products, that there is an increase in affinity of all the allosteric ligands studied, especially in the Kx of gallamine where the overall change is 10,000 fold, indicating the extent that the binding of gallamine is affected by the K523E mutation and the PB buffer. For strychnine, CMB and brucine the overall changes are also large (9-78 fold) for both parameters (Kx and Kocc).

Comparing the differences between these two Δ values for Kx relative to Kocc we observe that in the overall changes in affinity there are big changes in both directions. For example for gallamine the overall change in Kocc is 20 times lower than the one obtained in Kx. On the other hand, for strychnine and CMB, the overall changes were found higher in the Kocc than in Kx by a factor of 6 and 9 respectively. Brucine did not show a difference between the overall changes obtained in Kx relative to Kocc.

The sensitivity factors (δ) are also summarised in Table 4.4. The highest change has been also found in gallamine, ca 10 fold for both Kocc and Kx. For the rest of the allosteric ligands, the sensitivity factors are practically unchanged. The sensitivity factors of the K523E mutant and PB buffer on the M_3 WT receptor in Hepes, are very similar for Kocc and Kx for all the allosteric ligands studied, indicating that the change found in buffer or mutant was similar in both Kx and Kocc for all the compounds.

Fig.4.12: Diagram of squares illustrating the different pathways that the factors (K523E mutation and switching to PB buffer), that increase the Kx affinity of allosteric modulators relative to M_3 WT in Hepes, can follow

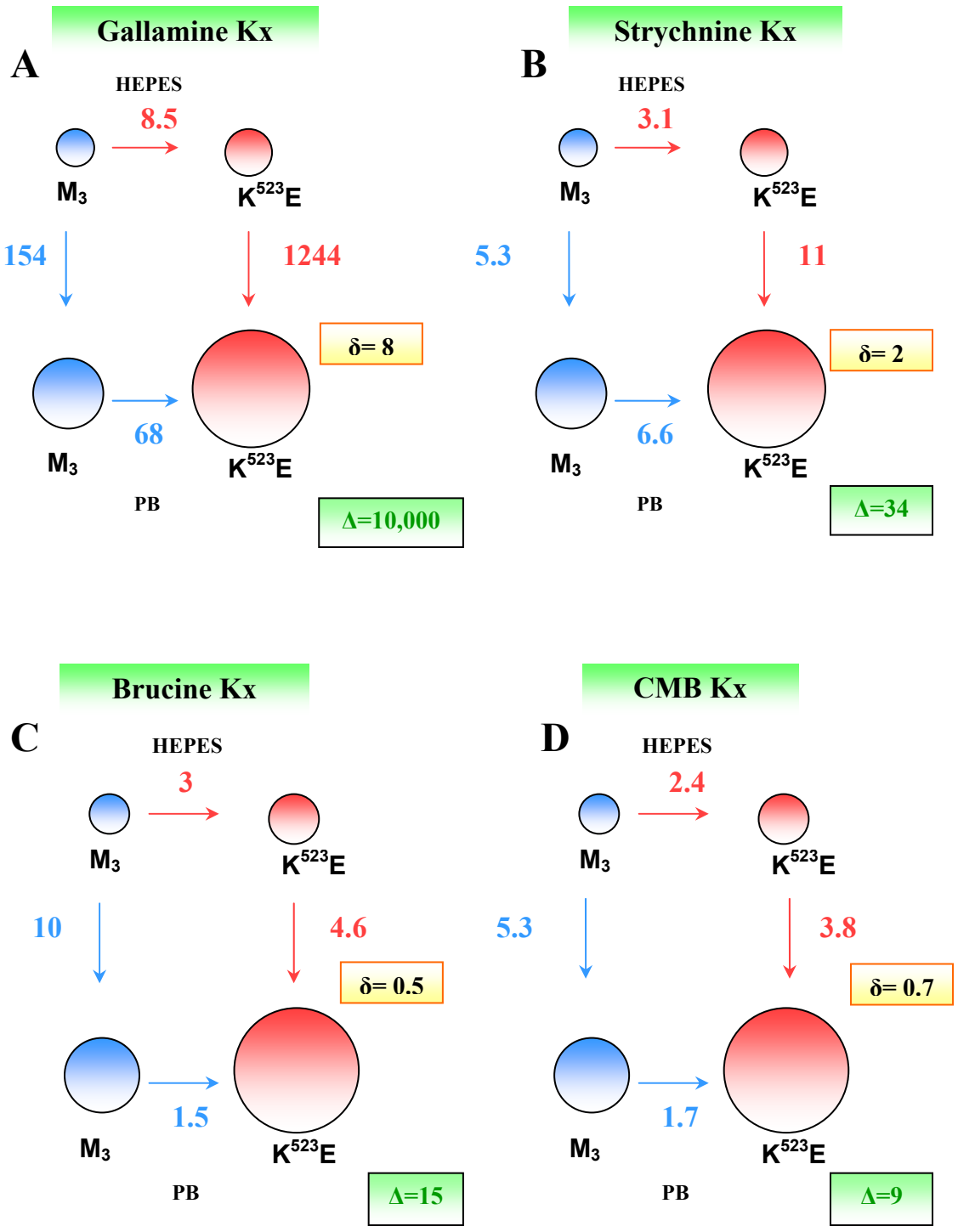

Table 4.4: Differences in binding affinity of ligands between M_3 receptor in Hepes and K523E mutant in PB (- fold)

	Δ (Kocc) Overall changes in affinity (fold)	Δ (Kx) Overall changes in affinity (fold)	δ (Kocc) Buffer or mutant Sensitivity (fold)	δ (Kx) Buffer or mutant Sensitivity (fold)
Gallamine	500	10,000	12	8
Strychnine	200	34	1.4	2
Brucine	10	15	0.5	0.5
CMB	78	9	2	0.7

Effects on cooperativities

The cooperativities that gallamine, strychnine, brucine and CMB have with [^{3}H]NMS at M_3 WT and mutations in three different buffers are illustrated symbolically in Tables 4.5 and 4.6. For ease of visualization, the data are summarised in two Tables. Table 4.5 focuses on the changes in cooperativity SAR's with mutation and how they are different under different incubation conditions. Table 4.6 focuses on how it is possible to change the cooperativity of the allosteric ligands by changing the incubation buffer.

This illustrates how we have demonstrated that cooperativities can be switched depending on the buffer used and the mutation studied. The individual allosteric compounds also showed very different patterns of cooperativities. Going from Tris to Hepes and to PB there is a tendency for the cooperativity of strychnine-related ligands to become more positive, i.e. cooperativity increases, α becomes greater. Gallamine instead, tends to become more negatively cooperative.

As a general finding, we have also observed, for the strychnine-related ligands, that for the particular mutant, K523E, the cooperativity has also increased, such that in PB, where the buffer effect and effect on mutation are combined, α was always greater than 1, even if α were less than 1 in the other buffers.

The tables illustrate how the effect of a mutation on cooperativity may be observed in one buffer and not another. It is important to know this possibility when comparing ones results with those from labs where the binding assay may have been carried out under different conditions. It is noteworthy that different cooperativities in functional studies from those observed in binding studies may be explained by the different conditions (buffer and temperature) used in the assays of binding, relative to the standard conditions used in functional assays.

Table 4.5: The changes in cooperativity SAR of four allosteric ligands at M_3 receptors as a function of mutation and incubation conditions

Tris Buffer	M_3	$K^{523}E$	$K^{523}Q$	$N^{132}G$
Cooperativity with [^{3}H]NMS				
Gallamine	-	--	--	-
Strychnine	0	+	-	-
Brucine	--	-	-	-
CMB	-	-	-	-
Hepes Buffer	M_3	$K^{523}E$	$K^{523}Q$	$N^{132}G$
Cooperativity with [^{3}H]NMS				
Gallamine	-	-	-	-
Strychnine	-	+	-	-
Brucine	-	0	-	-
CMB	-	-	-	-
PB Buffer	M_3	$K^{523}E$	$K^{523}Q$	$N^{132}G$
Cooperativity with [^{3}H]NMS				
Gallamine	--	--	--	--
Strychnine	+	++	+	0
Brucine	-	+	0	0
CMB	-	+	-	-

Table 4.5: The estimates of cooperativities are represented by symbols:

--: $0 < \alpha < 0.01$; - : $0.02 < \alpha < 0.8$; **0**: $0.81 < \alpha < 1.2$; +: $1.21 < \alpha < 3$; ++:$3.1 > \alpha > 10$

Table 4.6: Effects of different ionic conditions on the cooperativities of the four allosteric ligands with NMS

Cooperativity with [^{3}H]NMS				
Gallamine	**M_3**	**$K^{523}E$**	**$K^{523}Q$**	**$N^{132}G$**
Tris	-	--	--	-
Hepes	-	-	-	-
PB	--	--	--	--
Strychnine	**M_3**	**$K^{523}E$**	**$K^{523}Q$**	**$N^{132}G$**
Tris	0	+	-	-
Hepes	-	+	-	-
PB	+	++	+	0
Brucine	**M_3**	**$K^{523}E$**	**$K^{523}Q$**	**$N^{132}G$**
Tris	--	-	-	-
Hepes	-	0	-	-
PB	-	+	0	0
CMB	**M_3**	**$K^{523}E$**	**$K^{523}Q$**	**$N^{132}G$**
Tris	-	-	-	-
Hepes	-	-	-	-
PB	-	+	-	-

Table 4.6: The estimates of cooperativities are represented with symbols:

--: $0< \alpha <0.01$; - : $0.02< \alpha <0.8$; **0**: $0.81 < \alpha < 1.2$; +: $1.21 < \alpha < 3$; ++:$3.1> \alpha > 10$

Buffer effects and the Jakubik et al. data

Our data discussed in the previous sections have illustrated how affinities and cooperativities can be modulated strongly by carrying out the binding assays under different conditions. We were aware that (Jakubik et al., 1997) had reported similar affinities and cooperativities for brucine at M_3 receptors and strychnine at M_1 receptors from those found in Hepes buffer in this study and in (Lazareno and Birdsall, 1995;Lazareno et al., 1998;Gharagozloo et al., 1999).

However their data for brucine at M_1 receptors and strychnine at M_3 receptors differed markedly from the concordant results of our experiments and those of (Lazareno and Birdsall, 1995;Lazareno et al., 1998) in Hepes buffer. There are over 10-fold changes in affinity as well as qualitative and quantitative differences in cooperativity.

As Jakubik et al., 1997 carried out their studies in a slightly different buffer from our Hepes buffer we decided to explore whether the Jakubik buffer was generating M_1/M_3 subtype selective changes in affinity and cooperativity. We reproduced exactly the Jakubik data for brucine at M_3 receptors and strychnine at M_1 receptors and in side-by side experiments and showed that the binding parameters obtained were very similar to those determined in Hepes buffer. However we found that our data for brucine at M_1 receptors and strychnine at M_3 receptors in the Jakubik buffer did not match that reported by Jakubik et al., (Fig 4.8) but agreed with our data in Hepes buffer. This showed that, in our hands, there is little difference in the binding of brucine and strychnine at M_1 and M_3 receptors between Hepes buffer and the Jakubik buffer. We confirmed using dissociation assays that our equilibrium and kinetic data matched the predictions of the allosteric ternary complex model. Jakubik et al did not perform dissociation assays to check the validity of the analysis of their data by the ATCM.

In conclusion, we have not found an explanation for the difference between our data and that reported by Jakubik et al. It is not due to different incubation conditions.

In summary:

- We confirmed that performing one point kinetic assays is valid to identify and measure allosteric interactions and to calculate the Log Kocc of allosteric ligands.

- We found that the K523E mutation has an important effect of increasing the affinities (both log Kx and log Kocc) of all the modulators tested, showing that this single residue has a clear role in the binding of allosteric modulators which bind to the gallamine site. We also found that affinities were increased to a greater extent by incubating in buffer with low ionic strength, PB.

- We have been able to quantify the magnitude of the changes produced at the M_3 receptor by combining these two factors (the effect of K523E mutation and the PB buffer) on affinities of the four allosteric compounds studied. Up to 10,000 fold changes in affinity generated.

- Two new parameters have been introduced in this study, overall affinity change (Δ) and sensitivity factor (δ).

- We have shown that cooperativities can be modulated strongly by a single mutation and by using different buffer conditions. The mutation K523E tended to make the cooperativity more positive in all the strychnine structure-related compounds studied.

- We were not successful in our attempt to find an explanation of the discrepancy between our data and that found by Jakubik et al., but we were able to show that this discrepancy is not due to different incubation conditions. We showed that the binding parameters obtained by carrying out binding assays under the two incubation conditions are comparable with each other.

Chapter 5. Characterization of the interactions between ACh and allosteric ligands that bind to the 'gallamine' binding site

5.1 Introduction

Given the current lack of sufficiently subtype-selective orthosteric mAChR ligands, allosteric modulators of mAChRs are potentially useful alternatives in the therapy of disorders that involve a mAChR component, such as cognitive dysfunction, schizophrenia, and a variety of pain states. Besides showing positive allosteric effects with an antagonist, it is obviously very important to find agents that show positive cooperativity with an agonist, especially with the endogenous neurotransmitter, acetylcholine. These are known as enhancers. An agent that has a specific effect on acetylcholine at only one subtype and, at the other subtypes, has different effects or no effect at all (neutral modulators) would exhibit a novel form of selectivity and be a potentially useful drug. A clear example of a possible therapeutic agent for the Alzheimer disease is a modulator which shows positive cooperativity only at M_1 muscarinic receptors.

Allosteric drugs can regulate receptor function in a selective way compared with agonists and antagonists. For the development of these potential therapeutic and selective allosteric drugs, the interactions between the endogenous neurotransmitter and the allosteric ligand are particularly important. To establish the relevant structure-activity relationships it is necessary to obtain quantitative binding data to define the allosteric interaction. In the case of allosteric agents this is particularly difficult, because two parameters, i.e., the affinity of the agent for the unliganded receptor and the cooperativity of its binding to neurotransmitter-occupied receptor to form the ternary complex, are required to define the interaction. The situation is even more complex when a third, radiolabeled, ligand must be used to detect the allosteric interaction between an allosteric agent and the neurotransmitter, because the effect of an allosteric agent depends, both quantitatively and qualitatively, on the nature of the particular

ligand occupying the 'primary' orthosteric binding site (Stockton et al., 1983;Tucek et al., 1990).

So far, we have quantified the interactions between several allosteric modulators and the radiolabelled antagonist [^{3}H]NMS to M_3 and M_1 WT receptors, and different mutated M_3 receptors under different incubation conditions. A question that could arise at this point is why the endogenous ligand [^{3}H]ACh has not been used to quantify the effects of the allosteric modulators directly as it would be clinically more relevant. High affinity [^{3}H]ACh binding to the M_2 and M_4 subtypes can be measured. However the ACh affinity for receptor G-protein complexes of M_1 or M_3 receptors is much lower and essentially no specific [^{3}H]ACh binding can be detected. In addition both the K_D and *Bmax,* of [^{3}H]ACh binding may be altered by perturbations of receptor-G protein coupling, so we did not attempt to investigate changes in [^{3}H]ACh binding. Consequently, indirect methods for detecting and quantifying the allosteric interaction between ACh and several allosteric modulators acting at muscarinic receptors need to be used. The methods used in this study were first described by (Lazareno and Birdsall, 1995) and were applied to generate quantitative data on allosteric interactions at muscarinic receptors and also at other G protein-coupled receptors.

In this section, the effect of several allosteric agents which bind to the 'gallamine' binding site on the binding of ACh to M_3, M_1 WT and M_3 mutated receptors have been studied under two different conditions. The alkaloid brucine is an enhancer only at M_1 receptors. In contrast its structurally related derivative, CMB, displays positive cooperativity exclusively at the M_3 receptor subtype. In order to further investigate the selective effects of these allosteric compounds with ACh, three singly mutated M_3 receptors have been studied using three different approaches. As shown previously, the ionic strength and the composition of the incubation buffer can have an important influence on the magnitude of the cooperativity. For that reason, two different incubation conditions have been also studied, Hepes and PB. This study could provide us with additional insights into the molecular basis that underlies the direction of cooperativity of an allosteric interaction, at M_1 and M_3 receptors.

The reason for using different methods is that we had a large number of different factors to measure. The first two methods used were necessary to identify qualitatively where

the interesting effects were occurring. The third method used was to quantify the allosteric effects detected using the previous two methods.

In this section the interactions of brucine, CMB and strychnine on the binding of ACh at M_3, M_1 and mutants in two buffers have been studied. We will only be focusing on cooperativities as all the affinity constants of the allosteric agents have been reported in more detail in the previous chapter, where the allosteric interactions of ligands that bind to the gallamine site with [^{3}H]NMS have been described.

5.2 Effects of an allosteric modulator on [^{3}H]NMS binding in the presence and absence of acetylcholine

5.2.1 Inhibition of [^{3}H]NMS binding by a fixed concentration of ACh and different concentrations of the modulator.

This is a semiquantitative assay which allows the effect of an agent on [^{3}H]NMS binding to be directly compared with its effect on unlabeled ACh binding. Radioligand binding is measured alone and in the presence of a range of concentrations of allosteric agent, (this is the first curve), and using the same concentrations of allosteric ligands but in the presence of a fixed concentration of unlabeled competitive ligand, ACh (second curve). All the experiments were performed in presence of 0.2 mM of GTP to minimise the effects of receptor-G protein coupling on the results.

The parameters that can be determined from this kind of assay are the affinity of the allosteric agent for the free receptor (Kx) and its cooperativity (α) with NMS, which is given by the direction of the first curve. These are the same parameters obtained in previous section in equilibrium binding assays, which was in absence of ACh. The inhibitory effect of the fixed concentration of ACh on the binding of [^{3}H]NMS in absence of the allosteric agent gives an estimation of the affinity of ACh for the unoccupied receptor. The effect of the presence of the allosteric ligand in the presence and absence of ACh gives an estimation of beta (β), the cooperativity between the allosteric ligand and ACh. This is obtained by fitting the data to the ternary complex model. As only one concentration of ACh is used, the measure of beta may require confirmation by further experiments.

The effects of two allosteric ligands, brucine and CMB, which have different patterns of positive cooperativity in the binding of [^{3}H]NMS and ACh have been studied at M_3 and M_1 WT, and three M_3 mutated receptors (K523E, K523Q and N132G) under two different incubation buffers, Hepes and PB. Because of time restrictions, Tris was not tested in these assays, as previous experiments did not show much difference in the results in this buffer compared to Hepes, and this latter buffer is closer to physiological in composition.

A fixed concentration of [^{3}H]NMS, normally its K_D for the receptor, and 20 μM of ACh have been used in all the experiments. The choices of the range of different concentrations of the allosteric ligands were made using the similar criteria as those applied in previous section in equilibrium studies (e.g. the highest concentration of allosteric ligand should not be more than 0.5 log units of the Kocc to avoid kinetic artifacts).

The affinities of brucine, CMB and ACh for the M_3 and M_1 WT and the K523E mutation under two different buffers and the semiquantitative estimates of cooperativities obtained in this kind of assay are shown in Tables 5.1 and 5.2.

To simplify following the sections, the results and graphs of the mutations K523Q and N132G will not be discussed as the results obtained are similar to M_3 WT. Only the results for K523E and M_3 and M_1 are described.

Effect of Brucine on ACh binding

Figure 5.1 shows the different pattern of cooperativities of brucine on the binding of [^{3}H]NMS in the absence of ACh (upper curve in all the graphs) and in the presence of ACh (lower curve) at M_3 and M_1 WT and the K523E mutated M_3 receptor in two different buffers. The curves are the fits to the ATCM with the cooperativities shown in Table 5.1 and 5.2 (pages 168 and 169).

At M_3 WT in Hepes, brucine has a negative cooperativity with [^{3}H]NMS as well as with ACh, whereas at the M_1 subtype, the cooperativity with [^{3}H]NMS is neutral and slightly positive with ACh. This neutral cooperativity with [^{3}H]NMS and positive cooperativity

Fig.5.1: Effect of brucine on the [^{3}H]NMS equilibrium curves in absence and presence of one concentration of ACh at the M_3 and M_1 WT and the K523E mutant in HEPES

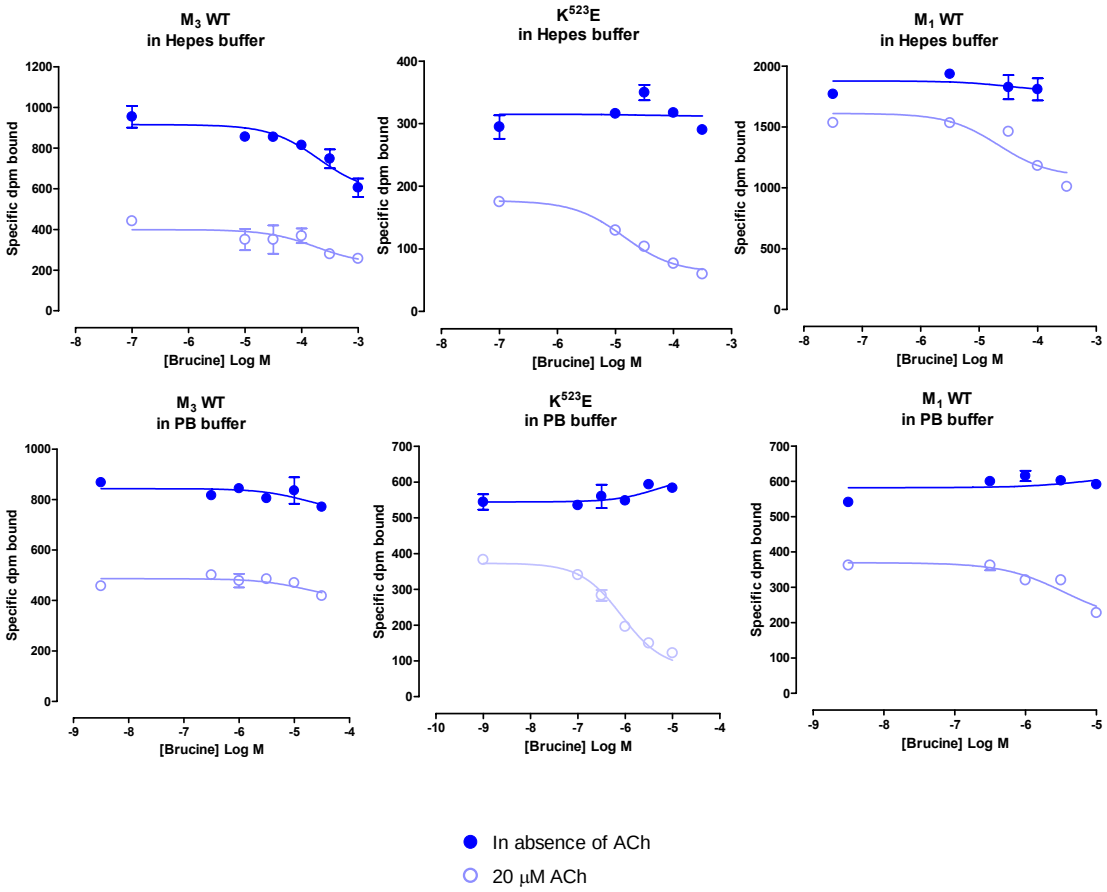

with ACh, is also seen at the mutant K523E, which has become qualitatively similar to M_1 WT, but showing an even higher positive cooperativity with ACh.

In PB buffer, cooperativities at M_1 are not changed whereas at K523E the cooperativity of brucine with [^{3}H]NMS became positive and with ACh even more positive than that found in Hepes. At M_3 WT in PB, the cooperativities, both with [^{3}H]NMS and ACh, were also changed, becoming neutral.

Effect of CMB on ACh binding

Figure 5.2 shows also the different pattern of cooperativities of CMB with [^{3}H]NMS and ACh at the M_3, M_1 WT and the mutated M_3 receptor in two buffer conditions.

In Hepes buffer the cooperativity between CMB and [^{3}H]NMS was negative at M_3, M_1 and the mutant K523E. This negative cooperativity remained in all the receptors when we incubated in PB buffer except for K523E which showed a switch from negative to positive cooperativity. This effect is shown in the upper curve of the K523E mutant in PB buffer panel in Fig 5.2 which shows the [^{3}H]NMS bound increasing with [CMB]. On the other hand, the cooperativity between CMB and ACh in Hepes buffer is positive at M_3 with the binding of [^{3}H]NMS in the presence of ACh decreasing, reflecting the increase in ACh potency in the presence of CMB. At K523E this positive cooperativity is increased, and at M_1 it is negative with ACh. In PB buffer, the positive cooperativities of M_3 and K523E with CMB were increased compared to Hepes, and at M_1 CMB cooperativity with ACh switched from negative to neutral.

It should be noted that it is not always possible to simply interpret these data. The effect of an allosteric ligand on the ability of ACh to inhibit [^{3}H]NMS binding reflects both the effect of the allosteric ligand on [^{3}H]NMS binding alone and on ACh binding. Depiction of the binding data as an 'affinity ratio' plot (Lazareno and Birdsall, 1995) or analysis of the data by the ATCM does provide an estimate of the cooperativity with ACh.

Fig.5.2: Effect of CMB on the [^{3}H]NMS equilibrium curves in absence and presence of one concentration of ACh at the M_3 and M_1 WT and the K523E mutant in HEPES

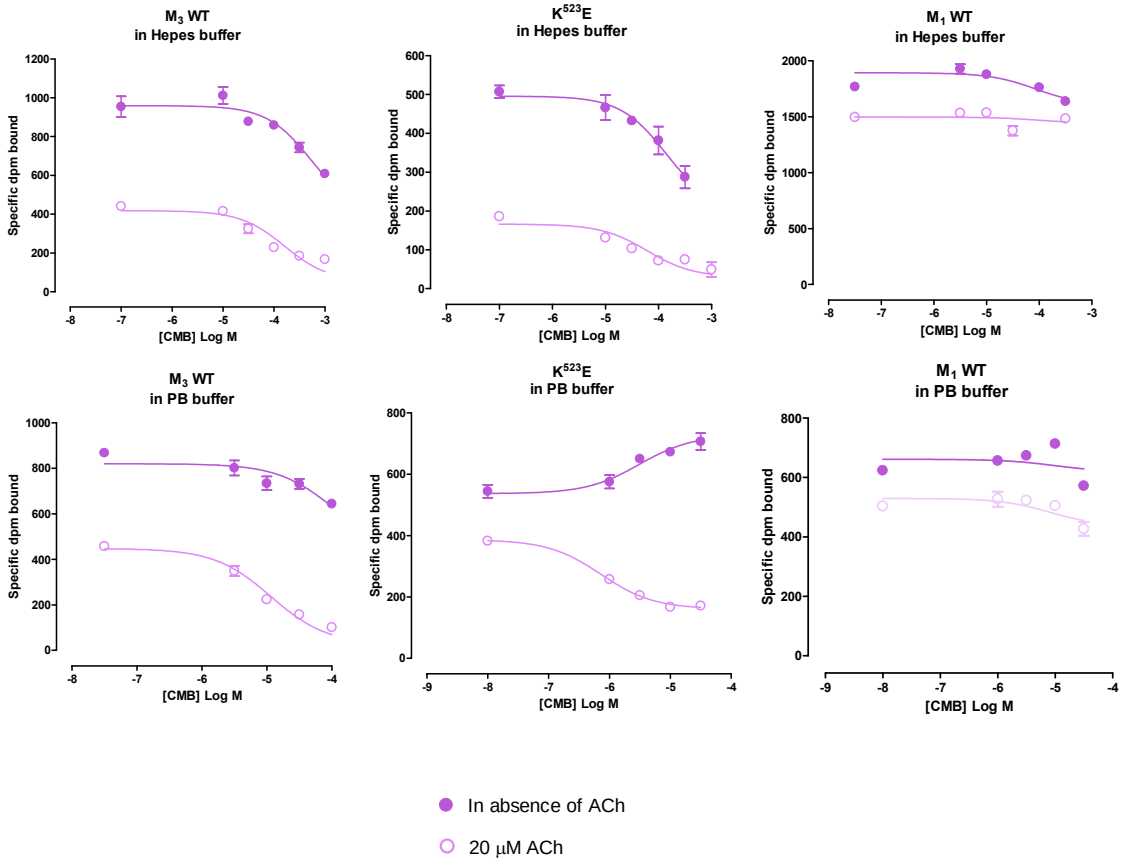

5.2.2 Inhibition of [^{3}H]NMS binding by different concentrations of ACh and a fixed concentration of the modulator

In this kind of experiment, different concentrations of ACh were used to be able to quantify further the cooperativity (β) of allosteric modulators with ACh. Only one concentration of the allosteric modulator is used in this case, which is selected based on the concentration which caused maximal effect without having a kinetic artefact. As only one concentration is used, it is necessary to fix the Kocc value in order to fit the data to the ternary complex model equation (equation 9 in *Material and Methods*). This equation is similar to that used previously, but with the nomenclature of the affinity constants and concentrations of the allosteric ligand and ACh reversed, to reflect which was the independent variable used in the data analysis. This experimental protocol allows the affinity of acetylcholine for the free receptor, in absence of the modulator to be precisely determined by its inhibition of [^{3}H]NMS binding. It measures the change of the affinity of acetylcholine in presence of an allosteric modulator, i.e a measure of the cooperativity of the allosteric modulator with acetylcholine. The cooperativity is positive if the curve is shifted to the left, enhancing the ACh potency, or negative if the curve is shifted to the right.

From the previous method we obtained the information about the potency of the allosteric ligand (Kx) which is necessary in order to choose the concentration of allosteric ligand to be used in this second method. It differs from the previous one as it gives information about the whole ACh dose-response curve. The ACh inhibition curve is shifted in a parallel fashion. It also serves as a test to see if there is something unusual happening such as a change in the slope factor of the ACh inhibition curve. However for the data reported in this chapter there is no evidence of allosteric ligands producing anything other than a parallel shift in the ACh inhibition curve.

Inhibition of [^{3}H]NMS by different concentrations of ACh and a fixed concentration of the CMB and brucine at M_3 and M_1 WT and the M_3 mutations, N132G, K523E and K523Q in two buffer conditions have been made. The parameters obtained are shown in Table 5.1 and 5.2 (pages 168 and 169). Fig 5.3 illustrates an example of how the ACh inhibition curve is shifted to the left by a sufficiently high concentration of CMB (300

μM) at M_3 receptors in Hepes. This shift represents the change of the ACh IC50 in presence of 300 μM CMB and a positive cooperativity between CMB and ACh.

Fig.5.3: Representative [^{3}H]NMS-ACh inhibition curves in absence and presence of one concentration of the modulator CMB in Hepes at M_3 WT

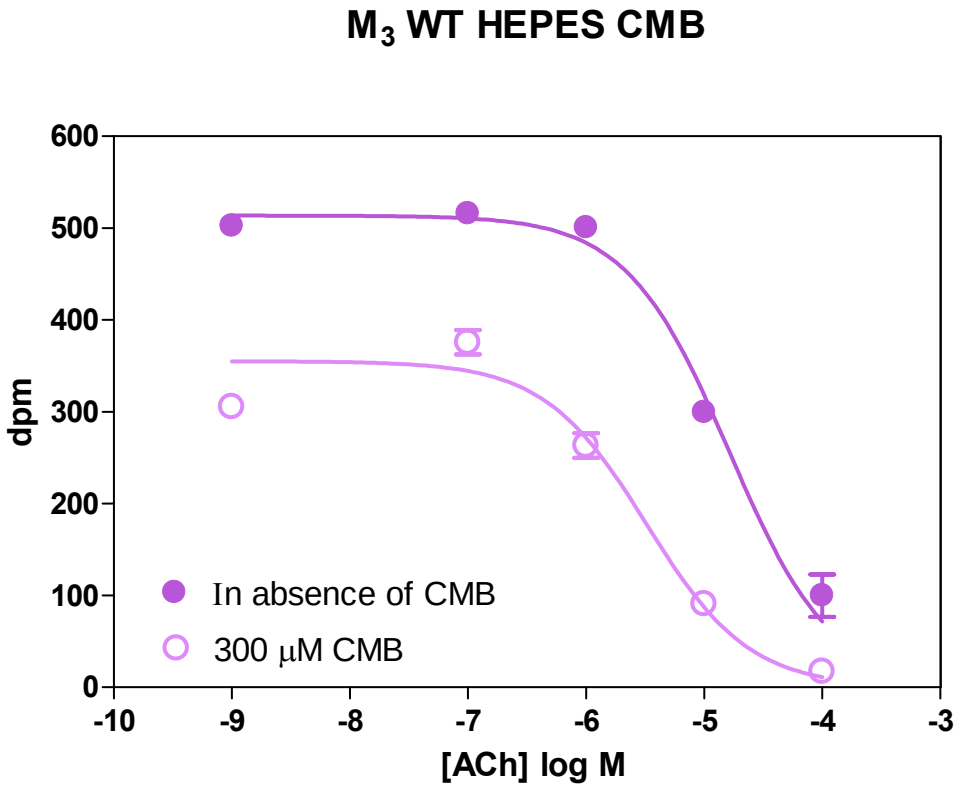

Fig 5.3: Equilibrium [^{3}H]NMS inhibition curves with different concentrations of ACh and in absence and presence on 300 μM CMB at M_3 membranes in Hepes. The first data points of both curves (-9) represent the effect of CMB in [^{3}H]NMS in absence of ACh. The data was fitted into the allosteric ternary complex model using non linear regression analysis. The log Kocc was constrained in the analysis

Therefore this cooperativity can be calculated using the ternary complex model equation, although there is still not enough data to quantify this parameter precisely. By looking at the first point of each curve we can visually estimate the cooperativity between [^{3}H]NMS and CMB, which in this particular case is shown to be negative, as in presence of 300 μM of CMB the [^{3}H]NMS binding is inhibited, indicating a negative cooperativity, which matches with the cooperativity observed in the previous chapter between CMB and [^{3}H]NMS at M_3 WT in Hepes.

To simplify the following sections, the results of the mutations K523Q and N132G will not be discussed as the results obtained are similar to M_3 WT. Only the results for K523E and M_3 and M_1 are described.

Effect of Brucine on the ACh inhibiton curve

At M_3 WT in Hepes, brucine has a weak negative cooperativity with ACh shifting the ACh curve slightly to the right. In contrast there is a shift to the left in the ACh inhibition curve at M_1 WT which is even higher at the mutant K523E in Hepes buffer. In PB buffer, the shift to the left at M_1 is not changed and becomes higher at K523E. At M_3 WT in PB the cooperativity is now neutral.

Effect of CMB on the ACh inhibiton curve

At M_3 WT in Hepes, CMB shifts to the left the ACh inhibition curve as is shown in Fig 5.3. This shift is also observed at K523E in Hepes, but the increase in ACh potency is even higher. At M_1 there is no change in the ACh IC50 indicating neutral cooperativity with CMB. In PB, the ACh IC50 was displaced to the left at M_3 and K523E even more than in Hepes. At M_1 WT the curve was displaced slightly to the left, indicating a shift in cooperativity between CMB and ACh at M_1 from negative in Hepes to neutral in PB.

All the parameters obtained in this section by studying the allosteric interactions between CMB and brucine with ACh at M_3 and M_1 WT and mutants in Hepes and PB was perfectly comparable with the data found in previous section. However, not enough information was obtained in order to determine β without constraining parameters in the ATCM. Values of β will be quantitated in the experiments described in next section.

5.2.3 Equilibrium binding assay with different concentrations of modulator and ACh

This type of assay measures ACh inhibition of [^{3}H]NMS binding (in the presence of GTP) in the absence and presence of three concentrations of the agent, allowing estimates of the agent affinity and its cooperativity with both [^{3}H]NMS and ACh to be made by fitting the data using the ternary complex model. In general, the full curves that are obtained yield an accurate estimate of beta with no need to make assumptions of any parameter.

Full curves for three different allosteric agents, brucine, CMB and strychnine at M_3, M_1 and K523E in two buffer conditions, Hepes and PB, are shown in Figure 5.4 and 5.5. Data for the affinities of the agents and their cooperativities with ACh are presented in Tables 5.1 and 5.2.

In these full curves, all the data points on the left of the figure represent the binding of [^{3}H]NMS in presence of different concentration of the allosteric agent in absence of ACh, so they give an estimation of alpha. As would be expected, with regard to [^{3}H]NMS binding, the values of alpha of all the compounds across the subtypes showed the same pattern as previously found in both Hepes and PB (Table 5.1 and 5.2).

The dark curves in Fig 5.4 and 5.5 (either blue or purple indicating the effect of brucine or CMB respectively) represent the [^{3}H]NMS binding inhibition curve in presence of different concentrations of ACh, the midpoint of the which gives us an estimation of ACh affinity. By adding increasing concentrations of allosteric ligands a progressive modulation on ACh binding can be observed. In general, if the curve is shifted to the left, the cooperativity of the allosteric modulator with ACh is positive. On the other hand if the shift is to the right, the cooperativity is negative. When there is no change, there is neutral cooperativity.

Fig.5.4: Inhibition by ACh of [^{3}H]NMS binding in the absence and presence of different concentrations of brucine at M_3 and M_1 WT and K523E in Hepes and PB

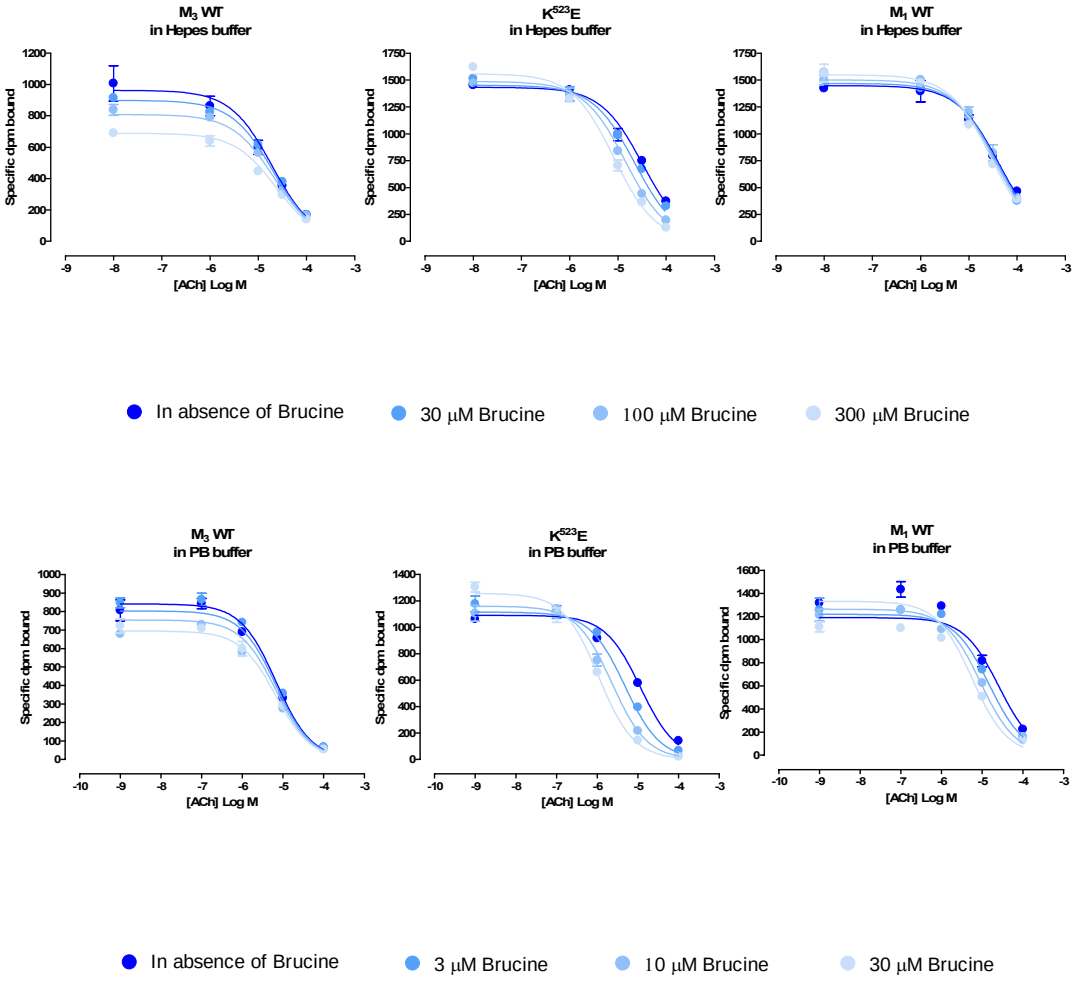

Fig 5.4: Inhibition by different concentrations of ACh of [^{3}H]NMS in absence and presence of a fixed concentration of brucine at M_3, M_1 and K523E in Hepes and PB. The first data points of both curves represent the effect of brucine in [^{3}H]NMS in absence of ACh. The data were fitted into the allosteric ternary complex model using non linear regression analysis

Fig.5.5: Inhibition by ACh of [^{3}H]NMS binding in the absence and presence of different concentrations of CMB at M_3 and M_1 WT and K523E in Hepes and PB

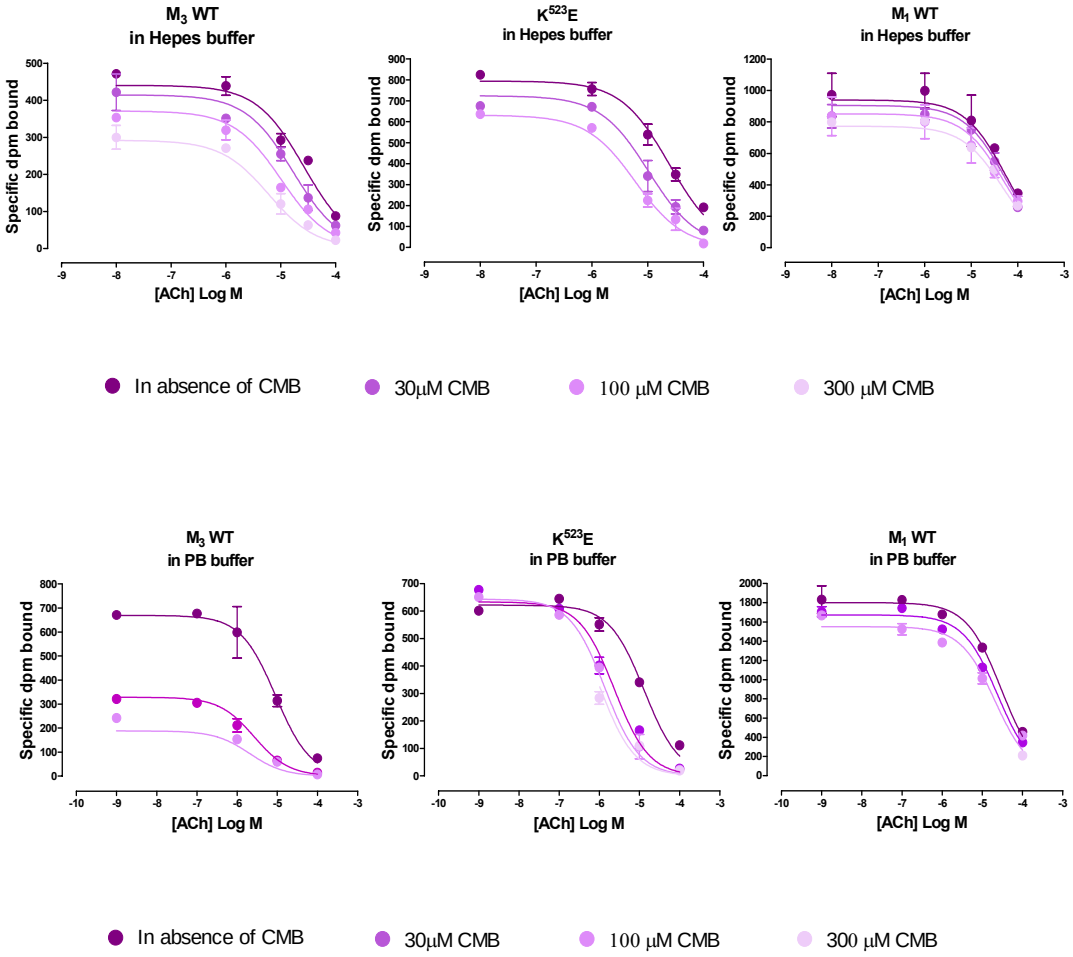

Fig 5.5: Inhibition by different concentrations of ACh of [^{3}H]NMS in absence and presence of a fixed concentration of CMB at M_3, M_1 and K523E in Hepes and PB. The first data points of both curves represent the effect of CMB in [^{3}H]NMS in absence of ACh. The data was fitted into the allosteric ternary complex model using non linear regression analysis

Brucine

With regard to ACh, brucine is known to have weak negative cooperativity with ACh at M_3 WT, whereas it acts as an enhancer at M_1 receptors and not at other subtypes. This cooperativity became even more positive at K523E. PB also tended to increase all the cooperativities with brucine, being neutral at M_3, more positive at M_1 and yielding a big positive cooperativity (over 30) at K523E (Fig 5.4).

CMB

CMB is known to be an exclusively M_3 enhancer whereas at M_1 it has negative cooperativity with ACh (Lazareno et al., 1998). This behaviour was reproduced in Fig 5.5. At K523E, the positive cooperativity was enhanced. As found for brucine, PB buffer tends to increase the cooperativities of CMB to all the receptors, being much more positive in M_3 and K523E and neutral at M_1 relative to Hepes.

Strychnine

The data in Table 5.1 and 5.2 confirms the known negative cooperativity at M_3 and M_1 of strychnine with ACh in Hepes, strongly negative at M_3 and weakly negative at M_1 (Lazareno and Birdsall, 1995). However the cooperativity of strychnine with ACh at K523E in this buffer was neutral. As was observed for brucine and CMB, in PB buffer, all the cooperativities of strychnine with ACh were increased, being only weakly negative at M_3, neutral at M_1, and positive at K523E.

Table 5.1: Binding parameters of the allosteric interactions between CMB, brucine and strychnine with [^{3}H]NMS and ACh at M_3 and M_1 WT and the M_3 mutants in Hepes

CMB

HEPES	*LogK_{CMB}*	*LogKocc (NMS)*	*α*	*LogK_{ACh}*	*LogKocc (ACh)*	*β*
M_3	3.46±0.05	[2.9]	(0.30±0.04)	5.01±0.06	(5.6)	4.2±0.5
$K^{523}E$	3.84±0.05	[3.7]	(0.47±0.06)	4.77±0.10	(5.6)	8.5±1.8
M_1	4.26±0.06	[4.0]	(0.57±0.07)	4.56±0.11	(4.4)	0.70±0.09
K523Q	3.78±0.08	[3.5]	(0.30±0.06)	4.81±0.06	(5.7)	9.1±1.0
N132G	3.65±0.16	[2.9]	(0.25±0.07)	4.92±0.09	(5.3)	3.7±1.6

Brucine

HEPES	*LogK_{Bruc}*	*LogKocc (NMS)*	*α*	*LogK_{ACh}*	*LogKocc (ACh)*	*β*
M_3	3.89±0.05	[3.4]	(0.42±0.05)	4.91±0.08	(4.8)	0.78±0.21
$K^{523}E$	4.39±0.08	[4.4]	(1.1±0.17)	4.72±0.11	(5.7)	22±6
M_1	4.74±0.05	[4.7]	(0.95±0.12)	4.60±0.11	(4.9)	2.2±0.2
K523Q	4.01±0.15	[3.6]	(0.47±0.16)	4.70±0.05	(4.7)	1.5±0.7
N132G	3.47±0.05	[3.3]	(0.67±0.25)	4.77±0.04	(4.9)	1.5±0.5

Strychnine

HEPES	*LogK_{Stry}*	*LogKocc (NMS)*	*α*	*LogK_{ACh}*	*LogKocc (ACh)*	*β*
M_3	4.30±0.07	[4.1]	(0.62±0.09)	4.94±0.08	(3.6)	0.05±0.04
$K^{523}E$	4.82±0.11	[5.1]	(2.1±0.56)	4.63±0.07	(4.6)	1.0
M_1	5.11±0.12	[4.9]	(0.50±0.11)	4.69±0.09	(4.5)	0.22±0.05
K523Q	4.26±0.03	[4.1]	(0.72±0.04)	4.79±0.01	(3.9)	0.12
N132G	4.25±0.04	[4.2]	(0.58±0.06)	4.73±0.12	(3.4)	0.05±0.01

For legends and footnotes see page 170

Table 5.2: Binding parameters of the allosteric interactions between CMB, brucine and strychnine with [^{3}H]NMS and ACh at M_3 and M_1 WT and the M_3 mutants in PB

CMB

PB	*LogK_{CMB}*	*LogKocc (NMS)*	*α*	*LogK_{ACh}*	*LogKocc (ACh)*	*β*
M_3	4.18±0.13	[3.7]	(0.39±0.11)	5.12±0.15	(6.3)	20±9
$K^{523}E$	4.62±0.15	[4.8]	(1.50±0.36)	4.67±0.15	(6.3)	22±5
M_1	5.39±0.10	[5.0]	(0.55±0.04)	5.01±0.13	(5.1)	1.2±0.1
K523Q	4.33±0.13	[3.9]	(0.22±0.11)	4.71±0.01	(6.0)	21
N132G	4.38±0.17	[3.6]	(0.18±0.07)	5.15±0.01	(5.9)	6.0

Brucine

PB	*LogK_{Bruc}*	*LogKocc (NMS)*	*α*	*LogK_{ACh}*	*LogKocc (ACh)*	*β*
M_3	4.89±0.02	[4.7]	(0.66±0.03)	5.30±0.06	(5.4)	1.0±0.1
$K^{523}E$	5.06±0.04	[5.4]	(1.94±0.23)	5.14±0.07	(6.7)	36±5
M_1	5.12±0.10	[5.2]	(1.35±0.24)	5.09±0.06	(5.8)	7.4±2.6
K523Q	4.59±0.06	[4.6]	(0.96±0.16)	4.97±0.03	(5.1)	1.4±0.2
N132G	4.38±0.06	[4.4]	(1.08±0.06)	5.16±0.10	(5.3)	2.0±0.5

Strychnine

PB	*LogK_{Stry}*	*LogKocc (NMS)*	*α*	*LogK_{ACh}*	*LogKocc (ACh)*	*β*
M_3	5.02±0.07	[5.3]	(1.51±0.23)	5.31±0.17	(4.8)	0.40±0.22
$K^{523}E$	5.85±0.01	[6.4]	(3.90±0.09)	5.13±0.03	(6.0)	8.1±1.6
M_1	6.04±0.07	[6.0]	(0.94±0.14)	5.14±0.15	(5.0)	0.81±0.20
K523Q	5.39±0.03	[5.6]	(1.29±0.11)	4.97±0.01	(4.9)	0.9
N132G	5.18±0.03	[5.2]	(1.04±0.07)	5.35±0.01	(4.7)	0.2

For legends and footnotes see page 170

Tables 5.1 and 5.2:

Binding parameters of the allosteric interactions between CMB, brucine and strychnine with [^{3}H]NMS and ACh at M_3 and M_1 WT and the M_3 mutants, N132G, K523E and K523Q. Starting from the left hand side of the table, the parameters shown are: (a) The Log Kx of the allosteric agents when the receptor is not occupied by [^{3}H]NMS. The mean value was obtained from equilibrium assays both in absence and presence of ACh. (b) The affinity of the allosteric agents when NMS is bound to the receptor (Log Kocc). It is shown in square brackets because this value has been constrained when fitting the data to the allosteric ternary complex model. This value was obtained in kinetic experiments (Table 4.2 previous chapter). α is the cooperativity between the allosteric agents and [^{3}H]NMS. This value has been calculated from the ratio between the log Kocc and the log Kx and is shown in brackets. (d) Log K_{ACh} is the affinity of ACh for the unoccupied receptors and the mean that has been obtained in equilibrium assays. (e) The log $Kocc_{ACh}$ is the affinity of ACh when the receptor is occupied by the allosteric agent. This mean value has been calculated from the product of $LogK_{ACh}$ and β, which is the last parameter shown. The β value was obtained from the analysis of equilibrium experiments in presence of ACh, applying the ATCM

5.3 Discussion

The alkaloid brucine has been reported to have positive cooperativity with ACh only at M_1 WT in Hepes (Lazareno et al., 1998). This positive cooperativity observed, ca 2 fold, is similar to the magnitude of the positive cooperativity between therapeutically effective benzodiazepine tranquilizers and GABA at $GABA_A$ receptors (Ehlert et al., 1983). At M_3 receptors the cooperativity of brucine with ACh is negative. The analogue, CMB, has been shown to have positive cooperativity only at M_3 receptors and negative cooperativity at M_1 in Hepes with ACh (Lazareno et al., 1998). Strychnine has been reported to have negative cooperativity with ACh at both subtypes (Lazareno et al., 1998;Jakubik et al., 1997).

This chapter describes the characterization of the allosteric interactions of brucine, CMB and strychnine with ACh at M_3 and M_1 WT, and the M_3 mutants N132G, K523E and K523Q in Hepes and PB by using three different methods to generate quantitative data on allosteric interactions (described in *Material and Methods* and in the *sections 5.2-4*). The previous chapter showed the characterization of the same allosteric interactions but with [^{3}H]NMS, which is a necessary step in order to analyse the data of this section using the allosteric ternary complex model equation.

The first two methods were sufficiently sensitive to allow us to detect and confirm small degrees of positive and negative cooperativities between allosteric modulators and ACh at muscarinic receptors. Both methods monitor different aspects of the binding of an allosteric agent and its allosteric effect on an unlabelled compound (the endogenous neurotransmitter, ACh). The first one describes the behaviour of the modulator on [^{3}H]NMS binding in absence and presence of a single concentration of ACh whereas the second one describes the behaviour of ACh inhibiting [^{3}H]NMS binding and how the IC50 of ACh is shifted in presence of single concentration of modulator. The first method can give an indication of the potency of the modulator and its cooperativity with both NMS and ACh but it does not examine whether the complex nature of the ACh inhibition curve has changed. The second method examines this latter possibility as well as quantifying the enhancement of inhibition of ACh potency by a single concentration of modulator. It does not measure the potency of the allosteric ligand α or β. In all these

experiments, the slope factors of the ACh inhibition curves were unchanged by modulator. This was not known (except for M_1 and M_3 WT at Hepes) and could not be assumed.

Full [^{3}H]NMS-ACh inhibition curves were also performed in the third method in order to quantify the cooperativity values of allosteric agents tested with ACh. This was analysed by using the allosteric ternary complex model equation. All the parameters obtained agreed with each other using the three methods. The cooperativities for strychnine, brucine and CMB at M_1 and M_3 agreed in general with literature data (Lazareno and Birdsall, 1995;Lazareno et al., 1998;Gharagozloo et al., 1999). However discrepancies were found between the data reported here and the data of Jakubik et at. This is shown in Table 5.3. They observed positive cooperativity with brucine at M_3 and neutral cooperativity with strychnine at M_1. We have no explanation for these discrepancies between the Jakubik data and other data in the literature. It is unlikely that slightly different buffer conditions used by Jakubik et al. could be an explanation because we found the allosteric properties of M_1 and M_3 receptors in this buffer to be very similar to that in Hepes (Table 4.3 and Fig. 4.8).

Table 5.3: Comparison of the cooperativity factors (β) for brucine and strychnine with ACh at M_1 and M_3 WT muscarinic receptors

	Strychnine	Brucine
	M_1	M_3
	Cooperativity (β)	
HEPES[a]	0.2	0.8
HEPES[b]	0.4	0.5
Jakubik data[c]	0.8	1.9

[a]: Parameters obtained from this thesis experiments (Table 5.1)

[b]: Published data (Lazareno and Birdsall, 1995;Lazareno et al., 1998)

[c]: β values from Jakubik et al.

The parameters obtained from the analysis of our full [^{3}H]NMS-ACh curves experiments were not significantly changed at the N132G and K523Q mutants relative to M_3 WT in any of the conditions tested (Tables 5.1 and 5.2). In contrast the parameters obtained at K523E were all increased in all the conditions. That indicates that this enhancement is not due to removal of the positive charge, as in the K523Q mutation this enhancement was not observed. For simplicity we will focus only in the effects observed at the K523E mutant relative to M_3 WT.

Cooperativity values obtained at M_3 WT and K523E are shown in Table 5.4 (shown as symbols). It indicates the strong effect of the K523E mutation on the cooperativity values of the three allosteric modulators tested with ACh, relative to M_3 WT. CMB has positive cooperativity with ACh and brucine and strychnine negative, the latter exhibiting strong negative cooperativity. However, at K523E, all the cooperativity values were enhanced relative to M_3 WT. In most of the cases the cooperativities were strongly positive. Brucine and CMB were enhancers at K523E in Hepes and PB and strychnine was enhancer in PB. Only between strychnine and ACh at K523E in Hepes was there neutral cooperativity, although it is worth noting that there was strong negative cooperativity at M_3 and so the cooperativity at K523E has substantially increased but not enough to make it an enhancer in Hepes.

The effect of buffer on the cooperativity values is also shown in Table 5.5. In PB buffer all the cooperativity values between brucine, CMB and strychnine with ACh were enhanced at M_3, M_1 WT and K523E relative to Hepes, indicating that incubation under low ionic strength increases cooperativity values.

Table 5.4: Effect of the K523E mutant on the cooperativity of three allosteric ligands with ACh relative to M_3 receptors in Hepes and PB

	Cooperativity with ACh	M_3	$K^{523}E$
Hepes (30°)	CMB	++	++
	Brucine	-	+++
	Strychnine	--	0
PB (20°)	CMB	+++	+++
	Brucine	0	+++
	Strychnine	-	++

--: 0< α <0.01; - : 0.02< α <0.8; **0**: 0.81 < α < 1.2; +: 1.21 < α < 3; ++:3.1> α > 10;+++: >10

Table 5.5: Effects of different ionic conditions on the cooperativities of the three allosteric ligands with ACh at M_3, M_1 WT and K523E

Cooperativity with ACh	M_3	$K^{523}E$	M_1
CMB			
Hepes (30°)	++	++	-
PB (20°)	+++	+++	0
Brucine			
Hepes (30°)	-	+++	+
PB (20°)	0	+++	++
Strychnine			
Hepes (30°)	--	0	-
PB (20°)	-	++	0

--: 0< α <0.01; - : 0.02< α <0.8; **0**: 0.81 < α < 1.2; +: 1.21 < α < 3; ++:3.1> α > 10;+++: >10

The above conclusions are represented in quantitative form for strychnine and brucine in Fig 5.6

This indicates that the mutant K523E:

- Showed enhanced cooperativity with ACh in presence of all allosteric ligands tested, compared to M_3 WT. The columns which illustrate K523E are higher in A, B, C and D relative to M_3 WT.
- Switches cooperativity of brucine with ACh from NEGATIVE to POSITIVE and strychnine from negative to neutral and positive in Hepes and PB respectively which is illustrated with the switch of the columns colour from blue to green and red.
- Has a behaviour for the interaction between brucine and ACh that is qualitatively comparable to the M_1 phenotype. The columns that illustrate K523E and M_1 in A and B are all red relative to the blue and green ones of M_3.

In addition the PB buffer tends to make cooperativity more positive. In this case all the columns B versus A and D versus C are higher.

Fig.5.6: Quantitative graphs of the log cooperativity values between brucine and strychnine with ACh at M_3 and M_1 WT and the mutant K523E in Hepes and PB

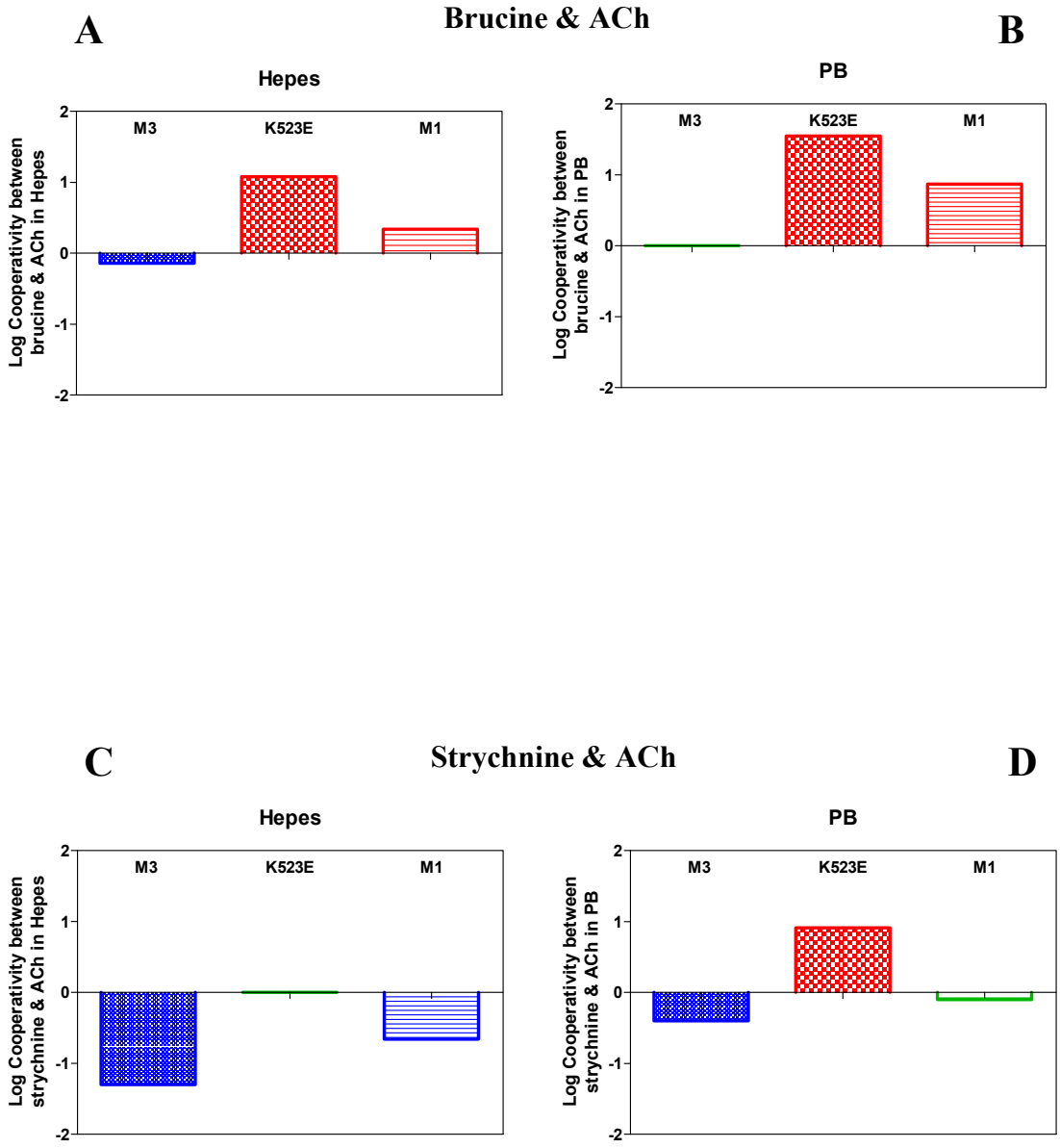

As defined in previous chapters, the cooperativity value β is the ratio between absolute values of affinities, specifically the log Kocc (affinity of the modulator in presence of ACh) and the logKx (affinity of the modulator for the unoccupied receptor). In order to further discuss the ability of K523E to modulate the cooperativity values between ACh and the three allosteric agents tested, we compared the affinity values of LogKocc of each modulator in presence of ACh ($LogKocc_{modulator}$ (ACh)) and the Log Kx at M_3 and K523E in Hepes and PB (Table 5.6). The logKocc value of the modulators when [^{3}H]NMS is bound (parameters obtained in Chapter 4) and the fold-change of the affinity values obtained relative to M_3 WT are also included in Table 5.6 for comparison. This and the subsequent table highlights the large changes in affinity that can be generated.

We can conclude by looking at these numbers, that the conformation of the receptor that is mainly changed by the K523E mutation is the one that has ACh and strychnine or brucine bound at the same time (the complex Allo-R-ACh which has the fold-changes shown in red). In Hepes for instance, the affinity of brucine at K523E when ACh is bound is 90 fold higher than at M_3 compared to only ca 3 fold higher when the receptor is unoccupied. If we compare the log Kocc of brucine to that when the receptor is occupied by [^{3}H]NMS, the difference is only ca 10 fold, indicating that the most sensitive changes are produced at the ACh occupied receptor. This conclusion can be generalised to the binding of brucine in PB, with a LogKoccBruc (ACh) at K523E 40 fold higher than M_3 WT, and to the binding of strychnine, which the LogKoccStrych(ACh) becomes ca 60 higher than M_3 in Hepes and remarkably higher (ca 160 fold) in PB. In contrast, the same changes are not seen when CMB binds, indicating that CMB binds in a different way from that of brucine and strychnine, generating much smaller effects at the ACh occupied receptor but comparable effects at the NMS occupied receptor.

It is also worth noting that the affinity values of ACh for the unoccupied receptors were buffer and mutant independent. However, this was very different when an allosteric ligand such as brucine or strychnine was bound at the K523E mutant (Tables 5.1 and 5.2), showing that the conformation of the receptors was more favourable when the two ligands (ACh and brucine or strychnine) were bound at the same time forming the

Table 5.6: Affinity parameters of brucine, strychnine and CMB for the unoccupied and ACh-occupied receptors at M_3 WT and K523E in Hepes and PB

	Hepes (30°)			PB (20°)		
Subtype	**$LogK_{Bruc}$**	***LogKocc $_{Bruc}$ (ACh)***	***LogKocc $_{Bruc}$ (NMS)***	**$LogK_{Bruc}$**	***LogKocc $_{Bruc}$ (ACh)***	***LogKocc $_{Bruc}$ (NMS)***
M_3	3.9	3.8	[3.4]	4.9	5.0	[4.7]
K523E	4.4	5.7	[4.4]	5.1	6.6	[5.4]
Increase in affinity relative to M_3 WT(fold)	**3**	**90**	**10**	**2**	**40**	**5**

	Hepes (30°)			PB (20°)		
Subtype	**$LogK_{Stry}$**	***LogKocc $_{Stry}$ (ACh)***	***LogKocc $_{Stry}$ (NMS)***	**$LogK_{Stry}$**	***LogKocc $_{Stry}$ (ACh)***	***LogKocc $_{Stry}$ (NMS)***
M_3	4.3	3.0	[4.1]	5.0	4.6	[5.3]
K523E	4.8	4.8	[5.1]	5.9	6.8	[6.4]
Increase in affinity relative to M_3 WT(fold)	**3**	**63**	**10**	**8**	**160**	**13**

	Hepes (30°)			PB (20°)		
Subtype	**$LogK_{CMB}$**	***LogKocc $_{CMB}$ (ACh)***	***LogKocc $_{CMB}$ (NMS)***	**$LogK_{CMB}$**	***LogKocc $_{CMB}$ (ACh)***	***LogKocc $_{CMB}$ (NMS)***
M_3	3.5	4.1	[2.9]	4.2	5.5	[3.7]
K523E	3.8	4.7	[3.7]	4.6	5.7	[4.8]
Increase in affinity relative to M_3 WT(fold)	**2**	**4**	**6**	**3**	**2**	**13**

ternary complex. The effect of K523E seems to be on the binding of the allosteric ligand and the transmission of the effects of the binding of ligands to the orthosteric site.

As shown in Chapter 4 (see *4.1.7 Discussion*), the effect of the mutant K523E and the PB buffer together on M_3 WT in Hepes, strongly increases the affinity of the three allosteric ligands studied when NMS is bound to the receptor. When ACh is bound to the receptor, even more dramatic increases in affinity are observed (Table 5.7). For example the brucine affinity is increased by a factor of 690 and the increase is 6,400 fold for strychnine. These are extraordinarily large changes in affinity and beg the question whether even greater changes might be produced with other allosteric ligands.

The fact that we have been able to modulate the cooperativity between allosteric agents and ACh, by introducing a residue corresponding to the M_1 subtype, and this ability of modulation is only due to the introduction of the residue E, as the neutral residue Q does not show comparable effects, may help one to understand better the mechanism of binding of these compounds to this allosteric site and in the future aid the development of therapeutically active drugs with novel mechanism of action.

In conclusion,

(a) Strychnine and brucine have similar behaviours in the way they bind to M_1, M_3 and K523E, whereas the binding of CMB is different.

(b) Brucine becomes an enhancer and strychnine shows neutral/positive cooperativity at K523E.

(c) Brucine and strychnine cooperativity values with ACh at K523E have a comparable behaviour to the M_1 phenotype. That does not occur with CMB, which keeps the M_3 phenotype (Fig 5.6).

(d) The positive cooperativity found between ACh and brucine at K523E in Hepes and PB is the highest cooperativity with ACh so far reported at M_3 receptors and comparable to the high value reported recently at M_4 receptors (Shirey et al., 2008) and Chang WY et al., 2008. Allosteric modulation of the muscarinic M_4 receptor as a novel approach to treating schizophrenia. Proceedings of the National Academy of Sciences (PNAS) *in press*.

Table 5.7: Effect of the K523E mutant and the PB buffer together relative to M_3 WT in Hepes on the affinity of three allosteric modulators when ACh is bound to the receptor

	LogKocc in presence of ACh		
	M_3 WT Hepes(30°)	$K^{523}E$ PB (20°)	Diff in affinity to M_3 WT
Brucine	3.8	6.6	**690 fold**
Strychnine	3.0	6.8	**6,400 fold**
CMB	4.1	5.7	**40 fold**

Chapter 6. Functional studies at M_3 and mutant muscarinic receptors

6.1 Introduction

The neurotransmitter ACh is released from the postganglionic parasympathetic nervous and activates muscarinic acetylcholine receptors exerting diverse physiological actions inside of the cell. The mechanism that M_3 muscarinic receptors use is shown in Fig 6.1 where ACh binds to the receptor changing its conformation from the inactive state to the active state, facilitating the binding of G protein, Gq/11 type (in the case of M_3 muscarinic subtype) to the receptor. At this binding step, Gq/11 has GDP bound and its interchange for GTP leads to the separation of the alpha subunit from the beta-gamma subunits which were forming the heterotrimeric G protein. The alpha subunit stimulates the membrane bound enzyme phospholipase C (PLC) which hydrolyses phosphoinositol 4,5-bisphosphate (PIP_2) into 1,2-diacylglycerol (DAG) and the second messenger inositol 1,4,5-triphosphate (IP_3). IP_3 is able to promote Ca^{2+} release from specialized intracellular compartments leading to physiological responses as smooth muscle contraction and glandular secretion.

In order to study the actions of ACh in functional assays we have used the phosphoinositide assay method (Jones et al., 1995). Stably transfected CHO cells with M_3 WT and mutant receptors were prelabelled with ^{3}H-myoinositol overnight and the production of ^{3}H-inositol-phosphates generated from PIP_2 during incubation in the absence and presence of muscarinic ligands (orthosteric or allosteric) was measured. The assays were always performed in the presence of Li^+ (lithium block) which inhibits the breakdown of inositol-phosphate to inositol and allows ^{3}H-inositol-phosphates to accumulate.

From the binding experiments described in previous chapters, we were able to determine ACh affinities for the different receptor species and how they were regulated by allosteric ligands. One of the main findings that we have shown in chapter 5 was the enhancer effect of brucine and CMB on ACh binding at the K523E mutant. Therefore

Fig.6.1: Modulator effects on ACh mediated phosphoinositol response

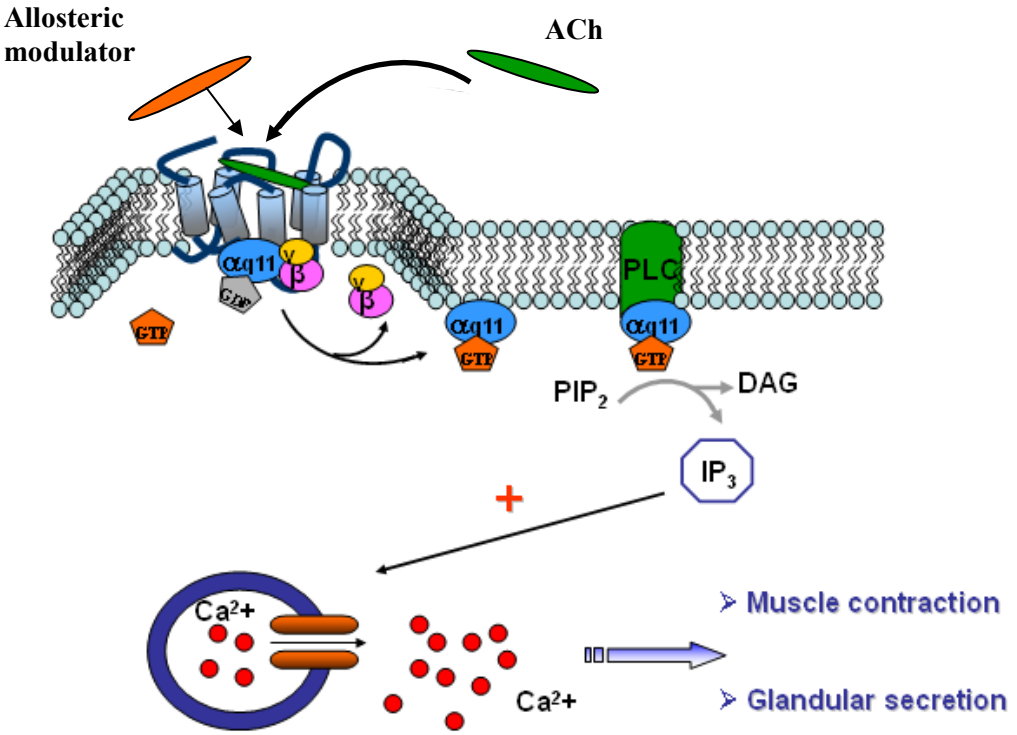

Fig.6.2: Theoretical agonist dose response curve and possible changes of the agonist potencies and Emax

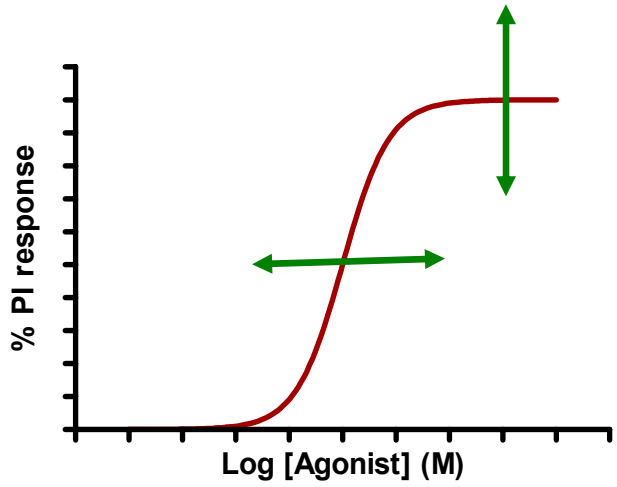

we wanted to determine whether the same allosteric effects found in binding assays could be observed in the modulation of ACh actions in functional assays.

The study of the effects of strychnine, brucine and CMB on the potency of ACh was performed by looking at the shifts in the ACh dose response curve in presence of three concentrations of the allosteric ligands. A theoretical agonist dose response curve is shown in Fig 6.2 illustrating by an arrow the possible directions of the shift that the presence of allosteric ligands could produce on the curve, relating to potency (horizontal arrow) and to Emax (vertical arrow). Dose response curves of different muscarinic agonists were also made at the M_3 WT and the mutants. A low efficacy agonist chosen was oxotremorine which, like ACh, is supposed to bind to the orthosteric site of muscarinic receptors. The molecule McN-A-343 was also chosen in this study. It is a M_1/M_4 preferring agonist whose mechanism is unknown but may be allosteric (Birdsall et al., 1983).

Constitutive activity studies were also performed and a cautionary finding came out of these studies, which will be described in an additional section.

6.2 Agonist dose-response curves at WT and mutant receptors

Phosphoinositide (PI) functional studies were performed in CHO cells stably transfected with M_3 WT and the K523E and N132G mutants. Initially ACh dose-response curves were for each construct. The normalised ACh dose-response curves of M_3 WT and the K523E and N132G mutants are shown in Fig 6.3. The data were analysed using non linear regression analysis to determine the EC50.

Basal data points were measured in presence of acetylcholinesterase (AChE), which breaks down ACh. The reason of using this enzyme for the basal data will be discussed later in this chapter. From the dose-response curves, we can estimate the Emax, which is the maximal ACh signalling capacity. In general we will not be focusing on this parameter as it is a function of the cell clone, the receptor expression level, and these are not being varied.

The potency values obtained for the WT and mutants are shown in Table 6.1. The -log EC50 for ACh at M_3 WT was 7.11±0.07. There was no significant difference between the EC50 values of the WT and the M_3 mutants except at the K523E where the potency was significantly reduced ($p<0.001$).

Oxotremorine dose response curves were also made for M_3 WT and the K523E, N132G mutants (Table 6.1). The -log EC50 values of oxotremorine for M_3 WT and K523E were similar to those of ACh at the equivalent receptor. In contrast the -log EC50 of oxotremorine was significantly weaker than ACh at the N132G mutant even though the -log EC50 for ACh was similar at the N132G mutant and the M_3 WT. It appears that the N132G mutation has selectively decreased oxotremorine signalling relative to ACh. Oxotremorine gave the same Emax value as ACh in all these studies, i.e. it was behaving as a full agonist.

Dose-response curves of the M_1/M_4 subtype low efficacy agonist, McN-A-343, were also generated at M_3 WT and the mutated receptors. The Emax, between 1-4% of what of ACh, was not high enough to fit the data to the sigmoidal dose curve equation and generate credible EC50 values for M_3 WT and K523E. On the other hand the N132G mutant had an increased Emax for McN-A-343, relative to the M_3 WT, allowing the

data to be fit, giving a -log EC50 value of 5.50±0.14. The Emax of McN-A-343 at N132G was 15 ± 3% of the ACh response.

Fig.6.3: ACh dose response curves for M_3 WT receptors and the M_3 mutants

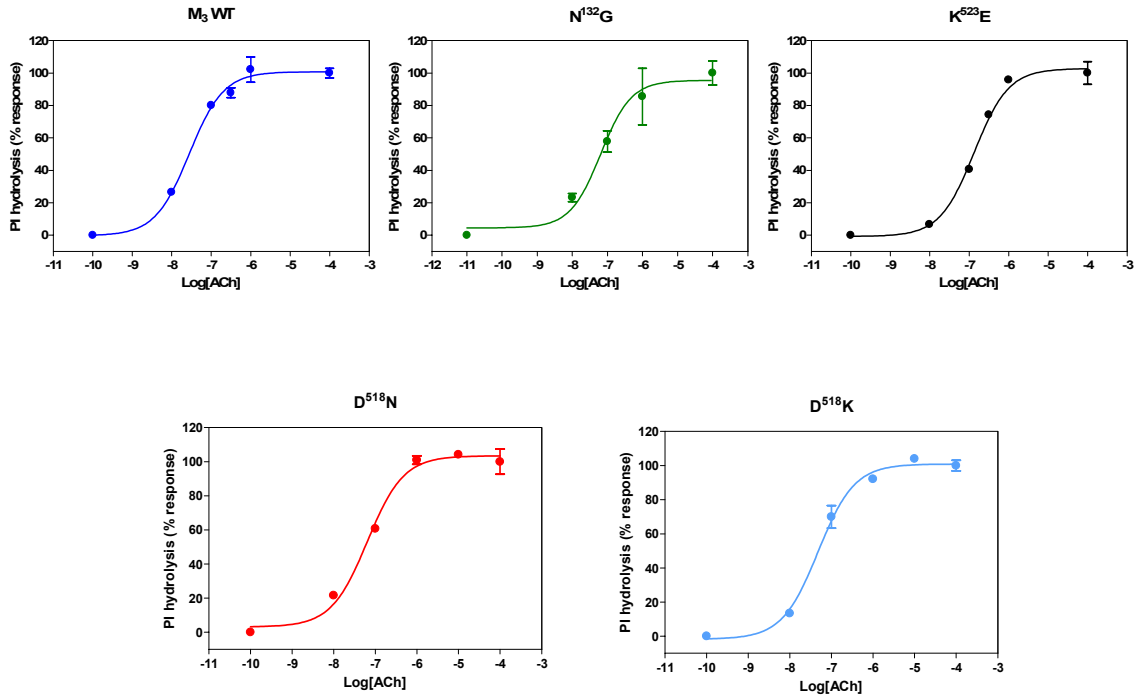

Fig. 6.3: ACh dose response curves for M_3 muscarinic WT and mutants illustrating the agonist activity of ACh. PI assays were performed on stably CHO cells transfected with the WT and mutant M_3 receptors cells were incubated with increasing concentrations of ACh (0.01-100 μM) for 1 hour at 37° under lithium block. The experimental data were fitted using non linear regression analysis with the slope factor fixed at 1. The data in each panel are the results of a single experiment.

Table 6.1: Potency of the muscarinic agonists ACh, oxotremorine and McN-A-343 at M_3 WT and the M_3 mutants

	Log EC50		
Subtype	**ACh**	**Oxotremorine**	**McN-A-343**
M_3	7.11±0.07(10)	7.05±0.09(5)	N.C.
K523E	6.49±0.08(8)	6.45±0.05(2)	N.C.
N132G	7.02±0.01(2)	6.65±0.10(2)	5.50±0.14(3)
D518N	7.18±0.01(1)	N.D.	N.D.
D518K	7.32±0.01(1)	N.D.	N.D.

Table 6.1: Potency values of ACh, oxotremorine and McN-A-343 at M_3 WT and mutants obtained from PI experiments. The EC50 values are mean ± SEM (number of experiments) and are expressed in log units.

N.C.: log EC50 not calculable because of a low Emax

N.D.: Not determined

6.3 Effects of Brucine, CMB and Strychnine on ACh and Oxotremorine responses at WT and mutant receptors (The K523E enhancer effect)

We have shown in Chapter 5 the effects that the allosteric ligands, brucine, CMB and strychnine, have on the binding of the endogenous agonist ACh at the M_3 WT receptors and the mutants. In those experiments different incubation conditions were used, one of them being Hepes buffer. This Hepes buffer resembles, in terms of ionic strength, the conditions used in functional experiments with living cells. In order to check that the allosteric effects seen in binding are transmitted to the cell function and are not just binding effects, functional assays were performed. We studied the modulation by those allosteric ligands of the ACh dose response curves by looking at the changes in the potency of ACh (EC50).

We have also studied the modulation by the allosteric ligands of oxotremorine agonism in order to give additional information about the molecular mechanism that allosteric ligands use to modulate the agonist response in the cell, i.e. whether the observed effects of the allosteric ligands is related to the structure or efficacy of the orthosteric agonist and if alpha is correlated with efficacy.

The data were analysed by the allosteric model with the curves in Fig. 6.4, 6.5 and 6.6 being the non-linear regression fits. The data from each panel are the results from a single experiment. ACh dose response curves were made in absence and presence of three different concentrations of brucine (30-300 μM) at M_3 WT and the K523E mutant receptor (Fig 6.4, upper two panels). The -log EC50 of ACh at M_3 WT receptors did not change in presence of brucine indicating neutral cooperativity, $\beta=1.0\pm0.2$. In these examples, where little or no change in EC50 was observed, the values of β were estimated by constraining the affinity of the allosteric ligand to the log Kx value found in binding studies. On the other hand, at K523E, the potency of ACh gradually shifts to the left with increasing concentrations of brucine, with a positive cooperativity of 16±7. Oxotremorine dose response curves are also shown in Fig 6.4 (lower two panels). There was no effect of brucine on the -log EC50 of oxotremorine at M_3 WT showing a similar effect to ACh, i.e. neutral cooperativity. The positive effect of brucine was also seen at the K523E mutation with oxotremorine, but this was an even higher value, $\beta=30\pm11$.

Fig.6.4: Effect of brucine on the potency of orthosteric agonists ACh and oxotremorine at the M_3 WT and K523E

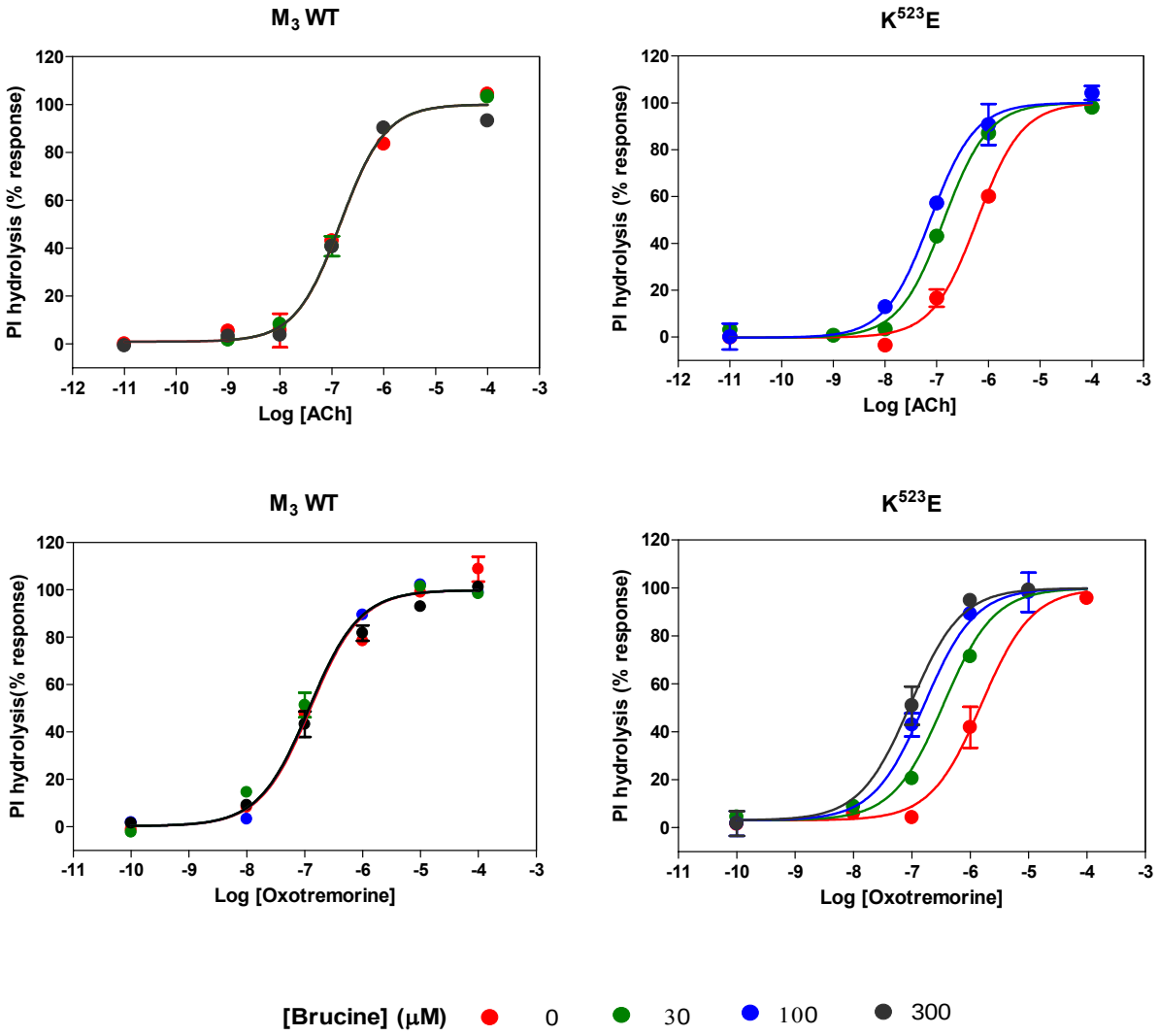

Fig.6.5: Effect of CMB on the potency of orthosteric agonists ACh and oxotremorine at M_3 WT and K523E

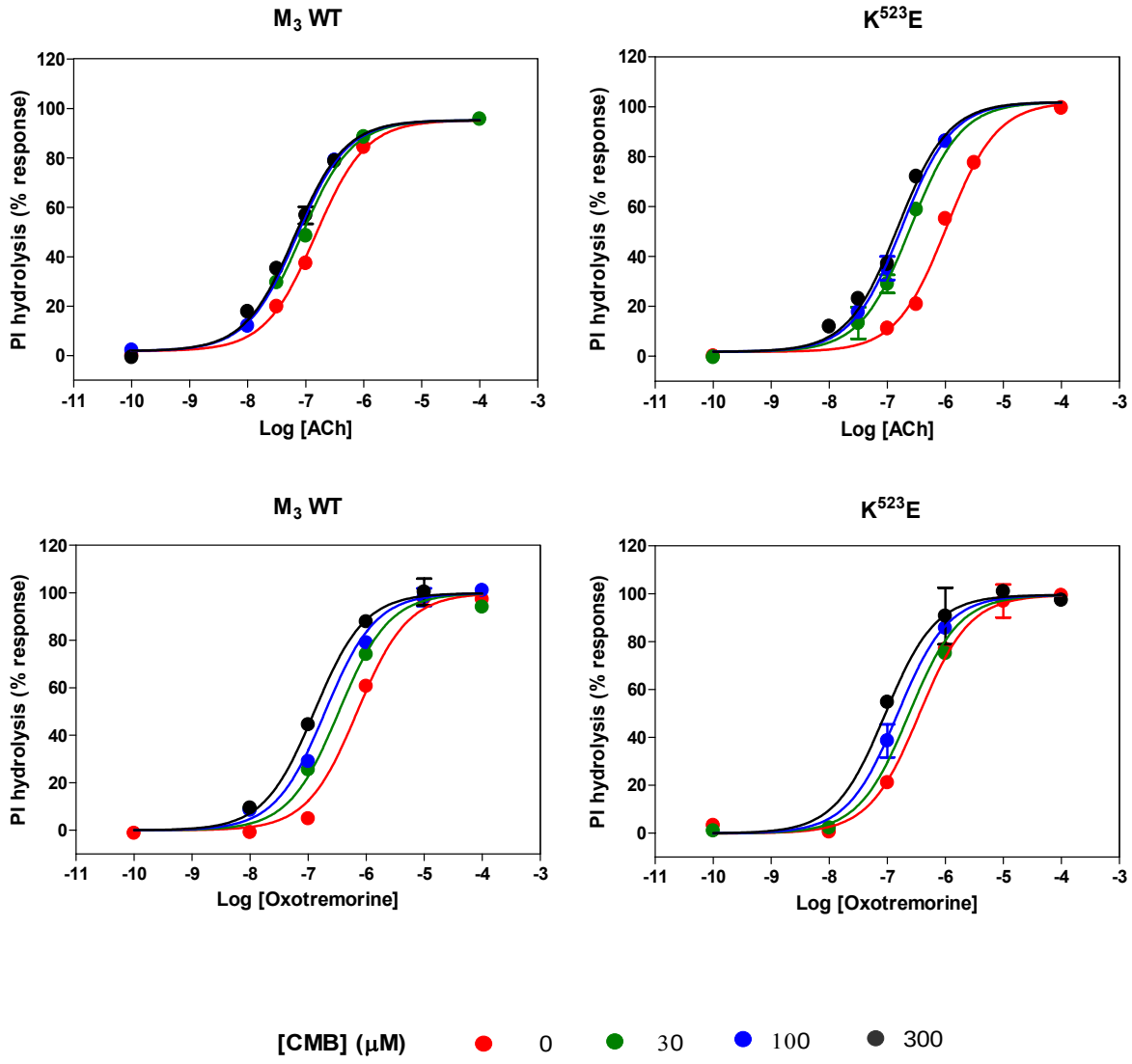

Fig.6.6: Effect of strychnine on the potency of the orthosteric agonist oxotremorine at M_3 WT and K523E

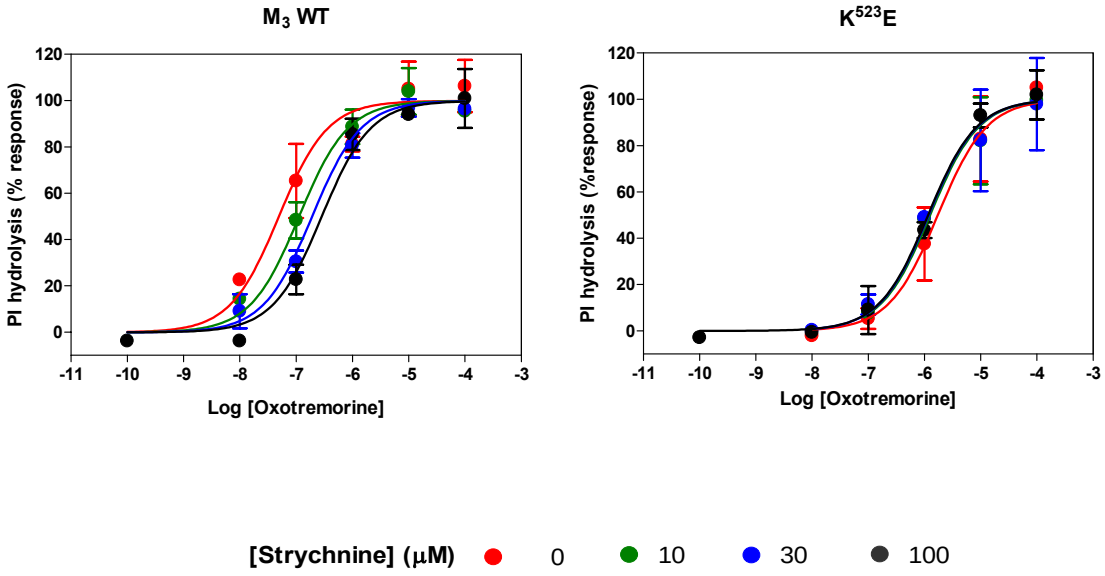

The effects of CMB on the potency of ACh at M_3 and the K523E mutant were also measured. The dose response curves obtained in absence and presence of three different concentrations of CMB (30-300 μM) are shown in Fig 6.5 (upper two panels). At M_3 WT we found that the potency of ACh slightly shifted to the left, with a positive cooperativity of ca 2.5±0.3. This effect was higher at K523E, β= 9.5±1.4. In Fig 6.5 (lower two panels) the oxotremorine dose response curves are illustrated in presence of the same three concentrations of CMB. The effect of CMB on oxotremorine -log EC50 at M_3 WT was with a β= 8.1. The potency of oxotremorine was also enhanced with CMB at K523E but the enhancement was slightly lower than that observed for ACh.

It has been reported that strychnine has a very strong negative cooperativity with oxotremorine at M_1 and M_3 receptors in binding studies (Jakubik et al., 1997). Taking into account that we have been showing so far that the K523E mutation tends to increase the cooperativity between allosteric modulators which bind to the gallamine site and orthosteric ligands, we wanted to examine whether this mutation was able to increase this strong negative cooperativity observed between strychnine and the agonist oxotremorine.

The effect of strychnine on oxotremorine dose-response curves at M_3 and K523E was also measured (Fig 6.6). The oxotremorine dose response curve is shifted to the right, indicating a negative cooperativity at M_3 WT, ca 0.13±0.07, agreeing with the binding data of Jakubik et al. Interestingly the potency of oxotremorine was not shifted to the right in presence of strychnine at the K523E mutation, the curves being slightly displaced to the left with a positive cooperativity of 1.5±0.7.

None of these compounds studied affected the basal or maximal responses or the slope of the ACh or oxotremorine dose-response curves. The direction of the cooperativity values of brucine, CMB and strychnine with the agonists ACh and oxotremorine are shown in Table 6.2.

Table 6.2: Effect of the K523E mutant on the cooperativity of three allosteric ligands with ACh and oxotremorine relative to M_3 receptors in functional studies

Compound	Cooperativity	
β with ACh	**M_3**	**K523E**
Brucine	0	+++
CMB	+	++
β with Oxo	**M_3**	**K523E**
Brucine	0	+++
CMB	++	++
Strychnine	-	+

Compound	Cooperativity	
β with ACh	**M_3**	**K523E**
Brucine	1.0±0.2	16±7
CMB	2.5±0.3	10±1
β with Oxo	**M_3**	**K523E**
Brucine	1.0±0.03	30±11
CMB	8.1±2.1	7±2
Strychnine	0.13±0.07	1.5±0.7

--: $0 < \alpha < 0.01$; - : $0.01 < \alpha < 0.9$; **0**: $0.9 < \alpha < 1.1$; +: $1.1 < \alpha < 3$; ++:3> α > 10;+++>10

Data shown are the means ±sem of 2 or 3 experiments

6.4 'Constitutive activity' of M_3 and mutant receptors and its modulation by inverse agonists and allosteric ligands

The ability of G-protein coupled receptors (GPCR) to activate their cognate G-proteins in the absence of an agonist is termed 'constitutive' receptor activity (Costa and Herz, 1989) and it depends on the concentration and expression level of the free activated receptor. Thus, certain ligands (termed inverse agonists and previously characterized as competitive antagonists) can inhibit agonist- independent receptor activity (Bond and Ijzerman, 2006;Nelson and Challiss, 2007). One of the most powerful tools used by researchers in this area has been the discovery of specific mutations which enhance the agonist independent activity, namely, constitutive active mutant receptors (CAM) (Seifert and Wenzel-Seifert, 2002).

In the case of the muscarinic acetylcholine receptors (mAChRs) (Spalding and Burstein, 2006), a number of studies have identified constitutively activating mutations, particularly in the predominantly Gq/11- coupled M_1, M_3, and M_5 receptor subtypes (Spalding et al., 1995;Spalding et al., 1997;Ford et al., 2002;Dowling et al., 2006;Nelson et al., 2006;Vogel et al., 1997). Spalding et al., 1995 first identified that mutation of adjacent serine (Ser465) and threonine (Thr466) residues at the junction between TM VI and the third extracellular loop results in a CAM-M_5 mACh receptor. Mutation of the equivalent residues of the other subtypes has also been demonstrated to enhance constitutive activity (Ford et al., 2002). The serine residue conserved in M_1 and M_5 and the equivalent asparagine residue corresponding to M_3, M_2 and M_4 are thus implicated in constraining the receptor to inactive state.

The mutant receptors displayed many of the characteristic properties of CAM-GPCRs, including enhanced agonist affinity and potency, in addition to an elevated basal functional activity (proportional to the receptor expression level), which was sensitive to the inverse agonist atropine (Ford et al., 2002).

As we are interested in the modulation on function of the M_3 muscarinic receptor by different allosteric ligands and also in two mutants located in the extracellular loops, i.e. N132G located in the first extracellular loop and K523E located in the third

extracellular loop, effects of orthosteric and allosteric ligands in the basal response were studied, performing constitutive activity assays. This initial idea was the result of our observing relatively high counts in the basal activity of the cells of M_3 WT and the mutant receptors.

Using the phosphoinositol hydrolysis method previously described, we found that the basal activity of the M_3 WT and the two mutants was decreased by 3.5 ± 0.6*, 2.8 ± 0.7* and 1.9 ± 0.2* fold respectively by the inverse agonist atropine (10^{-7}M) indicating that there might be apparent constitutive activity (Fig 6.7). In this section the asterisk denotes a significant difference relative to basal activity ($p<0.05$).

Initial studies indicated that this apparent constitutive activity could be enhanced or inhibited by different allosteric muscarinic ligands, sometimes in a mutant sensitive manner (Fig. 6.8). N-chloromethylbrucine (300μM) enhanced ^{3}H-IP production at WT, N132G and K523E by 1.5 ± 0.2*, 1.5 ± 0.2* and 1.8 ± 0.6* fold respectively whereas brucine (300μM) was neutral at WT and N132G (fold increase 1.0 ± 0.1, 0.9 ± 0.1) and enhanced ^{3}H-IP production 3.8 ± 0.4* fold at K523E. In contrast, strychnine (100μM) inhibited ^{3}H-IP production at WT by a factor of 0.61 ± 0.03* but had no effect at the two mutated receptors.

Fig.6.7: Effect of atropine (10^{-7}M) on 'basal' activity

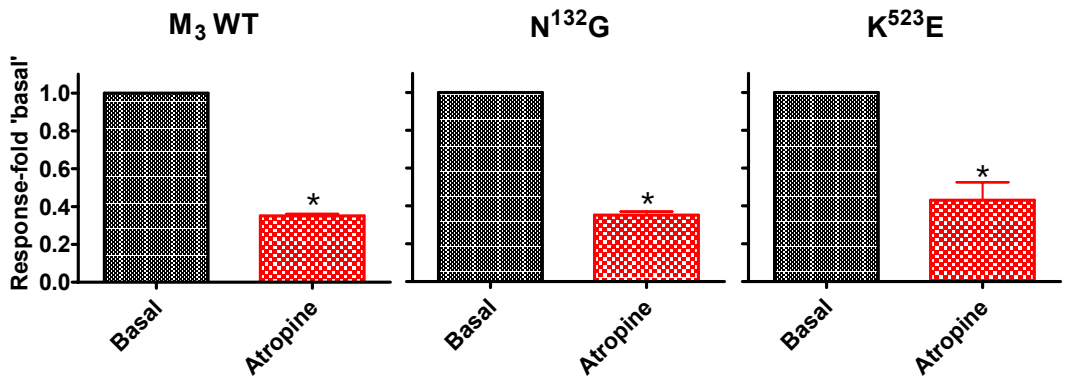

Each data point is the mean of duplicate points and representative of 2-4 experiments

Fig.6.8: Effects of allosteric modulators that bind to the 'gallamine' allosteric site on function

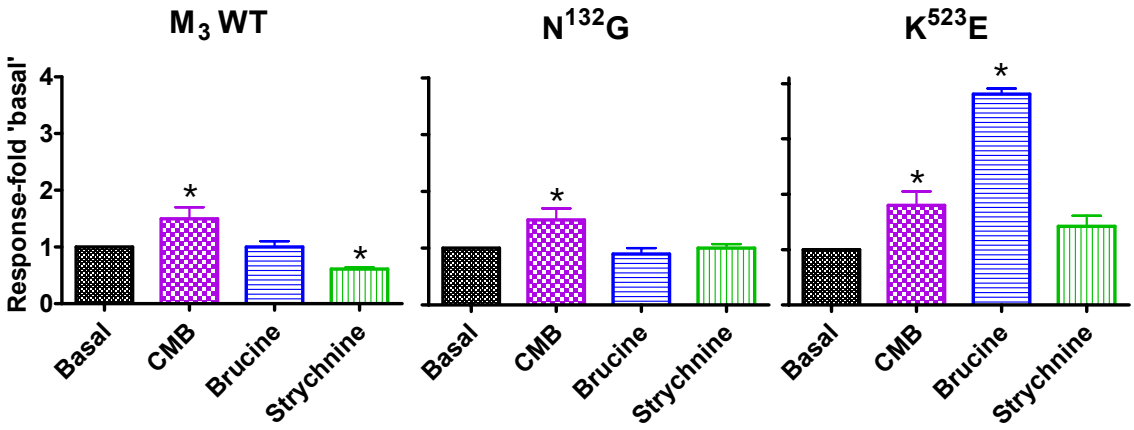

Each data point is the mean of duplicate points and representative of 2-4 experiments

As the behaviour of these four allosteric ligands mimicked their ability to act as allosteric enhancers or inhibitors of ACh at WT, N132G and K523E, cells were incubated with the enzyme acetylcholinesterase (AChE, 0.05-5U/ml), which breaks down the molecule ACh. This reduced ^{3}H-IP production to the levels found in the presence of atropine in the three cell lines, eliminating the constitutive activity and indicating that ACh was present in the assay (Fig 6.9). In the presence of AChE (2.5U/0.5ml), N-chloro-methylbrucine (300μM), brucine (300μM) and strychnine (100μM) had no effect on basal activity (Fig 6.10), i.e. they were not allosteric agonists at the WT or the two mutant M_3 receptors. The research in this section was presented orally to the British Pharmacological Society Meeting in December 2007 and the abstract has been published (Iarriccio and Birdsall, 2008).

Fig.6.9: Effect of acetylcholinesterase on the basal activity at the M_3 WT and mutants

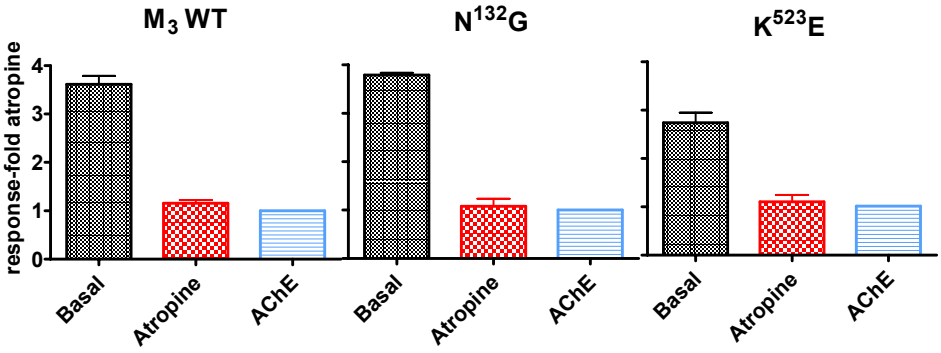

Each data point is the mean of duplicate points and representative of 2-4 experiments

Fig.6.10: Effect of allosteric modulators that bind to the 'gallamine' site on function in the presence of AChE

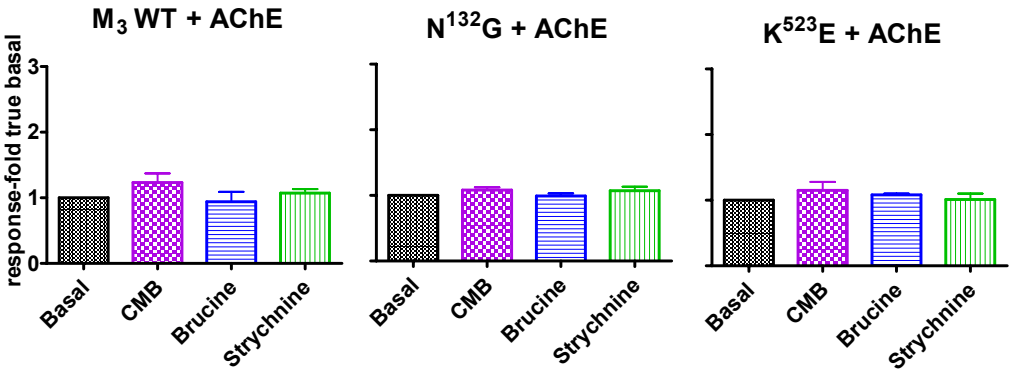

Each data point is the mean of duplicate points and representative of 2-4 experiments

6.5 Discussion

In order to study the modulation by four allosteric ligands of the stimulation of the M_3 WT receptors and mutants by ACh, dose response curves were generated. We needed initially to measure the ACh log EC50 at the M_3 WT and compare it with the mutants to see whether there is a change. Only in K523E was there any change in the ACh -log EC50 which was reduced 4 fold relative to M_3 WT. This decrease could be due to a reduced expression level or to a reduction in signalling efficacy.

We also measured the oxotremorine log EC50 in order to gain some additional information at molecular level about the mechanism of agonists binding and response. In this assay oxotremorine was a full agonist at the WT receptor and all mutants examined. The potency of oxotremorine was similar that of ACh in the WT and the K523E mutant receptor. However at N132G there was a 2.5 fold reduction in oxotremorine potency which was not observed for ACh. This indicates that signalling efficacy of oxotremorine, relative to ACh, may have been reduced in N132G.

The low efficacy agonist McN-A-343 did not show any appreciable response at M_3 WT. This was expected according to literature (Hu and el-Fakahany, 1990;Heldman et al., 1996), although in the N132G mutant the efficacy was higher, indicating that this residue could be hindering the signalling efficacy of McN-A-343, and when we remove the N, it becomes better. The literature (Hu and el-Fakahany, 1990;Heldman et al., 1996) shows that the efficacy of McN-A-343 at the M_1 subtype is higher relative to M_3 WT maybe generating an M_1 phenotype. Thus at N132G, oxotremorine signalling efficacy seems to be decreased whereas that of McN-A-343 increased, in a ligand-dependent change in efficacy.

Concerning the effects of the allosteric modulators on ACh stimulation, we have been able to reproduce all the effects that we have seen in binding, indicating that the allosteric modulation seen in binding is transmitted to the cellular response. We have been able to see the same switch of cooperativity from neutral to positive between M_3 WT and K523E in functional studies for brucine as was seen in binding studies. It was difficult to get accurate estimates of log Kx because of the noise in the functional data

and the relatively small effects. However all the dose-response curves could be well fitted by constraining the log Kx values to those seen in the binding studies with the calculated values of cooperativities agreeing with those found in binding studies. This is an indication of the receptors behaving similarly in binding and function under similar conditions and that the changes in agonist binding in the presence of allosteric modulators are reflecting a change in agonist affinity, not agonist efficacy.

The same effects are reproduced with oxotremorine indicating a similar mechanism of binding and action. At K523E, brucine and CMB are even stronger enhancers of oxotremorine than those of ACh. We can conclude that the enhancement of ACh affinity by an allosteric ligand is transmitted into an equivalent enhancement of the response and that at the K523E mutant, brucine is now a ACh enhancer.

The effect of K523E on strychnine binding is also large. The strong negative cooperativity that strychnine has at M_3 is changed to neutral cooperativity indicating that this residue is clearly involved in modulating the cooperativity, not only with antagonists as described in Chapter 4 but also with agonists. K523E makes the conformation of the receptor more favourable for the cooperative binding of an allosteric ligand and an agonist (or antagonist).

With regards to the constitutive activity studies we can conclude that there is a need to be aware that ACh may be present in some functional assays. We estimated the ACh concentration when present in our assay, to be ca. 2-10 nM. The explanation of how we have calculated this concentration is illustrated in Fig 6.11 where an ACh dose response curve with two different basal data points is represented. The upper basal data point is the one that we obtained in absence of AChE and the basal data point below is the true basal data point in presence of AChE. The difference between these two points is the stimulation of the endogenous ACh. Going across the curve horizontally, gives us the concentration of ACh at which there is a given level of stimulation. In this particular example the concentration of ACh is between 6-8 nM. In studies of constitutive activity of muscarinic receptors, an AChE control is needed as all the publications working in cell lines that we are aware of, did not include this control This artifact can generate apparent constitutive activity and apparent agonism of allosteric enhancers, especially

when ACh is potent and/or when there is strong positive cooperativity with ACh (e.g. where brucine is acting as an enhancer at K523E, ($\alpha = 10$)).

Having solved the problem of high basal activity, we found some interesting results which are described in the next chapter.

Fig.6.11: Illustration of the estimation of the ACh concentration found in functional studies

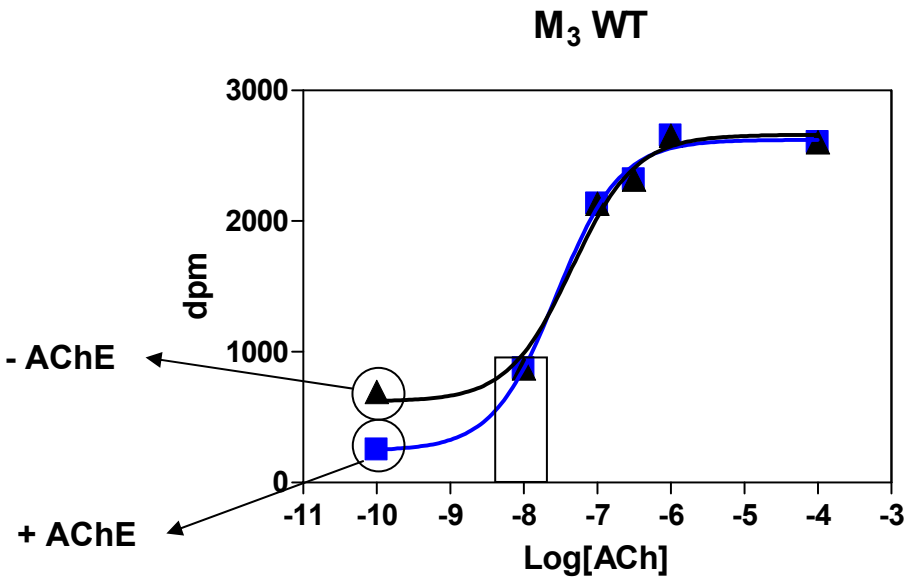

Chapter 7. Actions of allosteric ligands that bind to the second allosteric binding site

7.1 Introduction

M_3 muscarinic receptors are one of the members of the 7-transmembrane helix family, the G-protein coupled receptors (GPCRs). Most drugs bind to the orthosteric site. This is the site where the endogenous ligand (ACh in the case of muscarinic receptors) binds and this is a highly conserved area of the receptor. However there is also a second binding site called the 'gallamine' binding site to which molecules like gallamine and strychnine bind. This site is thought to be located on the extracellular loops. As this region of the receptor is much less conserved than the orthosteric site, it could be potentially a subtype selective drug target. A second allosteric site has been found (Lazareno et al., 2000;Lazareno et al., 2002), but the location of this site is not known. This second allosteric site binds molecules like WIN 51708 and 62,577 and staurosporine.

The indolocarbazole staurosporine (Fig 7.1) was discovered to have a number of biological activities, ranging from anti-fungal to anti-hypertensive (Ruegg and Burgess, 1989). The interest in these activities resulted in a large investigative effort in chemistry and biology and the discovery of its potential for anti-cancer treatment (Ruegg and Burgess, 1989). The main biological activity of staurosporine is the inhibition of protein kinases through a competitive interaction at the ATP binding site of the kinases.

Staurosporine has been also found to have allosteric effects at M_1-M_4 muscarinic receptors (Lazareno et al., 2000). The interactions of staurosporine and some other staurosporine-like compounds have been studied with [^{3}H]NMS and ACh at M_1-M_4 using equilibrium and non equilibrium radioligand studies (Lazareno et al., 2000). Staurosporine was found to inhibit [^{3}H]NMS dissociation from all the subtypes having the smallest effect, 3 fold maximal inhibition, at M_3 receptors. According to this study, staurosporine showed positive cooperativity with [^{3}H]NMS at M_1 and M_2 receptors,

neutral cooperativity with [^{3}H]NMS at M_4 receptors, and was inactive or neutrally cooperative at M_3 receptors. It had negative cooperativity with ACh at M_1, M_2, and M_4 subtypes and was neutral with ACh or inactive at M_3 receptors. Staurosporine had *K*d values for unoccupied receptors in the μM range. Functional assays were only done at M_1 receptors where 10 μM staurosporine reduced basal activity and Emax. The potency of ACh at M_1 receptors was also reduced, ca 2.9 fold which was consistent with the 3.6 fold increase in the IC50 of ACh predicted in [^{3}H]NMS binding studies.

The steroid-like compounds WIN 51,708 and WIN 62,577 were also found to act allosterically at muscarinic receptors (Lazareno et al., 2002). One of the main findings of this study was that WIN 62,577 is an allosteric enhancer of low positive cooperativity at M_3 receptors. These compounds are also antagonists of rat, but not human, neurokinin NK1 receptors, but importantly, they are centrally active (Venepalli et al., 1992) as they are able to cross blood-brain barrier (Ukai et al., 1995;Nikolaus et al., 1999;De Araujo et al., 2001), which is a prerequisite for a drug therapy for human central nervous system disorders.

WIN 62,577 can be considered in simplistic terms as a fusion of an aromatic heterocyclic system with an alicyclic ring system, especially a steroid structure (Fig 7.1). Modification of either moiety can generate substantial changes in affinity, cooperativity, and subtype selectivity (Lazareno et al., 2002). WIN 62,577 contains a double bond in the steroid moiety (Fig 7.1) and was found to inhibit [^{3}H]NMS dissociation from M_1, M_2 and M_4 receptor. In contrast, WIN 62,577, like WIN 51,708, had no measurable effect on [^{3}H]NMS dissociation from M_3 receptors. However, the allosteric action of WIN compounds at M_3 receptors was shown in this paper. They showed that WIN was clearly occupying the receptors as it was able to inhibit the binding of another allosteric analogue of WIN, PG987.

WIN 62,577, showed only small negative cooperativity with [^{3}H]NMS at all subtypes. It is worth noting that the potency and small degree of negative cooperativity found with [^{3}H]NMS for both WIN compounds at M_3 receptors in equilibrium assays would predict some activity at M_3 receptors in the off-rate assay, but no activity was observed. With respect to ACh, WIN 62,577 was also negatively cooperative at M_2 and M_4 receptors, almost neutral at M_1 receptors, and showed a small but nonsignificant positive

interaction with ACh at M_3 receptors (1.8). This positive cooperativity was confirmed in more detailed assays, where full [^{3}H]NMS-ACh curves were constructed in the absence and presence of three concentrations of WIN 62,577.

In the present study the interactions of staurosporine and WIN 62,577 with [^{3}H]NMS and ACh at M_3 WT and mutants have been studied at M_3 WT and the N132G, K523E and K523Q mutation under three different conditions, using equilibrium and dissociation radioligand assays. These experiments have provided some confirmation that, at M_3 receptors and the mutants, these ligands binds to a different site from the gallamine binding site.

Functional studies were also performed to measure the effect of WIN 62,577 on ACh stimulation. Some quantitative discrepancies were found for the K523E mutant regarding the cooperativity predicted from the binding experiments and unanticipated results were found concerning the activity of WIN compound at M_3 WT.

Fig.7.1: Chemical structure of staurosporine and WIN 62,577

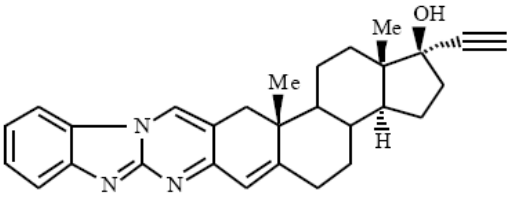

WIN 62,577

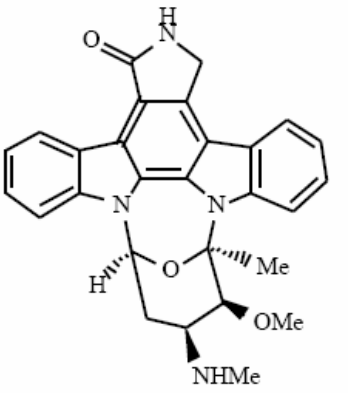

Staurosporine

7.2 Effect of mutations and incubation conditions on the allosteric interaction of WIN 62,577 and staurosporine on [^{3}H]NMS binding and kinetics

The effects of staurosporine and WIN 62,577 on the dissociation rate constant (k_{-1}) of [^{3}H]NMS at M_3 WT and N132G, K523E, K523Q mutations under three different conditions were measured by doing dissociation radioligand assays. One point kinetic assays were used to measure the log Kocc of the compounds by measuring the [^{3}H]NMS dissociated alone and in the presence of three different concentrations of the modulators. The equation used to analyse the data to give estimates of the k_{-1} and log Kocc using only one equation is described in *Material and Methods*.

The effects of staurosporine and WIN 62,577 on the dissociation of [^{3}H]NMS at M_3 WT in Hepes are illustrated in Fig 7.2 where the top data point (shown at -1) in the curve represents binding before dissociation starts and that at -8 in this figure and in Figures 7.3 and 7.4, are that found in the absence of modulator. The curve for staurosporine extrapolates to this value showing that this allosteric agent can completely block [^{3}H]NMS dissociation at a sufficient high concentration. In the case of WIN 62,577 the data show no effect on [^{3}H]NMS dissociation (horizontal line). The parameters estimates, describing the slowing effects of these two compounds at M_3 WT and the mutants in the three buffers, are summarised in Table 7.1.

Staurosporine inhibited [^{3}H]NMS dissociation at M_3 WT and N132G, K523E, K523Q mutations in the three buffer conditions used. The log Kocc value in Hepes was ca 4.9 at M_3 WT, and there was no significant difference in this value at the N132G and K523Q mutants. The K523E mutant showed an increase ($p<0.01$) in the Kocc value of ca 2 in Hepes buffer relative to M_3 WT. This small increase in the Log Kocc value of K523E relative to M_3 WT in Hepes is illustrated in Fig 7.3. The same effects of staurosporine on the dissociation of [^{3}H]NMS at M_3 WT and the M_3 mutants were seen in Tris buffer.

The effects of staurosporine and WIN 62,577 on the dissociation of [^{3}H]NMS at M_3 WT and the mutants in PB buffer were also measured. These effects are illustrated in Fig 7.4 (only M_3 WT and the K523E mutant shown). The log Kocc value of M_3 WT in PB was

ca 5.3, the same value that the one obtained at the K523E mutant in PB. The log Kocc values of M_3 WT are slightly sensitive ($p<0.05$) to PB buffer, ca 3 fold higher.

Fig.7.2: One time point kinetic analysis of the dissociation of [^{3}H]NMS from M_3 WT receptors in absence and presence of three different concentrations of staurosporine and WIN 62,577 in HEPES

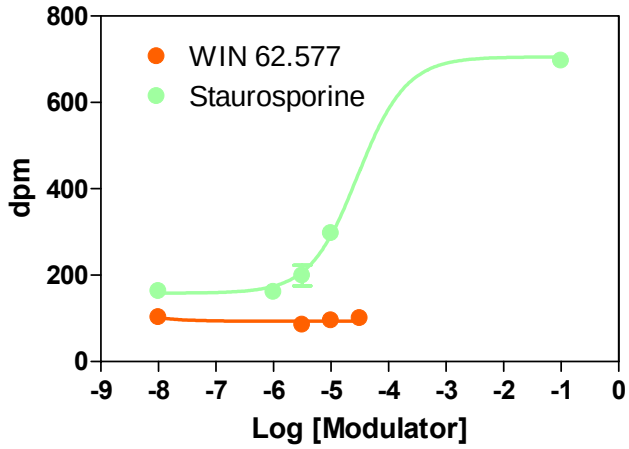

Fig.7.3: One time point kinetic analysis of the dissociation of [^{3}H]NMS from M_3 WT and the K523E mutation in absence and presence of three different concentrations of staurosporine in HEPES

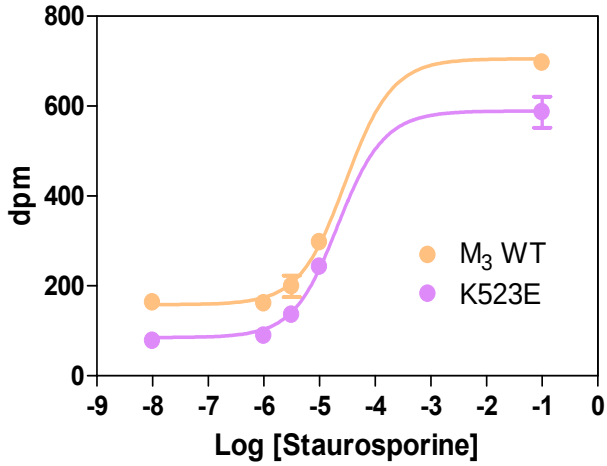

Table 7.1: Binding parameters for the allosteric interactions of staurosporine and WIN 62,577 with NMS obtained from equilibrium (log Kx) and kinetic (log Kocc) experiments at M_3 WT and mutants in three different incubation conditions

Staurosporine		Equilibrium assay			Off rate assay
			Cooperativity		
	Subtype	log Kx	NMS	log KoccNMS	-log EC50
TRIS	M_3	5.50±0.04	0.2	[4.75]	4.75±0.09
	N132G	5.60±0.06	0.1	[4.75]	4.75±0.05
	K523E	5.75±0.08	0.3	[5.19]	5.19±0.01
	K523Q	5.78±0.07	0.2	[5.02]	5.02±0.01
HEPES	M_3	5.26±0.08	0.4	[4.86]	4.86±0.02
	N132G	5.27±0.13	0.3	[4.67]	4.67±0.03
	K523E	5.52±0.08	0.4	[5.17]	5.17±0.06
	K523Q	5.69±0.07	0.2	[5.05]	5.05±0.13
PB	M_3	5.62±0.05	0.4	[5.27]	5.27±0.12
	N132G	5.69±0.03	0.3	[5.10]	5.10±0.12
	K523E	6.41±0.06	0.2	[5.31]	5.31±0.12
	K523Q	6.11±0.05	0.2	[5.28]	5.28±0.02

WIN 62,577		Equilibrium assay		Off rate assay
			Cooperativity	
	Subtype	log Kx	NMS	-log EC50
TRIS	M_3	[5.2]	0.14±0.01	N.D.
	N132G	[5.2]	0.32±0.04	N.D.
	K523E	[5.2]	0.60±0.50	N.D.
	K523Q	[5.2]	0.36±0.20	N.D.
HEPES	M_3	[5.3]	0.31±0.05	N.D.
	N132G	[5.3]	0.32±0.09	N.D.
	K523E	[5.3]	0.29±0.11	N.D.
	K523Q	[5.3]	0.20±0.07	N.D.
PB	M_3	[5.5]	0.25±0.05	N.D.
	N132G	[5.5]	0.17±0.04	N.D.
	K523E	[5.5]	0.20±0.01	N.D.
	K523Q	[5.5]	0.53±0.09	N.D.

The staurosporine binding parameters (top) show the equilibrium parameters obtained using the ATCM and constraining the log Kocc to the value shown in the square brackets to the log EC50 obtained in the off-rate assays. The WIN 62,577 binding parameters (bottom) show the affinity values determined from equilibrium assays (in square brackets). These values were constrained to be shared between M_3 and the mutants to determine the cooperativity estimates. The computer estimates of the error of the WIN 62,577 affinities were ± 0.2-0.3 log units. Each estimate is the mean of duplicate values of 2 independent experiments. N.D.: Not detected

Fig.7.4: One time point kinetic analysis of the dissociation of [^{3}H]NMS from M_3 WT and the K523E mutation in absence and presence of three different concentrations of staurosporine in PB

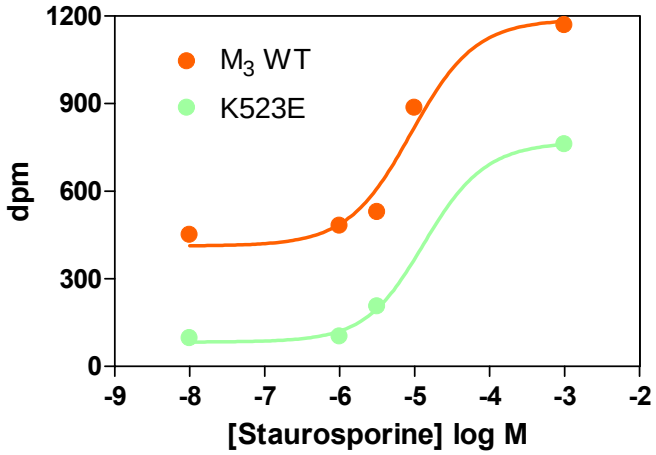

This buffer sensitivity was also observed at the N132G and K523Q mutants but not at K523E. The K523E mutation showed an increase ($p<0.01$) in the log Kocc value of ca 2 and 1.6 fold in Hepes and PB buffer respectively relative to M_3 WT.

WIN 62,577 had no measurable effect on [^{3}H]NMS dissociation from M_3 WT and from any of the M_3 mutants in any of the three different buffers used. From these data alone there is no evidence that WIN 62,577 has an allosteric action at M_3 receptors and mutants (but see *Discussion* of this chapter).

Equilibrium assays were also performed in order to study the interactions of staurosporine and WIN 62,577 with [^{3}H]NMS at M_3 WT and the mutants under three different conditions. The log Kx and the cooperativity estimates of the test compounds were obtained from nonlinear regression analysis for these compounds using the allosteric equation (described in *Material and Methods*) and they are shown in Table 7.1.

The staurosporine log Kx values are insensitive to buffers at M_3 WT and the N132G mutants, having values of ca 5.5. At the K523E and K523Q mutants there is a similar tendency of the staurosporine log Kx values to be increased relative to M_3 in Tris and Hepes buffer. This similarity in log Kx value for these two mutants differs from the difference in log Kx seen for all the 'gallamine site' compounds tested in previous chapters, indicating a different mechanism of staurosporine binding to the receptor. On the other hand, in PB there is a bigger difference between log Kx of K523E relative to M_3 WT, ca 6 fold. The K523Q log Kx is higher, ca 3 fold, relative to M_3 WT, but the increase is not as big as for the K523E mutant. The cooperativity values between [^{3}H]NMS and staurosporine are also shown in Table 7.1, and they are calculated from the ratio between the log Kocc obtained in kinetic assays and the log Kx obtained in equilibrium assays. These cooperativiy values are all negative and insensitive to buffer composition and to any mutation.

To estimate WIN 62,577 affinities at equilibrium we used the allosteric ternary model (ATCM) constraining affinities of WIN in Hepes to be shared. This was because of the small and similar effects on [^{3}H]NMS binding that were observed. The data were compatible with a log Kocc value of 5.4±0.3 and the alpha factor is in the range of 0.2-0.3 irrespective of the mutants. The same analytical method was applied to the data with WIN in PB to get a log Kocc 5.4±0.3 and an alpha factor in the range of 0.1-0.3. In Tris buffer the Log Kocc was 5.3±0.5 with a range of the alpha factor being 0.3-0.6. The log Kx values of WIN 62,577 at M_3 WT and mutants appeared to be similar (ca 5.5) under the three different conditions. This suggests that the binding of WIN 62,577 to the M_3 receptor is insensitive to buffer conditions and it is not perturbed by any mutation, as K523E and K523Q mutants have equal effects on WIN binding relative to M_3 WT. The cooperativity values are all negative within a range of 0.1-0.5.

These Kx values of WIN 62,577 obtained in equilibrium assays are compatible with the ones obtained in experiments performed in presence of ACh described in next section, where more precise values could be obtained.

7.3 Effect of mutations on the equilibrium allosteric interaction of WIN 62,577 with ACh

To characterize these interactions further, the equilibrium effects of WIN 62,577 on equilibrium ACh binding were measured. Because of time constraints, it was only possible to test this compound on M_3 WT and the mutants in Hepes buffer. This buffer was chosen as the parameters obtained under this condition were anticipated to be comparable to those obtained in functional assays. To determine the allosteric effects on ACh affinity, we used an indirect assay of ACh binding that measures the inhibition of [^{3}H]NMS binding by unlabeled ACh. This is because [^{3}H]ACh does not usefully bind to M_1 or M_3 receptors; in any case, GTP is included in the assay to minimize the effect of G-protein coupling on the affinity of ACh. The effects of a range of concentrations of test agent on [^{3}H]NMS binding are measured in the absence and presence of a single concentration of ACh. The data are plotted against increasing concentrations of the test agent, WIN 62,577.

Fig 7.5 shows representative plots from equilibrium assays for WIN 62,577 binding to M_3 WT and the N132G, K523E and K523Q mutations in Hepes buffer. The Log Kx for WIN 62,577 did not change at any of the mutants relative to M_3 WT (as assumed in previous section). The parameter estimates are summarised in Table 7.2. WIN 62,577 showed a neutral cooperativity at M_3 WT receptors with ACh and negative cooperativity at the three mutations. At the N132G mutant the cooperativity was only slightly negative, ca 0.7, but the K523E and K523Q mutants exhibited higher negative cooperativity, ca 0.4.

These results demonstrate the lack of effect of the mutations on log Kx that was inferred in the previous section.

Table 7.2: Equilibrium binding parameters of WIN 62,577 and ACh at M_3 WT and mutants in Hepes buffer

WIN 62,577		Equilibrium assay		
	Subtype	log Kx	Log K_A	β ACh
HEPES	M_3	5.49±0.08	4.90±0.08	1.1±0.4
	N132G	5.52±0.10	4.77±0.04	0.7±0.2
	K523E	5.58±0.05	4.72±0.11	0.4±0.2
	K523Q	5.60±0.05	4.70±0.05	0.4±0.2

Table 7.2: These values were obtained from [^{3}H]NMS equilibrium assays with different concentrations of WIN 62,577 and in absence and presence of one concentration of ACh (20 μM) at M_3 WT and mutants in Hepes. All these experiments were carried out in the presence of 0.2 mM GTP. By using the ATCM to analyse the data the cooperativity values between WIN 62,577 and ACh were estimated. Values are reported as a mean ± S.E.M. Each estimate is the mean of duplicate values from 2-3 independent experiments.

Fig.7.5: Effect of WIN 62,577 on the [^{3}H]NMS equilibrium curves in absence and presence of a single concentration of ACh at M_3 WT and the mutants in HEPES

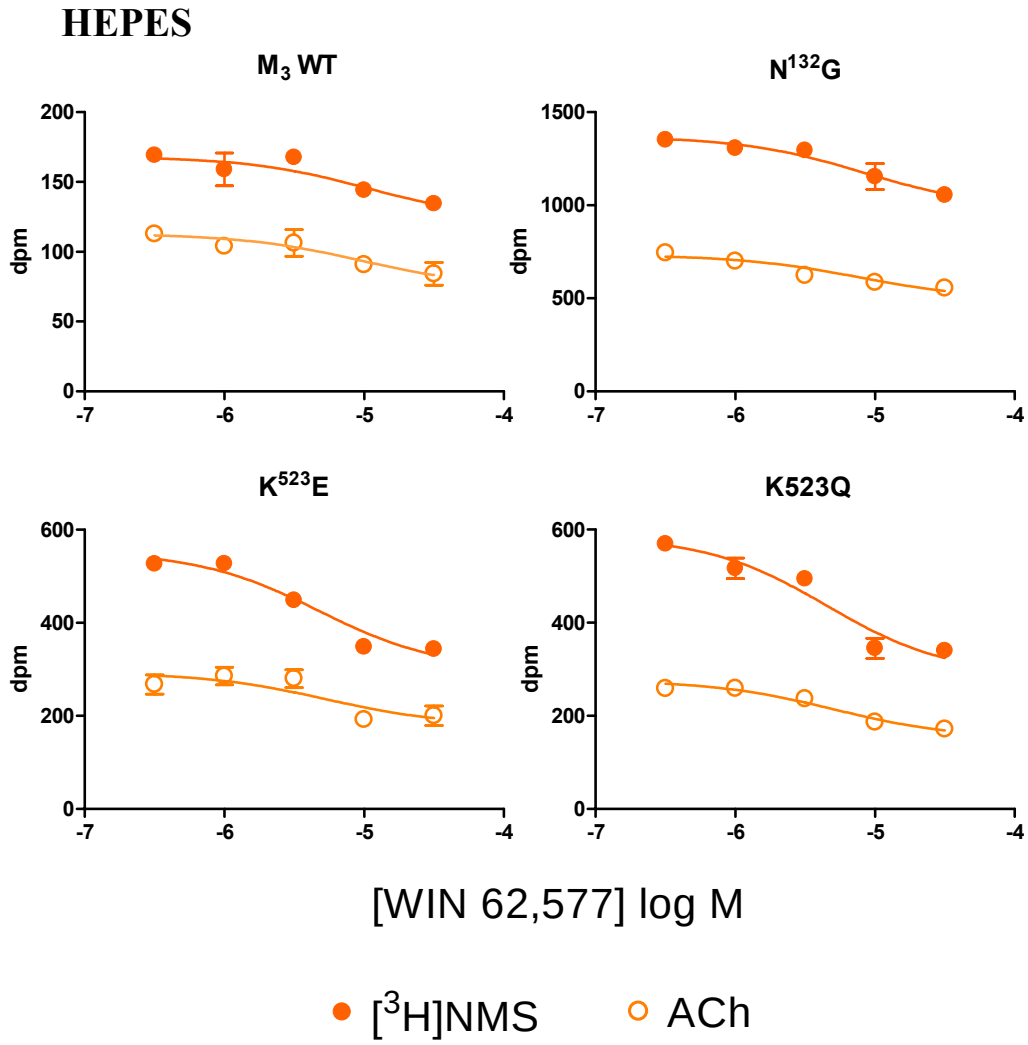

Fig 7.5: Effect of WIN 62,577 on the binding of [^{3}H]NMS in the absence (full circles) and presence (open circles) of ACh at M_3 WT receptors and mutants in Hepes buffer. The experiment was repeated three times with very similar results

7.4 Effects of WIN 62,577 on receptor function and its modulation of ACh actions

In functional studies, Chapter 6, we have demonstrated and discussed the 'apparent' constitutive activity found during the investigation of the effects of mutations in the 1st and 3rd extracellular loops of M_3 receptors, on the ^{3}H-IP production by allosteric ligands. This 'apparent' constitutive activity could be modulated in a ligand- and mutant- dependent manner.

We were able to inhibit this 'apparent' constitutive activity by adding 10^{-7} M of the inverse agonist atropine. This activity was also eliminated by the presence of the specific enzyme AChE, and indicated that ACh was presence in the assays.

Similar functional experiments were also performed in presence of WIN 62,577 in the M_3 WT, N132G and K523E stably transfected cells. Fig 7.6 shows the effect of WIN 62,577 on the 'apparent' basal activity of M_3 WT and the N132G and K523E mutations **in absence of AChE**, where this 'basal activity' is not affected at M_3 and N132G (1.0 ± 0.2, 1.0 ± 0.1 fold respectively). However at the K523E mutation the basal activity was increased by 100 μM of WIN 62,577 1.6 ± 0.1* fold, indicating that is acting as an 'apparent' allosteric agonist at this particular mutant. But in fact, as we have discussed in the functional studies chapter, ACh was present in the assay and the effect that we see is a neutral cooperativity of the WIN 62,577 compound with ACh at M_3 WT and the N132G mutant and a positive cooperativity at the K523E mutant.

In order to look at the effects of WIN 62,577 on the 'true' basal activity of M_3 WT and N132G and K523E mutant receptors (Fig 7.7), we added AChE in the assay to eliminate any possible presence of ACh. Surprisingly, we found that in the absence of ACh, WIN 62,577 (100 μM) did stimulate M_3 WT, N132G and K523E receptors (2.3 ± 0.2*, 1.6 ± 0.2* and 1.9 ± 0.6* fold respectively) acting as an allosteric agonist. The maximum WIN response is 5-15% of the maximum ACh response.

Fig.7.6: Effect of WIN 62,577 on function in the absence of AChE

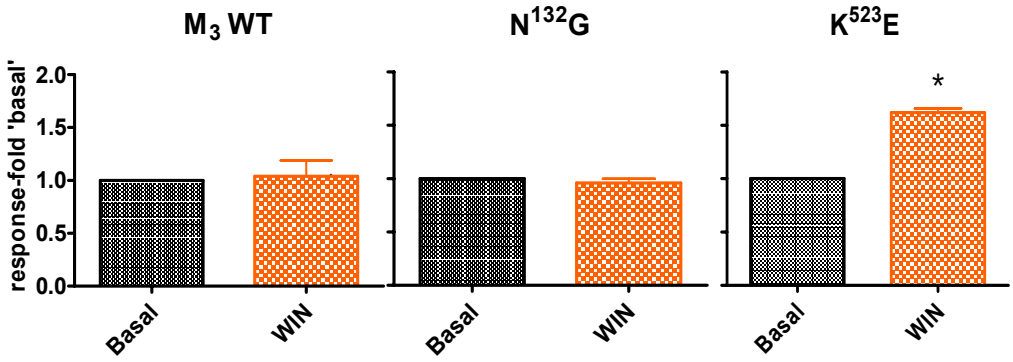

** p< 0.05*

Fig.7.7: Effect of WIN 62,577 on function in the presence of AChE

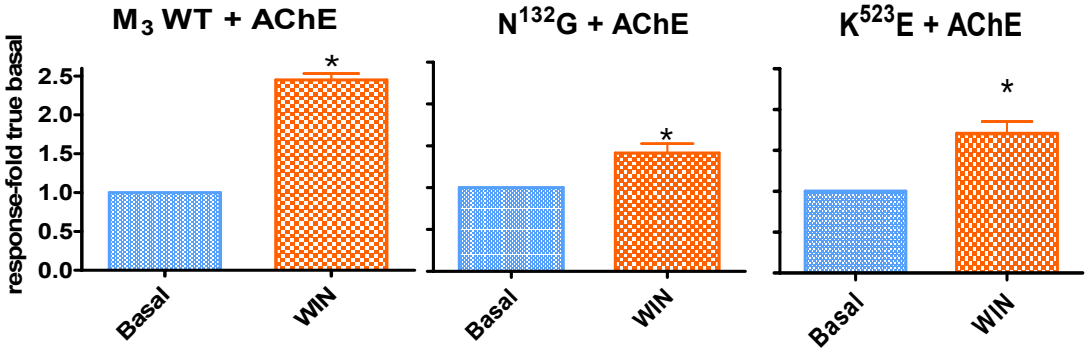

** p < 0.05*

To further investigate the allosteric agonism behaviour of the WIN 62,577 compound at the M_3 WT and the mutants dose-response curves were generated with increasing concentrations of WIN (1μM-100μM) all in presence of AChE (Fig 7.8 and 7.9). Two additional ACh controls were included (both in the absence of AChE); one in presence of 100 μM ACh in order to measure the maximal response (Emax, normalized to 100%) and the other control was the presence of 0.01 μM ACh, which is the approximate concentration that we estimated to be present in previous assays.

Figure 7.8 illustrates the challenge of obtaining good dose-response curves because of the low signal. Nevertheless it was possible to obtain estimates of the potencies of WIN 62,577. These are illustrated in Fig 7.9, and are summarised in Table 7.3. The potencies of WIN agree well with those found in binding assays (Table 7.1) and indeed those dose-response curves could be fitted well if the EC50 values were constrained to the binding values (data not shown).

WIN 62,577 and staurosporine dose-response curves in presence of 0.01 μM ACh were also generated in order to quantify the cooperativity values (β) between ACh and the two allosteric ligands at M_3 WT and the N132G and K523E mutants. The estimates of β are shown in Table 7.4. The β value of WIN 62,577 with ACh at M_3 WT and the N132G mutant was ca 1, i.e. neutral, matching the neutral cooperativity seen in binding experiments. At the K523E mutant this β value was slightly positive, ca 1.7, which is different from the negative cooperativity seen in binding experiments. On the other hand, staurosporine shows positive cooperativity with ACh in functional experiments with a value between 1.8-2.6 at M_3 WT and the mutants. Because of time constraints, the interaction of staurosporine with ACh in binding experiments was not measured although in the literature (Lazareno et al., 2000) it has been reported that, in binding experiments, staurosporine has a neutral cooperativity with ACh at M_3 receptors in Hepes (or is inactive).

Fig.7.8: Effect of different concentrations of WIN 62,577 on the 'true' basal activity of M_3 and the N132G and K523E mutants relative to the maximal response of ACh

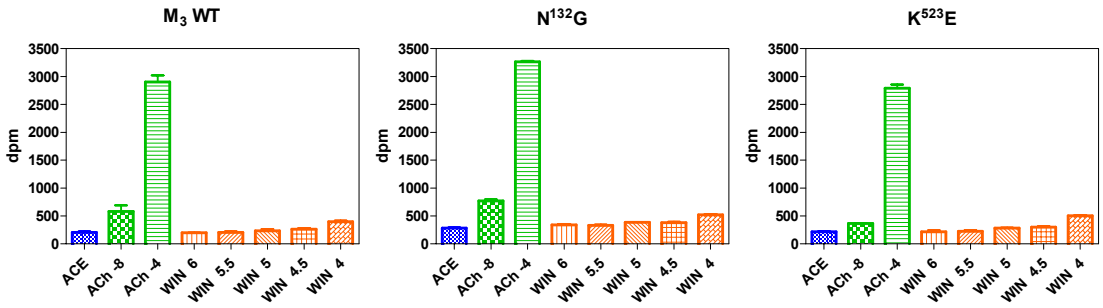

Data from a single experiment, with the mean values shown in Table 7.3

Fig.7.9: WIN 62,577 dose response curves at M_3 WT and the N132G and K523E mutants

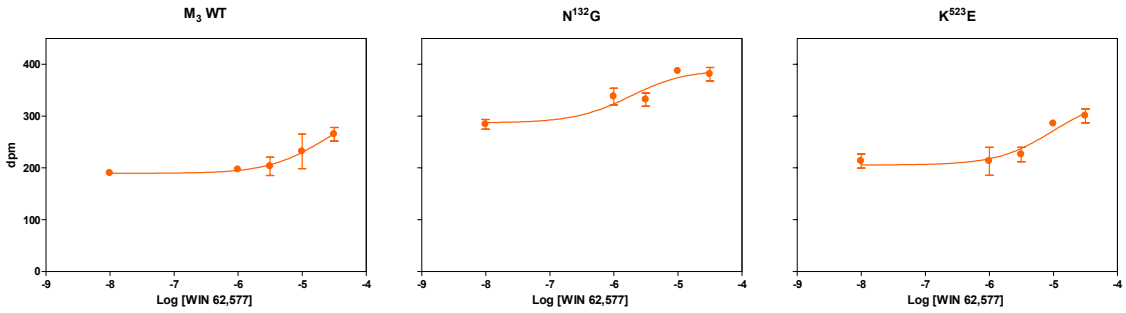

Data from a single experiment, with the mean values shown in Table 7.3

Table 7.3: Potency and Emax values of ACh and WIN 62,577 at M_3 WT and the N132G and K523E mutants

	ACh		WIN 62,577	
	Log EC50	**Emax%**	**Log EC50**	**Emax%**
M_3 WT	-7.11 ± 0.06	(100)	-5.63 ± 0.35	12 ± 2
N132G	-7.02 ± 0.18	(100)	-5.74 ± 0.31	7 ± 2
K523E	-6.53 ± 0.08	(100)	-5.20 ± 0.39	10 ± 2

Table 7.3: Potency values of ACh and WIN 62,577 at the M_3 WT and mutants obtained from dose-response curves. The stimulation by ACh is considered as 100% of the receptor stimulation. The WIN response is 5-15% of the maximum ACh response. Each estimate is the mean of duplicate values from 2-11 independent experiments

Table 7.4: Cooperativity (β) values between ACh and WIN 62,577 or staurosporine at M_3 WT and the N132G and K523E mutants

	WIN 62,577 and ACh		Staurosporine and ACh	
	Beta		**Beta**	
M_3 WT	0.94±0.19	Neutral	2.55±0.22	Positive
N132G	0.87±0.02	Neutral	1.81±0.56	Positive
K523E	1.65±0.20	Positive	1.86±0.45	Positive

7.5 Discussion

The allosteric interactions of staurosporine and WIN 62,577 with [^{3}H]NMS at M_3 WT and the N132G and K523E mutants were measured in dissociation and equilibrium experiments in Hepes and PB buffers.

The dissociation of [^{3}H]NMS was inhibited by staurosporine at M_3 WT and at the mutants. The potency of staurosporine for the [^{3}H]NMS-occupied receptor was mutant independent in the three buffers, although a tendency for the affinity to be slightly increased at the K523E mutant in Hepes and Tris was observed. No inhibition of [^{3}H]NMS dissociation by WIN 62,577 at M_3 WT or any of the mutants at any buffer condition was detected.

In equilibrium binding studies in Hepes and Tris, there was a tendency for the staurosporine affinity values to be increased equally at the K523E and K523Q mutants. In PB buffer the log Kx was 6 fold and 3 fold higher at K523E and K52EQ respectively relative to M_3 WT. With regards the affinity values of WIN 62, 577 in the equilibrium binding studies using [^{3}H]-NMS alone there was not enough information to precisely calculate the log Kx values. In addition the log Kocc values could not be used to constrain the fit because WIN 62,577 did not affect [^{3}H]NMS dissociation. Therefore the log Kocc could not be constrained in the equation. We had to share the log Kx parameters between M_3 WT and the mutants which gave us an estimation of the log Kx for WIN. Even though the errors were big there is no evidence which indicates that the log Kx was mutant or buffer sensitive.

In contrast to most muscarinic allosteric agents, WIN 62,577 does not inhibit dissociation of [^{3}H]NMS from M_3 receptors and mutants at high concentrations, although (Lazareno et al., 2002) showed that this modulator clearly occupies the receptor and inhibits the effect of another allosteric agent, PG987. We can make the assumption that WIN 62,577 slows the [^{3}H]NMS association rate, as obidoxime acts in a similar manner at the 'gallamine'site, it has no effect on [^{3}H]QNB dissociation from the M_2 receptors (at low ionic strengths).

The allosteric interactions between WIN and ACh were also measured at the M_3 WT and mutants in the Hepes buffer, which is relatively close to physiological. The

cooperativity at M_3 WT was neutral, although it was shifted to negative cooperativity at the K523E and K523Q mutants, indicating that both mutations have small and equal effects on WIN binding but only in the ternary complex with ACh where the affinity was decreased ca 2 fold. The finding that WIN 62, 577 exhibited neutral cooperativity with ACh in binding (α=1.1±0.4) may appear to be in conflict with the reported, that WIN 62,577 has low positive cooperativity with ACh in binding (Lazareno et al., 2002). However their data (α=1.8±0.5, α=1.39±0.03) are not significantly different from ours and this illustrates the difficulty in measuring precise cooperativity values when $\alpha \approx 1$.

The mutant and buffer insensitivity of WIN 62,577 binding shows an indication that the mechanism of binding of the WIN compound is different from that seen at gallamine site. Furthermore the equal effects of the mutants K523E and K523Q suggests that the WIN site and the 'gallamine' site maybe located in different regions of the receptor. In Chapter 5, we showed that interactions between ACh and strychnine-like compounds were completely different from those of WIN 62,577 described in this chapter. PB tended to make cooperativity more positive and there was a clearly enhancement produced exclusively by K523E and not K523Q on the ACh binding when strychnine-like compounds were present.

The neutral cooperativity between WIN and ACh in binding at M_3 receptors was also found in functional experiments. However we saw a discrepancy between what we saw in binding and function at K523E. The negative cooperativity seen in binding between WIN and ACh was switched to positive in functional studies, going from values of 0.4 to 1.7. This clearly indicates a different behaviour from what is occurring in binding. This discrepancy might happen as WIN 62,577 behaves unexpectedly in absence of ACh at the M_3 and mutant receptors. This will be discussed in the following paragraph. Cooperativity values between staurosporine and ACh have been also calculated in functional studies, suggesting that staurosporine could be acting as an enhancer at M_3 WT and the N132G and K523E mutations. However caution should be applied in this interpretation as staurosporine may have other intracellular effects caused by its ability to inhibit kinases.

Apparent constitutive activity was seen at a certain point during the investigation of the effect of several allosteric modulators on ACh stimulation in functional studies. We showed that ACh was present in the assays in the previous chapter (functional studies).

Therefore, as a control to eliminate the ACh, the enzyme AChE was added. The WIN 62,577 effect on the basal activity of M_3 and mutants has been studied in presence of AChE. It has been shown than in presence of AChE, WIN 62,577 is an allosteric agonist activating the receptor from its allosteric site. This novel finding has also been confirmed by performing the corresponding WIN dose-response curves and obtaining the EC50 values of WIN at M_3 WT and the mutants. The potency values obtained agreed well with those found in binding assays emphasizing the quality of the data and the ability to activate the receptors was due to a specific action of WIN at the receptors and not to another mechanism.

Chapter 8. Overall conclusions

GPCR structural studies have proceeded largely in the absence of a high-resolution X-ray crystal structure, in contrast to many other proteins. The publication in 2000 of structure of the inactive state of bovine rhodopsin (Palczewski et al., 2000) has certainly been useful and it has provided the possibility to create rhodopsin-based models of muscarinic receptors. Unfortunately it has only limited application for the study of allosteric binding sites because the extracellular loops, where the allosteric sites are predicted to be located, are difficult to model due to their flexibility. In addition this is a non-conserved region among members of Family A GPCRs, including the muscarinic receptor subtypes. Very recently a new high-resolution crystal structure of the human beta 2 adrenergic receptor, also a member of Family A biogenic amine GPCRs, has been reported (Cherezov et al., 2007;Rasmussen et al., 2007). New prospects have arisen with the release of this new structure as it shows some differences from the rhodopsin model. There is a major difference in the E2 loop which instead of facing down into the receptor, is facing up. This may be due to the presence of an extra conserved disulfide bond in the second loop in addition to the conserved disulfide bond found in many Family A GPCRs. Rhodopsin-based models created so far for Family A receptors and the theoretical interpretations might have to be revised to take into account this new model because structural differences in the ligand binding site and other regions might be found. This new model highlights the challenges in using rhodopsin as the template for the study of this large family. It is important to emphasize the generation of experimental results in order to compare and validate the theoretical models.

The Family A (rhodopsin-like) receptors represent the largest subfamily of GPCRs. Within this family, the most extensive structural studies of allosteric binding sites have been on mAChRs. This is in part due to the fact that the earliest allosteric modulation was noted for this receptor family, reviewed in (Christopoulos and Kenakin, 2002;Birdsall and Lazareno, 2005). In addition there are series of structurally diverse allosteric modulators that recognize at least one common allosteric site, on all five subtypes of mAChR. Two basic approaches generally have been used in most mutagenesis studies of allosterism at mAChR. The first has involved site-directed

mutagenesis of residues that are conserved across each of the five subtypes of receptors, aiming to find a common pattern in the allosteric binding site. The second, more widespread, approach has involved creation of chimeric receptors and mutagenesis of nonconserved residues in an attempt to delineate the structural basis of modulator selectivity for different subtypes (Christopoulos and Kenakin, 2002;Birdsall and Lazareno, 2005).

In this thesis, three residues of the human M_3 muscarinic receptor, not conserved between the five muscarinic subtypes and located in the extracellular loops have been selected to be studied. Several allosteric compounds, known to have different allosteric interactions between M_3 and M_1 receptors, have been used in order to investigate a potential role of residues in the subtype selective allosteric modulation. We have shown that one of these residues, K523, when substituted with the corresponding charged residue in M_1 receptors, (and not when replaced by an uncharged residue) plays an important role in regulating both the affinity and the cooperativity of certain allosteric compounds.

We have also confirmed that the binding of both orthosteric and allosteric ligands to muscarinic receptors can be very sensitive to the incubation conditions of the binding assay (Tränkle et al., 1996;Schröter et al., 2000;Pedder et al., 1991;Birdsall et al., 1979). This sensitivity has been exploited to expose or amplify differences in the binding properties of the mutants from those of the WT receptors. The different buffers conditions were chosen to exploit differences in buffer, (Tris, Hepes, phosphate), presence of 100 mM NaCl, absence of Mg^{2+}, and different incubation temperatures, rather than to investigate the roles of the individual variables in allosteric phenomena at muscarinic receptors. The three buffers also represent those commonly used in muscarinic receptor studies and thus facilitate comparison of the results reported here with those in the literature. The ionic strengths of the PB, Tris and Hepes buffers are ca 0.01, 0.06 and 0.20 respectively.

This chapter concentrates on the main new findings: the different binding properties in PB, the different properties of the K523E mutant, and the potentiating effect of the combination of these two phenomena. In addition the possible location of K523 and other residues in three different models relating to the structure of the M_3 receptor are presented and discussed.

1. Influence of PB relative to Hepes:

Orthosteric ligands and the orthosteric site

We did not find significant differences between the [^{3}H]NMS affinity constants in Hepes and Tris. However, the affinity of [^{3}H]NMS for the receptors in PB buffer is increased, the k_{-1} values are decreased and the k_{+1} (calculated) values are increased (relative to Hepes and Tris buffer) without exception at M_3, M_1 and the mutant receptors. One of the explanations for the effect of PB buffer on the NMS binding properties is that the lower ionic strength of the buffer PB might be facilitating the binding of the NMS, there being less interference from cations. This may explain why the k_{+1} was faster at RT in PB than at 37° in Hepes. The results obtained indicate that the different incubation conditions produce substantial perturbations of the binding properties of [^{3}H]NMS. The ACh affinity constants were also increased, ca 3-4 fold, at M_3, M_1 and the mutant receptors. These perturbations could give more information about the nature of the binding processes and the modes of binding and this was illustrated with the putative selective M_3 antagonists darifenacin, solifenacin and SVT-40776. Different patterns of PB sensitivity were found. For the M_3 WT and mutants, darifenacin and solifenacin affinity values were ca 3 fold higher in PB than in Hepes or Tris. Contrarily at M_1 receptors, darifenacin and solifenacin affinity values were unaffected by PB but increased in Hepes relative to PB. The affinity of SVT-40776 was buffer insensitive at both M_3 and M_1 WT receptors. This indicates different ways of binding of these molecules between M_3 and M_1 receptors.

Allosteric ligands acting at the 'gallamine or common' allosteric site

In all the studies carried out with allosteric ligands in this thesis the data could be fitted satisfactory to the ATCM, validating the use of this model.

The effects on binding affinities and the interaction with **[^{3}H]NMS** have been studied. We always found an increase in affinity of allosteric ligands at both the unoccupied and [^{3}H]NMS occupied receptors in PB buffer, relative to Hepes or Tris, without exception at M_3, M_1 and the mutants. This change was particularly pronounced for gallamine, especially for the affinity for the unoccupied receptor which was 150 fold higher at M_3, relative to Hepes. The change was even greater at K523E (over 1200 fold) indicating an

increased influence of the buffer in K523E compared to M_3 WT. The effects of PB on the potencies of the three strychnine related compounds, for both the unoccupied and the [^{3}H]NMS occupied receptors, were also different in M_3 and K523E. Although the effects on the affinities were less than for gallamine, (the exception being the change in logKocc of brucine which is similar to that of gallamine), the incubation buffer still made a profound change in the SAR of these three particular ligands when they bind to M_3 and K523E.

PB also has influence on the affinity constants of the three allosteric ligands, strychnine, brucine and CMB, when the receptor is occupied by **ACh**, increasing all these affinity constants without exception at M_3 and M_1 WT and at the K523E mutant. PB affected equally the logKocc(ACh) of brucine and CMB, with an increase of ca 10 fold at M_3 WT and K523E. Only the Kocc(ACh) of strychnine was more affected by the PB buffer, which was 40 fold higher at M_3 WT and 100 fold higher at K523E relative to Hepes.

For the first time the effects of buffer conditions on the cooperativity values for different allosteric modulators with **[^{3}H]NMS** have been investigated in detail. At M_3 WT in Hepes the alpha values of gallamine, strychnine, brucine and CMB with [^{3}H]NMS were all less than 1. By incubating in PB buffer, the cooperativity of gallamine with [^{3}H]NMS was changed to be more strongly negative. We were also able to switch the cooperativity of strychnine from negative to positive whereas the alpha values of brucine and CMB were unaffected.

Between **ACh** and strychnine, brucine or CMB, all the cooperativity values were more positive in PB relative to Hepes at M_3, M_1 and K523E, indicating a general tendency of PB to increase the value of beta. We also were able to switch the direction of cooperativity values by incubating in PB. The cooperativity between brucine and ACh at M_3 WT was changed from negative in Hepes to neutral in PB. Between strychnine and ACh at M_1 and K523E the cooperativity was also changed from negative to neutral and from neutral to positive respectively. To our knowledge this is the first time that changes in cooperativity values between allosteric agents and ACh based on different buffer conditions have been reported.

The results of this study give us an indication of how much the affinity constants can vary, depending on the conditions of the binding assay. The magnitude and direction of the perturbations depends on both structure of the ligand and subtype with which is interacting. For example, the smallest range of affinity change was around 3 fold (ACh affinity) whereas the affinity of gallamine for K523E can vary 10,000 fold relative to M_3. As a consequence, both the structure-binding relationships of a given receptor may dramatically change as well as the selectivity of a drug for the different receptors. The explanation of why there are such variations in affinity both within and between subtypes and mutations is not known. The binding site for competitive antagonists and agonists is thought to lie in a pocket formed by seven hydrophobic transmembrane domains, of the receptor (Hulme et al., 1990). However, within the putative transmembrane domains there is a strong residue conservation between subtypes. Conserved amino acid residues containing most of the hydrophilic side chains point towards the central pore whereas the hydrophobic residues are on the outside, facing the lipid bilayer (Hulme et al 1990). If this model is valid, the muscarinic receptor binding site might be considered as a conserved hydrophilic pocket within the membrane, although there are antagonists which are quite hydrophobic, so hydrophobic residues may form part of the binding site. The model may well explain the difficulties in designing very selective competitive antagonists as well as the relative insensitive of the affinity constants of most antagonists to the ionic environment. The exception of this behaviour are allosteric ligands which binds to the 'common' allosteric site and can form ternary complex with the receptor-antagonist binary complex. The structural determinants for gallamine binding, which is a very polar molecule, are quite different from those of the competitive antagonists. Its binding may involve several acidic residues on the extracellular loops on the receptor which are accessible to the cations in the buffer, hence explaining the sensitivity of gallamine binding to ionic strength.

The interaction of allosteric agents with orthosteric-occupied receptors is known to depend on the buffer conditions in an allosteric-specific fashion (Ellis et al., 1991;Schröter et al., 2000). The authors showed that gallamine had the strongest buffer dependence of a series of allosteric modulators studied at M_2 muscarinic receptors. Comparison of logKocc of different allosteric ligands at [^{3}H]NMS occupied M_2 receptors using two different buffer conditions has been performed (Tränkle et al., 1996). They revealed that the binding affinity of allosteric ligands is generally lower in

Tris buffer (in presence of divalent cations) than in the low ionic strength medium PB (in absence of divalent cations) (Tränkle et al., 1996). Those two buffer compositions resembled to our Tris and PB buffers. They found that generally the allosteric agents were more potent to retard the [^{3}H]NMS dissociation at M_2 in the low ionic strength buffer. It has also been suggested that Mg^{2+} competes with allosteric modulators for binding to [^{3}H]NMS-occupied M_2 receptors, possibly via interaction with the acidic amino acids in the extracellular loops of the receptor protein (Burgmer et al., 1998) giving a possible explanation of the differences found between buffer conditions. They showed that at high concentrations of Mg^{2+} ($\geq$10 mM) the equilibrium of [^{3}H]NMS is inhibited. On the other hand, at lower concentrations of Mg^{2+} retard [^{3}H]NMS dissociation but the equilibrium binding is unchanged. According to this, our Tris or PB buffer would not affect the equilibrium binding of [^{3}H]NMS, and in Hepes it would be inhibited. Our data generally have shown similar effects on the affinity constants of ligands in Hepes and Tris buffer.

Allosteric ligands acting at the WIN site

WIN 62,577 has been reported to bind allosterically, like staurosporine, to a second allosteric site on muscarinic receptor (Lazareno et al., 2002). The ability of WIN 62,577 to cross the blood-brain barrier makes it a potential drug in the therapy for human central nervous system disorders. For that reason the allosteric interactions between WIN and ACh was also measured at the M_3 WT and mutants in a buffer which was similar to physiological, Hepes.

The staurosporine binding affinity constants for the [^{3}H]NMS-occupied M_3 receptor are slightly sensitive ($p<0.05$) to buffer but not for the [^{3}H]NMS-occupied K523E receptor. PB or Tris does not have any influence on the lack of effect of WIN 62,577 on [^{3}H]NMS dissociation from M_3 WT and from the M_3 mutants. The WIN 62,577 affinity constants of at M_3 WT and mutants appeared to be similar (ca 5.3) under the three different conditions.

2. Influence of K523E relative to M_3

Orthosteric ligands and the orthosteric site

None of the mutants have any effect on [^{3}H]NMS binding affinity although the NMS affinity is different for M_3 and M_1. These residues separately, are not responsible for the NMS subtype selectivity. However [^{3}H]NMS dissociation from the K523E mutant becomes faster, ca 2-2.7 fold, regardless of the incubation conditions. [^{3}H]NMS dissociation at the K523Q is also faster, although not as much. The positively charged residue, lysine, might be interfering in the dissociation of NMS from the receptor. The mutations do not interfere in the conformation of the orthosteric binding site of the receptor, only in the dissociation (and association) kinetics. Residue 523 might be on the pathway taken by NMS to and from its binding site.

As found for NMS, the affinity values of ACh and atropine are not affected either by any mutation in any of the conditions. There were also no significant effects of K523E on affinity values for darifenacin, solifenacin, tolterodine and SVT-40776 relative to M_3 WT indicating that the residue studied is not important for the binding selectivity of these M_3 antagonists.

It seems that this residue is not important for the binding of any of the orthosteric ligands. It does not affect the structure of the orthosteric binding site but it might be on the pathway for the orthosteric ligands in and out of the receptor.

Allosteric ligands and 'gallamine' or 'common' allosteric site

We have investigated the effects on binding affinities and the interaction with **[^{3}H]NMS**. One of our main findings has been the increase in the affinity constants of the four allosteric ligands studied at K523E relative to M_3 WT, which were independent of the structure of the ligand and the buffer conditions used. This increase in affinity differed, especially for gallamine, for the unoccupied receptors which was higher relative to the strychnine related compounds. For example in PB the increase in gallamine affinity was ca 70 fold higher relative to M_3 WT. Contrarily, the effect of K523E was greater on the affinity of strychnine, brucine and CMB for the [^{3}H]NMS

occupied receptors. Again we see a difference in the mode of binding of the polycationic agent gallamine and the other three related compounds. Only for gallamine were increases in affinity constants found at the K523Q mutant, but these were not as high as found for K523E. This suggests that the positive charge of lysine is interfering with the binding of gallamine, but not with the other compounds. This is another indication of different mode of binding between gallamine and the strychnine related compounds.

The allosteric interaction with **ACh** has also been inivestigated. In contrast to the studies on prototypical modulators with [^{3}H]NMS, there have been only a few studies to date on the effect of allosteric site mutations on the actions of orthosteric agonists. To date, only the mutation Y82A at the M_1 receptor (Baig et al., 2005) has been shown to increase the affinity of ACh in the presence of WIN 62,577 and WIN 51,708 and to switch the direction of the cooperativity between ACh and WIN 62,577 or WIN 51,708 from negative to positive. A study investigating the effects of allosteric-site mutation on the mode of binding of possible allosteric muscarinic agonists such as AC-42 and McN-A-343 has also been reported (May et al., 2007a), but in functional studies no effect of mutation on the direction of the cooperativity between ACh and the allosteric agonists was found.

Nevertheless this is the first time to our knowledge that the changes produced by a single mutation on the affinity constants of ACh in presence of prototypical allosteric modulators have been reported. This is important as ACh is the endogenous neurotransmitter for muscarinic receptors. The changes produced on the binding parameters of allosteric ligands in presence of ACh are also novel results. The introduction of the negative residue, E, substituting for the positive charge of the lysine at position 523, made the ternary complex of the three allosteric modulators with the receptor-ACh complex more favourable. This was so especially for brucine and strychnine, where the affinity constants for the ACh occupied receptor were increased ca 90 and 160 fold respectively relative to M_3 WT. Therefore at K523E the binary complex ACh-receptor becomes more favourable for brucine and strychnine (both tertiary amines) and not as favourable for CMB (a quaternary ligand), showing a different behaviour in the mode of binding between strychnine and brucine with CMB or equivalently, a change in the SAR.

Another important finding of this particular mutant, K523E, was the change in the direction of cooperativity that was observed between **[^{3}H]NMS** and strychnine and brucine, from negative to positive and neutral cooperativity respectively in Hepes. The K523E mutation generates differences in the structure of the 'common' allosteric site when the orthosteric site is unoccupied or occupied by NMS. As discussed earlier this mutation does not affect the structure of the orthosteric site.

Another important consequence of the findings described earlier was the switch in cooperativity with **ACh** that was created by the K523E mutation. As mentioned before, only the Y82A mutant at M_1 receptors has been reported to switch the cooperativity between ACh and WIN compounds (Baig et al., 2005). To our knowledge is the first time that a switch in cooperativity between ACh and prototypical modulators created by a single mutation has been observed. Not only that but the increase of this cooperativity has been the highest that has been reported at M_3 receptors, a value of ca 35 relative to a weak negative cooperativity found at M_3 WT in Hepes. This cooperativity value is much higher than the positive cooperativity between therapeutically effective benzodiazepine tranquilizers and GABA at $GABA_A$ receptors (Ehlert et al., 1983). Brucine has become a strong enhancer at K523E and strychnine has become neutral in Hepes and positive in PB. The K523E mutation of the M_3 receptor generates aspects of the M_1 phenotype, but with even higher positive cooperativities with ACh. This shows that cooperativity values can be changed dramatically at M_3 muscarinic receptors by mutation and raises the possibility that by changing the structure of the allosteric ligands new drugs showing various patterns of cooperativities, including large cooperativities with ACh across a range of receptor subtypes, may be developed.

There is some very recent progress in the area with the development of selective M_4 enhancers with large cooperativities with ACh. These novel allosteric molecules have the potential to be used to differentially regulate specific aspects of mAChR modulation of function in the treatment of multiple central nervous system disorders, such as schizophrenia (Shirey et al., 2008) and Chang WY et al., 2008. Allosteric modulation of the muscarinic M_4 receptor as a novel approach to treating schizophrenia. Proceedings of the National Academy of Sciences (PNAS) *in press*.

Allosteric ligands acting at the WIN site

The K523E mutation showed similar effect on the staurosporine and WIN 62,577 binding affinity constants for the **[^{3}H]NMS**-occupied receptor, relative to the M_3 WT.

The K523E and K523Q mutations had a similar effect on the staurosporine binding affinity constants for the unoccupied receptors; i.e. to be increased relative to M_3 in Tris and Hepes buffer. In PB there was a bigger difference relative to M_3 WT, ca 6 fold relative to the difference found in Hepes and Tris. The K523Q affinity for the unoccupied receptor was also higher in PB, ca 3 fold, relative to M_3 WT, but the increase was as big as for the K523E mutant.

The affinity of WIN 62,577 for the unoccupied receptor at M_3 WT and the mutants appeared to be similar (ca 5.5). This suggests that the binding of WIN 62,577 to the M_3 receptor is not perturbed in K523E and K523Q. This similarity in affinity constant for these two mutations differs from the very large differences in affinity seen for all the 'gallamine site' compounds tested in previous chapters, indicating a different mechanism of WIN 62,577 binding to the receptor.

The cooperativity values between staurosporine or WIN 62,577 and **[^{3}H]NMS** are all negative and insensitive to buffer composition and to any mutation. This suggests that the binding of WIN 62,577 to the M_3 receptor and to the mutant receptors is insensitive to buffer conditions, showing an important difference compared to the binding of all the 'gallamine' compounds studied in previous sections.

The cooperativity between WIN 62,577 and **ACh** at M_3 WT was neutral, although this value was shifted to negative at the K523E and K523Q mutation, indicating that both have small and equal effects on WIN binding but only in the ternary complex with ACh where the cooperativity was decreased ca 2 fold.

3. Combined effects of PB and K523E

We have demonstrated in this study that the two major factors affecting the allosteric binding parameters, PB buffer and the K523E mutation, mutually potentiate each others effects. In order to illustrate that finding, square diagrams were constructed in the discussion of chapter 4. We have introduced two new parameters in order to describe the combination of these two effects, *overall changes in affinities* and *sensitivity factors*, for the affinities of the unoccupied and the [^{3}H]NMS and ACh occupied receptors. We have been able to obtain extremely high overall changes in affinities, e.g. the effect of both PB and K523E together, results in a ca 10,000 fold higher gallamine affinity for the unoccupied receptor at K523E in PB, relative to M_3 WT in Hepes. We also have obtained an overall change in affinity of 690 for brucine and 6400 fold for strychnine at the ACh occupied receptor for K523E in PB, relative to M_3 WT in Hepes. These are extraordinarily large changes in affinity and beg the question whether even greater changes might be produced with other allosteric ligands.

The fact that we have been able to modulate so strongly the cooperativity between allosteric agents and ACh, by introducing a single residue, E, corresponding to the M_1 subtype, and that the neutral residue substitution, Q, does not show comparable effects, may help one to understand better the mechanism of binding of these compounds to this allosteric site and, in the future, aid the development of therapeutically active drugs with novel mechanisms of action.

It seems that K523E has a quite specific effect, enhancing the affinity of allosteric ligands and facilitating the transmission of the conformational change produced by their binding to the gallamine site. And yet the mutation per se. does not affect binding of orthosteric ligands in the absence of an allosteric ligand. K523E increases log Kx, α and sensitivity to PB. In conclusion, the effect of K523E seems to be on the binding of certain allosteric ligands and the transmission of the effects of their binding to the orthosteric site.

The two factors together, PB buffer and the K523E mutation did not affect to the binding parameters of the ligands that bind to the WIN site, showing another indication of difference between the two allosteric sites.

4. Allosterism and function

For the ligands acting at the gallamine site, all the effects of the allosteric modulators on ACh binding, where examined, have been reproduced in ***functional studies*** indicating that the allosteric modulation seen in binding is transmitted to the cellular response. Similar results were observed for the action of these allosteric ligands on the oxotremorine stimulation of inositol phosphate production.

With regards to the constitutive activity studies and possible allosteric agonism generated by the mutations, we can conclude that there is a need to be aware that ACh may be present in functional assays. In studies of constitutive activity of muscarinic receptors, an AChE control is needed as all the publications working on cell lines that we are aware of, have not included this control. We did not detect any constitutive activity or allosteric agonism for the allosteric ligands that bind to the 'gallamine' site.

However, a novel finding was that in presence of AChE, WIN 62,577 is an allosteric agonist activating the receptor from its allosteric site. The potency values for WIN at the WT and mutant receptors obtained agreed well with those found in binding assays.

5. The possible location of K523 using different receptor models

Three different models relating to the structure of the M_3 muscarinic receptor have been generated and are shown below (Fig 8.1) with the extracellular part of the receptor facing outwards. The first model corresponds to the model of M_1 muscarinic receptor of Ed Hulme and Jose Saldanha (Hulme et al., 2003b;Lu et al., 2001). The second is the M_3 rat muscarinic receptor model constructed by the Jurgen Wess group (Han et al., 2005b). This is a three-dimensional model of the inactive state of the rat M_3 muscarinic receptor and was built via homology modeling using the high resolution x-ray structure of bovine rhodopsin as a template. The third model corresponds to the beta 2 adrenergic receptor, whose its crystal structure has been released very recently (Rasmussen et al., 2007;Cherezov et al., 2007). In this last model the loop does not extend across the top of the receptor. The residues in white on all three models correspond to the equivalent residues that in this study have been mutated in the human M_3 receptor. The residue on

the top corresponds to the residue D518, in the middle is the residue K523 and the one on the bottom is N132. The corresponding residues in the M_1 receptor are K392, E397 and G81 and in β_2 D300, K305 and K97. Two important conserved Trp residues (101 and 400 in M_1 receptors) which are known to be important for the allosteric binding are also shown in red (W400 in the top and W101 in the bottom). In the figure it is very interesting that the three residues chosen for this study are located in a quite similar positions in the three models and that the two tryptophan residues are similarly positioned and relatively close to the residue equivalent to K523. It might be expected, at the simplest level of interpretation, that the residues important for the binding of allosteric ligands would be clustered. In this context, residue D518 is separated from the other coloured residues and this may explain why the mutation of this residue had no effect on the binding of allosteric ligands. Similarly N132 is on the edge of the cluster formed by K523 and the two tryptophan residues compatible with its small effects on binding.

Fig.8.1: Models of M_1, M_3 muscarinic and β_2 adrenergic receptors

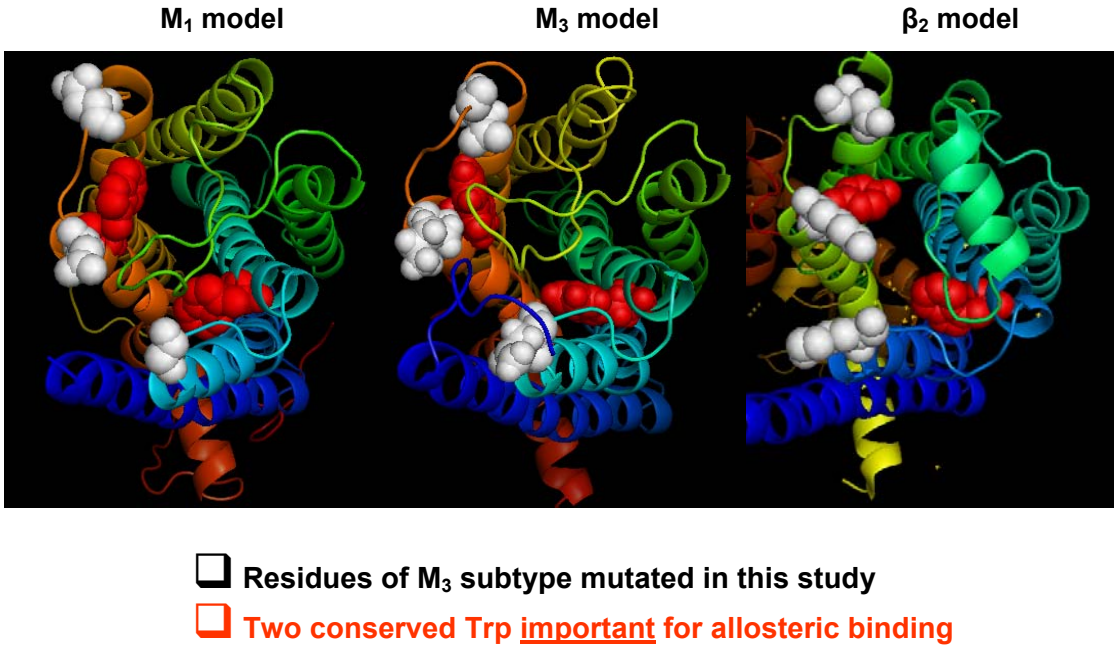

Various studies have used the approach of mutating non conserved residues of the extracellular loops in order to test their possible role in the allosteric interactions. These

kind of studies have been performed in most of the cases on the M_2 muscarinic subtype, as it has the highest affinity for the prototypical and the first allosteric agent found, gallamine. (Leppik et al., 1994) found an acidic epitope ^{172}EDGE^{175}, located in the second extracellular loop of the M_2 receptor subtype, to be important for gallamine affinity, showing the importance of the acidic residues for the binding of that allosteric modulator. The substitution of this acidic epitope into the epitope which corresponds to the M_1 subtype, ^{174}LAGQ^{177}, gave the same affinity for gallamine as for M_2. The residue Asn^{419} in M_2 has also been shown to play an important role in gallamine binding. In M_3 the triplet located in the E3 loop, Lys^{523}Phe^{525}Asn^{527} (KFN), has been shown to be important in regulating the cooperativity of gallamine, and also the residue located in the E1 loop, Arg133 (Krejci and Tucek, 2001;Jakubik et al., 2005). The residues D^{518}S^{519}Lys^{523}Phe^{525}Asn^{527} (DSKFN) at M_3 were mutated to the corresponding position of M_2. This mutant had the E3 loop equivalent to that of M_2 and switched the negative cooperativity found for alcuronium with [^{3}H]NMS in M_3 to the positive cooperativity shown in M_2.

A three-dimensional model of the M_2 receptor in the NMS-occupied state has been built on the basis of the crystal structure of bovine rhodopsin by (Jöhren and Höltje, 2002). Structurally different ligands such as gallamine, caracurine V salts or W84 (a hexamethonium-derivative) have been docked (Ellis and Seidenberg, 2000;Voigtländer et al., 2003;Huang et al., 2005). By using molecular modelling and site-directed mutagenesis approaches they have found that residues as Tyr^{177}, N^{419} and Thr^{423} are also important for the allosteric modulation of these compounds, although they indicated that each modulator has a different selectivity pattern, i.e. the residue Thr^{423} has been found to be critical for the binding of caracurine V related compounds, whereas for gallamine binding Asn^{419} plays a more important role but not for W84, which interacts with Tyr^{177} at M_2.

Previous studies have proposed that prototypical modulators of mAChRs recognize at least one allosteric site that involves the extracellular loops, particularly the E2 loop and E3 loop and its environs (Matsui et al., 1995, Gnagey et al., 1999, Leppik et al., 1994, Krejci and Tucek, 2001, Mohr and Tränkle, 2003 and Huang et al., 2005), thus highlighting that this region plays an important role in determining not only the actions of orthosteric ligands, but those of allosteric ligands as well. The E2 loop has also been

predicted to contribute directly to the orthosteric binding site by adopting a conformation similar to that found in the crystal strucure of the inactive state of rhodopsin whereby the β4 strand of the loop folds inwards towards the TM core regions that are crucial for the binding of orthosteric ligands (Shi and Javitch, 2002). Avlani et al. have postulated flexibility in the E2 loop in order to allow orthosteric ligands (often hydrophilic) to gain entrance from the extracellular space into the corresponding TM cavity. To that purpose, cysteine substitutions in two residues from the E2 loop and E3 loop (V171 and N419 in M_2) predicted to be close to each other were made and they significantly inhibit the binding of orthosteric and allosteric ligands via disulfide bond formation, compatible with the constrained E2 loop having dramatically reduced its flexibility. The E2 loop has been suggested to have a "gatekeeper" role.

Fig 8.2 shows the models described in Fig 8.1 but with additional residues 'space-filled'. The residue shown in white is the one which made the biggest effects in this study (equivalent to K523E in M_3). The Trp residues are again shown in red, and are less visible than in Fig. 8.1. Non conserved residues between the 5 muscarinic subtypes which have been shown to be important for the binding of allosteric ligands are shown in purple in their equivalent positions in the three structures. The residues are Arg^{133} in the E1 loop of M_3, in the E2 loop ^{172}EDGE^{175} and Tyr^{177} in M_2 and in the E3 loop the triplet KFN in M_3 and Thr^{423} in M_2. Finally conserved residues which are being shown not to be important for the allosteric binding at M_1 receptors (Matsui et al., 1995) are shown in yellow. In the M_1 muscarinic model it seems that the non-yellow residues are separated from each other. This lack of clustering also seems to be present in the beta 2 structure and the yellow and the coloured residues are interspersed. As with the models shown in Fig. 8.1, it might be expected that a satisfactory possible model of the allosteric site would show a cluster of red, purple and white residues without interspersed yellow residues. It might be that the second disulphide bond in the E2 loop of the beta 2 receptor (absent in muscarinic receptors) is constraining the loop. However it seems that in the M_3 model of Wess all these important residues for allosteric binding are clustered, including the K523, the residue studied, which seems to be where the action is happening. This model rationalises the important role of this residue in the binding of allosteric ligands to the gallamine site.

Fig.8.2: Models of M_1, M_3 muscarinic and β_2 adrenergic receptors showing the possible location of the 'common' allosteric site

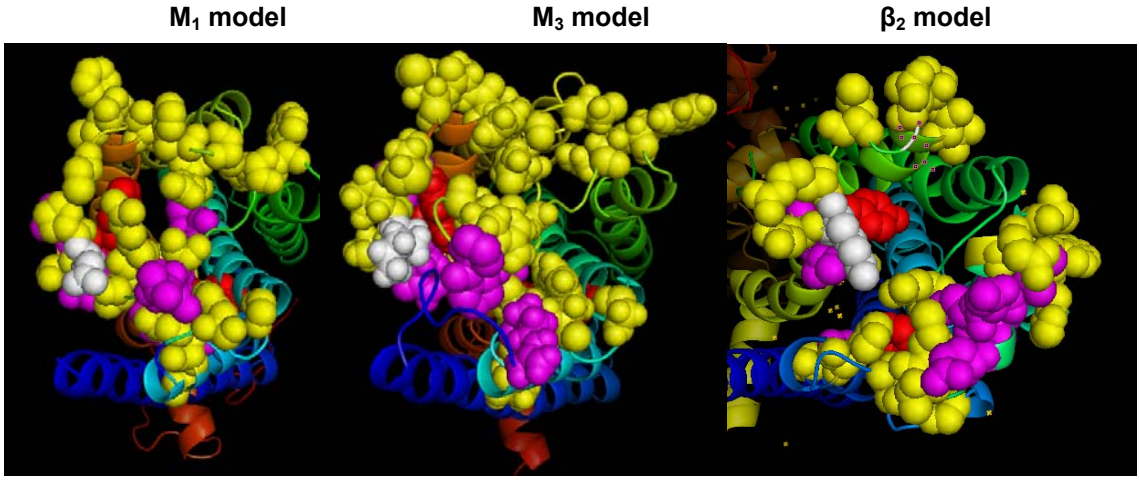

In summary, the **main results and conclusions** of this thesis are:

1. The M_3 receptor mutants, K523E, D518K and N132G, in which the substituted residues were those corresponding to the M_1 subtype, have been studied. In addition the uncharged mutants, K523Q and D518N, were also created.

2. Radioligand binding experiments revealed that one mutant, K523E, had a profound potentiating effect on the binding of prototypical modulators gallamine, strychnine, brucine and N-chloromethylbrucine, but had minimal effects on the binding of a number of orthosteric ligands. Switches from negative to positive cooperativity were observed.

3. At K523E, the affinities of the strychnine-related ligands were also increased up to 160 fold at the receptor-ACh complex, with up to 35 fold positive cooperativity being observed.

4. The dramatic changes in cooperativities and affinities of allosteric ligands at K523E, did not result in generation of the M_1 phenotype. The K523Q data suggest that the large changes in K523E result from the introduction of the negatively charged glutamate residue and not the loss of the positively charged lysine.

5. The effect of K523E seems to be solely on the binding of allosteric ligands that bind to the 'gallamine' site and the transmission of the effects of their binding to the orthosteric site.

6. For the ligands acting at the gallamine site, all the effects of the allosteric modulators on ACh binding have been reproduced in functional studies, indicating that the allosteric modulation, seen in binding, is transmitted to the cellular response.

7. A novel and unexpected finding is that WIN62,577 is an allosteric agonist at M_3 muscarinic receptors and at K523E and N132G.

8. Low (nanomolar) concentrations of ACh may be present in assays of muscarinic receptor function and may give misleading interpretations of data. These artefacts were removed by preincubation with acetylcholinesterase.

9. In a phosphate buffer of low ionic strength (PB) the affinity constants of almost all the compounds studied, both orthosteric and allosteric, were increased relative to a Hepes buffer of higher ionic strength.

10. Cooperativities have also been switched between negative and positive by changing buffer.

11. WIN 62,577, an allosteric ligand which binds to a different allosteric site from the prototypical modulators, and SVT-40776 a new M_3 selective antagonist, have different modes of binding to M_3 receptors.

12. The two factors affecting the allosteric binding parameters of M_3 receptors, PB and the mutation K523E, mutually potentiate each others effects. 10,000 fold changes in the affinity at the unoccupied receptor and 6400 fold increases in affinity at the ACh occupied receptor have been observed.

13. The possible location of K523, relative to other residues on the external loops of muscarinic receptors shown to be important for the binding of allosteric ligands, has been explored using different models based on the X-ray structures of rhodopsin and the β_2 adrenergic receptor.

Chapter 9. Future directions

The following list highlights interesting points that have arisen during this study and would benefit from further investigation to provide a more comprehensive understanding of the molecular basis of allosteric ligand binding to muscarinic acetylcholine receptors.

1. We have shown the extraordinary large changes in the affinity of three allosteric ligands that the mutant K523E and PB generate together when NMS or ACh are bound to the receptor. This finding raises the question of whether even greater changes might be produced with other allosteric ligands and other orthosteric ligands. Experiments using a range of other allosteric ligands, with similar and with different structures, and which bind to the 'common' and to the second allosteric site, would help to answer that question.

2. The fact that the ACh affinity was enhanced by the K523E mutation in presence of brucine and strychnine leads to the question of whether this affinity could be even more enhanced by further mutations. There are certain mutants which have been shown to enhance the ACh affinity by themselves, CAMs (constitutive active mutants), at the junction between TM VI and the third extracellular loop. At M_3 receptors the N514Y mutation has been shown to display many of the common properties exhibited by CAMs, such as enhanced agonist potency and binding affinity. The study of the double mutant N514Y/K523E could give an indication whether the effect of increasing ACh affinity is enhanced synergistically by both mutants, whether they oppose each other or whether the enhancement of ACh affinity is created by the same mechanism of action.

3. To ascertain whether or not the residue located at the 523 position at M_3 receptors has an important role in the absolute or subtype selective modulation of the cooperativity between allosteric ligands and ACh at the other three subtypes, it would be interesting to construct the K523N, K523D and K523V mutants (the residues found at equivalent positions in M_2, M_4 and M_5 receptors) and study their allosteric interactions between brucine, strychnine and CMB with ACh in binding and functional experiments. Furthermore, the substitution

of the residue E in the equivalent position of the other subtypes would answer the question whether this particular residue is important for creating a favourable conformation of the receptor between the allosteric ligands and ACh only at M_3 receptors or it can be generalized to the other subtypes. In the case of M_1 receptors it may be necessary to also mutate the lysine residue in the E3 loop to achieve the desired effect.

4. From this study, it was apparent that WIN 62,577 was activating the M_3 muscarinic receptors from its allosteric site. In order to study whether this compound is an M_3 selective allosteric partial agonist or it produces this effect at other subtypes, further functional experiments with WIN 62,577 will be necessary. Another approach to further investigate this agonism would be to perform Ca^{2+} assays, where the stimulation of the receptor by WIN 62,577 is measured by the increase in intracellular [Ca^{2+}] in a fluorescence assay. Alternatively, ERK assays or assays of β-arrestin binding could be used. The agonist actions of analogues of WIN 62,577 could be investigated. It may be that activation by WIN 62,577 generates a different conformational activated state from that exhibited by orthosteric agonists and will give 'stimulus trafficking' (selective activation of one signalling pathway).

5. A model of the active state of the M_3 msucarinic receptor using rhodopsin and beta 2 adrenergic as a templates with the ACh docked inside and the brucine docked in the extracellular part of the receptor at the WT receptor and the mutant K523E will give us additional information at a molecular level of the mechanism of binding and how this residue is modulating the binding of these two ligands at the same time.

6. If AC-42 or desmethylclozapine are allosteric agonists but acting at a different allosteric site, are those agonist actions and those of WIN 62,577 synergistic?

7. The response of AC-42 at the W101A mutant in M_1 is increased from 50% to 100%. In addition, the clozapine response is increased from 13% to 96 % at the Y106A mutant in M_1. The affinity of ACh is substantially reduced at these two mutants. Combinations of these mutations, together with K523E at M_3 would determine whether further increases in the allosteric ligand actions are seen.

8. Exploration of the effects of the K523E mutation on the binding of atypical allosteric ligands, like Duo3, tacrine and the pentacyclic carbazoles in high and low ionic strength conditions will give information as to whether these compounds maintain their atypical behaviour and behave similarly to the strychnine-related compounds.

9. It might be interesting to investigate the effect of the K523E mutation on the kinetics of a very highly hydrophobic ligand such as ^{3}H-QNB to see whether its mode of access to the orthosteric site is different from that of polar ligands. In this context it is worth noting than, in PB, gallamine speeds up [^{3}H]QNB dissociation (Ellis et al., 1991), and the question arises is whether QNB accesses the orthosteric site via the TM helices?

10. A novel small molecule potentiator, LY2033298 has a very high degree of positive allosteric enhancement of acetylcholine potency (ca 35 fold) at M_4 and it is a potential drug for treatment of schizophrenia, as it has been shown to be active in vivo (Chang WY et al., 2008. *Allosteric modulation of the muscarinic M_4 receptor as a novel approach to treating schizophrenia*. Proceedings of the National Academy of Sciences (PNAS) *in press*.). Mutational analysis identified a key amino acid located in the third extracellular loops which is negatively charged (D^{432}) of the human M_4 receptor to be important for selectivity and agonist potentiation by LY2033298. Interestingly this residue corresponds to the same position of the residue K523 at M_3 receptor. A study of the binding and the cooperativity with ACh of LY2033298 at the mutant K523E or K523D in order to try to reproduce the activity observed at M_4 will help to understand whether a negative charge in that position it is also have the same effect at M_3. Equally the question is whether the D432K mutation at M_4 abolishes the enhancing effect of LY2033298. Analogous studies using the related compound, VU10010, which potentiates the M_4 response to ACh ca 50-fold, could be done (Shirey et al., 2008).

11. In order to test the possible therapeutic use of the K523E enhancer effect, it would be attractive to generate mutant mice that selectively express the K523E mutant in β-pancreatic cells in mice which have the GSIS decreased. The administration of a suitable allosteric enhancer to those mutant mice would increase GSIS, and indicate a possible therapeutic role for M_3 enhancers.

Chapter 10. References

Ahren B (2000) Autonomic Regulation of Islet Hormone Secretion--Implications for Health and Disease. *Diabetologia* **43**:393-410.

Anagnostaras SG, Murphy G G, Hamilton S E, Mitchell S L, Rahnama N P, Nathanson N M and Silva A J (2003) Selective Cognitive Dysfunction in Acetylcholine M1 Muscarinic Receptor Mutant Mice. *Nat Neurosci* **6**:51-58.

Avlani VA, Gregory K J, Morton C J, Parker M W, Sexton P M and Christopoulos A (2007) Critical Role for the Second Extracellular Loop in the Binding of Both Orthosteric and Allosteric G Protein-Coupled Receptor Ligands. *J Biol Chem* **282**:25677-25686.

Baig A, Leppik R and Birdsall N (2005) The Y82A Mutant of the M_1 Receptor Has Increased Affinity and Cooperativity With Acetylcholine for WIN 62,577 and WIN 51,708. *pA2online* **3**:119P.

Baldwin JM, Schertler G F and Unger V M (1997) An Alpha-Carbon Template for the Transmembrane Helices in the Rhodopsin Family of G-Protein-Coupled Receptors. *J Mol Biol* **272**:144-164.

Ballesteros J and Weinstein H (1995) Integrated Methods for the Construction of Three Dimensional Models and Computational Probing of Structure-Function Relations in G-Protein Coupled Receptors. *Methods Neurosci* **25**:366-428.

Barlow RB, Berry K J, Glenton P A, Nilolaou N M and Soh K S (1976) A Comparison of Affinity Constants for Muscarine-Sensitive Acetylcholine Receptors in Guinea-Pig Atrial Pacemaker Cells at 29 Degrees C and in Ileum at 29 Degrees C and 37 Degrees C. *Br J Pharmacol* **58**:613-620.

Barlow RB, Birdsall N J and Hulme E C (1979) Temperature Coefficients of Affinity Constants for the Binding of Antagonists to Muscarinic Receptors in the Rat Cerebral Cortex. *Br J Pharmacol* **66**:587-590.

Basile AS, Fedorova I, Zapata A, Liu X, Shippenberg T, Duttaroy A, Yamada M and Wess J (2002) Deletion of the M5 Muscarinic Acetylcholine Receptor Attenuates Morphine Reinforcement and Withdrawal but Not Morphine Analgesia. *Proc Natl Acad Sci U S A* **99**:11452-11457.

Billington CK and Penn R B (2003) Signaling and Regulation of G Protein-Coupled Receptors in Airway Smooth Muscle. *Respir Res* **4**:2.

Birdsall NJ, Burgen A S, Hulme E C, Stockton J M and Zigmond M J (1983) The Effect of McN-A-343 on Muscarinic Receptors in the Cerebral Cortex and Heart. *Br J Pharmacol* **78**:257-259.

Birdsall NJ, Burgen A S, Hulme E C and Wells J W (1979) The Effects of Ions on the Binding of Agonists and Antagonists to Muscarinic Receptors. *Br J Pharmacol* **67**:371-377.

Birdsall NJ and Lazareno S (2005) Allosterism at Muscarinic Receptors: Ligands and Mechanisms. *Mini Rev Med Chem* **5**:523-543.

Birdsall NJM, Farries T, Gharagozloo P, Kobayashi S, Lazareno S and Sugimoto M (1999) Subtype-Selective Positive Cooperative Interactions Between Brucine Analogs and Acetylcholine at Muscarinic Receptors: Functional Studies. *Molecular Pharmacology* **55**:778-786.

Bissantz C (2003) Conformational Changes of G Protein-Coupled Receptors During Their Activation by Agonist Binding. *J Recept Signal Transduct Res* **23**:123-153.

Bluml K, Mutschler E and Wess J (1994a) Functional Role in Ligand Binding and Receptor Activation of an Asparagine Residue Present in the Sixth Transmembrane Domain of All Muscarinic Acetylcholine Receptors. *J Biol Chem* **269**:18870-18876.

Bluml K, Mutschler E and Wess J (1994b) Insertion Mutagenesis As a Tool to Predict the Secondary Structure of a Muscarinic Receptor Domain Determining Specificity of G-Protein Coupling. *Proc Natl Acad Sci U S A* **91**:7980-7984.

Bohr C, Hasselbalch KA and Krogh A (1904) Ubereinen in Biologischen Beziehung Wichtigen Einfluss, Den Die Kohlen-Sauerspannung Des Blutes Auf Dessen Sauerstoffbindung Ubt. *Skand Arch Physiol* **16**:402-412.

Bond RA and Ijzerman A P (2006) Recent Developments in Constitutive Receptor Activity and Inverse Agonism, and Their Potential for GPCR Drug Discovery. *Trends Pharmacol Sci* **27**:92-96.

Bonner TI, Buckley N J, Young A C and Brann M R (1987) Identification of a Family of Muscarinic Acetylcholine Receptor Genes. *Science* **237**:527-532.

Bonner TI, Young A C, Brann M R and Buckley N J (1988) Cloning and Expression of the Human and Rat M5 Muscarinic Acetylcholine Receptor Genes. *Neuron* **1**:403-410.

Bosch L, Iarriccio L and Garriga P (2005) New Prospects for Drug Discovery From Structural Studies of Rhodopsin. *Curr Pharm Des* **11**:2243-2256.

Bourne HR (1997) How Receptors Talk to Trimeric G Proteins. *Curr Opin Cell Biol* **9**:134-142.

Bradford MM (1976) A Rapid and Sensitive Method for the Quantitation of Microgram Quantities of Protein Utilizing the Principle of Protein-Dye Binding. *Anal Biochem* **72**:248-254.

Brown DA, Forward A and Marsh S (1980) Antagonist Discrimination Between Ganglionic and Ileal Muscarinic Receptors. *Br J Pharmacol* **71**:362-364.

Bruns RF and Fergus J H (1990) Allosteric Enhancement of Adenosine A1 Receptor Binding and Function by 2-Amino-3-Benzoylthiophenes. *Mol Pharmacol* **38**:939-949.

Budd DC, Willars GB, McDonald JE, Tobin AB (2001) Phosphorylation of the $G_{q/11}$-coupled M3-muscarinic receptor is involved in receptor activation of the ERK-1/2 Mitogen-activated Protein Kinase Pathway. *J Biol Chem* **276**:4581-7.

Buller S, Zlotos D P, Mohr K and Ellis J (2002) Allosteric Site on Muscarinic Acetylcholine Receptors: a Single Amino Acid in Transmembrane Region 7 Is Critical to the Subtype Selectivities of Caracurine V Derivatives and Alkane-Bisammonium Ligands. *Mol Pharmacol* **61**:160-168.

Burgmer U, Schulz U, Tränkle C and Mohr K (1998) Interaction of Mg2+ With the Allosteric Site of Muscarinic M2 Receptors. *Naunyn Schmiedebergs Arch Pharmacol* **357**:363-370.

Caulfield MP (1993) Muscarinic Receptors--Characterization, Coupling and Function. *Pharmacol Ther* **58**:319-379.

Caulfield MP and Birdsall N J (1998) International Union of Pharmacology. XVII. Classification of Muscarinic Acetylcholine Receptors. *Pharmacol Rev* **50**:279-290.

Chapple CR (2000) Muscarinic Receptor Antagonists in the Treatment of Overactive Bladder. *Urology* **55**:33-46.

Chapple CR and Nilvebrant L (2002) Tolterodine: Selectivity for the Urinary Bladder Over the Eye (As Measured by Visual Accommodation) in Healthy Volunteers. *Drugs R D* **3**:75-81.

Cherezov V, Rosenbaum D M, Hanson M A, Rasmussen S G, Thian F S, Kobilka T S, Choi H J, Kuhn P, Weis W I, Kobilka B K and Stevens R C (2007) High-Resolution Crystal Structure of an Engineered Human Beta2-Adrenergic G Protein-Coupled Receptor. *Science* **318**:1258-1265.

Chess-Williams R, Chapple C R, Yamanishi T, Yasuda K and Sellers D J (2001) The Minor Population of M3-Receptors Mediate Contraction of Human Detrusor Muscle in Vitro. *J Auton Pharmacol* **21**:243-248.

Christopoulos A and Kenakin T (2002) G Protein-Coupled Receptor Allosterism and Complexing. *Pharmacol Rev* **54**:323-374.

Christopoulos A and Mitchelson F (1997) Pharmacological Analysis of the Mode of Interaction of McN-A-343 at Atrial Muscarinic M2 Receptors. *Eur J Pharmacol* **339**:153-156.

Clark AL and Mitchelson F (1976) Inhibitory Effect of Gallamine on Muscarinic Receptors. *British Journal of Pharmacology* **58**:323-331.

Costa T and Herz A (1989) Antagonists With Negative Intrinsic Activity at Delta Opioid Receptors Coupled to GTP-Binding Proteins. *Proc Natl Acad Sci U S A* **86**:7321-7325.

Dale HH (1914) The actions of certain esteres and ethers of choline, and their relation to muscarine. *J Pharmacol Exp Ther* **6**:147.

De Araujo JE, Huston J P and Brandao M L (2001) Opposite Effects of Substance P Fragments C (Anxiogenic) and N (Anxiolytic) Injected into Dorsal Periaqueductal Gray. *Eur J Pharmacol* **432**:43-51.

Dong BJ (2005) Cinacalcet: An Oral Calcimimetic Agent for the Management of Hyperparathyroidism. *Clin Ther* **27**:1725-1751.

Dowling MR, Willets J M, Budd D C, Charlton S J, Nahorski S R and Challiss R A (2006) A Single Point Mutation (N514Y) in the Human M3 Muscarinic Acetylcholine Receptor Reveals Differences in the Properties of Antagonists: Evidence for Differential Inverse Agonism. *J Pharmacol Exp Ther* **317**:1134-1142.

Drews J (2000) Drug Discovery: a Historical Perspective. *Science* **287**:1960-1964.

Duttaroy A, Zimliki C L, Gautam D, Cui Y, Mears D and Wess J (2004) Muscarinic Stimulation of Pancreatic Insulin and Glucagon Release Is Abolished in M3 Muscarinic Acetylcholine Receptor-Deficient Mice. *Diabetes* **53**:1714-1720.

Eglen RM (2005) Muscarinic Receptor Subtype Pharmacology and Physiology. *Prog Med Chem* **43**:105-136.

Eglen RM, Choppin A, Dillon M P and Hegde S (1999) Muscarinic Receptor Ligands and Their Therapeutic Potential. *Curr Opin Chem Biol* **3**:426-432.

Eglen RM, Choppin A and Watson N (2001) Therapeutic Opportunities From Muscarinic Receptor Research. *Trends Pharmacol Sci* **22**:409-414.

Eglen RM, Reddy H, Watson N and Challiss R A (1994) Muscarinic Acetylcholine Receptor Subtypes in Smooth Muscle. *Trends Pharmacol Sci* **15**:114-119.

Ehlert FJ (1985) The Relationship Between Muscarinic Receptor Occupancy and Adenylate Cyclase Inhibition in the Rabbit Myocardium. *Mol Pharmacol* **28**:410-421.

Ehlert FJ (1988) Estimation of the Affinities of Allosteric Ligands Using Radioligand Binding and Pharmacological Null Methods. *Mol Pharmacol* **33**:187-194.

Ehlert FJ, Roeske W R, Yamamura S H and Yamamura H I (1983) The Benzodiazepine Receptor: Complex Binding Properties and the Influence of GABA. *Adv Biochem Psychopharmacol* **36**:209-220.

Ellis J, Huyler J and Brann M R (1991) Allosteric Regulation of Cloned M1-M5 Muscarinic Receptor Subtypes. *Biochem Pharmacol* **42**:1927-1932.

Ellis J and Seidenberg M (1992) Two Allosteric Modulators Interact at a Common Site on Cardiac Muscarinic Receptors. *Mol Pharmacol* **42**:638-641.

Ellis J and Seidenberg M (2000) Interactions of Alcuronium, TMB-8, and Other Allosteric Ligands With Muscarinic Acetylcholine Receptors: Studies With Chimeric Receptors. *Mol Pharmacol* **58**:1451-1460.

Farrens DL, Altenbach C, Yang K, Hubbell W L and Khorana H G (1996) Requirement of Rigid-Body Motion of Transmembrane Helices for Light Activation of Rhodopsin. *Science* **274**:768-770.

Feldberg W and Krayer O (1933) *Naunyn Schmiedebergs Arch Exp Pathol Pharmakol* **172**.

Felder CC, Bymaster F P, Ward J and DeLapp N (2000) Therapeutic Opportunities for Muscarinic Receptors in the Central Nervous System. *J Med Chem* **43**:4333-4353.

Fetscher C, Fleichman M, Schmidt M, Krege S and Michel M C (2002) M(3) Muscarinic Receptors Mediate Contraction of Human Urinary Bladder. *Br J Pharmacol* **136**:641-643.

Fisahn A, Yamada M, Duttaroy A, Gan J W, Deng C X, McBain C J and Wess J (2002) Muscarinic Induction of Hippocampal Gamma Oscillations Requires Coupling of the M1 Receptor to Two Mixed Cation Currents. *Neuron* **33**:615-624.

Fisher A, Brandeis R, Haring R, Bar-Ner N, Kliger-Spatz M, Natan N, Sonego H, Marcovitch I and Pittel Z (2002) Impact of Muscarinic Agonists for Successful Therapy of Alzheimer's Disease. *J Neural Transm Suppl*189-202.

Fisher A, Pittel Z, Haring R, Bar-Ner N, Kliger-Spatz M, Natan N, Egozi I, Sonego H, Marcovitch I and Brandeis R (2003) M1 Muscarinic Agonists Can Modulate Some of the Hallmarks in Alzheimer's Disease: Implications in Future Therapy. *J Mol Neurosci* **20**:349-356.

Ford DJ, Essex A, Spalding T A, Burstein E S and Ellis J (2002) Homologous Mutations Near the Junction of the Sixth Transmembrane Domain and the Third Extracellular Loop Lead to Constitutive Activity and Enhanced Agonist Affinity at All Muscarinic Receptor Subtypes. *J Pharmacol Exp Ther* **300**:810-817.

Fredriksson R and Schioth H B (2005) The Repertoire of G-Protein-Coupled Receptors in Fully Sequenced Genomes. *Mol Pharmacol* **67**:1414-1425.

Fritze O, Filipek S, Kuksa V, Palczewski K, Hofmann K P and Ernst O P (2003) Role of the Conserved NPxxY(x)5,6F Motif in the Rhodopsin Ground State and During Activation. *Proc Natl Acad Sci U S A* **100**:2290-2295.

Fryer AD and Jacoby D B (1998) Muscarinic Receptors and Control of Airway Smooth Muscle. *Am J Respir Crit Care Med* **158**:S154-S160.

Garriga P and Manyosa J (2002) The Eye Photoreceptor Protein Rhodopsin. Structural Implications for Retinal Disease. *FEBS Lett* **528**:17-22.

Gautam D, Han S J, Hamdan F F, Jeon J, Li B, Li J H, Cui Y, Mears D, Lu H, Deng C, Heard T and Wess J (2006) A Critical Role for Beta Cell M3 Muscarinic Acetylcholine Receptors in Regulating Insulin Release and Blood Glucose Homeostasis in Vivo. *Cell Metab* **3**:449-461.

Gether U, Asmar F, Meinild A K and Rasmussen S G (2002) Structural Basis for Activation of G-Protein-Coupled Receptors. *Pharmacol Toxicol* **91**:304-312.

Gether U and Kobilka B K (1998) G Protein-Coupled Receptors. II. Mechanism of Agonist Activation. *J Biol Chem* **273**:17979-17982.

Gharagozloo P, Lazareno S, Miyauchi M, Popham A and Birdsall N J (2002) Substituted Pentacyclic Carbazolones As Novel Muscarinic Allosteric Agents: Synthesis and Structure-Affinity and Cooperativity Relationships. *J Med Chem* **45**:1259-1274.

Gharagozloo P, Lazareno S, Popham A and Birdsall N J (1999) Allosteric Interactions of Quaternary Strychnine and Brucine Derivatives With Muscarinic Acetylcholine Receptors. *J Med Chem* **42**:438-445.

Gillberg PG, Sundquist S and Nilvebrant L (1998) Comparison of the in Vitro and in Vivo Profiles of Tolterodine With Those of Subtype-Selective Muscarinic Receptor Antagonists. *Eur J Pharmacol* **349**:285-292.

Gilon P and Henquin J C (2001) Mechanisms and Physiological Significance of the Cholinergic Control of Pancreatic Beta-Cell Function. *Endocr Rev* **22**:565-604.

Gnagey AL, Seidenberg M and Ellis J (1999) Site-Directed Mutagenesis Reveals Two Epitopes Involved in the Subtype Selectivity of the Allosteric Interactions of Gallamine at Muscarinic Acetylcholine Receptors. *Mol Pharmacol* **56**:1245-1253.

Gomeza J, Shannon H, Kostenis E, Felder C, Zhang L, Brodkin J, Grinberg A, Sheng H and Wess J (1999a) Pronounced Pharmacologic Deficits in M2 Muscarinic Acetylcholine Receptor Knockout Mice. *Proc Natl Acad Sci U S A* **96**:1692-1697.

Gomeza J, Zhang L, Kostenis E, Felder C, Bymaster F, Brodkin J, Shannon H, Xia B, Deng C and Wess J (1999b) Enhancement of D1 Dopamine Receptor-Mediated Locomotor Stimulation in M(4) Muscarinic Acetylcholine Receptor Knockout Mice. *Proc Natl Acad Sci U S A* **96**:10483-10488.

Grigorieff N, Ceska T A, Downing K H, Baldwin J M and Henderson R (1996) Electron-Crystallographic Refinement of the Structure of Bacteriorhodopsin. *J Mol Biol* **259**:393-421.

Gu Z, Zhong P and Yan Z (2003) Activation of Muscarinic Receptors Inhibits Beta-Amyloid Peptide-Induced Signaling in Cortical Slices. *J Biol Chem* **278**:17546-17556.

Gupta S, Sathyan G and Mori T (2002) New Perspectives on the Overactive Bladder: Pharmacokinetics and Bioavailability. *Urology* **60**:78-80.

Hamilton SE, Loose M D, Qi M, Levey A I, Hille B, McKnight G S, Idzerda R L and Nathanson N M (1997) Disruption of the M1 Receptor Gene Ablates Muscarinic Receptor-Dependent M Current Regulation and Seizure Activity in Mice. *Proc Natl Acad Sci U S A* **94**:13311-13316.

Hamilton SE and Nathanson N M (2001) The M1 Receptor Is Required for Muscarinic Activation of Mitogen-Activated Protein (MAP) Kinase in Murine Cerebral Cortical Neurons. *J Biol Chem* **276**:15850-15853.

Hammer R, Berrie C P, Birdsall N J, Burgen A S and Hulme E C (1980) Pirenzepine Distinguishes Between Different Subclasses of Muscarinic Receptors. *Nature* **283**:90-92.

Hammer R and Giachetti A (1982) Muscarinic Receptor Subtypes: M1 and M2 Biochemical and Functional Characterization. *Life Sci* **31**:2991-2998.

Han SJ, Hamdan F F, Kim S K, Jacobson K A, Bloodworth L M, Li B and Wess J (2005a) Identification of an Agonist-Induced Conformational Change Occurring Adjacent to the Ligand-Binding Pocket of the M(3) Muscarinic Acetylcholine Receptor. *J Biol Chem* **280**:34849-34858.

Han SJ, Hamdan F F, Kim S K, Jacobson K A, Brichta L, Bloodworth L M, Li J H and Wess J (2005b) Pronounced Conformational Changes Following Agonist Activation of the M(3) Muscarinic Acetylcholine Receptor. *J Biol Chem* **280**:24870-24879.

Hayashi MK and Haga T (1997) Palmitoylation of Muscarinic Acetylcholine Receptor M2 Subtypes: Reduction in Their Ability to Activate G Proteins by Mutation of a Putative Palmitoylation Site, Cysteine 457, in the Carboxyl-Terminal Tail. *Arch Biochem Biophys* **340**:376-382.

Hegde SS and Eglen R M (1999) Muscarinic Receptor Subtypes Modulating Smooth Muscle Contractility in the Urinary Bladder. *Life Sci* **64**:419-428.

Hejnova L, Tucek S and el-Fakahany E E (1995) Positive and Negative Allosteric Interactions on Muscarinic Receptors. *Eur J Pharmacol* **291**:427-430.

Heldman E, Barg J, Fisher A, Levy R, Pittel Z, Zimlichman R, Kushnir M and Vogel Z (1996) Pharmacological Basis for Functional Selectivity of Partial Muscarinic Receptor Agonists. *Eur J Pharmacol* **297**:283-291.

Hock C, Maddalena A, Raschig A, Muller-Spahn F, Eschweiler G, Hager K, Heuser I, Hampel H, Muller-Thomsen T, Oertel W, Wienrich M, Signorell A, Gonzalez-Agosti C and Nitsch R M (2003) Treatment With the Selective Muscarinic M1 Agonist Talsaclidine Decreases Cerebrospinal Fluid Levels of A Beta 42 in Patients With Alzheimer's Disease. *Amyloid* **10**:1-6.

Hogger P, Shockley M S, Lameh J and Sadee W (1995) Activating and Inactivating Mutations in N- and C-Terminal I3 Loop Junctions of Muscarinic Acetylcholine Hm1 Receptors. *J Biol Chem* **270**:7405-7410.

Hu JR and el-Fakahany E E (1990) Selectivity of McN-A-343 in Stimulating Phosphoinositide Hydrolysis Mediated by M1 Muscarinic Receptors. *Mol Pharmacol* **38**:895-903.

Huang XP and Ellis J (2007) Mutational Disruption of a Conserved Disulfide Bond in Muscarinic Acetylcholine Receptors Attenuates Positive Homotropic Cooperativity Between Multiple Allosteric Sites and Has Subtype-Dependent Effects on the Affinities of Muscarinic Allosteric Ligands. *Mol Pharmacol* **71**:759-768.

Huang XP, Prilla S, Mohr K and Ellis J (2005) Critical Amino Acid Residues of the Common Allosteric Site on the M2 Muscarinic Acetylcholine Receptor: More

Similarities Than Differences Between the Structurally Divergent Agents Gallamine and Bis(Ammonio)Alkane-Type Hexamethylene-Bis-[Dimethyl-(3-Phthalimidopropyl)Ammonium]Dibromide. *Mol Pharmacol* **68**:769-778.

Hubbell WL, Altenbach C, Hubbell C M and Khorana H G (2003) Rhodopsin Structure, Dynamics, and Activation: a Perspective From Crystallography, Site-Directed Spin Labeling, Sulfhydryl Reactivity, and Disulfide Cross-Linking. *Adv Protein Chem* **63**:243-290.

Hulme EC, Birdsall N J and Buckley N J (1990) Muscarinic Receptor Subtypes. *Annu Rev Pharmacol Toxicol* **30**:633-673.

Hulme EC, Birdsall N J, Burgen A S and Mehta P (1978) The Binding of Antagonists to Brain Muscarinic Receptors. *Mol Pharmacol* **14**:737-750.

Hulme EC, Lu Z L and Bee M S (2003a) Scanning Mutagenesis Studies of the M1 Muscarinic Acetylcholine Receptor. *Receptors Channels* **9**:215-228.

Hulme EC, Lu Z L, Saldanha J W and Bee M S (2003b) Structure and Activation of Muscarinic Acetylcholine Receptors. *Biochem Soc Trans* **31**:29-34.

Iarriccio L and Birdsall N J (2008) Modulation of the Activity of Wild-Type and Mutant M_3 Muscarinic Receptors in CHO Cells by Allosteric Ligands-a Cautionary Tale. *pA2online* **5**:011P.

Ikeda K, Kobayashi S, Suzuki M, Miyata K, Takeuchi M, Yamada T and Honda K (2002) M(3) Receptor Antagonism by the Novel Antimuscarinic Agent Solifenacin in the Urinary Bladder and Salivary Gland. *Naunyn Schmiedebergs Arch Pharmacol* **366**:97-103.

Jakubik J, Bacakova L, el-Fakahany E E and Tucek S (1997) Positive Cooperativity of Acetylcholine and Other Agonists With Allosteric Ligands on Muscarinic Acetylcholine Receptors. *Mol Pharmacol* **52**:172-179.

Jakubik J, Krejci A and Dolezal V (2005) Asparagine, Valine, and Threonine in the Third Extracellular Loop of Muscarinic Receptor Have Essential Roles in the Positive Cooperativity of Strychnine-Like Allosteric Modulators. *J Pharmacol Exp Ther* **313**:688-696.

Jensen AD, Guarnieri F, Rasmussen S G, Asmar F, Ballesteros J A and Gether U (2001) Agonist-Induced Conformational Changes at the Cytoplasmic Side of Transmembrane Segment 6 in the Beta 2 Adrenergic Receptor Mapped by Site-Selective Fluorescent Labeling. *J Biol Chem* **276**:9279-9290.

Jöhren K and Höltje H D (2002) A Model of the Human M2 Muscarinic Acetylcholine Receptor. *J Comput Aided Mol Des* **16**:795-801.

Jones PG, Curtis C A and Hulme E C (1995) The Function of a Highly-Conserved Arginine Residue in Activation of the Muscarinic M1 Receptor. *Eur J Pharmacol* **288**:251-257.

Kahn SE (2001) Clinical Review 135: The Importance of Beta-Cell Failure in the Development and Progression of Type 2 Diabetes. *J Clin Endocrinol Metab* **86**:4047-4058.

Kimura Y, Vassylyev D G, Miyazawa A, Kidera A, Matsushima M, Mitsuoka K, Murata K, Hirai T and Fujiyoshi Y (1997) Surface of Bacteriorhodopsin Revealed by High-Resolution Electron Crystallography. *Nature* **389**:206-211.

Kitazawa T, Hashiba K, Cao J, Unno T, Komori S, Yamada M, Wess J and Taneike T (2007) Functional Roles of Muscarinic M2 and M3 Receptors in Mouse Stomach Motility: Studies With Muscarinic Receptor Knockout Mice. *Eur J Pharmacol* **554**:212-222.

Kobilka BK (2007) G Protein Coupled Receptor Structure and Activation. *Biochim Biophys Acta* **1768**:794-807.

Krejci A and Tucek S (2001) Changes of Cooperativity Between N-Methylscopolamine and Allosteric Modulators Alcuronium and Gallamine Induced by Mutations of External Loops of Muscarinic M(3) Receptors. *Mol Pharmacol* **60**:761-767.

Kristiansen K (2004) Molecular Mechanisms of Ligand Binding, Signaling, and Regulation Within the Superfamily of G-Protein-Coupled Receptors: Molecular Modeling and Mutagenesis Approaches to Receptor Structure and Function. *Pharmacol Ther* **103**:21-80.

Kurtenbach E, Curtis C A, Pedder E K, Aitken A, Harris A C and Hulme E C (1990) Muscarinic Acetylcholine Receptors. Peptide Sequencing Identifies Residues Involved in Antagonist Binding and Disulfide Bond Formation. *J Biol Chem* **265**:13702-13708.

LaCroix C, Freeling J, Giles A, Wess J and Li Y F (2008) Deficiency of M2 Muscarinic Acetylcholine Receptors Increases Susceptibility of Ventricular Function to Chronic Adrenergic Stress. *Am J Physiol Heart Circ Physiol* **294**:H810-H820.

Langmead CJ, Fry V A, Forbes I T, Branch C L, Christopoulos A, Wood M D and Herdon H J (2006) Probing the Molecular Mechanism of Interaction Between 4-n-Butyl-1-[4-(2-Methylphenyl)-4-Oxo-1-Butyl]-Piperidine (AC-42) and the Muscarinic M(1) Receptor: Direct Pharmacological Evidence That AC-42 Is an Allosteric Agonist. *Mol Pharmacol* **69**:236-246.

Lazareno S and Birdsall N J (1995) Detection, Quantitation, and Verification of Allosteric Interactions of Agents With Labeled and Unlabeled Ligands at G Protein-Coupled Receptors: Interactions of Strychnine and Acetylcholine at Muscarinic Receptors. *Mol Pharmacol* **48**:362-378.

Lazareno S, Buckley N J and Roberts F F (1990) Characterization of Muscarinic M4 Binding Sites in Rabbit Lung, Chicken Heart, and NG108-15 Cells. *Mol Pharmacol* **38**:805-815.

Lazareno S, Dolezal V, Popham A and Birdsall N J (2004) Thiochrome Enhances Acetylcholine Affinity at Muscarinic M4 Receptors: Receptor Subtype Selectivity Via Cooperativity Rather Than Affinity. *Mol Pharmacol* **65**:257-266.

Lazareno S, Gharagozloo P, Kuonen D, Popham A and Birdsall N J M (1998) Subtype-Selective Positive Cooperative Interactions Between Brucine Analogues and Acetylcholine at Muscarinic Receptors: Radioligand Binding Studies. *Molecular Pharmacology* **53**:573-589.

Lazareno S, Popham A and Birdsall N J (2000) Allosteric Interactions of Staurosporine and Other Indolocarbazoles With N-[Methyl-(3)H]Scopolamine and Acetylcholine at Muscarinic Receptor Subtypes: Identification of a Second Allosteric Site. *Mol Pharmacol* **58**:194-207.

Lazareno S, Popham A and Birdsall N J (2002) Analogs of WIN 62,577 Define a Second Allosteric Site on Muscarinic Receptors. *Mol Pharmacol* **62**:1492-1505.

Lee AM, Jacoby D B and Fryer A D (2001) Selective Muscarinic Receptor Antagonists for Airway Diseases. *Curr Opin Pharmacol* **1**:223-229.

Leppik RA, Miller R C, Eck M and Paquet J L (1994) Role of Acidic Amino Acids in the Allosteric Modulation by Gallamine of Antagonist Binding at the M2 Muscarinic Acetylcholine Receptor. *Mol Pharmacol* **45**:983-990.

Levey AI (1993) Immunological Localization of M1-M5 Muscarinic Acetylcholine Receptors in Peripheral Tissues and Brain. *Life Sci* **52**:441-448.

Levey AI, Edmunds S M, Heilman C J, Desmond T J and Frey K A (1994) Localization of Muscarinic M3 Receptor Protein and M3 Receptor Binding in Rat Brain. *Neuroscience* **63**:207-221.

Li CK and Mitchelson F (1980) The Selective Antimuscarinic Action of Stercuronium. *Br J Pharmacol* **70**:313-321.

Li JH, Han S J, Hamdan F F, Kim S K, Jacobson K A, Bloodworth L M, Zhang X and Wess J (2007) Distinct Structural Changes in a G Protein-Coupled Receptor Caused by Different Classes of Agonist Ligands. *J Biol Chem* **282**:26284-26293.

Lin SW and Sakmar T P (1996) Specific Tryptophan UV-Absorbance Changes Are Probes of the Transition of Rhodopsin to Its Active State. *Biochemistry* **35**:11149-11159.

Loewi O and Navratil (1926) *E Arch Ges Physiol* **214**:678.

Longo FM and Massa S M (2004) Neuroprotective Strategies in Alzheimer's Disease. *NeuroRx* **1**:117-127.

Lu ZL, Curtis C A, Jones P G, Pavia J and Hulme E C (1997) The Role of the Aspartate-Arginine-Tyrosine Triad in the M1 Muscarinic Receptor: Mutations of Aspartate 122 and Tyrosine 124 Decrease Receptor Expression but Do Not Abolish Signaling. *Mol Pharmacol* **51**:234-241.

Lu ZL, Saldanha J W and Hulme E C (2001) Transmembrane Domains 4 and 7 of the M(1) Muscarinic Acetylcholine Receptor Are Critical for Ligand Binding and the Receptor Activation Switch. *J Biol Chem* **276**:34098-34104.

Lu ZL, Saldanha J W and Hulme E C (2002) Seven-Transmembrane Receptors: Crystals Clarify. *Trends Pharmacol Sci* **23**:140-146.

Lullmann H, Ohnesorge F K, Schauwecker G C and Wassermann O (1969) Inhibition of the Actions of Carbachol and DFP on Guinea Pig Isolated Atria by Alkane-Bis-Ammonium Compounds. *Eur J Pharmacol* **6**:241-247.

Marino MJ, Williams D L, Jr., O'Brien J A, Valenti O, McDonald T P, Clements M K, Wang R, DiLella A G, Hess J F, Kinney G G and Conn P J (2003) Allosteric Modulation of Group III Metabotropic Glutamate Receptor 4: a Potential Approach to Parkinson's Disease Treatment. *Proc Natl Acad Sci U S A* **100**:13668-13673.

Matsui H, Lazareno S and Birdsall N J (1995) Probing of the Location of the Allosteric Site on M1 Muscarinic Receptors by Site-Directed Mutagenesis. *Mol Pharmacol* **47**:88-98.

Matsui M, Motomura D, Karasawa H, Fujikawa T, Jiang J, Komiya Y, Takahashi S and Taketo M M (2000) Multiple Functional Defects in Peripheral Autonomic Organs in Mice Lacking Muscarinic Acetylcholine Receptor Gene for the M3 Subtype. *Proc Natl Acad Sci U S A* **97**:9579-9584.

May LT, Avlani V A, Langmead C J, Herdon H J, Wood M D, Sexton P M and Christopoulos A (2007a) Structure-Function Studies of Allosteric Agonism at M2 Muscarinic Acetylcholine Receptors. *Mol Pharmacol* **72**:463-476.

May LT, Leach K, Sexton P M and Christopoulos A (2007b) Allosteric Modulation of G Protein-Coupled Receptors. *Annu Rev Pharmacol Toxicol* **47**:1-51.

May LT, Lin Y, Sexton P M and Christopoulos A (2005) Regulation of M2 Muscarinic Acetylcholine Receptor Expression and Signaling by Prolonged Exposure to Allosteric Modulators. *J Pharmacol Exp Ther* **312**:382-390.

Meanwell NA and Kadow J F (2007) Maraviroc, a Chemokine CCR5 Receptor Antagonist for the Treatment of HIV Infection and AIDS. *Curr Opin Investig Drugs* **8**:669-681.

Michal P, Lysikova M, el-Fakahany E E and Tucek S (1999) Clozapine Interaction With the M2 and M4 Subtypes of Muscarinic Receptors. *Eur J Pharmacol* **376**:119-125.

Mohr K, Tränkle C and Holzgrabe U (2003) Structure/Activity Relationships of M2 Muscarinic Allosteric Modulators. *Receptors Channels* **9**:229-240.

MONOD J, CHANGEUX J P and JACOB F (1963) Allosteric Proteins and Cellular Control Systems. *J Mol Biol* **6**:306-329.

Nelson CP and Challiss R A (2007) "Phenotypic" Pharmacology: the Influence of Cellular Environment on G Protein-Coupled Receptor Antagonist and Inverse Agonist Pharmacology. *Biochem Pharmacol* **73**:737-751.

Nelson CP, Gupta P, Napier C M, Nahorski S R and Challiss R A (2004) Functional Selectivity of Muscarinic Receptor Antagonists for Inhibition of M3-Mediated

Phosphoinositide Responses in Guinea Pig Urinary Bladder and Submandibular Salivary Gland. *J Pharmacol Exp Ther* **310**:1255-1265.

Nelson CP, Nahorski S R and Challiss R A (2006) Constitutive Activity and Inverse Agonism at the M2 Muscarinic Acetylcholine Receptor. *J Pharmacol Exp Ther* **316**:279-288.

Niijima A (1989) Neural Mechanisms in the Control of Blood Glucose Concentration. *J Nutr* **119**:833-840.

Nikolaus S, Huston J P and Hasenohrl R U (1999) Reinforcing Effects of Neurokinin Substance P in the Ventral Pallidum: Mediation by the Tachykinin NK1 Receptor. *Eur J Pharmacol* **370**:93-99.

Nilvebrant L, Andersson K E, Gillberg P G, Stahl M and Sparf B (1997) Tolterodine--a New Bladder-Selective Antimuscarinic Agent. *Eur J Pharmacol* **327**:195-207.

Ohtake A, Saitoh C, Yuyama H, Ukai M, Okutsu H, Noguchi Y, Hatanaka T, Suzuki M, Sato S, Sasamata M and Miyata K (2007) Pharmacological Characterization of a New Antimuscarinic Agent, Solifenacin Succinate, in Comparison With Other Antimuscarinic Agents. *Biol Pharm Bull* **30**:54-58.

Olianas MC, Maullu C and Onali P (1999) Mixed Agonist-Antagonist Properties of Clozapine at Different Human Cloned Muscarinic Receptor Subtypes Expressed in Chinese Hamster Ovary Cells. *Neuropsychopharmacology* **20**:263-270.

Palczewski K, Kumasaka T, Hori T, Behnke C A, Motoshima H, Fox B A, Le T, I, Teller D C, Okada T, Stenkamp R E, Yamamoto M and Miyano M (2000) Crystal Structure of Rhodopsin: A G Protein-Coupled Receptor. *Science* **289**:739-745.

Pebay-Peyroula E, Rummel G, Rosenbusch J P and Landau E M (1997) X-Ray Structure of Bacteriorhodopsin at 2.5 Angstroms From Microcrystals Grown in Lipidic Cubic Phases. *Science* **277**:1676-1681.

Pedder EK, Eveleigh P, Poyner D, Hulme E C and Birdsall N J (1991) Modulation of the Structure-Binding Relationships of Antagonists for Muscarinic Acetylcholine Receptor Subtypes. *Br J Pharmacol* **103**:1561-1567.

Peralta EG, Ashkenazi A, Winslow J W, Smith D H, Ramachandran J and Capon D J (1987) Distinct Primary Structures, Ligand-Binding Properties and Tissue-Specific Expression of Four Human Muscarinic Acetylcholine Receptors. *EMBO J* **6**:3923-3929.

Pierce KL, Premont R T and Lefkowitz R J (2002) Seven-Transmembrane Receptors. *Nat Rev Mol Cell Biol* **3**:639-650.

Proska J and Tucek S (1994) Mechanisms of Steric and Cooperative Actions of Alcuronium on Cardiac Muscarinic Acetylcholine Receptors. *Mol Pharmacol* **45**:709-717.

Proska J and Tucek S (1995) Competition Between Positive and Negative Allosteric Effectors on Muscarinic Receptors. *Mol Pharmacol* **48**:696-702.

Quastel JH, Tennenbaum M and Wheatley A H (1936) Choline Ester Formation in, and Choline Esterase Activities of, Tissues in Vitro. *Biochem J* **30**:1668-1681.

Ramon E, Cordomi A, Bosch L, Zernii E Y, Senin I I, Manyosa J, Philippov P P, Perez J J and Garriga P (2007) Critical Role of Electrostatic Interactions of Amino Acids at the Cytoplasmic Region of Helices 3 and 6 in Rhodopsin Conformational Properties and Activation. *J Biol Chem* **282**:14272-14282.

Rasmussen SG, Choi H J, Rosenbaum D M, Kobilka T S, Thian F S, Edwards P C, Burghammer M, Ratnala V R, Sanishvili R, Fischetti R F, Schertler G F, Weis W I and Kobilka B K (2007) Crystal Structure of the Human Beta2 Adrenergic G-Protein-Coupled Receptor. *Nature* **450**:383-387.

Rattner A, Sun H and Nathans J (1999) Molecular Genetics of Human Retinal Disease. *Annu Rev Genet* **33**:89-131.

RIKER WF, Jr. and WESCOE W C (1951) The Pharmacology of Flaxedil, With Observations on Certain Analogs. *Ann N Y Acad Sci* **54**:373-394.

Rosenbaum DM, Cherezov V, Hanson M A, Rasmussen S G, Thian F S, Kobilka T S, Choi H J, Yao X J, Weis W I, Stevens R C and Kobilka B K (2007) GPCR Engineering Yields High-Resolution Structural Insights into Beta2-Adrenergic Receptor Function. *Science* **318**:1266-1273.

Rosenblum K, Futter M, Jones M, Hulme E C and Bliss T V (2000) ERKI/II Regulation by the Muscarinic Acetylcholine Receptors in Neurons. *J Neurosci* **20**:977-985.

ROSZKOWSKI AP (1961) An Unusual Type of Sympathetic Ganglionic Stimulant. *J Pharmacol Exp Ther* **132**:156-170.

Ruegg UT and Burgess G M (1989) Staurosporine, K-252 and UCN-01: Potent but Nonspecific Inhibitors of Protein Kinases. *Trends Pharmacol Sci* **10**:218-220.

Sachpatzidis A, Benton B K, Manfredi J P, Wang H, Hamilton A, Dohlman H G and Lolis E (2003) Identification of Allosteric Peptide Agonists of CXCR4. *J Biol Chem* **278**:896-907.

Sarria B, Naline E, Zhang Y, Cortijo J, Molimard M, Moreau J, Therond P, Advenier C and Morcillo E J (2002) Muscarinic M2 Receptors in Acetylcholine-Isoproterenol Functional Antagonism in Human Isolated Bronchus. *Am J Physiol Lung Cell Mol Physiol* **283**:L1125-L1132.

Savarese TM, Wang C D and Fraser C M (1992) Site-Directed Mutagenesis of the Rat M1 Muscarinic Acetylcholine Receptor. Role of Conserved Cysteines in Receptor Function. *J Biol Chem* **267**:11439-11448.

Scarselli M, Li B, Kim S K and Wess J (2007) Multiple Residues in the Second Extracellular Loop Are Critical for M3 Muscarinic Acetylcholine Receptor Activation. *J Biol Chem* **282**:7385-7396.

Schoneberg T, Schulz A and Gudermann T (2002) The Structural Basis of G-Protein-Coupled Receptor Function and Dysfunction in Human Diseases. *Rev Physiol Biochem Pharmacol* **144**:143-227.

Schröter A, Tränkle C and Mohr K (2000) Modes of Allosteric Interactions With Free and [3H]N-Methylscopolamine-Occupied Muscarinic M2 Receptors As Deduced From Buffer-Dependent Potency Shifts. *Naunyn Schmiedebergs Arch Pharmacol* **362**:512-519.

Seifert R and Wenzel-Seifert K (2002) Constitutive Activity of G-Protein-Coupled Receptors: Cause of Disease and Common Property of Wild-Type Receptors. *Naunyn Schmiedebergs Arch Pharmacol* **366**:381-416.

Sheikh SP, Vilardarga J P, Baranski T J, Lichtarge O, Iiri T, Meng E C, Nissenson R A and Bourne H R (1999) Similar Structures and Shared Switch Mechanisms of the Beta2-Adrenoceptor and the Parathyroid Hormone Receptor. Zn(II) Bridges Between Helices III and VI Block Activation. *J Biol Chem* **274**:17033-17041.

Sheikh SP, Zvyaga T A, Lichtarge O, Sakmar T P and Bourne H R (1996) Rhodopsin Activation Blocked by Metal-Ion-Binding Sites Linking Transmembrane Helices C and F. *Nature* **383**:347-350.

Shi L and Javitch J A (2002) The Binding Site of Aminergic G Protein-Coupled Receptors: the Transmembrane Segments and Second Extracellular Loop. *Annu Rev Pharmacol Toxicol* **42**:437-467.

Shi L and Javitch J A (2004) The Second Extracellular Loop of the Dopamine D2 Receptor Lines the Binding-Site Crevice. *Proc Natl Acad Sci U S A* **101**:440-445.

Shirey JK, Xiang Z, Orton D, Brady A E, Johnson K A, Williams R, Ayala J E, Rodriguez A L, Wess J, Weaver D, Niswender C M and Conn P J (2008) An Allosteric Potentiator of M4 MAChR Modulates Hippocampal Synaptic Transmission. *Nat Chem Biol* **4**:42-50.

Spalding TA and Burstein E S (2006) Constitutive Activity of Muscarinic Acetylcholine Receptors. *J Recept Signal Transduct Res* **26**:61-85.

Spalding TA, Burstein E S, Brauner-Osborne H, Hill-Eubanks D and Brann M R (1995) Pharmacology of a Constitutively Active Muscarinic Receptor Generated by Random Mutagenesis. *J Pharmacol Exp Ther* **275**:1274-1279.

Spalding TA, Burstein E S, Wells J W and Brann M R (1997) Constitutive Activation of the M5 Muscarinic Receptor by a Series of Mutations at the Extracellular End of Transmembrane 6. *Biochemistry* **36**:10109-10116.

Spalding TA, Ma J N, Ott T R, Friberg M, Bajpai A, Bradley S R, Davis R E, Brann M R and Burstein E S (2006) Structural Requirements of Transmembrane Domain 3 for Activation by the M1 Muscarinic Receptor Agonists AC-42, AC-260584, Clozapine, and N-Desmethylclozapine: Evidence for Three Distinct Modes of Receptor Activation. *Mol Pharmacol* **70**:1974-1983.

Spalding TA, Trotter C, Skjaerbaek N, Messier T L, Currier E A, Burstein E S, Li D, Hacksell U and Brann M R (2002) Discovery of an Ectopic Activation Site on the M(1) Muscarinic Receptor. *Mol Pharmacol* **61**:1297-1302.

Stengel PW and Cohen M L (2002) Muscarinic Receptor Knockout Mice: Role of Muscarinic Acetylcholine Receptors M(2), M(3), and M(4) in Carbamylcholine-Induced Gallbladder Contractility. *J Pharmacol Exp Ther* **301**:643-650.

Stengel PW, Yamada M, Wess J and Cohen M L (2002) M(3)-Receptor Knockout Mice: Muscarinic Receptor Function in Atria, Stomach Fundus, Urinary Bladder, and Trachea. *Am J Physiol Regul Integr Comp Physiol* **282**:R1443-R1449.

Stockton JM, Birdsall N J M, Burgen A S V and Hulme E C (1983) Modification of the Binding-Properties of Muscarinic Receptors by Gallamine. *Molecular Pharmacology* **23**:551-557.

Strader CD, Fong T M, Tota M R, Underwood D and Dixon R A (1994) Structure and Function of G Protein-Coupled Receptors. *Annu Rev Biochem* **63**:101-132.

Strosberg AD (1997) Structure and Function of the Beta 3-Adrenergic Receptor. *Annu Rev Pharmacol Toxicol* **37**:421-450.

Strosberg AD and Nahmias C (2007) G-Protein-Coupled Receptor Signalling Through Protein Networks. *Biochem Soc Trans* **35**:23-27.

Sur C, Mallorga P J, Wittmann M, Jacobson M A, Pascarella D, Williams J B, Brandish P E, Pettibone D J, Scolnick E M and Conn P J (2003) N-Desmethylclozapine, an Allosteric Agonist at Muscarinic 1 Receptor, Potentiates N-Methyl-D-Aspartate Receptor Activity. *Proc Natl Acad Sci U S A* **100**:13674-13679.

Takeuchi J, Fulton J, Jia Z P, bramov-Newerly W, Jamot L, Sud M, Coward D, Ralph M, Roder J and Yeomans J (2002) Increased Drinking in Mutant Mice With Truncated M5 Muscarinic Receptor Genes. *Pharmacol Biochem Behav* **72**:117-123.

Taylor P and Brown J H (2006) *oodman Gilman's The Pharmacological Basis of Therapeutics* **11th edn Ch. 7 (ed. Brunton, L. L.)**:183–200 (McGraw–Hill, New York.

Themmen AP and Verhoef-Post M (2002) LH Receptor Defects. *Semin Reprod Med* **20**:199-204.

Tobin AB, Totty NF, Sterlin AE, Nahorski SR (1997) Stimulus-dependent phosphorylation of G-protein-coupled receptors by casein kinase 1alpha. *J Biol Chem* **272**:20844-9.

Tränkle C, Dittmann A, Schulz U, Weyand O, Buller S, Jöhren K, Heller E, Birdsall N J, Holzgrabe U, Ellis J, Höltje H D and Mohr K (2005) Atypical Muscarinic Allosteric Modulation: Cooperativity Between Modulators and Their Atypical Binding Topology in Muscarinic M2 and M2/M5 Chimeric Receptors. *Mol Pharmacol* **68**:1597-1610.

Tränkle C, Kostenis E, Burgmer U and Mohr K (1996) Search for Lead Structures to Develop New Allosteric Modulators of Muscarinic Receptors. *J Pharmacol Exp Ther* **279**:926-933.

Tränkle C and Mohr K (1997) Divergent Modes of Action Among Cationic Allosteric Modulators of Muscarinic M2 Receptors. *Mol Pharmacol* **51**:674-682.

Tucek S, Musilkova J, Nedoma J, Proska J, Shelkovnikov S and Vorlicek J (1990) Positive Cooperativity in the Binding of Alcuronium and N-Methylscopolamine to Muscarinic Acetylcholine Receptors. *Mol Pharmacol* **38**:674-680.

Ukai M, Shinkai N, Ohashi K and Kameyama T (1995) Substance P Markedly Ameliorates Scopolamine-Induced Impairment of Spontaneous Alternation Performance in the Mouse. *Brain Res* **673**:335-338.

van Koppen CJ and Nathanson N M (1990) Site-Directed Mutagenesis of the M2 Muscarinic Acetylcholine Receptor. Analysis of the Role of N-Glycosylation in Receptor Expression and Function. *J Biol Chem* **265**:20887-20892.

Venepalli BR, Aimone L D, Appell K C, Bell M R, Dority J A, Goswami R, Hall P L, Kumar V, Lawrence K B, Logan M E and . (1992) Synthesis and Substance P Receptor Binding Activity of Androstano[3,2-b]Pyrimido[1,2-a]Benzimidazoles. *J Med Chem* **35**:374-378.

Vilaro MT, Mengod G and Palacios J M (1993) Advances and Limitations of the Molecular Neuroanatomy of Cholinergic Receptors: the Example of Multiple Muscarinic Receptors. *Prog Brain Res* **98**:95-101.

Vogel WK, Sheehan D M and Schimerlik M I (1997) Site-Directed Mutagenesis on the M2 Muscarinic Acetylcholine Receptor: the Significance of Tyr403 in the Binding of Agonists and Functional Coupling. *Mol Pharmacol* **52**:1087-1094.

Voigtländer U, Jöhren K, Mohr M, Raasch A, Tränkle C, Buller S, Ellis J, Höltje H D and Mohr K (2003) Allosteric Site on Muscarinic Acetylcholine Receptors: Identification of Two Amino Acids in the Muscarinic M2 Receptor That Account Entirely for the M2/M5 Subtype Selectivities of Some Structurally Diverse Allosteric Ligands in N-Methylscopolamine-Occupied Receptors. *Mol Pharmacol* **64**:21-31.

Waelbroeck M (1994) Identification of Drugs Competing With D-Tubocurarine for an Allosteric Site on Cardiac Muscarinic Receptors. *Mol Pharmacol* **46**:685-692.

Waelbroeck M (2003) Allosteric Drugs Acting at Muscarinic Acetylcholine Receptors. *Neurochem Res* **28**:419-422.

Waelbroeck M, Camus J and Christophe J (1989) Determination of the Association and Dissociation Rate Constants of Muscarinic Antagonists on Rat Pancreas: Rank Order of Potency Varies With Time. *Mol Pharmacol* **36**:405-411.

Wallis RM and Napier C M (1999) Muscarinic Antagonists in Development for Disorders of Smooth Muscle Function. *Life Sci* **64**:395-401.

Wallis R (1996) The Binding Profile of the Novel Muscarinic Receptor Antagonist Darifenacin Against the Five Cloned Human Muscarinic Receptors Expressed in CHO Cells. *Br J Pharmacol* **130P**.

Wang P, Luthin G R and Ruggieri M R (1995) Muscarinic Acetylcholine Receptor Subtypes Mediating Urinary Bladder Contractility and Coupling to GTP Binding Proteins. *J Pharmacol Exp Ther* **273**:959-966.

Ward SD, Curtis C A and Hulme E C (1999) Alanine-Scanning Mutagenesis of Transmembrane Domain 6 of the M(1) Muscarinic Acetylcholine Receptor Suggests That Tyr381 Plays Key Roles in Receptor Function. *Mol Pharmacol* **56**:1031-1041.

Ward SD, Hamdan F F, Bloodworth L M and Wess J (2002) Conformational Changes That Occur During M3 Muscarinic Acetylcholine Receptor Activation Probed by the Use of an in Situ Disulfide Cross-Linking Strategy. *J Biol Chem* **277**:2247-2257.

Wess J (1996) Molecular Biology of Muscarinic Acetylcholine Receptors. *Crit Rev Neurobiol* **10**:69-99.

Wess J (1997) G-Protein-Coupled Receptors: Molecular Mechanisms Involved in Receptor Activation and Selectivity of G-Protein Recognition. *FASEB J* **11**:346-354.

Wess J (1998) Molecular Basis of Receptor/G-Protein-Coupling Selectivity. *Pharmacol Ther* **80**:231-264.

Wess J (2003) Novel Insights into Muscarinic Acetylcholine Receptor Function Using Gene Targeting Technology. *Trends Pharmacol Sci* **24**:414-420.

Wess J (2004) Muscarinic Acetylcholine Receptor Knockout Mice: Novel Phenotypes and Clinical Implications. *Annu Rev Pharmacol Toxicol* **44**:423-450.

Wess J, Eglen R M and Gautam D (2007) Muscarinic Acetylcholine Receptors: Mutant Mice Provide New Insights for Drug Development. *Nat Rev Drug Discov* **6**:721-733.

Wess J, Gdula D and Brann M R (1991) Site-Directed Mutagenesis of the M3 Muscarinic Receptor: Identification of a Series of Threonine and Tyrosine Residues Involved in Agonist but Not Antagonist Binding. *EMBO J* **10**:3729-3734.

Wess J, Maggio R, Palmer J R and Vogel Z (1992) Role of Conserved Threonine and Tyrosine Residues in Acetylcholine Binding and Muscarinic Receptor Activation. A Study With M3 Muscarinic Receptor Point Mutants. *J Biol Chem* **267**:19313-19319.

Wess J, Nanavati S, Vogel Z and Maggio R (1993) Functional Role of Proline and Tryptophan Residues Highly Conserved Among G Protein-Coupled Receptors Studied by Mutational Analysis of the M3 Muscarinic Receptor. *EMBO J* **12**:331-338.

Whiting PJ (2003) GABA-A Receptor Subtypes in the Brain: a Paradigm for CNS Drug Discovery? *Drug Discov Today* **8**:445-450.

Wise A, Gearing K and Rees S (2002) Target Validation of G-Protein Coupled Receptors. *Drug Discov Today* **7**:235-246.

Wolfe BB and Yasuda R P (1995) Development of Selective Antisera for Muscarinic Cholinergic Receptor Subtypes. *Ann N Y Acad Sci* **757**:186-193.

Wyman J and Allen D (1951) The Problem of Heme Interactions in Haemoglobin and the Basis for the Bohr Effect. *J Polymer Sci* **7**:499-518.

Yamada M, Miyakawa T, Duttaroy A, Yamanaka A, Moriguchi T, Makita R, Ogawa M, Chou C J, Xia B, Crawley J N, Felder C C, Deng C X and Wess J (2001) Mice Lacking the M3 Muscarinic Acetylcholine Receptor Are Hypophagic and Lean. *Nature* **410**:207-212.

Zahn K, Eckstein N, Tränkle C, Sadee W and Mohr K (2002) Allosteric Modulation of Muscarinic Receptor Signaling: Alcuronium-Induced Conversion of Pilocarpine From an Agonist into an Antagonist. *J Pharmacol Exp Ther* **301**:720-728.

Zawalich WS, Zawalich K C, Tesz G J, Taketo M M, Sterpka J, Philbrick W and Matsui M (2004) Effects of Muscarinic Receptor Type 3 Knockout on Mouse Islet Secretory Responses. *Biochem Biophys Res Commun* **315**:872-876.

Zeng XP, Le F and Richelson E (1997) Muscarinic M4 Receptor Activation by Some Atypical Antipsychotic Drugs. *Eur J Pharmacol* **321**:349-354.

Zhang W, Basile A S, Gomeza J, Volpicelli L A, Levey A I and Wess J (2002a) Characterization of Central Inhibitory Muscarinic Autoreceptors by the Use of Muscarinic Acetylcholine Receptor Knock-Out Mice. *J Neurosci* **22**:1709-1717.

Zhang W, Yamada M, Gomeza J, Basile A S and Wess J (2002b) Multiple Muscarinic Acetylcholine Receptor Subtypes Modulate Striatal Dopamine Release, As Studied With M1-M5 Muscarinic Receptor Knock-Out Mice. *J Neurosci* **22**:6347-6352.

Zhu SZ, Wang S Z, Hu J and el-Fakahany E E (1994) An Arginine Residue Conserved in Most G Protein-Coupled Receptors Is Essential for the Function of the M1 Muscarinic Receptor. *Mol Pharmacol* **45**:517-523.

Zorn SH, Jones S B, Ward K M and Liston D R (1994) Clozapine Is a Potent and Selective Muscarinic M4 Receptor Agonist. *Eur J Pharmacol* **269**:R1-R2.

Chapter 11. Acknowledgements

I would like to first thank my thesis director, **Dr. Pere Garriga**, for giving me the opportunity to allow me to undertake this PhD study. For all the suggestions, ideas and very long discussions (sometimes many hours..) that we have had. For your advice both in science and in life. For having your door always open for anything I have needed and for supporting me until the end to successfully finish my thesis. I wish you all the best for the future. *Moltes gràcies Pere*

I would like to emphasize my deepest gratitude to the co-director of my thesis, **Dr. Nigel Birdsall** for making this project possible, starting from his very warm welcome to NIMR to convert my manuscript into a thesis. With immense knowledge, wisdom and patience he has guided my work. For sharing your incredible enthusiasm for doing science with me and teaching me to pay close attention to the details. For your support and encouragement at all the up and down moments. For all the help in the writing and for making such a great effort to have it corrected in a short time. I wish you all the best in your life and I will always be grateful to you. Thank you very much Nigel!

I also want to express my sincere gratitude to **Dr. Arthur Christopoulos**, who gave me the opportunity to work in his lively group in Melbourne for 6 months and provided me some of the starting material, for being responsible for the project having a beginning and instilling in me the enthusiasm for the allosterism. Thank you, Arthur, for your expert advice and your warm character.

To everybody from my lab in Terrassa!! *A* **Eva***, siempre dispuesta a ayudarme en cualquier cosa. Especialmente a* **Laia***, por su tolerancia, por guiarme al principio y por ser mi compañera sobre todo en momentos difíciles que hemos pasado en el labo…A* **Mónica***, por la ráfaga de buen humor y buen rollo con la que vino. A todos los cubanos del lab, a* **Dasiel***, por ese divertidísimo primer año!! A* **Darwin, Wilber y Mileidys***, gracias por esa maravillosa acogida en Sicilia!* I wish also to thank the rest of the GBMI group, especially to **Dra. Marga Morillo**, to **Dra. Margarita Calafell**, and to **Dr. Tzanko Tzanov**. I would like to thank **Maria Amor Duch**, responsible for the UPC radioactivity service, *por tu paciencia y ayuda, por hacerme la vida mucho más fácil con todo el tema de radiactividad*. To **Alicia Enrich**, from Salvat, *me ayudaste mucho al principio con todos los conceptos de* radioligand binding!

Many thanks to all the members of Arthur's lab, especially **Elizabeth Guida**, who was the person who generated some stable cells lines and subcloned the coding sequence of the human M_3 WT. Elizabeth has enabled me to overcome the frustrations of molecular biology and has given me excellent first hand instruction of various procedures used in this study, becoming also a good friend, thank you very much "Big F."! To **Vimesh Avlani** for his patient explanations of concepts and terminologies and his big help in analyzing results. To **Lauren May** for all the useful advices and explanations about allosterism and of course…all the laughs and funny moments. To **Karen, Olivia**…

I would like to thank to all the Division of Physical Biocehmistry at NIMR, to **Asma** and **Guillaume** for their useful and nice help at the beginning of my work in the lab. But if I have to thank someone in this Division, this is **Natali**, who offered me her friendship from the very beginning…and specially, for being so sweet and supportive always and letting me live with you all the time that I have needed….I will never forget that! Also to **Chris T**. for being always so nice and sweet to me, and of course the best "taxi driver"! Thanks for everything Chris. To **Chris M.** for being so kind, and of course…I have to thank you for all the DVDs that I borrowed! They entertained me during numerous evenings. To S**imone K.,** for your support (and to **Ben**). To **Marta M**., we met for only a short time, but thank you for your energy! Good luck finishing your PhD! And to the rest of the group, **Iwan, Andy, Rachel, Fred, Sarah**, **Stephan**….for all those spontaneous nice dinners and fun going out nights!!!.

To my numerous flatmates in Barcelona….among them, **Salvatore**, *ya que fue un placer compartir piso contigo, gracias por todo Salva.* **Jillian** and **David**, *por esas fantásticas fiestas en Castillejos!* To **Anna** and **Neus**, *que aunque fue cortito pero intenso!! Mil gracias por todas esas tertuliejas que tuvimos. Como no, a* **Elvira***, que has sido un apoyo enorme para mi en Barcelona, y por todos esos viajecitos de buceo. Y a* **Rovins** *claro!! Por tu increíble alegría y generosidad.* To my favourite Catalans **Eva, Laura E**. (la otra) y **Mónica**, *ha sido fantástico encontrarme con vosotras en Barcelona, por enseñarme vuestros rincones maravillosos en Catalunya y por hacerme disfrutar mucho más la naturaleza. De verdad, que me ha encantado, moltes gràcies!*

To **Rocio**, *por donde empezar "chuti"…si empezamos todo esto juntas…y lo más bonito es que también lo acabamos juntas…Por la inolvidable y entrañable aventura de Utrecht. Pero sobre todo mil gracias por tu incondicional apoyo, por estar siempre ahí,*

y por ser tan buena amiga. (And to **Dani**, *gracias por tu increíble energía y buen humor).* To **Miriam**, *hemos vivido tantas cosas…gracias, por ser tan especial, dulce y cariñosa, por apoyarme siempre a pesar de la distancia, y por siempre ser mi amiga.* To *"mamá"* **Teresita**…*jejeje...que voy siguiendo tus pasos…mil gracias por toda tu apoyo y energía, por hacerme reír tanto, por todos tus consejillos y por las fantásticas tertuliejas.* To **Dan** for your support, generosity and for the immense joy that you always transmit to me. To **Marco**, and in short, thanks to all the Utrecht family!

A mis compis de facultad, sobre todo a **Elena Briones, Marina, Eva y Elena Blanco**, *gracias por todos esos momentos en los que nos hemos reído y disfrutado tanto. A* **Maria B.**, *la chisca, por todas las risas y fantásticas conversaciones que siempre hemos tenido, y espero duren siempre. Y a* **Jorge,** *claro.*

A mis amigas de toda la vida, las de siempre, a las que adoro y que siempre están ahí incondicionalmente, **Patricia, María y Maite**, *que haría sin vosotras!. Y a "uuhuhhu",* **Isra**, *por tu alegría y cariño, y estar siempre ahí, a* **Alvarito**, *por tu apoyo siempre que nos vemos, a* **Miguel Ángel,** *por preocuparse, y a* **Laura S.**, *gracias por todo.*

A mi querida **abuelita**, *a mi tía* **Julia y Juan** *por el cariño y apoyarme siempre, gracias. A mis hermanos* **Luis** (*responsable de la impresión y la portada de esta tesis, mil gracias!)* **y Fernando**, *a los que adoro y admiro, por cuidarme tanto y darme siempre un apoyo incondicional, a* **Paloma y Elena**, *por su cariño, por su apoyo y por ser como hermanas para mi y a los maravillosos* **sobrinos** *que me han dado, que son unos soletes enormes y ya no se vivir sin ellos. Y por último y más importante a mi* **madre**, *ya que sin ti no habría podido acabar esta tesis, por tu generosidad, por estar siempre conmigo, en los buenos y en los malos momentos, por tu apoyo incondicional. Por darlo todo. Esta tesis es para ti mamá, te quiero mucho.*

Nobody said it was easy,
Nobody said it would be so hard,
I was just guessing at numbers and figures…
Pulling the puzzles apart…
Questions of science, science and progress…
Do not speak as loud as my heart.
No one ever said it would be this hard…

"The Scientist",
A Rush of Blood to the Head, Coldplay, 2002